National University of Ireland, Cork

University College Cork — Coláiste na hOllscoile Corcaigh

Department of Civil and Environmental Engineering

Head of School: Prof. Liam Marnane

Supervisors: Prof. Gerard Kiely

Dr. Matteo Sottocornola (Waterford Institute of Technology, Waterford, Ireland)

Dr. Damiano Gianelle (Fondazione Edmund Mach, San Michelle all'Adige, Italy)

Measurements of the carbon, energy and water balance in an Italian alpine peatland and simulating the vegetation and carbon dynamics in three different peatlands

Thesis presented by

Johannes Wilhelmus Maria Pullens MSc.

For the degree of

DOCTOR OF PHILOSOPHY

September 2017

Table of Contents

Declaration

This is to certify that the work I am submitting is my own and has not been submitted for another degree, either at University College Cork or elsewhere. All external references and sources are clearly acknowledged and identified within the contents. I have read and understood the regulations of University College Cork concerning plagiarism.

Johannes Wilhelmus Maria Pullens

Acknowledgements

This project has been funded with support from Fondazione Edmund Mach.

I am grateful to my supervisors, in random order, Dr. Damiano Gianelle, Dr. Matteo Sottocornola and Professor Ger Kiely, whom I thank for the existence of this study and for the guidance, the patience and the help during my PhD.

I would also like to thank the current and former members of the DASB group (Barbara, Mirco, Michele, Lorenzo, Mauro, Roberto, Maurizio, Claudia, Kaja, Karolina, Francesco and Damiano) for their help and friendship. In particular Roberto Zampedri and Mauro Cavagna for their help in the field and for the maintenance of the tower. I would also like to thank Prof. Steve Frolking for giving me the opportunity to visit him and work together; it has been a great experience and has been very helpful. I would like to thank IRSAE for their travel support through mobility grants.

I would also like to thank the cost action PROFOUND, and in particular, Florian Hartig and Maurizio Bagnara, for the opportunity to do a Short Term Scientific Mission. During this STSM, I have learned many new skills and met many interesting people.

Special thanks to my friends, too numerous to mention with whom I enjoyed many coffee breaks and nights out/diners, also when the amount of PhD students decreased I was sure I had people to count on. Without all of you, this period would have felt much longer and the PhD much heavier.

Finally, a special word of thanks goes to my family and friends in the Netherlands who supported me throughout the complete study, even though 1000 kilometres distance. Many thanks for all the visits to Italy or all the other places. Thanks to technology, we could have kept in close contact and we did not miss any single important moment.

Abstract

The stored carbon in the soil of peatlands is a result of a long-term imbalance between the decomposition and the biomass production. Peatlands occur all over the world but are mainly located in the northern hemisphere. Up to now, peatlands in the Alps have not received much attention, because they are not the dominant ecosystem. In this study, we investigated the carbon, water and energy balance of a small-scale fen in the Italian Alps over four years (2012-2015). During the four-year period, the carbon fluxes were measured by an eddy covariance system. Over this period, the peatland was a carbon source based on CO_2 emissions (net ecosystem exchange (NEE): 103.5, 262.9, 175.7, 1807.7 g C-CO_2 m^{-2} yr^{-1}). During a 10-month period, December 2013-September 2014 a methane analyser was installed at the peatland, which measured small methane (CH_4) fluxes (3.2 g C-CH_4 m^{-2}).

Dissolved Organic Carbon (DOC) plays an important role in the carbon balance of ecosystems. To assess the DOC fluxes of the peatland the hydrology of the peatland was modelled with the model GEOtop. GEOtop is a process-based distributed model of the water and energy budget and was applied for four years. The modelled energy fluxes are comparable to the fluxes measured by the on-site eddy covariance tower. The model was able to simulate the volumetric water content temperature accurately over the four years. During snow cover, the model had difficulties simulating the soil temperature due to insulation by the snow. In 2014-2015, the DOC concentrations were measured. The modelled water cycle was used to quantify the loss of dissolved organic carbon (DOC) and to calculate the carbon balance of the peatland. Based on the DOC measurements and the modelled discharge, an extrapolation of the DOC export was made, which resulted in an average loss of DOC 7.7, 12.3, 13.8, 8.0 g C m^{-2} yr^{-1} over the four years. The combination of the DOC, CO_2 and CH_4 fluxes indicate

that the peatland is acting as a carbon source for all four subsequent years with a carbon balance of 112.3, 273.8, 190.8 and 95.3 g C m^{-2} yr^{-1} for 2012, 2013, 2014 and 2015 respectively.

To study the functioning of three different peatlands over the world the NUCOM-Bog (NUtrient cycling and COmpetition Model) was applied. Bayesian techniques have been used to calibrate the model for each site specific and for a multi-site calibration. The combination of site-specific and multi-site calibration has the potential to gain insights in the functioning of different peatlands and to identify how the vegetation of peatlands will change over time in respect to climate change. The marginal parameter uncertainty of the multi-site calibration compared to the site-specific calibration, indicate that with the multi-site calibration the parameter uncertainty can be reduced by using information from multiple sites.

1 Introduction

1.1 General Introduction

Peatlands occupy only 3 % of the earth surface but store up to 30% of the global soil organic carbon (Gorham 1991) and are therefore important ecosystems. In the world's largest terrestrial soil carbon pool, over millennia peatlands have stored up to 547 (473-621) petagram (1 Pg = 10^{15} gram) of soil organic carbon in the form of peat (Gorham 1991, Yu 2012). This amount is approximately half the amount of greenhouse gas carbon dioxide (CO_2) in the atmosphere (Rydin and Jeglum 2015). The carbon cycle in peatlands involves processes such as net primary production, which is the difference of the CO_2 absorbed by plants during photosynthesis, and the CO_2 released (respired) by the plant and the soil, as a product of soil decomposition. Therefore, peatlands played and play an important role in the global carbon cycle. Peatlands occur all over the world but are mainly located in the northern hemisphere (Parish et al. 2008, Yu et al. 2010, Schuur et al. 2015). There most research is done on the vulnerability of the carbon storage in respect to climate change and permafrost degradation (Frolking et al. 2001, Camill 2005, Dorrepaal et al. 2009). Over the last decades an increase in interest for the carbon stock and fluxes of tropical peatlands has been seen (Page et al. 2011, Evans et al. 2014). While other peatlands located on high altitudes did not receive this increase in interest.

Up to now, peatlands in the Alps have not received much attention, since they are not the dominant ecosystem (Parish et al. 2008). So far the only research done on alpine peatlands has been focused on their restoration and management (van der Knaap et al. 2011, Ammann et al. 2013). In the Alps, small peatlands formed in lakes in mountain saddles, when the glaciers retreated. Over thousands of years, dead plant material has accumulated in these lakes and has formed layers of dead organic material. In this

way, the carbon has been stored in these peatlands. The fact that the peatlands are small in area does not make these peatlands less important. It is therefore important to understand how these small-scale peatlands function, to see what their current state is and to identify their threats. Only in this case it is possible to understand how these alpine peatlands will respond to the current climate change, which is expected to have a high impact on the temperature and the precipitation of these high altitudes regions (Beniston et al. 1997, Beniston 2006, IPCC 2007, 2013).

1.2 Aims and Scopes

This study investigates the functioning and the water, energy and carbon budgets of the Monte Bondone peatland in Italy. The carbon budget in peatlands is mainly composed of two greenhouse gasses CO_2 and CH_4 and dissolved organic carbon (DOC) in stream water. These carbon fluxes were quantified and their seasonal and annual variability was investigated and correlated with meteorological drivers (e.g. temperature, precipitation).

This study includes in total 4 years of eddy covariance CO_2 measurements, 10 months of eddy covariance CH_4 measurements and 4 years of DOC flux extrapolation via discharge modelling in addition to meteorological and environmental measurements over the 4 years (2012-2015).

This study was divided into three sub-projects, each of them with a specific aim:

A) Measure and calculate the carbon dioxide and methane fluxes at the Monte Bondone peatland site.
B) Use the hydrological model GEOtop to simulate the water balance of the complete catchment and to analyse the DOC export of the peatland.
C) To increase our understanding of peatland functioning through the model comparison of different peatland types in different climatic conditions.

1.3 Thesis Layout

This thesis contains nine chapters, a list of references and three appendices. Following this present introduction, Chapter 2 is a literature review addressing different types of peatlands, their importance for the global carbon balance and methods to study the peatlands. The methodologies used to perform this work and description of the study sites used are presented in chapter 3. Chapter 4 focuses on three year of carbon fluxes of an alpine peatland located on Monte Bondone, in the northeast of Italy. Chapter 5 presents a modelling study of the hydrology of the same alpine peatland. In this chapter, the fluxes from the previous chapter are combined with the modelled discharge and the measured dissolved organic carbon fluxes. Chapter 6 is dedicated to the description of the NUCOMBog R package, a software used for simulating vegetation, water, carbon and nitrogen dynamics in peatlands. In chapter 7 the previously described software is calibrated for different peatlands and the differences are discussed, in respect to a multi-site calibration. Chapter 8 presents a general discussion of this thesis, conclusions, while chapter 9 gives recommendations for future research. This is followed by the reference list and four appendices, which include two published papers from the current PhD study, one published paper from the previous Master studies (but related to this PhD study) and the manual of the NUCOMBog R package described in Chapter 6.

2 Literature review

2.1 The carbon balance of peatlands

The stored carbon in the soil of a peatland is a result of a long-term imbalance between the decomposition and the biomass production between the atmosphere and the biosphere. This misbalance is called the net ecosystem exchange (NEE), which is the difference between the gross primary production (GPP) and ecosystem respiration (R_{eco}). In peatlands due to the waterlogged conditions, the decomposition is lower than the biomass production. Globally it is estimated that peatlands are currently a net carbon sinks of around 830 Tg/year of carbon (1 Tg = 10^{12} gram) (Mitsch et al. 2013).

Other components of the carbon balance are methane (CH_4) and dissolved organic carbon (DOC) fluxes. Under the anaerobic conditions in the soil the decomposition of organic material generates methane (CH_4). The carbon can also be dissolved in water and be lost via runoff or discharge or streams

2.2 Different types of peatlands

Peatlands are wetlands with at least a 30-40 cm thick peat layer, depending on the which country's definition is used (Gorham 1991). They can exist in different types, based on the local climatic situations and peatlands are therefore region bound. The different types of peatlands have different origins and function in different ways. Peatlands can originate in locations where the biomass production is bigger than the biomass decay. The decomposition of the produced biomass in peatlands is limited, due to the waterlogged soils (Clymo 2004). Over time, this partially decomposed material can become a thick layer: this is called peat.

There are different types of peatlands, which will be discussed separately. The driving factor of which type of peatland can develop is based on the climatic situations

(Gorham 1957, Wheeler and Proctor 2000) and on the geological features of the area (Wheeler and Proctor 2000). Ombrotrophic peatlands, commonly called bogs, are rainwater fed and have therefore less nutrients and minerals, while minerotrophic peatlands, fens, are being fed by water from streams and springs; this water has percolated through soil and potentially rock, which, depending on the type of soil, could result in higher levels of nutrients and minerals (Wheeler and Proctor 2000). These differences in water sources and the dissolved nutrients and minerals result in different types of vegetation and have therefore different ecosystem dynamics (Sottocornola et al. 2009).

The geology of the location plays an important role in the hydrology of the area. A wet area or soil reduces the decomposition, due to anaerobic conditions of the soil. The slow decomposition can lead to an imbalance between the decomposition and the biomass production. If the soils are too steep, no water can stagnate and no organic material accumulate, and therefore no peatland can evolve over time. Since the biomass production and decomposition are both slow the formation of a peatland takes thousands of years (Wheeler and Proctor 2000).

2.2.1 Raised bog

Raised bogs are discreet, raised, dome-shaped peatlands, which started as fens but became, due to their growth in elevation, independent of the ground water (Gore 1983). The main vegetation in raised bogs is *Sphagnum* mosses. The capitulum, the growing part of the mosses, is growing upwards and this vertical increase results in lower parts of the moss becoming buried. Due to a lack of light these parts will die. These dead plant parts have a high water holding capacity, due to large structural cells (hyaline cells) which retain the water (Clymo and Hayward 1982). This has the effect that the raised bogs can hold the precipitation and retard percolation (Gorham 1957).

These mosses also change the acidity of the peat by taking up cations and secreting H^+ ions (Clymo 1964) and thereby decrease the decomposition rate of the peat even more (Hobbie 1996, Tallis 1998, Lang et al. 2009, Biester et al. 2014).

The surface of raised bogs can be divided in different microforms: hummocks, lawns and hollows (Tallis 1998). These microforms can be distinguished on the base of their elevation over the water table: Hummocks are the highest microforms, where hollows are the lowest and therefore the wettest microforms. Lawns are microforms which are at an elevation between hummocks and hollows.

2.2.2 Blanket bog

A blanket bog is a type of peatland that as the name suggests, forms a blanket over the topology and on slopes with a gradient up to 20-25° (Tallis 1998). Blanket bogs distribution is restricted to climates with high precipitation, cool summers and mild winters (Hammond 1978). Due to the high precipitation, the minerals in the soil, such as iron, are dissolved and deposited lower in the soil. This so called iron pan (van Breemen 1995), forms an impermeable layer and makes the soil therefore much wetter. Over millennia, under these conditions the peat could accumulate and spread. The general vegetation of blanket bogs in the northern hemisphere are mainly graminoids, in particular *Molinia caerulea* (purple moor-grass) and *Schoenus nigricans* (black-top sedge) and blanket bogs have a lower amount of *Sphagnum* moss cover compared to raised bogs (Gorham 1957, Sottocornola 2007). The surface of blanket bog is divided in the same microforms as the raised bog.

2.2.3 Fen

A fen type of peatland is always located in the lowest region of their catchment, a location where the groundwater and surface water can accumulate. After the last ice age (110,000 – 11,700 years ago), when the ice retreated, the water stagnated and

formed lakes in the depressions made by the glaciers. Due to the warmer climate, plants colonized these newly formed pools. When these plants died off, they sunk to the bottom of the pool, where, due to the lack of oxygen, they decompose slowly. Over time this layer of dead organic matter became thicker and thicker. Due to the location in the catchment, these infilled pools are also dependent on soil water and have therefore a different vegetation than bogs. In fens, sedges (*Carex* sp.) and graminoids (*Molinia caerulea* and *Eriophorum vaginatum*) are the most abundant plant species. Due to the dissolved nutrients and minerals in the groundwater the presence of *Sphagnum* mosses is suppressed (Wheeler and Proctor 2000).

2.2.4 Aapa mire

Aapa mire is a Finnish term for a large, complex, cold-climate wetland. These wetlands are, like fens, depended on soil water and are therefore minerotrophic (Laitinen et al. 2007). Aapa mires are located in the boreal area, where winter air temperature can drop significantly below zero degrees Celsius (Parish et al. 2008). The topography of aapa mires has usually a mosaic of specific topography formed as a result of frost heaving and the flow of snowmelt water. The topography shows high (strings) and low regions (flarks). These flarks are much wetter than the strings, where the water is drained fast. Aapa mires are usually slightly concave (Laitinen et al. 2007) and due to the very wet condition *Sphagnum* mosses are located more towards the edge of the mire, while in the centre mainly sedges are present (Mäkilä et al. 2001).

2.3 Importance of peatlands

Apart from carbon sequestration peatlands also provide other ecosystem services, which can have a big impact on the local scale. Peatlands, due to their water dependency tend to make the local climate cooler and more humid (Parish et al. 2008). The water dependence also helps to store water and in this way regulate the peak

discharges after precipitation events, in particular in bogs (Clymo and Hayward 1982, Tahvanainen 2011, Gao et al. 2016). Peatlands also have the ability to purify the big amount of water passing through by removing pollutants (Joosten, H., Clarke 2002, Lavoie et al. 2016).

Peatlands are unique and complex ecosystems and share many attributes with lakes and with terrestrial ecosystems are have therefore a high biodiversity (Parish et al. 2008). Peatlands are often the last remaining natural areas in degraded landscapes (Parish et al. 2008), which results in providing havens for biodiversity (Bridgham et al. 2006). Due to the uniqueness of the peatland ecosystem, peatlands also provide recreational and cultural services. Another ecosystem service provided by peatlands is the production of peat. This peat can be harvested and can serve many purposes, so is peat used for horticulture (Minkkinen et al. 2008, Weissert and Disney 2013, Woziwoda and Kopeć 2014), but through combustion peat can also be used as energy source (Bridgham et al. 2006, Weissert and Disney 2013, Woziwoda and Kopeć 2014, Abdalla et al. 2016).

2.3.1 Peatlands under climate change

The soil of the peatlands, in which the carbon is stored, is not a stable storage; the carbon is particularly vulnerable to climate change (Frolking et al. 2011). Due to climate change the air temperatures are globally raising and changes in the precipitation regime are expected (IPCC 2007, 2013). The distribution of the precipitation is likely to change to more intense periods of rain and longer periods of drought, so more extreme patterns in dry and wet regions on the planet (Donat et al. 2017). Since peatlands are highly dependent on water, the effects of the changes in precipitation can play a big role, in both the plant productivity as the decomposition of the peat (Ise et al. 2008, Fenner and Freeman 2011). When the soils of the peatlands

become drier due to less precipitation and longer periods without precipitation, more oxygen can reach the peat and this will result in higher decomposition rates (Minkkinen et al. 2008, Juszczak et al. 2013, Moore et al. 2013, Petrescu et al. 2015, Miller et al. 2015, Bragazza et al. 2016). The effect of the drier soils on the plant productivity is less frequently measured, however a general trend of reduced plant productivity can be seen (Frolking et al. 2011). On the other hand, a drop in water table depth below 20 cm will result in a decrease in CH_4 emissions, due to oxygenation of the carbon (Jungkunst et al. 2008, Couwenberg et al. 2010, Mitsch et al. 2013, Andersen et al. 2013, Gong et al. 2013). In peatlands where the water table is low, a raise in water table will reduce the CO_2 emissions and will also lead to changes in the vegetation composition and can therefore even reverse the net ecosystem carbon balance (Hendriks et al. 2007, Waddington et al. 2015). A raise in water level will result to an increase in bryophyte and a lower vascular plant cover, in particular *Sphagnum* mosses (Potvin et al. 2014, Järveoja et al. 2016). These mosses are known to be hard to decompose due to their high recalcitrance (Andersen et al. 2013), and will therefore result in a positive effect on the peat depth and hence stored carbon in the soil. A raise in water table could also result in more runoff and therefore a removal of organic matter through Dissolved Organic Carbon (DOC) in the water (Strack et al. 2008). The uncertainty in the range and sign of the changes in the precipitation regime makes it difficult to predict the impact on a global scale. On a plot or ecosystem scale the changes in precipitation regime might change the carbon balance from a carbon sink to a carbon source (Li et al. 2007, Frolking et al. 2011).

The expected temperature rise will lead to an increase in evapotranspiration and an increase in soil temperature. The increase in soil temperature will result in higher soil respiration due to higher microbial activity (Kirschbaum 1995, Dorrepaal et al. 2009, Smith and Fang 2010, Bond-Lamberty and Thomson 2010, Blok et al. 2016, Bragazza

et al. 2016, Wilson et al. 2016, Wohlfahrt and Galvagno 2017). The increase in evapotranspiration will result in a lowering of the water table (Roulet et al. 1992, Moore et al. 2013) and will therefore also result in higher soil respiration due to oxidation of the peat (Bond-Lamberty and Thomson 2010). The increase in temperature will likely result in a higher productivity due to a higher vascular plant cover (Moore et al. 1998, Bu et al. 2011). Expected is that the respiration will be bigger than the higher net primary production, changing from carbon sink to carbon source, which will intensify climate warming by positive feedback (Bu et al. 2011).

Globally the effects of climate change can be predicted, but at finer resolutions the effects are more uncertain. For example, the climate scenarios for mountainous regions are not in line with each other. There is evidence that there is Elevation-Dependent Warming (EDW, Giorgi et al. 1997, Beniston et al. 1997, Beniston 2006, Eccel et al. 2012, Pepin et al. 2015), but for every mountainous area the drivers can be different (Beniston et al. 1997, Im et al. 2010, Pepin et al. 2015). For each site the topography, slope, aspect and exposure is different, which results in different scales of warming. For example, shorter snow cover results in a decrease in albedo, which will result in an increase in surface absorption of the incoming radiation and therefore an increase in air temperature. The daily mean air temperature at 2 metre above a snow-covered is 0.4°C colder than over an not snow-covered area (mean value for 1961-2012 in Switzerland, (Scherrer et al. 2012), for more examples and mechanisms, see Pepin et al. (2015)). Despite the uncertainties in the climate change scenarios, it is important to know and understand what any possible effects of climate change can be and how ecosystems will respond.

Climate change can turn peatlands from a carbon sink to a carbon source, i.e. changing from a net uptake of carbon to a net emission of carbon. However, climate change is

a rather slow process and due to the changes in precipitation and temperature, the vegetation of peatlands is likely to change (Bauer et al. 2007, Sottocornola et al. 2009, Taylor et al. 2016). Lower water table values can facilitate the invasion of shrubs and tree species in peatlands (Stine et al. 2011, Blok et al. 2011, Holmgren et al. 2015, Bart et al. 2016, Kamocki et al. 2016). The encroachment of the woody plants will lead to the soils becoming drier due to higher transpiration by trees (Lewis et al. 2013, Woziwoda and Kopeć 2014). These drier soils will positively feedback more woody plant species invading, eventually turning these ecosystems into grasslands and/or forests depending on the local climate (Dieleman et al. 2015).

Even if the general response of global peatlands to climate change is likely to be small, the change in net greenhouse gas emissions may persist for centuries (Frolking et al. 2011).

2.3.2 Disturbances of peatlands

Apart from climate change also human have caused disturbances on peatlands. Peat can be used for many purposes, such as a fossil fuel and for horticultural purposes (Bridgham et al. 2006, Minkkinen et al. 2008, Weissert and Disney 2013, Woziwoda and Kopeć 2014, Abdalla et al. 2016). Peatlands are also converted to agricultural fields or to forests for wood production through drainage and fertilization. Drainage ditches are dug, normally a combination of closely spaced plough furrows and more widely spaced deep (0.5 – 2.0 m) ditches are used (Lewis 2011). An effect of these drainage ditches is the lowering of the water table, which makes the peatlands easier to access by machineries. However due to the drainage also the soil respiration increases (Hatala et al. 2012), the vegetation changes (Talbot et al. 2014, Gatis et al. 2016) and the stability of the soil decreases, which can lead to erosion (Minkkinen et al. 2008, Frolking et al. 2011, Zanello et al. 2011, Haahti et al. 2016) and peatland

subsidence (Couwenberg et al. 2010, Zanello et al. 2011, Hatala et al. 2012, Potvin et al. 2014, Harpenslager et al. 2015b).

2.3.3 Mechanisms of restoration

Nowadays the importance of peatlands in relation to carbon stocks and emissions is better known and attempts are being made to restore the managed, harvested and drained peatlands. Several techniques are involved in restoring the peatlands to "re-establish self-regulatory mechanisms that will lead back to functional peat accumulating ecosystems" (Quinty and Rochefort 2003). As an initial step, the drainage ditches are being closed so that the water table can rise and the soil respiration is lowered (Taylor et al. 2016). By doing so plant species which are not adapted to high water table will die and less management has to be performed (Bellamy et al. 2012). Natural revegetation of peatlands by mosses is a slow process due to the low growth rate of the mosses (Quinty and Rochefort 2003). When the managed peatland has been used as agricultural field, first the nutrient rich topsoil has to be removed, to remove the added fertilizer and nutrients (Harpenslager et al. 2015b). When the peatland is completely harvested and the drainage has been blocked the site is usually left to restore (e.g. Hendriks et al. 2007, Aslan-Sungur et al. 2016). The North-American approach to peatland restoration is based on the use of donor peat for the restoration of reclaimed peatlands (Quinty and Rochefort 2003, Strack et al. 2015, Murray et al. 2017). This technique aims to speed up the process of making the peatland a carbon sink again, by transferring the top layer of a pristine, intact peatland to the degraded or reclaimed peatlands (Strack et al. 2015, Murray et al. 2017). This technique is not widely used yet, but the initial results indicate that this technique can be potentially used to turn degraded or reclaimed peatlands into peat accumulating peatlands again.

2.4 Methods to study the carbon balance in peatlands

2.4.1 Eddy covariance

The method used in this project to study the ecosystem greenhouse gas exchange is the eddy covariance technique. "The eddy covariance method provides measurements of gas emission and consumption rates, and also allows measurements of momentum, sensible heat, and latent heat (e.g., evapotranspiration, evaporative water loss, etc.) fluxes integrated over areas of various sizes" (Burba 2013). This technique was proposed around 1950 and but experienced a rapid growth since 1990 (IRRI 2012), with a maximum of around 6000 articles published in 2015 (Figure 2-1).

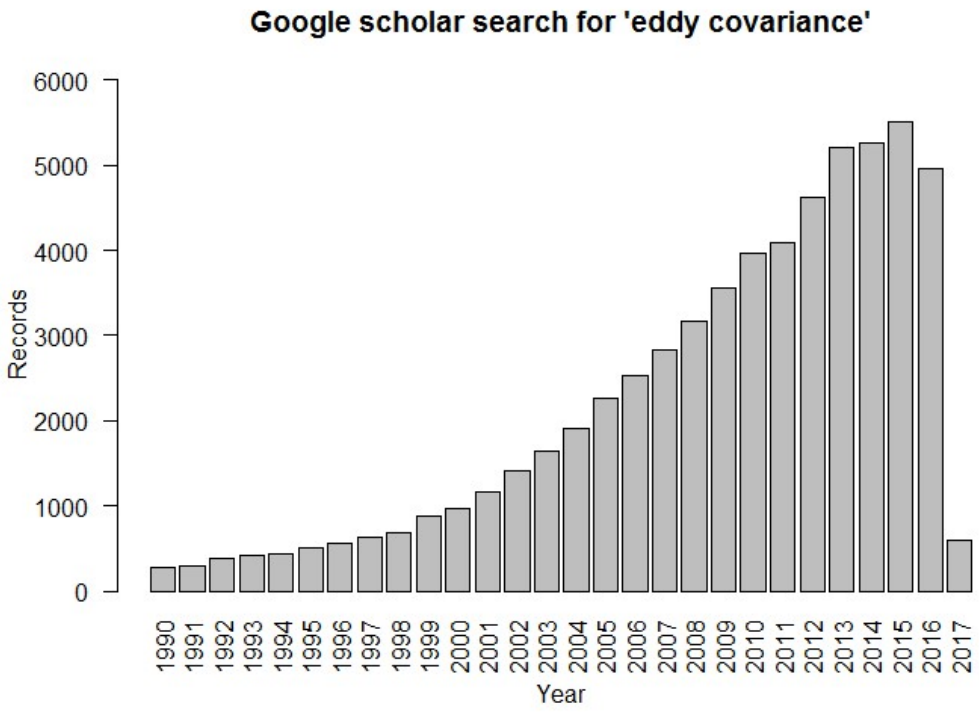

Figure 2-1 Number of occurrences with the keyword "Eddy covariance" on Google scholar (data until 05/02/2017 used)

An eddy covariance system consists in two fast response instruments that have to be combined: a 3D sonic anemometer and an infrared gas analyser (IRGA). The

anemometer measures the turbulent movements of the air, the so called eddies (Figure 2-2)

Figure 2-2 Representation of the eddies over a forest, where an eddy covariance tower is located (Burba 2013)

The IRGA has a path along which specific gas molecules are measured. This path can be either open or 'enclosed'. Two examples of instruments are the LI7500, and LI7200 (both manufactured by Licor, Lincoln, NE, USA). On one side of the path a laser is located while on the other side the detector is located. Every time the laser hits a specific gas molecule, in the case of these two sensors, CO_2 and H_2O, a fraction of the energy of the laser beam is absorbed. By calculating how much energy is absorbed, the amount of CO_2 and H_2O molecules in the air can be measured.

Figure 2-3 Drawing of the LI7550Rs, Open path InfraRed Gas Analyser. 1) Laser source and detector 2) open path with laser beam 3) scratch-resistant lenses 4) chopper motor and chopper wheel. (source: http://www.licor.com/)

Both the anemometer and the gas analyser have to work very fast, since air movements are fast, in particular when the eddies are very small. Therefore, both instruments are usually measuring at a 10-20 Hz range. The fluctuations around the mean of the wind speed, direction and the concentrations of CO_2 and H_2O in the air are correlated with each other. In this way, the fluxes of the gasses are measured, a flux is the transfer of a quantity per unit area per unit time. The raw 10 Hz data is averaged on site to half-hourly data, the standard for flux data. Many types of software are available to further process the raw data (e.g. EddyPro, TK3, EddyUH). With this software, the raw data can be corrected and filtered. The eddy covariance techniques measures the net ecosystem exchange (NEE). This can be expressed in the following formula:

$$NEE = GPP + R_{eco} \quad (2.1)$$

in which GPP is the Gross Primary Production and R_{eco}, ecosystem respiration. In this thesis, the atmospheric sign convention is used, so a negative sign of the flux represents an uptake by the ecosystem. Due to this used convention, the GPP values are negative and the R_{eco} values are positive.

As a guideline the instruments have to be set up at least 1.5 m above the surface and 1,5-2 times the height of the canopy (Burba 2013), in this case the eddies can fully develop. The height of the instruments should also not be set too high, since the eddy covariance system measures the fluxes transported by wind. If the instruments are too high, the footprint of where the fluxes originate can be outside of the region of interest.

One of the main strengths of the eddy covariance technique is that minor disturbance of the measured ecosystem is involved. Another advantage of this technique is that the measurements are done on ecosystem-level and that the technique is working around the clock with minor maintenance. While with other techniques such as chamber measurements, only a part of the ecosystem is measured and only short periods of measurements can be done. Nevertheless, do both techniques provide an insight in the functioning of the ecosystem, but on different spatial and temporal scales.

The eddy covariance technique is based on a number of assumptions. These are: 1) the air is properly mixed. This assumption does not always hold since during night time the atmosphere might become very stable, due to no incoming radiation and reduced wind speeds (Massman and Lee 2002). The air might become stratified, and no mixing will occur. This cause of disturbances can be reduced by a proper setup of the eddy covariance system and a prior check of the wind speeds. In case of stable condition, the anemometer will not be able to measure eddies and therefore the data cannot be used. The friction velocity, u*, is used to discriminate between ‘good’ and ‘bad’ night-time flux data. The filter can be applied when there is a clear correlation between the friction velocity and the night-time flux data (Papale et al. 2006). When the night-time fluxes are depended on the friction velocity it means that the air is not properly mixed below this friction velocity (Aubinet et al. 2012). 2) The eddies need to be able to reach the anemometer and the gas analyser without any obstruction. 3) The

instruments are positioned in such a way that the footprint of the tower is the area of interest. 4) The terrain is horizontal and uniformed, when the terrain is uneven the eddies cannot fully develop or do not reach the tower. 5) Instruments should be able to measure at a high frequency, in this way also the small, high frequency eddies can be measured.

Before the data can be analysed and processed via specific software the data needs to be filtered, the data needs to be filtered for:

1) The quality flag of the fluxes, if this quality flag is different from 0 or 1 ("0" means high quality fluxes, "1" means fluxes are suitable for carbon budget analysis) (Moncrieff et al. 2004);

2) Fluxes, which were measured when the atmosphere was stable. The fluxes with a friction velocity, u*, lower than a pre-calculated value during night-time (PAR < 20 μmol m^{-2} s^{-1}) (Papale et al. 2006);

3) Fluxes when the CO_2 mixing ratio, the concentration of CO_2 in the air, was smaller than 250 or bigger than 500 μmol mol^{-1} (ppm);

4) Fluxes when the CO_2 fluxes are above or below pre-set seasonal thresholds;

5) Fluxes when less than 70 % of the fluxes originated from inside the peatland (the footprint can be calculated by using the footprint model of Kljun et al. (2004). The data that is filtered out, cannot be used for further analysis and is therefore coded missing.

2.4.1.1 Gap filling missing data

Gaps in the data might occur due to several reasons; malfunctioning of the system, power outage, disturbance in the path of the IRGA or the data is coded missing because of specific filters used in the software to process the data. Several techniques to fill

these gaps can be used, ranging from simple techniques such as linear interpolation to very complex algorithms, such as artificial neural networks (Zhao and Huang 2015). In the global eddy covariance flux measurement network, FLUXNET (Baldocchi et al. 2001), the data is gap filled by using a look up table gap filling technique (Reichstein et al. 2005). In this technique, missing values are replaced by the average value under similar meteorological condition. The window in which the method is looking for similar results is 7 days; if there are no similar conditions found the method increased the window with steps of 7 days. The environmental factors used for the gap filling are: Global radiation, Temperature (soil or air), relative humidity, Vapour pressure deficit (VPD) and u* (friction velocity). This gap filling technique has also the option to partition the measured NEE into GPP and R_{eco} (see equation 2.1). With the gap filled data a continuous dataset is created, which can be used to calculate annual carbon balances, interannual variability of ecosystems or serve as an input for model exercises.

2.4.2 Peatland models

Another method to study ecosystems is by using computer simulations. These models are simplified and abstracted representations of reality. A review of literature reveals a wide range of models from simple models, in which the processes are simplified. Due to this 'simplicity' the models are also computational fast and can be used to simulate the formation of peat over millennia (e.g. Bog growth model (BGM, Clymo 1984) and the Holocene peat model (HPM, Frolking et al. 2010)). On the other side in more complex models more biological processes are incorporated and also more realistic specified (e.g. Peatbog (Wu and Blodau 2013) and McGill Wetland Model (MWM, St-Hilaire et al. 2010)). Due to their complexity the models are computationally slower, but the models can represent the biological processes on a sub-daily or even sub-hourly time step, for example to models that simulate vegetation

changes due to nutrient and light competition (NUCOM-Bog (Heijmans et al. 2008)). The choice of model depends on the requirements of the user, as increasing model complexity is generally associated with an increase in cost in terms of data requirements, user input and computational power. The advantage of using models is that the user can simulate a complete ecosystem without having to manipulate the ecosystem itself. Despite the fact that models are a representation of the reality, more insights in the functioning of the system can be gained by implementing them. The dynamics in peatlands are slow and with the help of models, a long period of time can be simulated in a shorter time step. By using models, the effects of climate change and/or management techniques on the vegetation and carbon dynamics can be investigated.

Since peatlands are highly dependent of water, peatland models need to incorporate the hydrology of the peatlands. The catchments where the peatlands are located are too big to conduct extensive field experiments and with the use of models, future scenarios can be investigated. Therefore, hydrological models have to be used. Hydrological models which simulate the soil-vegetation-atmospheric interactions (SVAT, such as GEOtop (Rigon et al. 2006)) can be used to assess the impact of hydrological changes on the water balance of peatlands.

3 Materials and Methods

3.1 Site descriptions

3.1.1 Monte Bondone

The main site used in this thesis is a fen type of peatland in the Italian Alps. This peatland is located on a plateau, Viote, on the Monte Bondone mountain, near Trento, in the Italian Alps (latitude 46º01'03 N, longitude 11º02'27 E) (Figure 3-1). The peatland is located on an altitude of 1563 m asl and is located in a relict glacial lakebed that was formed during the last ice age (Cescatti et al. 1999). The average annual precipitation during 1958-2008 was 1290 mm yr^{-1} with an average air temperature of 5.4 ˚C (Eccel et al. 2012). During winter, the peatland is typically covered by snow from late October-beginning of November till early May. On the east side of the peatland a mountaintop, Palon (2090 m asl), is located. From this mountaintop, all precipitation enters the peatland, either via runoff or via seepage. In the peatland, there are two distinct entry points of seepage, which result in two superficial streams, these two streams merge into one stream that flows out of the peatland (Figure 3-2).

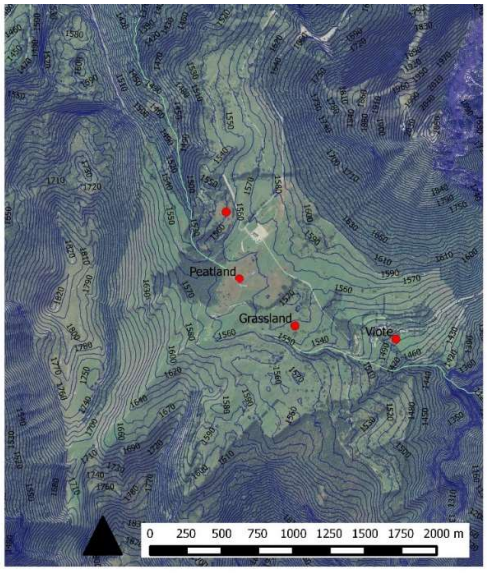

Figure 3-1 An overview of Monte Bondone site. The names refer to the sites of which data has been used. Giardino Botanico and Viote are two meteorological towers of Meteo Trentino. Grassland is an eddy covariance tower located at an alpine grassland (Marcolla et al. 2011, Sakowska et al. 2015); Peatland is the location of the eddy covariance tower at the peatland. The plotted contour lines have an interval of 10 meters

In 1914, 0.35 hectares of the peatland was harvested for burning by removing the peat top layer (Cescatti et al. 1999), which is still visible today (Figure 3-2). This area is mainly covered by *Campylium stellatum*, *Scorpidium cossonii* and *Carex rostrata* today. The depth of the complete peatland ranges from 0.82 m at the border (Cescatti et al. 1999, Zanella et al. 2001) to 4.3 m in the centre (Dalla Fior 1969). Recent measurements have indicated that in the centre of the peatland the mineral soil can be as deep as 7 meters (data not shown).

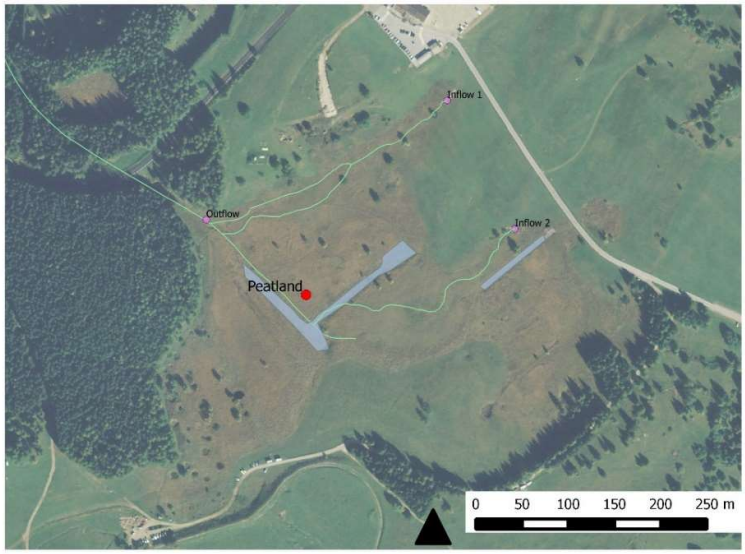

Figure 3-2 Aerial view of the peatland site, with in blue the areas where peat extraction has taken place in 1914. The highlighted area is 0.35 hectares. the turquoise line is a stream running through the peatland

3.1.1.1 Vegetation

The vegetation of the area is very heterogeneous: the areas closest to the eddy covariance tower are mainly dominated by *Molinia caerulea* forming big tussocks, while in the depressions the main vegetation consists of *Carex rostrata*, *Valeriana dioica, Scorpidium cossonii* and scattered *Sphagnum* spp. The southwestern area of the peatland is dominated by *Eriophorum vaginatum*, with high tussocks of *Carex nigra* covering the lower areas. *Sphagnum* spp. as well as *Trichophorum alpinum* and *Drosera rotundifolia* occur close to the outflow stream. In the eastern part of the peatland, between the two inflow streams, there are some short hummocks with *Calluna vulgaris* and *Sphagnum* section *acutifolia*. At this part of the peatland, there is no influence from the incoming streams.

3.1.1.2 Instrumentation

Since the summer of 2011 at the centre of the peatland a four-meter tower was operational. On this tower multiple meteorological sensors were installed. A shielded probe (Rotronic M103A, Bassersdorf, Germany) measured air temperature and relative humidity at 2 metre height. The incoming and outgoing, shortwave and far-infrared radiation were measured by a CNR1 (Kipp & Zonen, Delft, the Netherland). The incoming Photosynthetically Active Radiation (PAR) was measured by a LICOR 190SZ sensor (Licor, Lincoln, NE, USA). All these radiometers were positioned on a horizontal side arm of the tower at a height of 3.5 metre above the soil surface.

On the first of July in 2012 an STP01 sensor (Hukseflux Thermal Sensors B.V, Delft, the Netherlands) was installed, which measures the soil temperature along a profile at 2, 5, 10, 20 and 50 cm depth below the surface. Soil temperature was also measured with four T107 temperature probes at 2 and 5 cm depth (Campbell Scientific, Logan, UT, USA), under a tussock of *M. caerulea* and under a *C. vulgaris* shrub. In the same locations as the T107, two volumetric water content probes (CS616, Campbell Scientific, Logan, UT, USA) were also buried at a depth of 5 cm.

Until the 16th of December 2013, the precipitation data from a meteorological station, located 400 meters away, was used (Meteo Trentino, station name: Giardino Botanico (46º01'18 N, 11º02'23 E)). Later it was measured on site with a heated tipping bucket rain gauge (model 52202 from Young, Traverse City, MI, USA). The snow height and the fresh snow density were measured at another Meteo Trentino weather station (Monte Bondone – Viote 46º00'49 N, 11º03'17 E) on the same plateau as the peatland.

All meteorological data was collected once a minute on a data logger (CR3000, Campbell Scientific, Logan, UT, USA) with a multiplexer (AM16/32, Campbell Scientific, Logan, UT, USA) and averaged or summed to half-hourly values.

The water table depth of the peatland was measured at 4 positions in the peatland, two at each inlet of water, one at the outflow and one at 3 metres distance from the tower with a pressure transducer (Dipper-PT, SEBA Hydrometrie GmbH & Co., Germany). The pressure transducer was installed inside a perforated pipe on the 14th of May 2014. The water level was measured every half-hour. The data of the pressure transducer was collected on an internal Flash memory card and downloaded at regular intervals.

Besides the meteorological sensors, the tower was equipped with an eddy covariance system mounted at 1.6 m above the soil surface. The system, consisting of a LI7500 open path CO_2/H_2O gas analyser, a LI7200 enclosed path CO_2/H_2O gas analyser (both from Licor, Lincoln, NE, USA) and a R3-100 3D sonic anemometer (Gill instruments, Lymington, Hampshire, UK), all operating at 20 Hz. In December 2013, a LI7700 open path CO_2 analyser (Licor, Lincoln, NE, USA) was also installed at the same height. For more information about the used instruments, see chapter 4.3.

3.1.1.3 Water samples

Water samples were taken to analyse the Dissolved Organic Carbon (DOC) and Total Dissolved Nitrogen (TDN) of the water, DOC can play a big role in the carbon footprint of ecosystem (Strack et al. 2008, Gielen et al. 2011). The water samples were taken from the autumn of 2014 to the early summer of 2015 (Table 3-1) at three locations (Figure 3-2).

Table 3-1 Date the water samples were taken. On each day at the three locations the water was collected.

02-09-2014	15-01-2015
11-09-2014	02-02-2015
02-10-2014	18-03-2015
29-10-2014	09-04-2015
18-12-2014	29-04-2015

At each date samples were taken at the two inflows of the peatland and at the outflow, in this way the net DOC and TDN loss could be qualified. The samples were collected in plastic bottles (Figure 3-3) and transported to the laboratory. At the laboratory each sample was filtered with a Millipore System, using Isopore™ Membrane filters 0.4 µm (Merck Millipore, Billerica, MA, USA), to make sure that no plant material or debris was in the sample. The filtered samples were then frozen at -20 ˚C, and later shipped to the department of agricultural sciences of the University of Bologna for further analysis.

At the University of Bologna the samples were melted and well mixed. From each sample a 2 ml aliquot was taken, where 30µl of 2M HCl was added. To eliminate inorganic C the samples were sparged for 3 minutes. After this step 50 µl of each sample was inserted in a TOC-V-RMN1 Shimadzu analyser and combusted at a temperature of 720°C. At least three measurements of organic carbon and total nitrogen (mineral and organic dissolved N) are performed of the same sample (a minimum of three to a maximum of five in order to have the lowest coefficient of variation among three measurements).

The concentration of C and N (mg L^{-1}) are calculated against the two calibration curves (0-10 mg L^{-1} of C or N). The calibration curves are regenerated every time the furnace is renewed, however, in every sequence of samples at least three standards are analysed with the same condition of the samples.

Figure 3-3 Bottles used to collect the water at the peatland site

The TDN in all streams was low; in stream 3 the TDN was lower than stream 2 (Figure 3-4). The average amount of TDN over this 9-month period is 0.19 mg/L, 0.34 mg/L and 0.26 mg/L for stream 1, 2 and 3 respectively. There was no significant difference ($p>0.5$) between the nitrogen going in and out the peatland. Compared to the DOC the nitrogen did not show seasonal dynamics around the time of snow arrival and snowmelt, the Total Dissolved Nitrogen was fairly constant over the measured period (Figure 3-4).

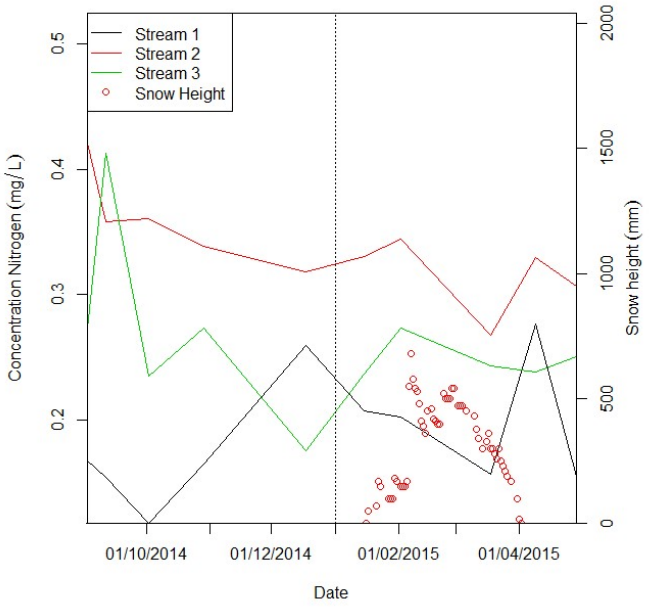

Figure 3-4 Total Dissolved Nitrogen in water sampled during 2014 and 2015 at two inflows/seepage (stream 1 and 2) and one outflow (stream 3). The snow height in mm is plotted with red dots.

3.1.1.4 Soil samples

Soil samples were collected on 3-4 July 2014 under all nine main vegetation types occurring in the fen (Figure 3-5). At each point, three soil samples replicates located at 1 m distance were collected at different depths (0-5, 50-55 and 100-105 cm). The shallow samples at 0-5 cm were taken with Eijkelkamp soil core sampler rings (diameter 5 cm, height 5 cm, volume 98 cm3), while at the depths of 50-55 and 100-105 cm the samples were collected with an Eijkelkamp split tube sampler (Eijkelkamp, Giesbeek, the Netherlands, same dimensions as the soil core sampler rings). No samples were taken in plant tussocks. For an elaborate explanation of the methods used to measure the Carbon/Nitrogen ratio and the Bulk density, see chapter 5.3.3.

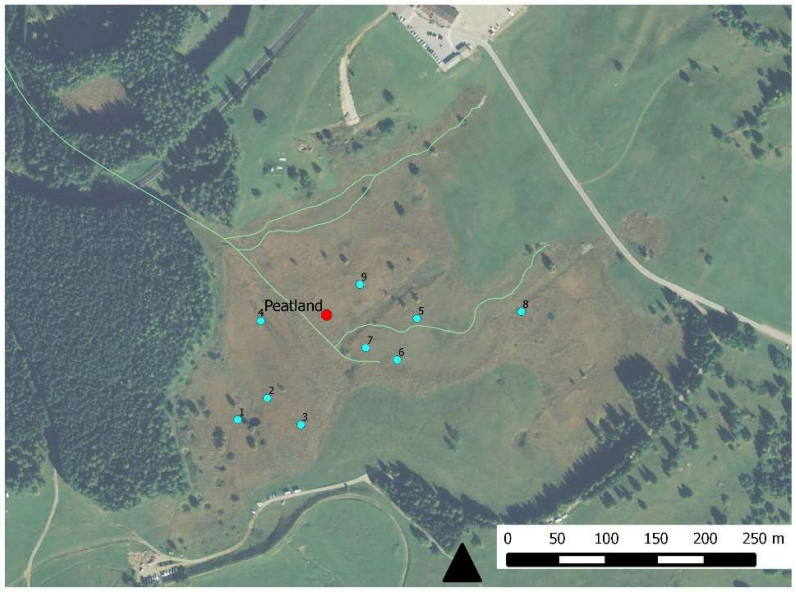

Figure 3-5 Overview of peatland with in the location of the eddy covariance tower (red), the stream (turquoise) and sampling points of the bulk density and carbon nitrogen ratio (light blue).

For hydraulic modelling hydraulic conductivity of the soil is a very important parameter. Hydraulic conductivity is a measure of how fast the water flows through a certain length of soil. In literature different methods are used to measure the hydraulic conductivity, such as the standing pipe technique (Hvorslev 1951) and Modified Cube Method (MCM, Beckwith et al. 2003). An advantage of the MCM over the standing pipe technique is that with MCM both the horizontal and the vertical hydraulic conductivity can be measured. Therefore in this study a modified method is used after Lewis et al. (2012), where the samples were covered with paraffin instead of gypsum. In August 2014 in total 5 plots were sampled, based on the biggest ranges of bulk density (Assouline 2006), and at each plot two samples were taken (0-10 and 40-50 cm depth). To reduce the damage to the peatland a square metal tube (12x12 cm) with a cutting edge was drive into the peatland to a depth of 70 cm. The tube was pulled out and due to the saturation of the peat the sample stayed in the sampler during the

retrieval. After retrieval of the column, samples at the mentioned depths were cut with a blunt knife. The samples were stored in a plastic bag and a container before being transported to the laboratory. Immediately after returning to the laboratory the cubes were cut to the correct size (10 by 10 by 10 cm) and sealed with molten paraffin (see Figure 3-6). To assure a good seal, the cubes were dipped into paraffin until the thickness of the paraffin was around 1 cm. The hydraulic conductivity was measured in the same way as is written in Lewis et al. (2012), but with a constant pressure head of 7 cm. The saturated hydraulic conductivity was calculated by using Darcy's law:

$$K_{sat} = \frac{Q * L}{A * \Delta h}$$

in which, K_{sat} is the saturated hydraulic conductivity (m s^{-1}), Q is the discharge (m^3 s^{-1}), L is the length of the sample (m), A is the area of one open side of the cube (m^2), and Δh is the difference in head between the top and bottom of the sample (m).

*Figure 3-6 Two cubes of paraffin covered peat blocks of 10*10*10 cm used for the measurement of hydraulic conductivity.*

3.1.2 Glencar

The Glencar site is an Atlantic blanket bog located in the Southwest of Ireland (51°55' N latitude, 9°55' W longitude, 150 m asl) (Sottocornola and Kiely 2010b). Mean annual temperature is 10.5 °C and mean annual precipitation is 2571 mm, where the summers are drier than the winters (McVeigh et al. 2014). The site is divided into four microforms based on their relative elevation: hummocks, high lawns, low lawns, and hollows. The distribution of the microform composition inside the eddy covariance footprint was estimated as 6% hummocks, 62% high lawns, 21% low lawns, and 11% hollows (Laine et al. 2006). Vascular plants cover about 30% of the bog surface, with the most common species being *Molinia caerulea*, *Calluna vulgaris*, *Erica tetralix*, *Narthecium ossifragum*, *Rhynchospora alba*, *Eriophorum angustifolium*, *Schoenus nigricans*, and *Menyanthes trifoliata*. The bryophyte component is not widespread, about 25% of the bog surface, and the principal species include a brown moss, *Racomitrium lanuginosum*, and *Sphagnum* mosses, covering about 10% each, so that large areas of the peatland are covered by bare soil (Sottocornola et al. 2009, McVeigh et al. 2014). At the Glencar site, an eddy covariance tower has been operational since 2003. For more information about the Glencar wetland, see McVeigh et al. (2014). In chapter 7 the monthly meteorological and eddy covariance data from the site from 2003-2012 is used, and meteorological data from a nearby meteorological station at Valentia (30 km west of the site, Met Éireann) from 1939 - 2003 is used.

3.1.3 Mer Bleue

The Mer Bleue peatland is a 2,800 ha ombrotrophic raised bog located in the Ottawa River Valley, 10 km east of Ottawa, Ontario, Canada (45.40° N longitude, 75.50° W latitude, 69 m asl). Mean annual temperature is 6.3 °C and ranges from –10.5 °C in January to 21.0 °C in July. Mean annual precipitation is 943 mm, 268 mm of which falls during the summer months (Bubier et al. 2006). During winter the snow cover

usually lasts from December to March with a maximum height of 0.6 and 0.8 m (Lafleur et al. 2003).

The dominant vegetation of Mer Bleue are mosses, *Sphagnum angustifolium*, *S. rubellum*, *S. magellanicum*, sedges, *Eriophorum vaginatum*, and shrubs, *Chamaedaphne calyculata*, *Ledum groenlandicum*, *Kalmia angustifolia*, and *Vaccinium myrtillodes*. On the site is a small fraction of trees (*Larix laricina*, *Betula papyrifera*, and *Picea glauca*) (Lafleur et al. 2001, Letts et al. 2005). At the Mer Bleue site, an eddy covariance tower has been operational since 1999. For more information about Mer Bleue, see Roulet et al. (2007). In chapter 7 the monthly meteorological and eddy covariance data from the site from 1999-2013 is used, and meteorological data from a nearby meteorological station at Ottawa International Airport (15 km south-west of the site, Environmental Canada) from 1939 - 1999 is used.

3.2 Pre-processing meteorological data

In case of missing meteorological data at the Monte Bondone peatland site (26% of the total, due to malfunctioning of the sensors or power shortage), the data were replaced by data from a nearby (500 meters horizontal distance) meteorological and eddy covariance tower located in a nutrient poor grassland (Marcolla et al. 2011, Sakowska et al. 2014). Because the towers are close to each other, no significant differences in temperature, PAR and relative humidity were found. Since the grassland tower is located on a different slope the precipitation data of the grassland was not used. For soil temperature a difference was expected between the grassland and the peatland, but there was a highly significant correlation between the half-hourly values from the two sites for all depths ($R^2 > 0.95$). If data were missing from the grassland site too (0.9 %), they were replaced by data from the two close Meteo Trentino meteorological stations (Giardino Botanico and Viote). The Giardino Botanico station

is located on the same slope as the eddy covariance tower and therefore the precipitation data of the Giardino Botanico station was used to fill the gaps. Soil temperature was not measured at these stations, but since no gap exceed 5 hours, gaps in the peatland time series were filled with linear interpolation.

The monthly data from Glencar (2003-2013) and from Mer Bleue (1999-2013) are downloaded from FLUXNET and are already gap filled and the NEE is partitioned into GPP and R_{eco}, this data is used for the model exercise with NUCOMBog (chapter 3.4.2 and chapter 7).

3.3 Eddy covariance

All Eddy covariance data collected were analysed using the EddyPro Software (version 5.1.1, LICOR, Lincoln, NE, USA). In this software, many filters are available and this program provides an easy interface for the user to implement specific filters. In this section only the filters used in this work are presented, for more details about the filters and the software please refer to the manual of EddyPro, which is available on the website of LICOR (www.licor.com). As already presented, it is possible that the fluxes or the measurements are affected by disturbances, to make sure that the used data is as clean as possible the following filters and corrections are applied.

Since for the eddy covariance a R3-100 3D sonic anemometer (Gill instruments, Lymington, Hampshire, UK) is used, a correction of the angle of attack for wind components has to be applied. Nakai and Shimoyama (2012) have shown that, after testing in a wind tunnel and on a meadow, the ultrasonic anemometers of Gill introduces errors depending on the angle of attack. This error affects “the heat, water vapor, and carbon fluxes, not only over forests and agricultural fields but also over smooth surfaces such as grasslands, wetlands, and tundra bogs” (Nakai and Shimoyama 2012).

For the open path InfraRed Gas Analyser (LI7500, LICOR) another correction has to be applied. After extensive testing a heating effect of the surface of this instrument was found, due to the electronics and the solar radiation loading (Burba et al. 2008). In particular in cold conditions, this heating changes the density fluctuations of the greenhouse gasses, which indicate an uptake of CO_2 during off-season periods. The Webb-Pearman-Leuning correction, WPL, is a technique to compensate for this heating effects (Webb et al. 1980).

Other options set for the calculation of the fluxes were the flagging policy and how the footprint of the flux tower was estimated. During this thesis the 0-1-2-system was used to indicate the quality of the fluxes (Foken et al. 2004), where "0" means high quality fluxes, "1" means fluxes are suitable for carbon budget analysis and "2" means fluxes that should be discarded.

The footprint prediction described by Kljun et al. (2004) was used, this method accounts for the roughness length of the vegetation and provides a fast and precise algebraic footprint estimation.

The processed fluxes were consecutive were coded missing when:

1) their quality flag was 2, which indicate "fluxes that should be discarded";
2) the friction velocity, u*, was lower than 0.2 m s^{-1} during night-time (Papale et al. 2006). The data was considered night-time when the Photosynthetic Active Radiation (PAR) was below 20 µmol m^{-2} s^{-1}. At night-time, with a low friction velocity the atmosphere is becoming too stable to measure eddies, the air is therefore not well mixed and stratification might occur;

3) the CO_2 mixing ratio of the air was smaller than 250 or bigger than 500 µmol mol^{-1};
4) the CO_2 fluxes were above or below seasonal thresholds (see chapter 4.8);
5) less than 70 % of the fluxes originated from inside the peatland.

Due to malfunctioning of the system and the subsequent filtering of the data, gaps occur in the data. To get an annual balance these gaps need to be filled. In this study the gaps are filed by using the online Reichstein tool (Reichstein et al. 2005; URL: http://www.bgc-jena.mpg.de/bgi/index.php/Services/REddyProcWeb). In this technique, missing values are replaced by the average value under similar meteorological condition. The window in which the method is looking for similar conditions is 7 days, if there are no similar conditions found the method increased the window with steps of 7 days. As a temperature input, soil temperature was used, since the snow cover in winter isolates the soil and as a subsequence, the soil does not freeze. This results in the continuation of biological processes going on in the soil.

3.4 Models

3.4.1 GEOtop

GEOtop is a process-based distributed model of the water and energy budget (Rigon et al. 2006). It requires a digital elevation model (DEM) to detail the topography, soil type, vegetation and river networks, also meteorological data is needed to calculate the water and energy balance of the given catchment. The model needed the following meteorological input: precipitation, air temperature, wind speed, wind direction, incoming short- and longwave radiation, which were all measured at the eddy covariance tower in the peatland (Pullens et al. 2016b). GEOtop incorporates precipitation and evapotranspiration to calculate storage, runoff and seepage. To

model the horizontal and vertical movement of the water in the soil a fully three-dimensional description of the Richards' equation is used (Endrizzi et al. 2014). For this model exercise the authors used GEOtop version 2, which also models freezing soils (Dall'Amico et al. 2011) and a multi-layered snow cover (Endrizzi et al. 2014), which is desirable for the site since it receives snow every winter. The GEOtop model is used in chapter 5, where more details about the model are provided.

3.4.2 NUCOM-Bog

In this thesis we will use the R package entitled NUCOMBog (Pullens et al. 2016a), which incorporates the NUCOM-Bog (NUtrient cycling and COmpetition Model (Heijmans et al. 2008)). The NUCOM-Bog model is derived from earlier NUCOM models (Berendse 1988, van Oene et al. 1999), the model simulates vegetation and carbon dynamics in peat bogs on a monthly time step. In the model, five plant functional types (PFTs) are represented: graminoids, shrubs, hummock, lawn and hollow mosses, where all PFTs compete for light and nitrogen (Figure 3-7).

As an input the model needs monthly precipitation, air temperature and potential evapotranspiration (Penman 1948), as well as annual ambient CO_2 concentration and nitrogen deposition. The model returns the monthly composition of the vegetation, the net ecosystem exchange, gross ecosystem production and heterotrophic respiration; also the water table depth is returned every month. The model is described in more details in Chapter 6 and 7.

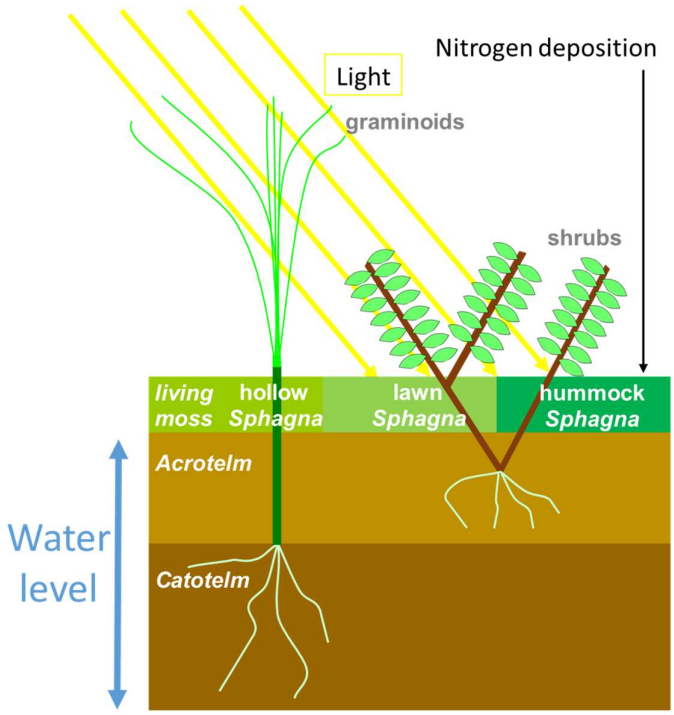

Figure 3-7 Schematic representation of NUCOM-Bog (adapted from Heijmans et al. 2008)

3.5 Calibration of NUCOM-Bog

In total the NUCOM-Bog model has too many parameters to be used in a model calibration exercise (>150 parameters) (Heijmans et al. 2008), therefore first a sensitivity analysis was performed. A sensitivity analysis indicates which parameters are the most sensitive, i.e. the parameters whose variation, even small, cause the bigger changes in the model output. This information is needed to get an idea of which parameters are the most important and allows us to focus the calibration effort on these parameters. The Morris function of the R-package "sensitivity" (Saltelli et al. 2008) which implements the Morris's elementary effects screening method (Morris 1991, Campolongo et al. 2007) is used. The Morris function 'walks' through the complete parameter range for each parameter specified, changing one parameter at a time (OAT-method). This function creates a Latin Hypercube with all the parameter combinations and subsequently starts running the model with all the parameter value sets. From the outputs of the model runs, the sensitivity of the model to different parameters are

derived. The most sensitive parameters will be used in the model calibration, since these parameters are the most important for the model outcome.

The aim of the calibration is to find the parameter distribution with the lowest mismatch with the data, therefore a Bayesian algorithm will be used, in this case, the DE-zs algorithm is used (Ter Braak and Vrugt 2008). DE-zs stands for Differential Evolution Markov Chain with a snooker updater, the algorithm starts with a set of parameters taken from the prior distribution. The prior distribution should not be taken too wide, since it might not have biological meaning and might not result in convergence of parameters (Gelman and Rubin 1992). From this initial set randomly sets are taken and these are the starting point of the Bayesian calibration. This method searches for the parameter distribution of all parameters, which returns the highest negative log likelihood:

$$\mathcal{L}(\theta|D) \propto p(D|\theta)$$

in which $\mathcal{L}$ is the likelihood of a set of parameters (θ), given outcome (D) is equal to the probability (p) of the observed outcome (D) given the parameter values (θ).

The DREAM algorithm runs a set number of parallel chains and during the run shares information among the parallel chains so that the proposal densities of randomised jumps are adjusted, resulting in accelerated movement of the MCMC chains towards an equilibrium (Vrugt et al. 2009). This equilibrium has the smallest log likelihood and hence the smallest error between the model and the data.

The DREAM algorithm is implemented in the R package “Bayesian Tools”, which is available on CRAN (Hartig et al. 2017).

4 Carbon fluxes of an alpine peatland in Northern Italy

J.W.M. Pullens[1,3], M. Sottocornola[2], G. Kiely[3], P. Toscano[4], D. Gianelle[1,5]

[1] Sustainable Agro-Ecosystems and Bioresources Department, Research and Innovation Centre – Fondazione Edmund Mach, San Michele all'Adige (TN), Italy

[2] Department of Science, Waterford Institute of Technology, Waterford, Ireland

[3] Hydromet, Department of Civil and Environmental Engineering and Environmental Research Institute, University College Cork, Cork, Ireland

[4] National Research Council–Institute for Biometeorology (CNR–IBIMET), Florence, Italy

[5] Foxlab Joint CNR-FEM Initiative, San Michele all'Adige (TN), Italy

Published in Agricultural and Forest Meteorology (2016) 220, 69-82, doi: 10.101/j.agrformet.2016.01.012

Keywords: Alpine peatland, carbon dioxide, methane, eddy covariance, minerotrophic fen, water table depth

4.1 Abstract

It is widely known that peatlands are a significant carbon (C) stock. Most peatlands are located in boreal and subarctic regions of the northern hemisphere but some occur also at high altitude and, contrary to the first; their contribution in terms of carbon sequestration is far less studied. In the Alps, there are numerous small peatlands, which are threatened by increasing temperatures and an alteration of their water balance. The aim of this study was to investigate the carbon fluxes of a small-scale fen in the Alps over three years (2012-2014).

During the study period, the peatland experienced a high interannual variation in weather conditions while it acted as a carbon source based on CO_2 emissions (NEE: 180.7 ± 65.2 g C – CO_2 m^{-2} yr^{-1}) for all three years. This was mainly due to the short net C uptake period (73 ± 7 days) and high respiration. Ecosystem respiration and summer gross primary production were both very high compared to other peatlands around the world and compared to a nearby low productive grassland. In wintertime, the soil did not freeze, resulting in a slow decomposition of the organic matter. Low methane fluxes were recorded during a 10-month measurement campaign, for a total of 3.2 g C – CH_4 m^{-2} over the December 2013-September 2014 period. Our findings suggest that the interannual variability of temperature and soil water content exert a strong influence on the carbon balance of peatlands of the Alps and that could further worsen depending upon the magnitude of climate change.

4.2 Introduction

Peatlands contain the largest terrestrial soil carbon (C) pool in the world (Gorham 1991). Northern peatlands store an estimated 547 (473-621) PgC (Yu et al. 2010), which is around 20 % of the total amount of global soil organic carbon (IPCC 2007), despite covering only about 3% of the land surface. Peatlands occur globally; however

the biggest and most studied areas are located in the northern hemisphere (Parish et al. 2008, Yu et al. 2010, Schuur et al. 2015). Most of researched peatlands are in high latitude regions and these peatlands are studied for the vulnerability of their carbon storage, the effects of climate change and permafrost degradation (Frolking et al. 2001, Camill 2005, Dorrepaal et al. 2009). Peatlands have been accumulating carbon for thousands of years. The decomposition of plant material is very slow due to the waterlogged soils and high recalcitrance of present *Sphagnum* mosses. The carbon can be released as the greenhouse gasses carbon dioxide (CO_2), methane (CH_4), or as Dissolved Organic Carbon (DOC) in waterbodies. Methane is only produced under anaerobic conditions (Wang et al. 2013). The emission of CO_2 in peatlands is has been linked to the presence of plants with aerenchyma, a tissue that can conduct methane from the soil to the atmosphere (Van Den Pol-Van Dasselaar et al. 1999, Carmichael et al. 2014). Aerenchyma tissue can be found mainly in sedges, so a high sedge abundance could potentially be an indicator of high methane emission (Smith 1970, Gebauer et al. 1995). It is estimated that peatlands contribute to around 33% of the annual global methane efflux (ca 645 Tg CO_2 $year^{-1}$, (Carmichael et al. 2014)).

Due to climate change, pristine peatlands can be potential carbon sources (Drösler et al. 2008, Dorrepaal et al. 2009, Bond-Lamberty and Thomson 2010, Frolking et al. 2011, Lawrence et al. 2013). The general global response of peatlands to climate change is hard to predict due to the uneven distribution of peatlands over the world, in addition to this only the most accessible peatlands are studied (Frolking et al. 2011).Warmer temperatures could lead to an increase in plant growth (net primary production, NPP) and an increase in ecosystem respiration (R_{eco}) (Beer and Blodau 2007, Smith and Fang 2010, Gong et al. 2013). The different magnitudes of these two contrasting fluxes could change peatlands from a carbon sink to a carbon source (Dorrepaal et al. 2009, Bond-Lamberty and Thomson 2010, Lawrence et al. 2013). A

difference in annual precipitation could result in a drop in the water table depth which will trigger faster decomposition of stored carbon, since more peat can be decomposed under aerobic conditions and simultaneously a reduction in CO_2 emissions (Jungkunst et al. 2008, Couwenberg et al. 2010, Mitsch et al. 2013, Andersen et al. 2013, Gong et al. 2013). On the contrary a rise in water table depth can reduce the decomposition (Murphy et al. 2009), increase the NPP (Sonnentag et al. 2010), with a positive effect on carbon accumulation, but with a negative effect in terms of increased CO_2 emissions (Lawrence et al. 2013, Petrescu et al. 2015, Vanselow-Algan et al. 2015).

To measure the net ecosystem CO_2 exchange (NEE) at an ecosystem level, the eddy covariance (EC) micrometeorological technique is typically used. This technique allows to measure turbulent fluxes, which are exchanged between vegetation canopy and the atmosphere (Baldocchi 2003). The advantage of this method is that it continuously measures the fluxes over a long period of time (years or even decades) and in a non-destructive way. In this way, the dynamics of ecosystems can be investigated and followed over time. NEE can then be partitioned to calculate the gross primary production (GPP) and ecosystem respiration (R_{eco}).

As highlighted by Drösler et al. (2008) measurements need to be done at different peatland ecosystems, to reach a better understanding of, and to upscale the greenhouse gas balance of peatlands regionally and/or globally. The difficulty with upscaling is that peatlands occur in different types: e.g. fen, aapa mire, blanket bog and raised bog, which are reliant on different water and nutrient sources, ombrotrophic (rainwater fed) vs minerotrophic (groundwater fed) (Wheeler and Proctor 2000). The differences in water sources, the dissolved minerals and nutrients can lead to different plant communities and therefore a different greenhouse gas balance. Measurements on pristine peatlands indicate that these untouched peatlands are mainly acting as a CO_2

sink (34.9 to 329 g C-CO_2 m^{-2} yr^{-1}) and as a methane source (3.2 to 32 g C-CO_2 m^{-2} yr^{-1}) (Roulet et al. 2007, Nilsson et al. 2008, Aurela et al. 2009, Lund et al. 2009, 2010, Bäckstrand et al. 2010, Sottocornola and Kiely 2010a, Sonnentag et al. 2010, Koehler et al. 2011, Beetz et al. 2013, Wu et al. 2013, McVeigh et al. 2014, Petrescu et al. 2015). On the contrary drained and managed wetlands often act as a CO_2 source (Hatala et al. 2012, Beyer and Höper 2015). Many factors are influencing the carbon balance, such as: vegetation, hydrology, ground water level (Murphy et al. 2009), human disturbance (Hendriks et al. 2007) and climatic variability (McVeigh et al. 2014). Peatlands with a high cover of bryophytes and a low cover of vascular plants, show lower GPP than peatlands with a high vascular plant cover (Beetz et al. 2013). Since peatlands are rather widespread, the climatic conditions are very important. A comparison of different peatlands can provide more information why some peatlands are bigger carbon sources than others (Drösler et al. 2008).

In the Alpine area, numerous small peatland fens are present. In the Alps the climatic conditions for these fens to develop into raised bogs are rare. This results in an infilling of non-peatland plant species (trees and grasses) into the peatland. The peatland fens in the Alps are being threatened by rising temperatures and changes in their precipitation regime (Beniston et al. 1997, IPCC 2007, 2013, Im et al. 2010, Eccel et al. 2012, Steger et al. 2013, Pepin et al. 2015). The predicted changes in precipitation can be opposite of sign and different in magnitude. Alpine fens are already experiencing modifications due to climate change with an acceleration of the infilling with trees (Stine et al. 2011). This is leading to the invasion of non-peatland plants typical of drier ecosystems that are turning the peatlands into grasslands and forests, with a consequent loss of both their stored soil carbon and their biodiversity (Stine et al. 2011). Tree encroachment for example is more persistent with global warming than it is with summer drought, while a combination of the two results in tree-dominated

peatlands (Heijmans et al. 2013, Holmgren et al. 2015). Despite the risks and the regular occurrence of peatlands in the Alps, their carbon and water cycle has been poorly studied because peatlands represent a small part of the dominant ecosystems in the Alps (Parish et al. 2008). To our knowledge the only research on Alpine peatlands focused on their restoration and management (van der Knaap et al. 2011, Ammann et al. 2013) while no attempt was taken to measure the carbon fluxes with an eddy covariance system.

The objectives of this paper are (i) to investigate three years of carbon and methane fluxes of a peatland in the Italian Alps, (ii) to study the inter annual variability of the carbon fluxes and (iii) to compare the fluxes of this alpine peatland with other peatlands.

We hypothesize that the peatland will be a small carbon sink, since the vegetation of the peatland grows very fast during the growing season. We assume that the carbon taken up during this period is more than the carbon released over the rest of the year, particularly when the peatland is covered with snow and all biological processes are slowed down or stopped. We also think that the peatland will have high methane fluxes, since the peatland has a high coverage of sedges.

4.3 Materials and Methods

4.3.1 Site

The study site is a 10 hectares minerotrophic relatively nutrient poor fen located at 1563 m a.s.l. on the Monte Bondone plateau (Figure 4.1), near Trento, in the Italian Alps (latitude 46º01'03 N, longitude 11º02'27 E). The peatland is placed in a relict glacial lakebed, that was formed during the last ice age (Cescatti et al. 1999), in a saddle shaped valley with a mountain top on the eastside (Palon, 2090 m a.s.l., Figure 4.1a). The runoff of the complete watershed flows on deep impermeable morainic

strata, which result into seepage into the fen (Cescatti et al. 1999). This seepage enters the peatland through two inflow streams; from the fen the water discharges in a stream (Figure 4.1). The average annual precipitation during 1958-2008 was 1290 mm $year^{-1}$ with an average air temperature of 5.4 °C (Eccel et al. 2012). The snow-free period typically lasts from early May to late October-beginning November.

The vegetation of the area is very heterogeneous: the areas closest to the tower are mainly dominated by *Molinia caerulea* forming big tussocks, while in the depressions the main vegetation consists of *Carex rostrata*, *Valeriana dioica, Scorpidium cossonii* and scattered *Sphagnum* spp. The southwestern area of the peatland is dominated by *Eriophorum vaginatum*, with high tussocks of *Carex nigra* covering the lower areas. *Sphagnum* spp. as well as *Trichophorum alpinum* and *Drosera rotundifolia* occur close to the outflow stream. In the eastern part of the peatland, between the two inflow streams, there are some short hummocks with *Calluna vulgaris* and *Sphagnum* section *acutifolia*. At this part of the peatland, there is no influence from the incoming streams.

In 1914, 0.35 hectares of the peatland was harvested for burning by removing the peat top layer (Cescatti et al. 1999), this is still visible today (Figure 4.1b). This area is mainly covered by *Campylium stellatum*, *Scorpidium cossonii* and *Carex rostrata* today. The depth of the peat ranges from 0.82 m at the border (Cescatti et al. 1999, Zanella et al. 2001) to 4.3 m in the centre (Dalla Fior 1969).

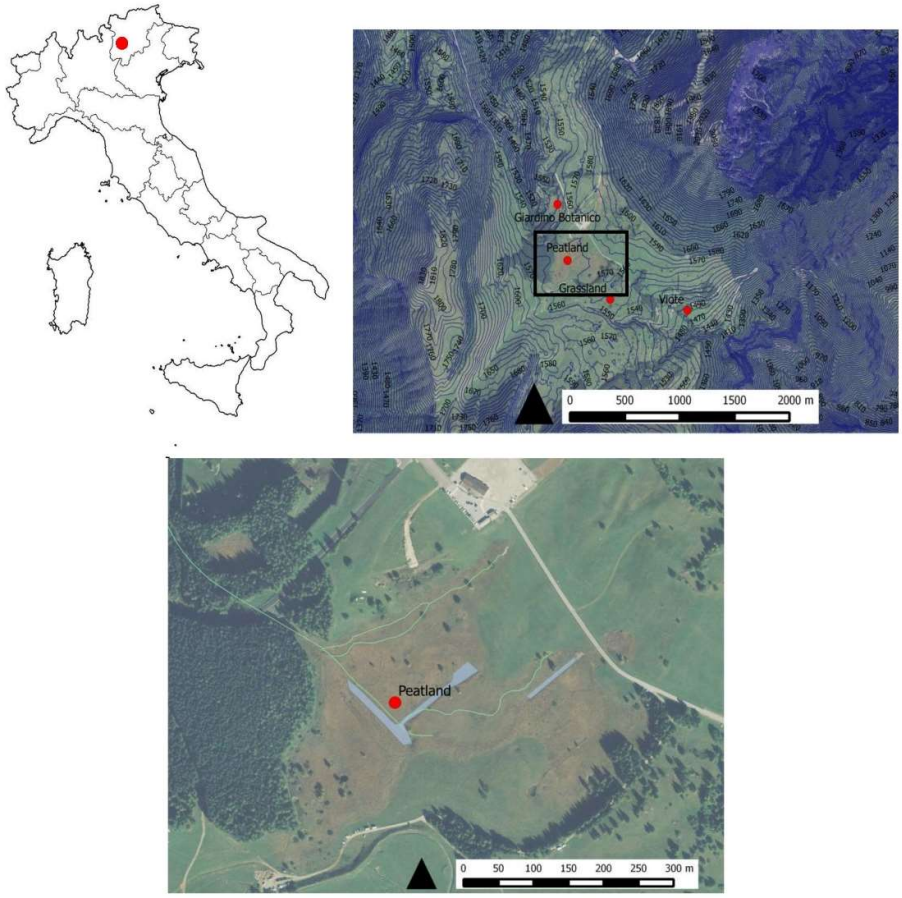

Figure 4-1 Top left) The location of the Peatland in respect to the topography of Italy, top right) An overview of Monte Bondone site. The names refer to the sites of which data has been used. Giardino Botanico and Viote are two meteorological towers of Meteo Trentino. Grassland is an eddy covariance tower located at an alpine grassland (Marcolla et al. 2011, Sakowska et al. 2015); Peatland is the location of the eddy covariance tower at the peatland. The plotted contour lines have an interval of 10 meters. Bottom) aerial view of the peatland site, with in blue the areas where peat extraction has taken place in 1914. The highlighted area is 0.35 hectares. the turquoise line is a stream running through the peatland.

4.3.2 Meteorological data

A four-meter tower was installed in the summer of 2011 at the centre of the peatland. The tower was equipped with multiple meteorological sensors. A shielded probe (Rotronic M103A, Bassersdorf, Germany) measured air temperature and relative humidity at 2 metre height. The incoming and outgoing, shortwave and far-infrared radiation were measured by a CNR1 (Kipp & Zonen, Delft, the Netherland), while the incoming Photosynthetically Active Radiation (PAR) was measured by a LICOR 190SZ sensor (Licor, Lincoln, NE, USA). All radiometers were positioned on a horizontal side arm of the tower at a height of 3.5 metre above the soil surface.

The soil temperature was measured along a profile at 2, 5, 10, 20 and 50 cm depth below the surface with a STP01 sensor (Hukseflux Thermal Sensors B.V, Delft, the Netherlands) from the 1st of July 2012. Soil temperature was also measured with four T107 temperature probes at 2 and 5 cm depth (Campbell Scientific, Logan, UT, USA), under a tussock of *M. caerulea* and under a *C. vulgaris* shrub. In the same locations as the T107, two volumetric water content probes (CS616, Campbell Scientific, Logan, UT, USA) were also buried at a depth of 5 cm.

A heated tipping bucket rain gauge (model 52202 from Young, Traverse City, MI, USA) measured precipitation. This instrument was installed on the 16th of December 2013. Before then, the data from a meteorological station, located 400 meters away, was used (Meteo Trentino, station name: Giardino Botanico (46º01'18 N, 11º02'23 E)). The snow height and density were measured at another Meteo Trentino weather station (Monte Bondone – Viote 46º00'49 N, 11º03'17 E) on the same plateau as the peatland.

All meteorological data was collected once a minute on a data logger (CR3000, Campbell Scientific, Logan, UT, USA) with a multiplexer (AM16/32, Campbell Scientific, Logan, UT, USA) and averaged or summed to half-hourly values. Missing meteorological data (26% of the total, due to malfunctioning of the sensors or power shortage) were replaced by data from a nearby (500 meters horizontal distance) meteorological and eddy covariance tower located in a nutrient poor grassland (Marcolla et al. 2011, Sakowska et al. 2014). Since the towers were very close to each other, no significant differences in temperature, PAR and relative humidity were found (data not shown). Since the grassland tower is located on a different slope the precipitation data of the grassland was not used. For soil temperature a difference was expected between the grassland and the peatland, but there was a highly significant

correlation between the half-hourly values from the two sites for all depths ($R^2 > 0.95$). If data were missing from the grassland site too (0.9 %), they were replaced by data from the two close Meteo Trentino meteorological stations (Giardino Botanico and Viote, Figure 4.1a). The Giardino Botanico station is located on the same slope as the eddy covariance tower and therefore the precipitation data of the Giardino Botanico station was used to fill the gaps in the precipitation data. Soil temperature was not measured at these stations, but since no gap exceed 5 hours, gaps in the peatland timeseries were filled with linear interpolation.

The water table depth of the peatland was measured at 3 metres distance from the tower with a pressure transducer (Dipper-PT, SEBA Hydrometrie GmbH & Co., Germany). The pressure transducer was installed inside a perforated pipe on the 14th of May 2014. The water level was measured every half-hour. The data of the pressure transducer was collected on an internal Flash memory card and downloaded at regular intervals.

4.3.3 Carbon and methane fluxes measurements

Besides the meteorological sensors, the tower was equipped with an eddy covariance system mounted at 1.6 m above the soil surface. The system, consisting of a LI7500 open path CO_2/H_2O gas analyser, a LI7200 enclosed path CO_2/H_2O gas analyser (both from Licor, Lincoln, NE, USA) and a R3-100 3D sonic anemometer (Gill instruments, Lymington, Hampshire, UK), all operating at 20 Hz. In December 2013, a LI7700 open path CH_4 analyser (Licor, Lincoln, NE, USA) was also installed at the same height. The data from both the LI7200 and LI7700 was collected and stored in an Analyser Interface Unit (LI7550); the data from the LI7500 was collected by Scanemone software (University of Tuscia, Italy) and stored on an industrial PC. Because both the LI7500 and the LI7200 were simultaneously operational, the signal

from the anemometer was split into a digital and an analogue signal: the digital signal was collected by the LI7550, where the data was combined with the data from the LI7200 and LI7700. The analogue signal was transferred to an indoor PCI unit of Gill, where it was computed with the data from the LI7500.

The intake tube of the enclosed path analyser (LI7200) was 98.7 cm long, with an internal diameter of 9 mm. The flow rate to suck air into the analyser was set to 15 L/min. To prevent condensation, the inlet tube was heated by a spiral resistor wire and insulated. Moreover, the intake tube was slightly tilted down, to avoid water entering the sensor cell. To prevent insects or other debris being drawn into the cell, a fine screen was added at the inlet of the intake tube.

All fluxes were analysed using the EddyPro Software (version 5.1.1, LICOR, Lincoln, NE, USA), applying a 2-D rotation and with the following corrections: 1) angle of attack for wind components for the Gill anemometer (Nakai and Shimoyama 2012); 2) a WPL 'Burba correction' was implemented on the data from the LI7500 to compensate for the density fluctuations of the gases because of the heating effect of this instrument (Burba et al. 2012); 3) the low-pass frequency response correction (Moncrieff et al. 1997).

Consecutive the fluxes were removed when: 1) their quality flag was different from 0 or 1 ("0" means high quality fluxes, "1" means fluxes are suitable for carbon budget analysis) (Moncrieff et al. 2004); 2) u* was lower than 0.2 m s^{-1} during night-time (PAR < 20 µmol m^{-2} s^{-1}) (Papale et al. 2006); 3) the CO_2 mixing ratio was smaller than 250 or bigger than 500 µmol mol^{-1}; 4) the CO_2 fluxes were above or below seasonal thresholds (Supplement Table 4.1); 5) less than 70 % of the fluxes originated from inside the peatland (the footprint was calculated by using the footprint model of Kljun et al. (2004)). After these filters the percentage of data gaps increased from 34% to

65% of gaps for the LI7200 and for the LI7500 from 53% to 74%. The former gap figures were due to system malfunctioning or power outage.

After the filters were applied, the relationship between the CO_2 fluxes computed from the data of the two infrared gas analysers was significant ($p < 0.05$, $R^2 > 0.92$, LI7200 = 0.09 + 0.99*LI7500, n= 7524). During the winter the R^2 value (0.2713) was lower than in the summer (0.8985), but R^2 was significant in all seasons.

Therefore, CO_2 fluxes computed with the LI7200 are presented here and gaps in this time series were filled with data computed from the open path sensor (LI7500). When both time series were missing or removed, (53 % of the data), the CO_2 fluxes were gap filled with the online Reichstein tool (Reichstein et al. 2005; URL: http://www.bgc-jena.mpg.de/bgi/index.php/Services/REddyProcWeb). The same tool was used to partition the measured NEE into GPP and R_{eco}. The environmental factors used for the gap filling were: Global radiation, Soil temperature at 5 cm, relative humidity, Vapor pressure deficit (VPD) and u* (friction velocity). The tool makes a look up table where gaps in the NEE data were filled with NEE with similar climatic conditions. The window in which the method is looking for similar results is 7 days, if there are no similar conditions found the method increased the window with steps of 7 days.

The methane sensor (LI7700) was active at this site from December 2013 until September 2014 and during this period there were minor problems with the data acquisition. Since the sensor has an open path the quality and availability of the data was susceptible to meteorological conditions (in total 66% of data gaps). The data was collected by a LI7550 and analysed with EddyPro. Only the fluxes with a quality flag of 0 and 1 were used (Moncrieff et al. 2004). Nevertheless, the data was very noisy and hard filters were applied: all fluxes outside the range of -0.04 to 0.05 μmol m^2 s^1

were discarded. After the filters, 30% of the data was considered good. The CH_4 fluxes were gap filled using the online Reichstein tool (Reichstein et al. 2005).

Due to the high amount of snow during the winter of 2013-2014 (up to 204 cm), on the 11th of March 2014 the complete LICOR setup was raised 1.5 metre above the snow level (3.1 m above soil surface). During the snowmelt in the early spring (the 29th of April 2014), the LICOR setup was lowered to its original position (1.6 m above soil surface).

An error analysis was performed by estimating uncertainties separately for the different error sources (Aurela et al. 2002). By combining these errors, an uncertainty of 23%, 21% and 30% for 2012, 2013 and 2014 was calculated for the annual balance. These values are in the same range as presented for eddy covariance measurements (Lafleur et al. 2001, Aurela et al. 2002, Richardson et al. 2008, Sottocornola and Kiely 2010a).

All analyses of the data were done with the half-hourly values of the fluxes and meteorological parameters, unless otherwise indicated. The data was analysed by using the R software version 3.2.1 (R Development Core Team. R Foundation for Statistical Computing 2017) with the zoo package (Zeileis and Grothendieck 2005). For the analysis the growing season is defined as the period where the cumulative NEE is declining, indicating an uptake of carbon. The micrometeorological sign convention is used in this paper, e.g. a negative sign means carbon sequestration.

A correlation coefficient analysis was performed to understand the main drivers of the measured carbon fluxes. Apart from the NEE, GPP and R_{eco} daily average values of air temperature, PAR, soil water content (SWC), VPD and daily sum of precipitation were used for this analysis. The Spearman correlations were calculated over three complete years and over each quarter of the years

4.4 Results

4.4.1 Meteorological data

The 2012 and 2014 annual temperatures of 5.1 °C and 5.0 °C, respectively, were close to the long-term average (1985-2008: 5.4 °C (Eccel et al. 2012)), while in 2013 the temperature was lower (4.3 °C). The seasonal temperatures in 2012 were close to the averages apart from higher temperatures in May and lower temperatures in December (Figure 4.2 and 4.3). In 2014 the spring and summer temperatures were colder, while in winter and autumn were warmer than the long-term average. The colder 2013 annual temperature was caused by colder temperatures in all seasons except in autumn, in particular in winter. The precipitation variation in the three years was also very pronounced, with annual values of 1650.4, 1740.6, and 2082.6 mm (for 2012, 2013 and 2014, respectively), all well above the long-term average of 1290 mm per year (Eccel et al. 2012). The first and third quarter of 2014 was wetter than the long-term average (Figure 4.2).

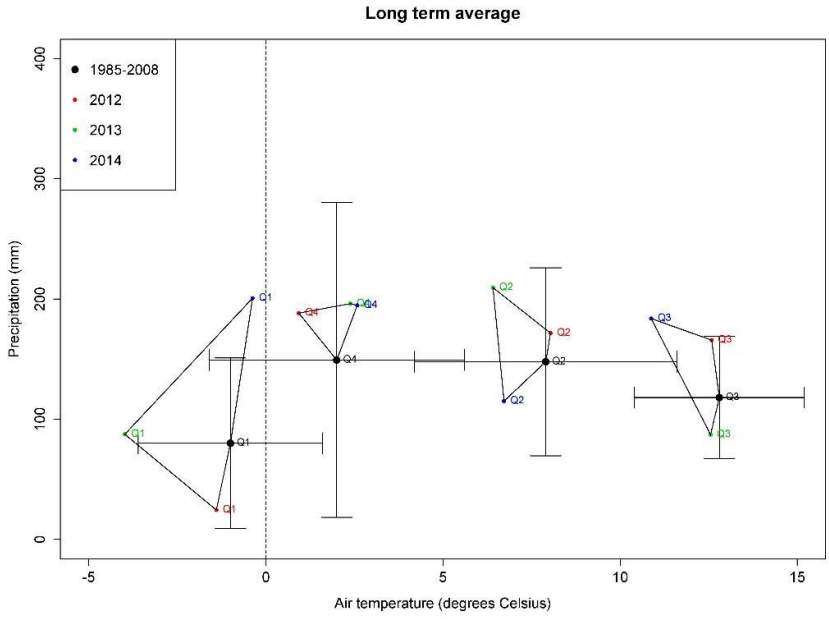

Figure 4-2 Quarterly average air temperature and precipitation for 2012, 2013 and 2014 compared with the long-term average and their variation (1985-2008, (Eccel et al. 2012))

2014 had particularly high precipitation in January and February and in July compared to the other years, while May and September were dryer (Figure 4.3). 2012 had a dry winter with little snowfall compared to the other two years and then regular precipitation throughout the year. 2013 had little precipitation in the winter, but a very wet spring. In July and August 2014, the radiation was consistent with the high amount of precipitation, with lower radiation than the other years (Figure 4.3). The annual daytime average PAR was 318 (2012), 290 (2013) and 287 (2014) µmol m^{-2} s^{-1}, while the average daytime PAR during the growing season was 1006 (2012), 948 (2013) and 942 (2014) µmol m^{-2} s^{-1}.

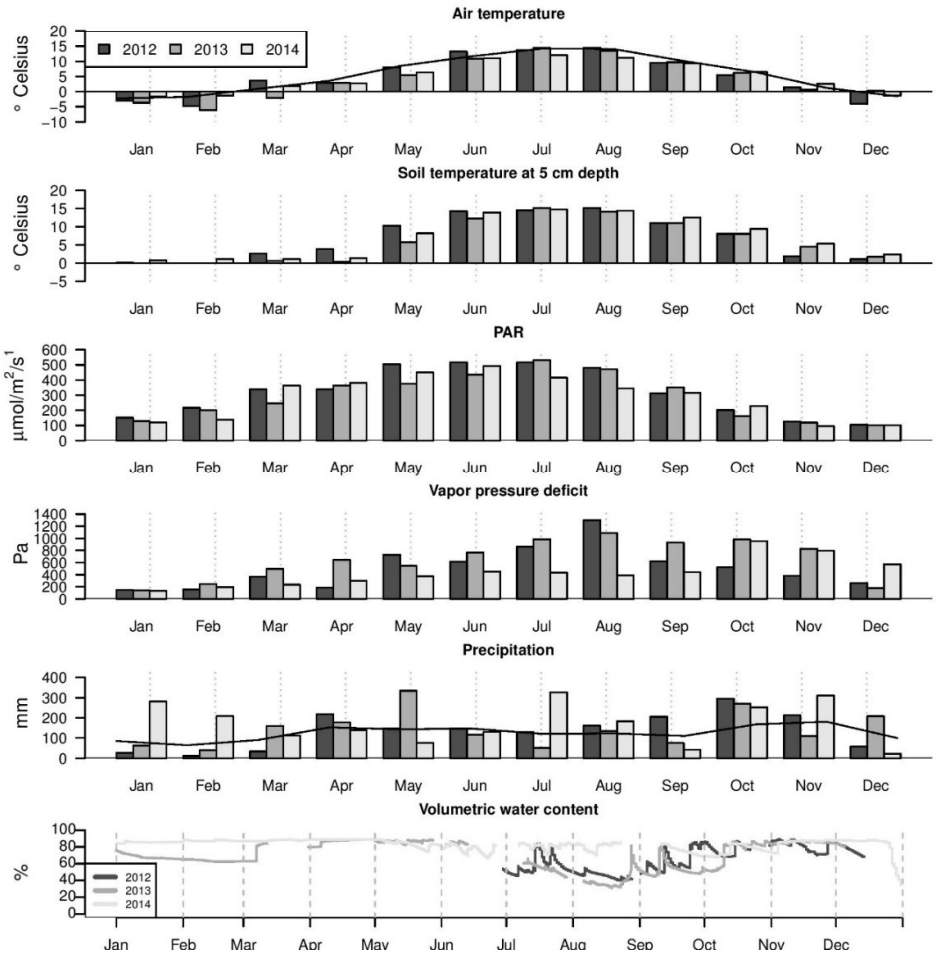

Figure 4-3 Monthly values for meteorological variables across 3 years: average air temperature with the long-term average (Eccel et al. 2012) as a solid line, average soil temperature at 5 cm depth, total photosynthetic active radiation (PAR), mean vapour pressure deficit, total precipitation, and volumetric water content under Calluna vulgaris at 5 cm depth

During the very wet summer 2014 the water table was around 17 cm below soil level, while in autumn it dropped to 60 cm deep following a very dry September and start of October (Figure 4.4). The mean water table depth was 27 cm below the surface over the measured period.

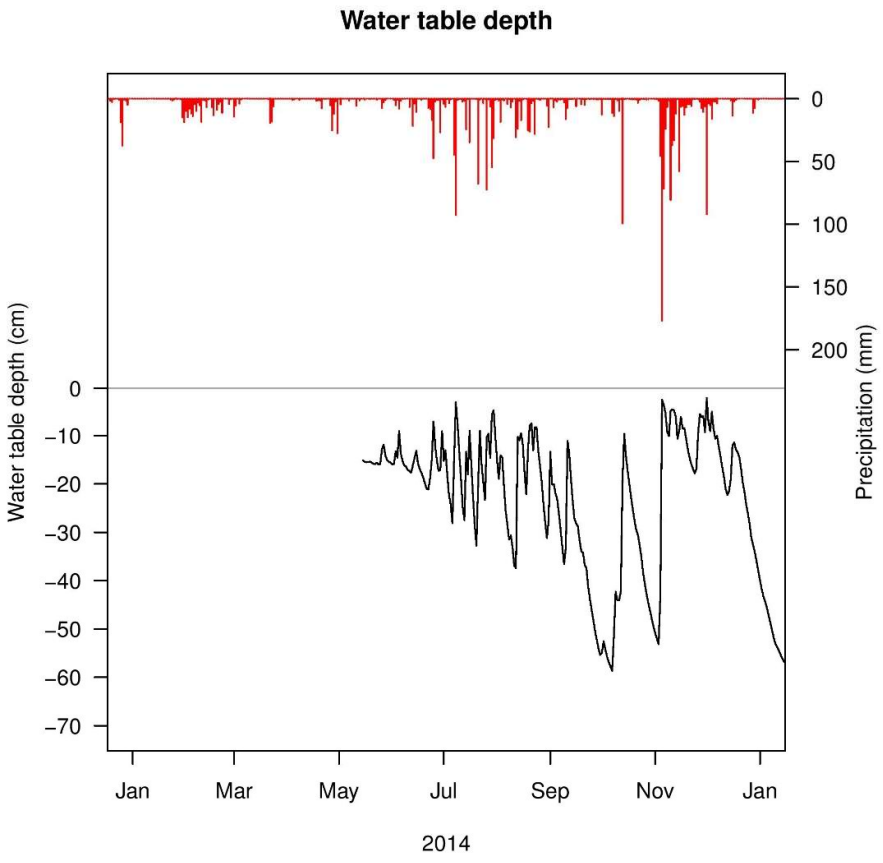

Figure 4-4 Daily water table depth and daily precipitation from 14th of May 2014.

During the winter, neither the soil temperature at 5 cm depth under *M. caerulea* and *C. vulgaris* dropped below 0 °C, because the snow cover and the layer of dead *M. caerulea* leaves were acting as insulators (Figure 4.3 and 4.5). In all years the soil temperature at 5cm depth was above 5 °C when the first snow fell, then it decreased to near 0°C in the following two months under the snow pack. The date at which the snow arrived was very variable with a range of 16 to 43 days difference. In 2011, the snow arrived the on 13th December; in 2012 it arrived on the 31st October, in 2013 on

the 15th November and in 2014 the snow did not arrive (it arrived the 16th of January 2015). The maximum snow height in the three winters, was very variable and ranged from 43 cm (2012), 101 cm (2013) to 204 cm (2014) (Figure 4.5). During the winters of 2011-2012 and 2013-2014, the snow density showed an increasing trend; while in the winter 2012-2013, there was a drop in snow density in the middle of the snow covered period. The peatland was covered with snow for 101, 173 and 157 days during the winter of 2012, 2013 and 2014, respectively. The long-term snow cover period average and the maximum snow height from 1985-2015 is 140 ± 29 days and 95 ± 52 cm, respectively (Meteotrentino). The difference in the snow water equivalent and amount of precipitation was responsible for the difference in SWC, which was higher in winter 2014 (above 80%) than in the other winters. During the summer season the SWC of the peatland never dropped below 31%, which was measured during the summer of 2013 (Figure 4.3). Conversely, in 2014, the wettest year, the SWC did not drop beneath 66% during the summer. Under the snow cover the SWC dropped to 60 % in 2013 compared to more than 80% in 2014, the annual average of the SWC was 74% over the three years.

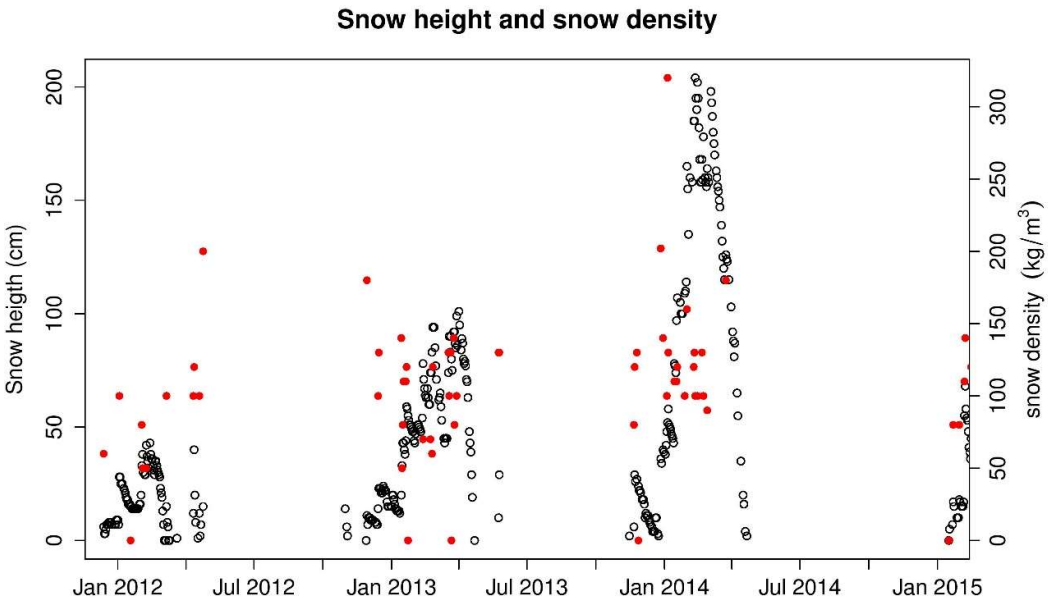

Figure 4-5 Measured snow height and snow density during the years 2012, 2013 and 2014. The snow height (cm) is depicted by the black dots and the snow density (kg/m3) by the red points. The values are not measured on site but at nearby a meteorological site.

4.4.2 Carbon and methane fluxes measurements

In all three years, the peatland was a source of CO_2 (Figure 4.6). The peatland acted as a carbon sink for only four months a year, June to September (Figure 4.6). The annual NEE measured at the Monte Bondone fen was 103.5, 262.9, 175.7 g C-CO_2 m^{-2} in the calendar years 2012, cooler 2013 and wettest 2014 respectively (Figure 4.6). In total, the net CO_2 uptake period (the period where NEE < 0) was 64, 75 and 81 days for 2012, 2013 and 2014 respectively. During this period, the uptake was 4.2, 2.8 and 3.5 g C-CO_2 m^{-2} p77er day. In 2013, the CO_2 uptake period started later than in 2014 (Figure 4.6 and 4.7), because of the long period of snow cover. The quarterly inter-annual variations showed that all seasons have the same trends, apart from higher daily emissions in the first quarter of 2014, compared to the other years (figure 4.8). This could have been driven by high SWC, which was higher than in the other years (Table 4.1). Interesting to see is that the lower annual NEE of 2012 can be explained by the shorter C uptake period, due to an increase in ecosystem respiration.

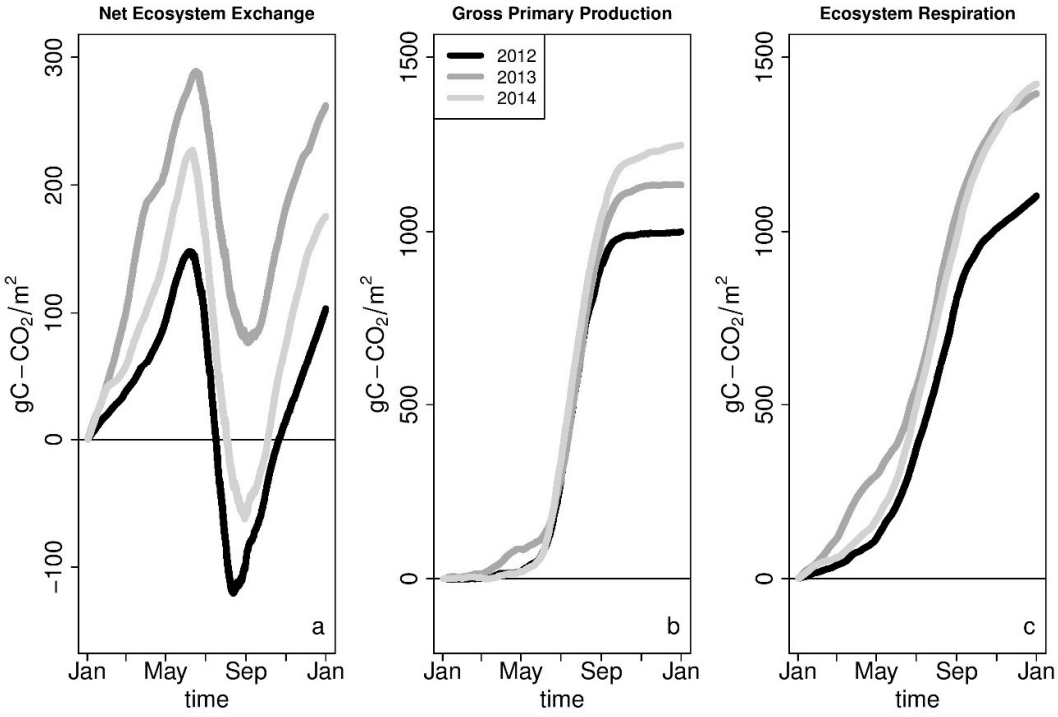

Figure 4-6a Cumulative NEE flux for each year b) Cumulative GPP flux for each year c) Cumulative R_{eco} flux for each year.

Table 4-1 Spearman's correlations between Net Ecosystem Exchange (g C-CO_2 m^{-2} s^{-1}), Gross Primary Production (g C-CO_2 m^{-2} s^{-1}), and ecosystem respiration (g C-CO_2 m^{-2} s^{-1}), and air temperature (°C), photosynthetic active radiation (µmol m^{-2} s-1), vapor pressure deficit (Pa), soil water content (%) and precipitation (mm) over three complete years and over each quarter of the years. All values are daily averages, apart from precipitation, which is a daily sum.

	NEE					GPP					R_{eco}				
	Air temp	PAR	VPD	SWC	Prec	Air temp	PAR	VPD	SWC	Prec	Air temp	PAR	VPD	SWC	Prec
Yearly	-0,34	-0,40	"-0,00"	0,18	0,07	0,82	0,65	0,57	-0,45	0,05	0,82	0,56	0,61	-0,56	0,06
Q1	-0,07	0,10	0,40	-0,70	0,08	0,23	0,34	0,46	0,06	0,16	0,03	0,23	0,46	-0,59	0,11
Q2	-0,33	-0,15	-0,20	0,34	0,09	0,74	0,29	0,42	-0,84	-0,18	0,82	0,29	0,38	-0,79	-0,15
Q3	-0,52	-0,63	-0,04	-0,11	-0,04	0,65	0,63	0,09	0,07	0,06	0,63	0,34	0,15	-0,14	0,13
Q4	0,67	0,29	0,64	-0,30	0,19	0,55	0,26	0,66	-0,09	0,24	0,68	0,24	0,72	-0,22	0,25

p<0,05

p<0,1

Light gray: $p < 0.05$
Dark gray: $p < 0.10$
White: $p > 0.1$

The gross primary production (GPP) was high between June and September for all years, with the highest production in July (168.7, 117.0 and 150.1 g C-CO_2 m^{-2} for 2012, 2013 and 2014, respectively). During May, the GPP was still very low, due to the late snowmelt. The annual GPP was 999.1, 1133.6 and 1248.2 g C-CO_2 m^{-2} for 2012, 2013 and 2014, respectively.

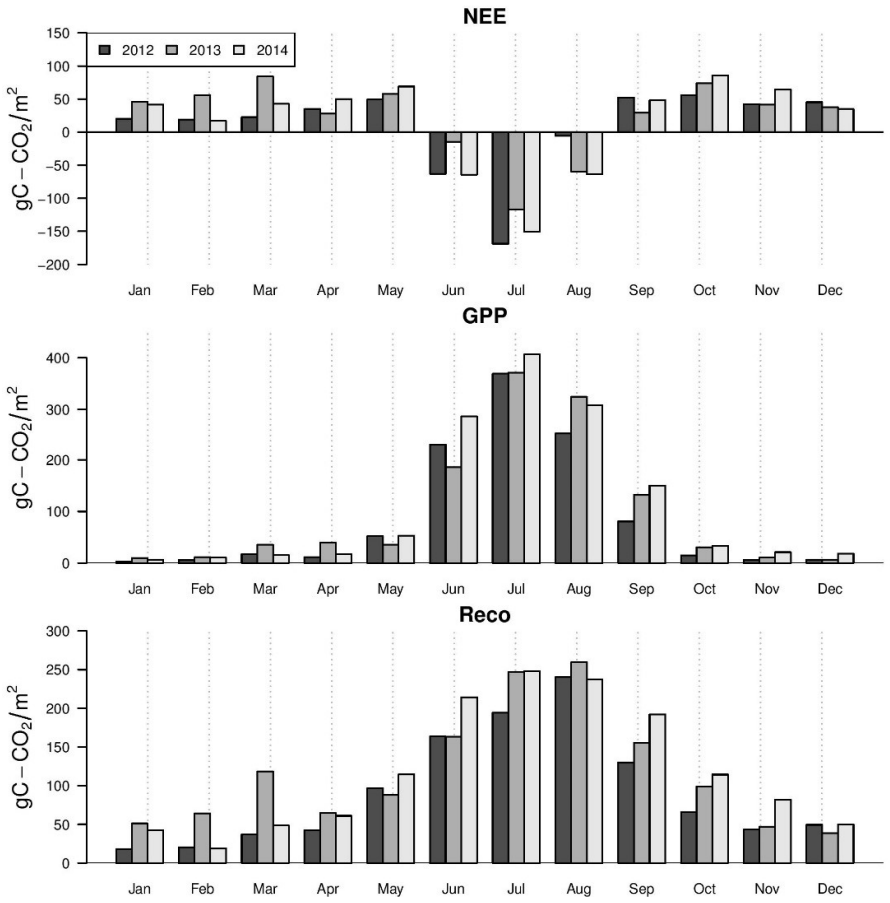

Figure 4-7 Monthly values for CO_2 exchange variable across 3 years: sums of Net Ecosystem Exchange (NEE), sums of Gross Primary Production (GPP) and sums of ecosystem respiration (R_{eco}).

During the three winters there was a slight variation in the NEE, where 2013 had the highest emissions despite having the coldest air temperature (figure 4.8). Through the winter of 2012 and 2014 the ecosystem respiration was low, compared to the ecosystem respiration of the winter of 2013 (Figure 4.7). During the winter of 2012-2013 the peatland was a big source of CO_2 and showed an elevated R_{eco} (compared to the other years) over the first three months of the year with a maximum monthly

emission of 118.2 g C-CO_2 m^{-2} (March 2013). During the summer months of all years (figure 4.8), the R_{eco} increased and showed the characteristic bell shape. In 2012, the R_{eco} was lower in all months, apart from May and December, compared to the other years. In wettest 2014, the R_{eco} was higher in June, September, October and November, compared to the same months of the other years. The annual ecosystem respiration (R_{eco}) was 1102.4, 1396.4 and 1423.8 g C-CO_2 m^{-2} in the calendar years 2012, 2013 and 2014.

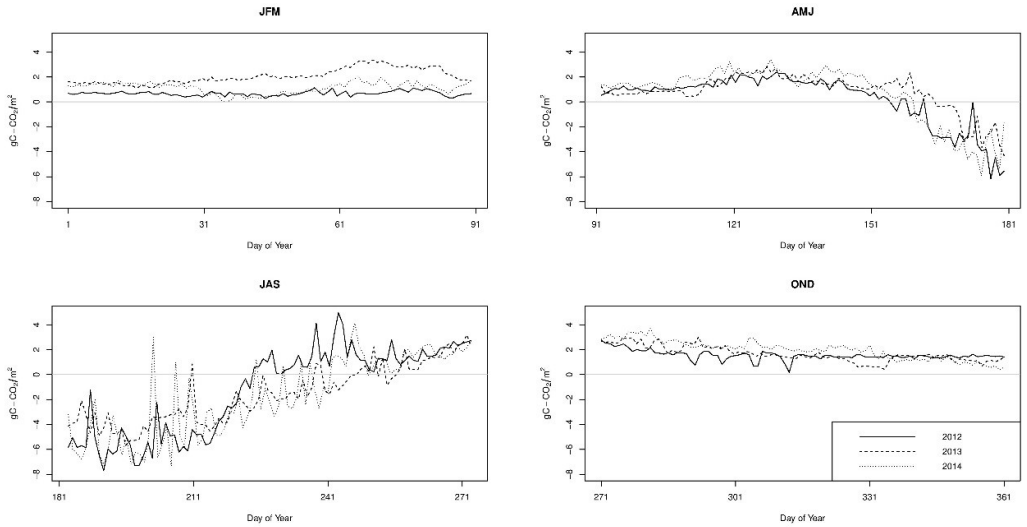

Figure 4-8 Quarterly daily NEE fluxes over three years. JFM = January February March, APJ = April May June, JAS; July, August, September, OND= October, November, December.

Based on the three years of carbon fluxes and meteorological measurements the correlation between the half-hourly values of NEE, R_{eco}, GPP and meteorological parameters were analysed. Frolking et al. (1998) described a correlation between NEE of peatlands and incoming radiation:

$$NEE = \frac{\alpha * PAR * GPP_{max}}{\alpha * PAR + GPP_{max}} - R$$

Where α is the initial slope of the rectangular hyperbola and R is the dark respiration value. For this analysis, only the data from the summer was used, where the midday

uptake was higher than 5 µmol m^{-2} s^{-1}. Over the data a rectangular hyperbola was fitted, since NEE becomes light saturated.

$$NEE = \frac{0.05 * PAR * GPP_{max}}{0.05 * PAR + GPP_{max}} - 6.4 \qquad R^2 = 0.83,\ p < 0.01$$

Over the complete years and all half-hourly data points, the GPP was linearly correlated to NEE.

$$GPP = 3.66 - 1.09 * NEE \qquad R^2 = 0.85,\ p < 0.01$$

While R_{eco} was exponentially correlated with the air temperature.

$$R_{eco} = e^{0.1029 * Tair} + 1.2656 \qquad R^2 = 0.58,\ p < 0.01$$

No comparison with soil temperature at 5 cm depth has been made since this variable was used to gap fill the data.

Over the three years, the daily values of NEE, GPP and R_{eco} are significantly correlated with Air temperature, PAR, VPD, soil water content and precipitation (Table 4.1). NEE is significantly correlated with air temperature, PAR and SWC. Interesting is that SWC has a negative relation with GPP and R_{eco}, which means that a decrease of SWC will increase the GPP and R_{eco}. Over the years, during all seasons the SWC had a significant correlation with inter-annual variability of NEE, but in the second quarter of the year (months: April, May, June) there was a positive correlation between NEE and SWC. During these months the soil was very wet, due to the snow melt (Figures 3 and 5). Overall an increase in NEE is correlated with an increase of air temperature and PAR and a decrease in NEE with an increase in SWC.

Methane fluxes measured over 10 month showed small emissions, generally not higher than 0.035 µmol CH_4 m^{-2} s^{-1} (Figure 4.9). Over this 10-month period, the total emission of the peatland was 3.2 g C – CH_4 m^{-2}. No relation between water table depth and

methane fluxes at half hourly, nor daily time steps was found. In addition, air pressure as a proxy for ebullition of methane bubbles did not explain the methane flux (data not shown, $R^2 < 0.001$, $p > 0.25$). The CH_4 fluxes also show no daily or monthly trend or relationship with any measured meteorological parameters (data not shown, $p > 0.10$).

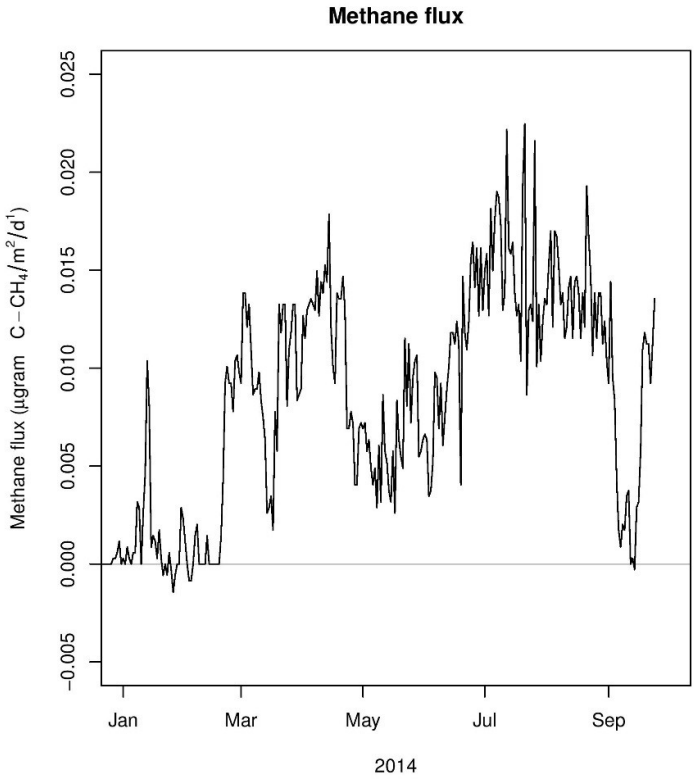

Figure 4-9 Half-hourly data points of measured CH_4 fluxes.

4.5 Discussion

The observed CO_2 emissions of this Alpine peatland were much higher than in all of the other untouched peatlands monitored with an eddy covariance system (Hendriks et al. 2007, Roulet et al. 2007, Aurela et al. 2009, Lund et al. 2009, Bäckstrand et al. 2010, Sonnentag et al. 2010, Beetz et al. 2013, McVeigh et al. 2014), since most of the low altitude northern latitude, pristine peatlands act as a carbon sink. The range of annual NEE (-329 to -9 g C-CO_2 m^{-2}), GPP (288 to 1215 g C-CO_2 m^{-2}) and R_{eco} (232 to 1307 g C-CO_2 m^{-2}) over different types of peatlands and altitudes are presented in

Table 4.2; all peatlands are either untouched (by anthropogenic disturbances), or these activities were minor and occurred more than 30 years ago, apart from The Horstermeer site which is a wetland restored around 20 years ago from an abandoned agricultural peat meadow (Hendriks et al. 2007). Compared to the peatlands presented in Table 4.2, which are all carbon sinks, the peatland at Monte Bondone had a significantly shorter active carbon uptake period (ANOVA, $p<0.01$). In spite of this short carbon uptake period, the annual GPP was very high. Only in one of the peatlands where fluxes are measured with an EC system (Horstermeer, NL), such a high annual GPP was measured. At the Horstermeer-site the annual GPP was high because of the long growing season (around 165 days) and the relatively eutrophic soil conditions (Hendriks et al. 2007). The GPP in other fens was less than half of the GPP measured at Monte Bondone. At these other sites more mosses and less vascular plants are present compared to the Monte Bondone peatland (Nilsson et al. 2008, Aurela et al. 2009, Sonnentag et al. 2010, Beetz et al. 2013, Wu et al. 2013). At our site, the abundant presence of *M. caerulea* was possibly resulting in high values of GPP (Aerts and Berendse 1989, Jarosz et al. 2008, Vanselow-Algan et al. 2015).

*Table 4-2 Comparison of Monte Bondone peatland with other peatlands of different types and locations, with the standard deviation in brackets (±). *For the methane fluxes of the Monte Bondone peatland no uncertainty can be given, since this value is derived from the 10 and a half-month data-period. [a] chamber measurements (Laine et al. 2007) [b] Negative values of water table depth are below soil level.*

Site	Glencar (McVeigh et al. 2014)	Fäjemyr (Lund et al. 2009, 2010)	Mer Bleue (Roulet et al. 2007)	Stordalen (Bäckstrand et al. 2010)	Horstermeer (Hendriks et al. 2007)	Sandhill fen (Sonnentag et al. 2010)	Friesinger Moos (Beetz et al. 2013)	Lompolojänkkä (Aurela et al. 2009)	Degerö Stormyr (Nilsson et al. 2008, Wu et al. 2013)	Monte Bondone peatland (this study)
Latitude	51.55 N	56.15 N	45.41 N	55.78 N	52.25 N	53.80 N	53.68 N	67.03 N	64.18 N	46.02 N
Longitude	9.55 E	13.33 E	75.48 W	3.23 W	5.04 E	104.62 E	8.82 E	24.49 E	19.55 E	11.03 E
Type	Blanket bog	Eccentric bog	Raised bog	Mixed Mire	Restored peatland	Fen	Fen	Fen	Poor fen	Fen
Elevation (m a.s.l.)	145-170	96	69	267	0	494	0	180	270	1563
Duration (years)	9	1	6	11	3	4	2	3	5	3
Length growing season (days)	Around 130	214	171 ± 22	169	163 ± 26	Around 180	218	119	153	73 ± 7
NEE (g C-CO_2 m^{-2} yr^{-1})	-55.7 ± 18.9	-80	-40.2 ± 40.5	-34.9 ± 4	-329 ± 88	-129.7 ± 74.7	-14 ± 75	-117 ± 83.4	-54 ± 5.6	180.7 ± 65.2
GPP (g C-CO_2 m^{-2} yr^{-1})	288 ± 17	Around 250	259 ± 52	Around 200	1215 ± 70	421.8 ± 69.2	630 ± 64	n.a.	448 ± 83	1191.0 ± 42.9
R_{eco} (g C-CO_2 m^{-2} yr^{-1})	232 ± 7	Around 250	230 ± 40	Around 150	886 ± 27	301.5 ± 30.0	617 ± 38	n.a.	404 ± 76	1307.7 ± 25.4
CH_4 (g C-CH_4 m^{-2} yr^{-1})	6.2 [a]	n.a.	3.7 ± 0.5	11 ± 12	32 ± 21	n.a.	4.7 ± 0.6	n.a.	11.5 ± 2.2	3.2*
Water table depth (cm)	-4.4 ± 1.4	-3.3 ± 7.8	-40 ± 10	-5 ± 10	-20 ± 25	-15 ± 10	-59 ± 20	2.5 ± 2.3	-10 ± 5	-27.6 ± 18

The R_{eco} of the Monte Bondone peatland is the highest value seen in Table 4.2; most of the sites have an ecosystem respiration of about 200-500 g C-CO_2 m^{-2} yr^{-1}. The great root biomass of *M. caerulea* when it is as widespread and developed as in Monte Bondone probably results in an increased root respiration and microbial respiration of root exudates compared to other plant communities (Gatis et al. 2016). The high R_{eco} during winter, with low air temperatures, was the effect of the snow insulation (Morgner et al. 2010), so the soil temperatures were still high enough to support decomposition even though the temperatures were close to zero degrees Celsius (Clein and Schimel 1995).

The fitted rectangular hyperbola on the NEE of the peatland at Monte Bondone shows a clear difference with other peatlands (Frolking et al. 1998). Frolking et al. (1998) found an average of 0.024 ± 0.008 for the initial slope of the rectangular hyperbola (α) and -2.38 ± 2.45 for the dark respiration (R) for peatlands, while at Monte Bondone the values were: 0.05 and -6.4, respectively. The higher value for the dark respiration could explain the high values of R_{eco}, while the higher value for α indicates a productive system. These high values are found at C3 crops or at grasslands (Ruimy et al. 1995).

The fluxes measured at the Bondone peatland were very different from those measured at the same time in a nearby managed poor grassland (*Sieversio-Nardetum strictae*), since the grassland was close to being CO_2 neutral (9.14 ± 75.21 g C-CO_2 m^{-2} (Marcolla et al. 2011)). The different NEE between the two sites are due to the higher winter ecosystem respiration in the peatland compared to the grassland. The high winter ecosystem respiration at the peatland, under the snow cover indicates that the microbes in the soil are still actively decomposing the high amount of stored soil carbon (Clein and Schimel 1995). The GPP of the peatland was also higher than the

GPP of the grassland (Marcolla et al. 2011) possibly because of the higher productivity of the peatland plants (as *M. caerulea*) compared to the less productive (*Festuca rubra* and *Nardus stricta*) Monte Bondone grassland plants (Marcolla et al. 2011, Sakowska et al. 2014) and to the management of the grassland. Each year around mid-July, the vegetation is cut and the biomass is removed, reducing the GPP and the R_{eco}.

During the three years the GPP as well as the duration of the net CO_2 uptake period increased; the same trend is not visible in NEE (figure 4.8). The high GPP in 2014 can be explained by the fact that the soil water content was high (Table 4.1), due to the high amount of precipitation. The plants could therefore keep their stomata open longer without having to cope with water stress (Oren et al. 1999).

The NEE and R_{eco} in February and March of 2013 were higher than in the same months of the other years (Figure 4.7). During this period the SWC was lower than in the winter of 2013-2014, which might indicate that the WTL was also lower. As a consequence, this could have resulted in a faster decomposition under aerobic condition of soil organic carbon.

Possible errors in the measured fluxes at the Monte Bondone site consist of high data loss due to unstable situations, rain, power failure and due to the snowfall. The total amount of data gaps for the open path analyser (74%) was higher than the enclosed path analyser (65%). The open path is much more susceptible to external influences, e.g. when it rains the laser path is blocked and no fluxes can be measured. In total 53 % of the data consisted of gaps, since not all the gaps of both analysers did not overlap. Another source of error can be the snowfall, when the snow fell the EC system should be lifted to maintain a constant height above the soil surface. In 2014 the EC system was raised, on the date that the EC system was raised the snow was close to the EC system. The snow height in 2014 increased very fast, which could have resulted in an

underestimation of fluxes due to a decrease of the footprint. At sites were snow is present during the winter, the height of the EC system should be increased according to the snow height. The methane open path sensor was more susceptible to influences, since the open path was longer, 50 cm compared to 12.5 cm of the open path CH_4 analyser, hence the low amount of data available from this sensor (30%).

In February and March 2013, the average air temperature was lower than in the other years. The combination of low air temperatures and snowfall leads to a snow pack with a low density, e.g. presence of macro pores (Massman et al. 1997, Bowling and Massman 2011). The increase in snow depth in February and March 2013 (Figure 4.5), possibly caused air to be trapped in the newly fallen snow pack. During daytime, the occasionally positive air temperature and the high level of incoming radiation resulted in snowmelt. Due to the high porosity of the snow the water migrated down and accumulated (Rempel 2007). During the nights, the air temperature dropped below zero again. This unfreezing and re-freezing process could have led to the formation of ice lenses in the snow pack. Ice lenses have the capability to trap the air underneath it (Mast et al. 1998), so that the CO_2 produced during the decomposition was being stored in the snow pack (Larsen et al. 2007). During the snowmelt the ice lenses melted and the stored gasses was released in pulses, measured as peaks of ecosystem respiration in February and March 2013 (Figure 4.7) (Monson et al. 2006, Larsen et al. 2007). Soil respiration in winter could be as much as 7-10 % of the annual ecosystem respiration (Monson et al. 2006), in March 2013, during snow melt, the ecosystem respiration was 8.5% of the annual ecosystem respiration.

The methane fluxes were not measured for a complete year and no correlation between methane fluxes and meteorological variables was found. Nevertheless, it is plausible that the methane fluxes at this site do not play a major role in the carbon balance due

to the low water table. During the measurements in 2014, the release of methane was a continuous diffusion process, even though the data showed many spikes. In our data there was no diurnal trend, which was also found by Rinne et al. (2007) at a peatland in Finland. It is difficult to measure methane fluxes with an eddy covariance setup, the micrometeorology plays a big role in the production of methane and the microbes which produce methane are not uniformly spread in the soil (Baldocchi et al. 2012, Bohn et al. 2013, Koebsch et al. 2015). The gap filling of methane is much more difficult compared to CO_2 data , therefore no consensus about the best method to gap fill methane data has been found in literature (Dengel et al. 2013). Methane can be released in bursts, which happens when there is a drop in the air pressure. This drop in pressure results in an over pressure of methane gas in the soil, which can result in the ebullition of methane gas (Tokida et al. 2007). After the snowmelt, the emission of methane increased a little, but overall the fluxes were at the lower range (3.2 g C-CH_4 m^{-2} over the 10-month study period), compared to other peatlands: 3.7 to 32 g C-CH_4 m^{-2} yr^{-1}, Table 4.2). This is remarkable since most of the peatland is covered by *M. caerulea*, which is known to be able to conduct methane through its aerenchyma (Van Den Pol-Van Dasselaar et al. 1999, Carmichael et al. 2014, Turetsky et al. 2014). The high cover of *M. caerulea* in this peatland does not directly link with high emissions of methane, while this relation was found in other peatlands (e.g. (Couwenberg et al. 2010, Turetsky et al. 2014, Vanselow-Algan et al. 2015). During the measurement of the CH_4 fluxes, the measured water table was deep, up to 17 cm in summer and even to 60 cm in autumn. Methane is only produced under anaerobic conditions and emitted with a shallow water table; with a deep water table the methane is oxidized in the upper aerobic soil layers (Wagner et al. 2003, Jungkunst et al. 2008). At Mer Bleue and the Friesinger Moor the amount of methane emitted is more or less the same and also the water table level has the same depth ((Roulet et al. 2007, Beetz

et al. 2013), Table 4.2). This coincides with the findings that the methane emissions with a water table level of more than 20 cm below soil level is close to zero (Wagner et al. 2003, Jungkunst et al. 2008, Couwenberg et al. 2010, Turetsky et al. 2014). At Stordalen and Glencar the water table level was much shallower and therefore the methane emission was much higher (Bäckstrand et al. 2010, Koehler et al. 2011, Turetsky et al. 2014). At Horstermeer the methane fluxes were very high and not comparable with other sites where methane fluxes were measured, since it is a restored peatland and the eutrophic soil was not excavated (Hendriks et al. 2007). It has to be stated that the methane fluxes and the water table depth at Monte Bondone were only measured during the wettest year (2014) and not for the complete year.

4.6 Conclusion

The study of carbon fluxes of an alpine peatland for 2012-2014 shows that the peatland at Monte Bondone acted as a significant carbon source, based on its CO_2 emissions. This is a major contrast to all other pristine peatlands studied to date, most of which are at elevations below 300 m a.s.l , which are sinks for carbon. The methane emissions of this site were very low, due to a low water table. Despite being very high, the GPP of the peatland during the growing season was not high enough to compensate for the even higher loss of carbon (R_{eco}) during the winter period. During the snow cover, the decomposition of organic matter was an ongoing process. The active carbon uptake period of the peatland was 73 ± 7 days. The start of the growing season was induced by the melt of the snow, so changes in the date of snowmelt could result in differences in the carbon balance of the peatland.

With climate change, the period with snow cover will be shorter, which can possibly result in a longer growing season (Aurela et al. 2004, Humphreys and Lafleur 2011). With a decrease of precipitation, part of the peatland will likely dry up, which will

lead to an overall increase in *M. caerulea* and will even make it possible for other species to colonize it. The surrounding area of the peatland is covered by grasses (*Sieversio-Nardetum strictae* association), which can invade the peatland when the water table drops (Stine et al. 2011). The increase in *M. caerulea* could result in a higher carbon uptake, while the eventual transition to grassland will have unknown consequences. However, the first years to decades the grassland might act as a carbon source, since the carbon in the soil will become unstable (Schwalm and Zeitz 2014). To gain a better insight in the effect of climate change on alpine peatlands, a longer time series of carbon measurements is needed as well as studies on changes in the hydrology and the vegetation of the peatland.

4.7 Acknowledgments

The authors would like to thank Roberto Zampedri and Mauro Cavagna, from Fondazione Edmund Mach, for the maintenance of the eddy covariance tower and for the collection of the data. The authors thank Dr. Beniamino Gioli from the National Research Council – Institute for Biometeorology, Florence for lending the open path methane sensor (LI7700). The authors also want to thank the Associate Editor Eva Falge and the two anonymous reviewers for their useful suggestions and comments.

4.8 Supplementary material

Supplement Table 4.1 Seasonal thresholds for CO_2 fluxes used for filtering the raw fluxes to remove the amount of noise in the data.

	Uptake (µmol s^{-1} m^{-2})	Loss (µmol s^{-1} m^{-2})
Winter	-4	5
Spring	-15	9
Summer	-35	15
Autumn	-15	9

4.9 Appendix I: Interannual variability of air temperature and precipitation compared to long-term data

The mean monthly air temperature and monthly precipitation for the years 2012-2014 have been compared to the long-term data (1958-2008 (Eccel et al. 2012)). The monthly mean air temperature values measured for 2012 and 2013 are within the long-term variation (Figure 4-10), apart from the air temperatures in February and December 2012 and in February 2013 where the air temperatures were slightly lower than the long-term average. In May 2013, the air temperature was also lower than the long-term average (5.5 ˚C and 8.5 ˚C, respectively). The summer of 2014 was lower than the long-term average (June 11.1 ˚C, and July 12.1 ˚C compared to the long-term average of 11.6 ˚C and 14.2 ˚C, respectively). Only March 2012 had monthly mean air temperature higher than the monthly long-term mean air temperature, resulting in three colder years (2012: 5.1 °C, 2013: 4.3 °C and 2014: 5.0 °C) compared to the long-term average (1958-2008: 5.4 °C, Eccel et al. (2012) and chapter 4.4.1 of this thesis).

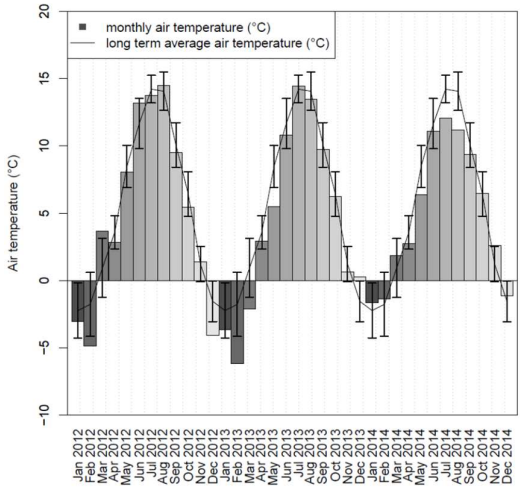

Figure 4-10 Monthly mean air temperature over the years 2012-2014 (bars) and the monthly long term mean air temperature (1958-2008) with standard deviation (line with error bars)

The variability in the precipitation data is higher than in the variability in air temperature data (Figure 4-11), also indicated by the high values of standard deviation

of the long-term monthly precipitation. In total seven months out of the thirty-six months had precipitation values that were not within the standard deviation of the long-term precipitation data (2012: September, 2013: May, July and 2014: January, February, June and October). Out of these seven months only two months had a lower precipitation compared to the long-term average (July 2013 and October 2014), for the other five months the precipitation was higher than the long-term average. The high amount of snow measured in 2014 can be related to the high amount of precipitation in January and February 2014. The precipitation variation in the three years was very pronounced, with annual cumulative values of 1650.4, 1740.6, and 2082.6 mm (for 2012, 2013 and 2014, respectively), all well above the long-term average of 1290 mm per year (Eccel et al. (2012) and chapter 4.4.1 of this thesis).

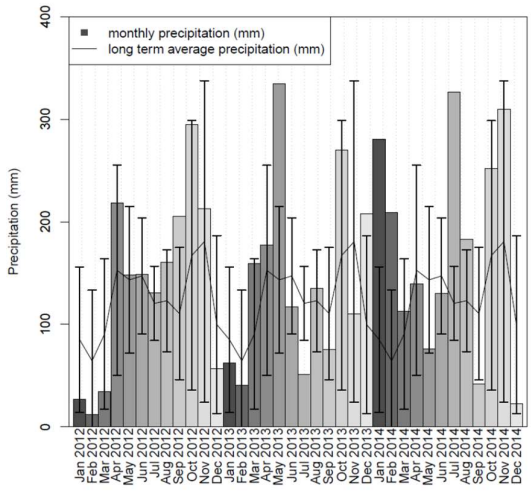

Figure 4-11 Monthly precipitation over the years 2012-2014 (bars) and the monthly long-term precipitation (1958-2008) with standard deviation (line with error bars)

4.10 Appendix II: A comparison of three gap filling techniques for eddy covariance fluxes and two NEE partitioning techniques

4.10.1 Introduction

A disadvantage of eddy covariance data is that it contains gaps due to malfunctioning of the system, bad meteorological conditions and the filtering of the data (chapter 3.3). To get an annual balance these gaps need to be filled, for which many methods are available (Moffat et al. 2007). The flux partitioning and gap-filling method (Reichstein et al. 2005) used in this thesis, while conventionally used world-wide, is compared against other gap filling methods to determine whether the interannual variability (IAV) of Net Ecosystem Exchange (NEE) is influenced by biases introduced by the used gap-filling technique (Moffat et al. 2007). The used method has been developed for forests and agricultural sites, and their direct utility to peatlands remains an open question. To assess the correctness of the gap filling technique, the used gap filling technique is compared to two other techniques (Mean diurnal variation (Falge et al. 2001) and artificial neural network (Dengel et al. 2013)). These three major gap filling techniques have previously been used in a study with short vegetation (Zhao and Huang 2015), as is present in the Monte Bondone peatland.

With an eddy covariance tower the NEE is continuously measured. The NEE is the difference between the Gross Primary Production (GPP) and ecosystem respiration (R_{eco}). Different partitioning tools are available to partition the NEE into GPP and R_{eco} fluxes (Stoy et al. 2006), in this chapter a night-time based and day-time based approach is used to partition the NEE fluxes gap filled using the three different gap filling techniques.

This study is has the objective to compare the three major gap filling techniques to identify changes in NEE fluxes when these different techniques are used and to asses

if the conventionally used world-wide gap filling technique (Reichstein et al. 2005) was a valid approach for the research site at the peatland of Monte Bondone.

4.10.2 Methods

In this chapter three different gap filling techniques are used: the mean diurnal variation technique (MDV, Falge et al. 2001), the artificial neural network technique (ANN, Dengel et al. 2013) and the look up table technique as used by FLUXENT (LUT, Reichstein et al. 2005). The NEE are later partitioned into GPP and R_{eco} fluxes based on a day-time based (Lasslop et al. 2010) and night-time based approach (Reichstein et al. 2005).

4.10.2.1 Gap filling

4.10.2.1.1 Mean Diurnal Variation

The mean diurnal variation technique (MDV, Falge et al. 2001) is the simplest gap filling technique of the three methods used in this chapter. In the MDV technique, a missing measurement is replaced by the mean for that half-hour of the adjacent days. For this exercise, the range of adjacent days in which the algorithm was looking for gaps was 14 days. A previous study has indicated that this range should be between 7 and 14 days, shorter periods were not enough to determine a mean from measurements and longer periods introduces error because of nonlinear dependence on environmental variables (Falge et al. 2001). Due to the gap distribution in the measured data a seven days window did not result in a gap filled dataset (data not shown).

4.10.2.1.2 Artificial Neural Network

The artificial neural network is a technique that finds nonlinear regressions between parameters. In this exercise, the net ecosystem exchange is correlated with day of year, time of the day, global radiation, soil temperature at 5 cm depth and the relative

humidity. These parameters are used, since they are also used in the look up table technique, which is used in this thesis. The non-gap filled dataset of the measurements (19268 data points) was randomly spilt into a training (14451 data points, 75% of total) and a test dataset (4817 data points, 25% of total). The training dataset was used to train the ANN and to find the nonlinear regressions between the parameters. The test dataset was used to validate the predicted NEE based on the ANN. The model was also cross-validated against the data by running the ANN method ten times on different training sets, the data presented in this chapter are the results of the ten runs, which were not significantly different ($p < 0.05$). For the implementation of the ANN, the R package Neuralnet was used (Fritsch et al. 2016), the ANN was configured to have 1 hidden layers with 3 neurons, as in Dengel et al. (2013).

4.10.2.1.3 Look up table

The look up table (Reichstein et al. 2005) is the methodology used by the FLUXNET community and is therefore the most used gap filling technique. With this technique missing values are replaced by the average value under similar meteorological condition within a certain timeframe, in this case 7 days or if no similar conditions are found the window is increased with steps of 7 days. Since this technique is used throughout the thesis, further explanation of the technique is presented in chapter 3.3 and 4.3.3.

4.10.2.2 Statistical errors

To compare the three different gap filling techniques the statistical sums were calculated using the individual observed NEE data and the predicted value the sum relative error (SRE) were as follows:

$$SRE = \frac{\sum o_i - \sum p_i}{\sum o_i}$$

in which a positive error indicates an overestimation and a negative error in underestimation by the respective method (Zhao and Huang 2015).

4.10.2.3 Partitioning

The NEE measurements of the eddy covariance tower can be partitioned into the Gross Primary Production (GPP) and ecosystem respiration (R_{eco}) fluxes. In this chapter, we will use two types of partitioning methods, a night-time based (Reichstein et al. 2005) and a day-time based (Lasslop et al. 2010) approach to partition the NEE fluxes.

4.10.2.3.1 Night-time based partitioning

Night-time data was selected according to a global radiation threshold of 20 W m^{-2}, this night-time NEE data is considered ecosystem respiration (Reichstein et al. 2005). In this method the partitioning of the NEE fluxes into GPP and R_{eco} is based on the Lloyd-and-Taylor (1994) model:

$$R_{eco}(T) = R_{eco,ref} \cdot e^{E_0 \cdot \left(\frac{1}{T_{ref}-T_0} - \frac{1}{T-T_0}\right)}$$

in which T is soil temperature at 5 cm and T_0 is kept constant at -46.02 ˚C, E_0 is the activation energy and T_{ref} a reference temperature, set constant at 10 ˚C. Both the E_0 and $R_{eco,ref}$ are estimated via this function. The GPP values are the difference between the NEE and the calculated R_{eco} fluxes.

4.10.2.3.2 Day-time based partitioning

The partitioning of the NEE into GPP and R_{eco} can also be calculated via the day-time based partitioning (Lasslop et al. 2010). In the day-time base approach the NEE was modelled using the common rectangular hyperbolic light–response curve (Falge et al. 2001) with the addition of the Lloyd-and-Taylor (1994) model, as presented by Gilmanov et al. (2003):

$$NEE = \frac{\alpha\beta R_g}{\alpha R_g + \beta} + R_{eco,ref} \cdot e^{E_0 \cdot \left(\frac{1}{T_{ref} - T_0} - \frac{1}{T - T_0}\right)}$$

In which α is the canopy light utilization efficiency (µmol C J^{-1}), β is the maximum CO_2 uptake rate of the canopy at light saturation (µmol C m^{-2} s^{-1}), R_g is the global radiation (W m^{-2}) and the same Lloyd-and-Taylor model as previously described.

4.10.3 Results

4.10.3.1 Gap filling

4.10.3.1.1 Mean Diurnal Variation

The MDV approach with a 14 days window resulted in a complete gap filled dataset of NEE, the cumulative NEE fluxes indicate that the peatland was a carbon source for all three years (as described in Pullens et al. (2016b)). The NEE fluxes show a big IAV over the three years (Figure 4-12 and Table 4-3). The MDV is the simplest gap filling approach used in this chapter and apart from a small artefact in July 2012 the technique is able to reproduce the characteristic sigmoid curve of NEE fluxes.

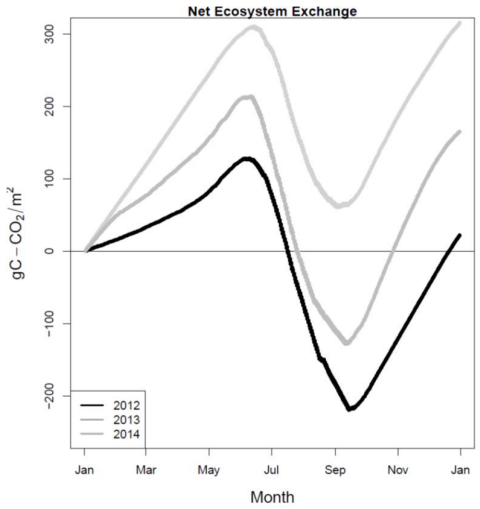

Figure 4-12 Cumulative Net Ecosystem Exchange (g C m^{-2} yr^{-1}) over three years based on the Mean Diurnal Variation gapfilling technique (Falge et al. 2001)

4.10.3.1.2 Artificial Neural Network

The ANN approach is the most complex gap filling technique used in this chapter, since first a model was fitted to a training dataset. This model was parameterized via nonlinear regression in which 1 layer with 3 hidden neurons were present, following the method described by Dengel et al. (2013). The ANN approach gives weights to each connection (Figure 4-13). The model is behaving as a black-box, but has been used to calibrate on the training dataset.

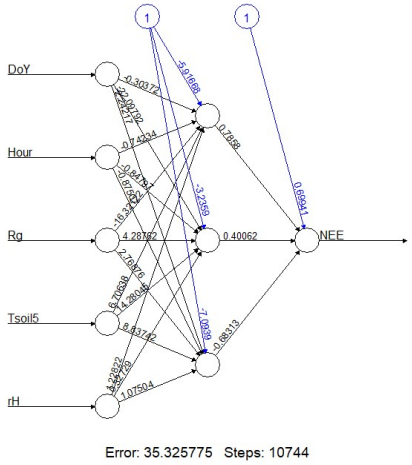

Figure 4-13 A neural network with the weights on each connection. The network has a hidden layer with 3 nodes.

Validation of the model behaviour was analysed by comparing the model output with the test dataset, that was excluded prior to the training. For comparison, the data was also tested against a fitted linear model with the same parameters (Figure 4-14). The ANN approach (modelled= -0.39 + 0.76*measured, R^2 = 0.75, RMSE = 3.57, NSE = 0.75) performed better than the linear model (modelled = -0.84 +0.42*measured, R^2=0.43, RMSE = 5.42, NSE = -0.43).

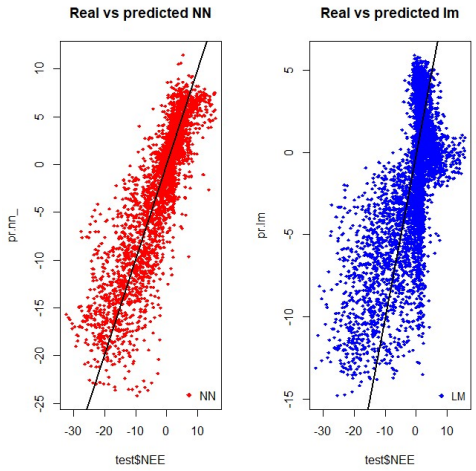

Figure 4-14 1:1 Plot of the model outputs of the artificial neural network and the linear model compared to the test dataset, a subset of the dataset not used for calibration.

The ANN was used to gap fill the NEE fluxes, the cumulative fluxes for all three years indicated that the peatland was a carbon source (Figure 4-15 and Table 4-3). The fluxes show little IAV over the three years, with the peatland being a stable carbon source of around 150 g C m^{-2} yr^{-1}.

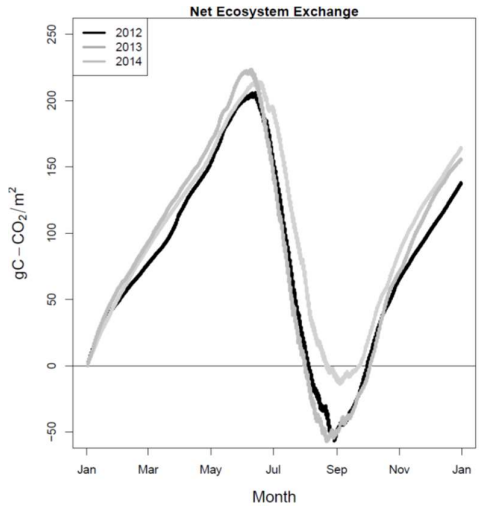

Figure 4-15 Cumulative Net Ecosystem Exchange (g C m^{-2} yr^{-1}) over three years based on the Neural Network gapfilling technique (Dengel et al. 2013)

4.10.3.1.3 Look up table

The results of the look up table are discussed in more depth in chapter 4, in this chapter also an uncertainty analysis was presented. The uncertainty analysis was performed

by estimating uncertainties separately for the different error sources (Aurela et al. 2002). By combining these errors, an uncertainty of 23%, 21% and 30% for 2012, 2013 and 2014 was calculated for the annual balance. These values are in the same range as presented for eddy covariance measurements (Lafleur et al. 2001, Aurela et al. 2002, Richardson et al. 2008, Sottocornola and Kiely 2010a).

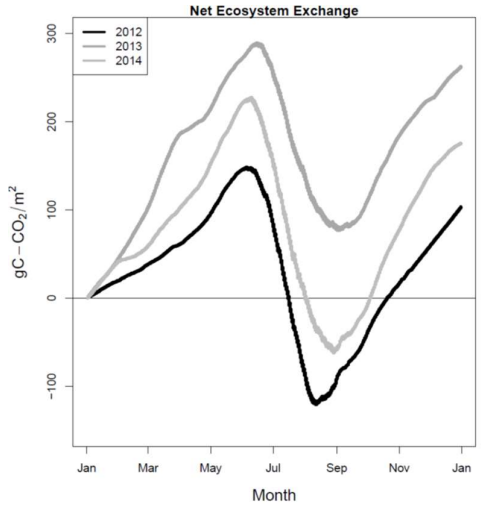

Figure 4-16 Cumulative Net Ecosystem Exchange (g C m^{-2} yr^{-1}) over three years based on the look-up Table gapfilling technique (Reichstein et al. 2005)

Based on all gap filling approaches the peatland was a carbon source for all three years (Figure 4-12, Figure 4-15, Figure 4-16 and Table 4-3). The ANN approach resulted in the highest cumulative NEE fluxes in 2012 and 2014, while in 2013 the MDV approach resulted in the highest cumulative NEE fluxes.

Table 4-3 Sum of Net Ecosystem Exchange (g C m^{-2} yr^{-1}) per year for three different gap filling techniques with mean values per year and per gap filling technique

NEE	MDV	ANN	LUT	Mean
2012	22.8	137.9	103.5	101.1
2013	316.2	164.5	262.9	257.9
2014	165.6	155.8	175.7	176.0
Mean	168.2	152.7	180.7	
Max-Min	293.4	26.6	159.4	

The sum of relative error (Table 4-4) shows that the MDV technique is underestimating the NEE fluxes in 2012, while being close to the measurements in 2013 and 2014, indicated by the small SRE values. The neural network is overestimating the observed NEE in 2012 and slightly underestimating the observed NEE fluxes in 2013 and 2014. While the look up table technique is overestimating the observed NEE fluxes for all three years. The mean SRE over the three years is the smallest for the ANN based approach.

Table 4-4 Sum of relative error (SRE) of Net Ecosystem Exchange per year for three different gap filling techniques with mean values per year and per gap filling technique

	MDV	ANN	LUT
2012	-3.55	1.51	1.64
2013	0.17	-0.31	2.21
2014	-0.06	-0.12	1.76
Mean	-1.14	0.36	1.87
Max-Min	3.72	1.82	0.57

4.10.3.2 Partitioning

Two methods of NEE flux partitioning are used, a night-time based (Reichstein et al. 2005) and a day-time based (Lasslop et al. 2010) approach. The night-time based approach is the approach most commonly used by the FLUXNET community.

The night-time based approach resulted in similar mean GPP and R_{eco} for all three gap filling techniques, with the look up table approach having the highest mean GPP and R_{eco}. The highest GPP and R_{eco} fluxes for 2012, 2013 and 2014 are for the ANN, LUT, MDV respectively. The biggest range of GPP and R_{eco} was based on the MDV gap filling approach.

Table 4-5 Sum of Gross Primary Production (g C m-2 yr-1) and ecosystem respiration (g C m-2 yr-1) per year for three different gap filling techniques based on Night-time partitioning with mean values per year and per gap filling technique

	MDV		ANN		LUT		Mean	
	GPP	R_{eco}	GPP	R_{eco}	GPP	R_{eco}	GPP	R_{eco}
2012	976.8	999.6	1033.9	1171.8	999.1	1102.6	1003.3	1091.3
2013	1059.3	1375.5	964.3	1128.8	1133.6	1396.5	1052.4	1300.3
2014	1296.2	1461.8	1119.2	1275.0	1248.2	1426.9	1221.2	1387.9
Mean	1110.8	1279.0	1039.1	1191.9	1127.0	1307.7		
Max-Min	319.4	462.2	154.9	146.2	249.1	324.3		

The day-time based approach resulted in similar mean GPP and R_{eco} for all three gap filling techniques, with the artificial neural network approach having the highest mean GPP and R_{eco}. The highest GPP fluxes for 2012, 2013 and 2014 are for the ANN, LUT and MDV respectively, while the highest mean R_{eco} fluxes are for ANN, LUT and ANN respectively. The biggest range of GPP and R_{eco} was based on the MDV gap filling approach.

Table 4-6 Sum of Gross Primary Production (g C m^{-2} yr^{-1}) and ecosystem respiration (g C m^{-2} yr^{-1}) per year for three different gap filling techniques based on Day-time partitioning with mean values per year and per gap filling technique

	MDV		ANN		LUT		Mean	
	GPP	R_{eco}	GPP	R_{eco}	GPP	R_{eco}	GPP	R_{eco}
2012	810.5	802.7	851.8	917.6	804.9	831.3	822.4	850.5
2013	857.0	1034.7	872.3	1006.1	878.8	1059.1	869.4	1033.3
2014	933.0	819.9	910.8	894.1	927.5	840.6	923.8	851.5
Mean	866.8	885.8	878.3	939.3	870.4	910.3		
Max-Min	122.5	232	59	112	122.6	227.8		

4.10.4 Discussion

With all three gap filling techniques the peatland was a carbon source for all three years, with 2013 having the highest carbon emission with all gap filling techniques. An interesting observation is that the NEE fluxes based on the ANN technique do not show the IAV shown by the other gap filling techniques, with MDV having the biggest range of NEE values. In 2012 the MDV had a low NEE flux (22.8 g C m^{-2} yr^{-1}) compared to the cumulative NEE fluxes based on the ANN and LUT approach (137.9 and 103.5 g C m^{-2} yr^{-1}, respectively). 2012 was also the year with the most data gaps (63.2% of the year, compared to 59.8 and 55.3 % for 2013 and 2014) indicating that the MDV technique is not preferred technique when big gaps are present in the dataset. This is also supported by the high negative SRE value (Table 4-4). When a big amount of data is missing, due to malfunctioning of the instruments or the subsequently filtering of the raw data, the ANN or LUT approach should be preferred. In 2013, the cumulative NEE fluxes gap filled with MDV are higher compared to the other two approaches, while in 2014 (the year with the lowest amount of gaps) the fluxes are in the same range of the other two methods, indicating the weaknesses of the approach

when a high amount of gaps and gaps of longer periods of time are present (Falge et al. 2001, Moffat et al. 2007).

The cumulative NEE fluxes gap filled with the ANN approach do not show a clear IAV, while the IAV is present in the gap filled NEE based on the other two approaches. IAV in the NEE fluxes were expected, due to the IAV the meteorological conditions (chapter 3.3). Potentially the reason that the IAV is lost is due to the selection of the parameters, although the same parameters are used in the LUT technique, where the IAV is present. Nevertheless, did the ANN compare well with the test dataset after the calibration. The addition of more parameters to the ANN could have resulted in a higher IAV, but for the comparison of the three gap filling techniques in this chapter the same parameters were used in the ANN and LUT methods.

For the three gap filling techniques over the three years the mean values of the annual sum of NEE are in the same range and showed that the peatland was a carbon source. The sum of relative error was the lowest for the ANN technique, but the IAV was lost. The look up table had higher SRE values indicating an overestimation of the NEE fluxes, nevertheless are the mean values of the annual sum of NEE in the same range indicating that the used method in the thesis is a valid approach.

The flux partitioning based on the night-time and day-time approach showed the same annual dynamics, with the highest GPP and R_{eco} values for the same year. The gap filling method resulting in the highest GPP and R_{eco} values per year did not correlate with the gap filling method resulting in the highest NEE values (

Table 4-3, Table 4-5 and Table 4-6). Based on the night-time approach the GPP and R_{eco} fluxes were much higher than based on the day-time approach, following the conclusions of Juszczak et al (2012) based on chamber measurements on peatland in Poland. The differences in the GPP and R_{eco} fluxes based on the two approaches do not have an impact on the work presented in this thesis, but should be taken into account when GPP and R_{eco} values are compared between sites and are used for modelling.

4.10.5 Conclusion

Three gap filling techniques are used in this chapter to gap fill three years of eddy covariance data measured from 2012-2014 at the peatland on Monte Bondone, Italy. This data was previously published by Pullens et al. (2016b) in Agricultural and Forest Meteorology. Three gap filling methods are used to identify changes in NEE fluxes when these different techniques are used: the Mean Diurnal Variability (Falge et al. 2001), the artificial neutral network (Dengel et al. 2013) and the Look up table (Reichstein et al. 2005) and two types of flux partitioning methods are used the night-time (Reichstein et al. 2005) and the day-time based approach (Lasslop et al. 2010). The neural network approach was the only gap filling method that reduces the interannual variability, that is present in the NEE with the other gap filling techniques. The mean values of the annual sum of NEE of all the gap filling techniques are in the same range and for all three years the peatland was a carbon source based on all three gap filling techniques. Based on the sum of relative error the look up table (Reichstein et al. 2005) is overestimating the NEE fluxes, nevertheless the mean values of the annual sum of NEE are in the same range indicating that the used method in the thesis is a valid approach.

The comparison of the two NEE separation techniques shows that with the day-time flux separation (Lasslop et al. 2010) both the GPP and the R_{eco} for the three gap filling techniques are lower than the GPP and R_{eco} calculated with the night-time flux separation approach (Reichstein et al. 2005). These differences indicate that the GPP and R_{eco} values provided in the literature should be treated with this uncertainty, in particular when the GPP and R_{eco} fluxes are used in models.

4.11 Appendix III: Spatially heterogeneous release of methane fluxes

The presented methane fluxes in chapter 4 are further analysed and described in this appendix to discuss the possible mechanisms for the spatially heterogeneous release of CH_4. The occurrence of ebullition has been tested by correlating the CH_4 fluxes with the measured air pressure, but due to the spatially heterogeneity of the field, the subsequent conclusion that ebullition does not play a role in this peatland was potentially stated as a too strong conclusion. For this reason, a more in-depth analysis of the non-gap filled CH_4 fluxes is performed in which the occurrence of ebullition or other heterogeneous mechanisms are investigated.

To test the occurrence of ebullition or other heterogeneous mechanisms, the correlation between the covariance of the CO_2, H_2O and CH_4 fluxes with the vertical wind speed (w'), when w' is positive, is tested. If the covariances of the fluxes and w' are correlated, the fluxes are turbulence-driven and hence no ebullition or other heterogeneous mechanisms are driving the CH_4 fluxes. The correlation between the covariance of the CO_2 and H_2O fluxes and w' is also analysed as a comparison for the correlation between the covariance of the CO_2 and CH_4 fluxes and w'. The non-gap filled data set is split into a day and night dataset to analyse differences in day and night time fluxes and correlations.

A high correlation between CO_2 and H_2O fluxes was found for both day (-0.7, $p < 0.05$) and night (0.33, $p < 0.05$), these values are set as a baseline to which the correlation with the CH_4 is measured. The CH_4 fluxes are tested for correlation between CO_2 and H_2O fluxes (both the day- and night-time fluxes, Table 4-7).

Table 4-7 Correlation coefficients between the covariances of the CO_2, H_2O and CH_4 fluxes and w' for both night- and day-time fluxes

	CO_2	H_2O
Day-time	0.08 ($p < 0.05$)	-0.15 ($p < 0.05$)
Night-time	-0.02 ($p > 0.1$)	-0.06 ($p < 0.05$)

Analysis show a weak correlation between the CH_4 fluxes and the CO_2 and H_2O fluxes for both night-and day-time. All correlation coefficients between CO_2 and CH_4 and H_2O and CH_4 are lower than the correlation coefficients between CO_2 and H2O, indicating that the CH_4 fluxes are not turbulence-driven. The results presented in this appendix indicate that, in contrast to the conclusion stated in chapter 4, ebullition and other heterogenous mechanisms and not turbulence are driving the CH_4 fluxes in the Monte Bondone peatland.

5 Water, energy and carbon balance of a peatland catchment in the Alps

J.W.M. Pullens[1,3 *], M. Sottocornola[2], G. Kiely[3], D. Gianelle[1,4], R. Rigon[5]

[1] Sustainable Agro-Ecosystems and Bioresources Department, Research and Innovation Centre – Fondazione Edmund Mach, San Michele all'Adige, Trento, Italy

[2] Department of Science, Waterford Institute of Technology, Waterford, Ireland

[3] Hydromet, Department of Civil and Environmental Engineering and Environmental Research Institute, University College Cork, Cork, Ireland

[4] Foxlab Joint CNR-FEM Initiative, San Michele all'Adige, Trento, Italy

[5] Department of Civil, Environmental and Mechanical Engineering, CUDAM, University of Trento, Trento, Italy

[*] Corresponding author: johannes.pullens@fmach.it

Under review at Water Resource Research, hence the American language

5.1 Abstract

Over millennia, peatlands have stored around 30% of the global soil organic carbon. The peat has formed and accumulated due to the slow decomposition rate of organic matter in waterlogged, anaerobic conditions. It is therefore important to understand the water cycle of peatlands to understand the functioning of peatlands. The water and energy cycle of an alpine catchment in Italy, which includes a peatland, was studied using the process-based hydrological model GEOtop and an appropriate set of in situ measurements to simulate 4 years (2012-2015) of water and energy fluxes. This is a challenging modelling exercise that has not been tried before with GEOtop, because it focuses on a complex (peatland, grassland, scree, bare rock) mountainous catchment. The GEOtop model was able to replicate the energy and water fluxes measured by an eddy covariance tower located in the peatland and the volumetric water content and soil temperature of the peatland accurately over the four year. This study shows that a process-based hydrological model can be used to study the water and energy dynamics of a peatland in a mountainous area.

Moreover, the modeled water cycle, together with a number of water sample analyses, was used to quantify the loss of dissolved organic carbon (DOC) and hence to calculate the full carbon balance of the peatland together with CO_2 and CH_4 fluxes measured by the eddy covariance tower.

5.2 Introduction

Peatlands are highly dependent on water, as in the waterlogged, anaerobic soils the decomposition of organic matter is very slow. The organic matter accumulates and can form a peat layer ranging from centimeters to meters. Over millennia, globally, peatlands have stored up to 547 (473-621) Pg of soil organic carbon, in the form of

peat (Gorham 1991, Yu 2012). This is equivalent to about 30% of the global soil organic carbon (Gorham 1991).

Pristine peatlands are today mainly acting as carbon sinks (e.g. Lund et al. 2010, McVeigh et al. 2014), while disturbed peatland predominantly act as carbon sources (e.g. Hendriks et al. 2007, Aslan-Sungur et al. 2016). The accumulated carbon in peatlands can be lost as CO_2, through ecosystem respiration, as methane (CH_4) emissions and/or as dissolved organic carbon (DOC) in stream runoff. The stored carbon in the soil is vulnerable to environmental and climate change (Lafleur et al. 2003, Camill 2005, Frolking et al. 2011, McVeigh et al. 2014, Aslan-Sungur et al. 2016). Apart from the climate change many factors can influence the fate of the stored carbon, such as: ground water level (Murphy et al. 2009, Sottocornola and Kiely 2010b, Lewis et al. 2013, Miller et al. 2015, Pullens et al. 2016b), management (Hendriks et al. 2007, Wilson et al. 2007, van der Molen et al. 2007, Baldocchi et al. 2012) and water cycle (Roulet et al. 2007, Koehler et al. 2011). The source of water (ombrotrophic or minerotrophic) and its dissolved minerals is important for peatland ecosystems; differences in water sources and the dissolved nutrients lead to different plant communities (Koerselman 1989). The water cycle plays a crucial role in the functioning of peatland ecosystems (Gorham 1957).

The level of the water table impacts the carbon balance of peatlands, since a raise in water table depth can result in higher methane emissions (Wagner et al. 2003, Jungkunst et al. 2008) and/or in more runoff and thus a removal of organic matter through DOC in the water. A rising water table will also reduce the soil respiration due to anaerobic soil conditions (e.g. Sonnentag et al. 2010, McVeigh et al. 2014, Strachan et al. 2016). Therefore, it is important to understand the dynamics of the water table and thus the water cycle of the peatland catchment. To understand these

dynamics, state of the art hydrological models can be used. A decrease in precipitation will lead to the drying of peatlands and less waterlogged soils, which will result in higher decomposition rates of the peat. The expected rising temperatures from climate change will result in higher evaporation and decomposition rates, which may change the peatlands from natural carbon sinks to carbon sources.

Many studied peatlands are located in high latitude regions, where the vulnerability of their carbon storage, the effects on climate change and permafrost degradation has been investigated (Frolking et al. 2001, Camill 2005, Dorrepaal et al. 2009). Beside the occurrence of peatlands at high latitudes, peatlands also occur at high elevation, although less research has been done on the latter, because they are not the dominant ecosystems in those areas (Parish et al. 2008). Even though there are numerous peatlands in the Alps, which are being threatened by rising temperatures and changes in the precipitation regime (Beniston et al. 1997, IPCC 2007, 2013, Im et al. 2010, Eccel et al. 2012, Steger et al. 2013, Pepin et al. 2015, Tudoroiu et al. 2016), their carbon, energy and water cycle has been little studied. As to the authors knowledge, the carbon fluxes has been studied continuously over multiple years in only one alpine peatland (Pullens et al. 2016b), which is the focus of this paper as well.

To analyze the energy and water cycles in complex ecosystems, hydrological models are an essential tool for water and environment resource management (Devia et al. 2015). There are various hydrological models available (see (Todini 2007)), ranging from models based on the unit hydrograph to complex process based catchment models (Beven and Kirkby 1979, Gregory et al. 1996, Rinaldo and Rodriguez-Iturbe 1996, Ewen et al. 2000, Vivoni et al. 2004, Rigon et al. 2006, 2016, Endrizzi et al. 2014). The requirements and research questions of the user determine the choice of the model (Devia et al. 2015). Because of the multiplicity of interactions responsible

for peatlands dynamics, a process-based model of the water and energy budget in conjunction with a series of in situ measurements was used (Fatichi et al. 2016).

In this paper the process-based hydrological model GEOtop (Rigon et al. 2006) was implemented on a catchment in the Italian Alps. GEOtop v. 2.0 models the energy and water budgets at and below the soil surface (Endrizzi et al. 2014) and provides the soil-vegetation-atmospheric interactions (SVAT) for complex terrain. It has previously been implemented by Lewis et al. (2013) to study the effect of afforestation on the hydrology of a blanket peatland in Ireland, where it was shown that GEOtop is suitable for modelling the hydrological processes in a peatland. The model is also able to reproduce the spatial patterns of land surface temperature and soil moisture and the energy balance components in alpine and pre-alpine environments (Bertoldi et al. 2006, 2010, 2014, Chiesa et al. 2014, Hingerl et al. 2016). To date, GEOtop has not been used to simulate the water and energy balance over multiple years of an alpine catchment, in which a fen type of peatland is located.

Specifically, the paper aims at investigating: (I) the possibility to simulate the water and energy budgets of an alpine peatland with a process-based model; and (II) the capability of the model to reproduce the observed interannual variability (2012-2015) of the energy fluxes in a mountain area. The two objectives are addressed using the GEOtop v 2.0 model and in situ measurements. The latter are: the bulk density, the hydraulic conductivity, meteorological conditions, carbon fluxes (CO_2 and CH_4), and discharge and dissolved organic carbon (DOC) out of the peatland area. The DOC loss can subsequently be used to estimate the main components of the ecosystem carbon budget which includes the fluxes of CO_2, CH_4 and DOC, where the CO_2 and CH_4 fluxes have been previously measured and published (Pullens et al. 2016b).

5.3 Materials and Methods

5.3.1 The site

The study site is a 10 hectare minerotrophic fen located at 1563 m asl on the Monte Bondone plateau, near Trento, in the Eastern Italian Alps (Figure 5-1a, 46°01' N, 11°02' E). The peatland is located in a 93 ha catchment and includes part of the Palon mountain and the surrounding slopes to the mountain tops (Cima verde, Dos d'Abramo and Cornetto). The catchment area was calculated by means of the Qgis software (version 2.6, Brighton) with the DEM (resolution 1 by 1 meter) provided by the Autonomous Province of Trento. The catchment consists of bare rock (limestone) and rock with a very shallow layer of soil, some managed grassland (cut once a year), coniferous forest (Norway spruce (*Picea abies*) and European larch (*Larix decidua*)) and a minerotrophic fen type peatland. The resolution of the catchment was rescaled to 25 by 25 m for computational reasons.

The peatland is a relic of an ancient lake that was formed by a glacier during the last ice age (Cescatti et al. 1999). The thickness of the peat layer ranges from 80 cm at the border to 4.4 meter in the center (Dalla Fior 1969), in 1914 the top peat layer of 0.35 ha of the peatland was harvested for fuel (Cescatti et al. 1999). The peatland has different microforms (from high to low), hummock, lawns and hollows, where the lawns are flat areas in the peatland. The peatland at Monte Bondone has a diverse vegetation (Figure 1b, Perucco et al. 2013): the lawns are dominated by either grasses, *Molinia caerulea* or sedges, *Carex nigra* and *Eriophorum vaginatum*, while the main vegetation in the hollows consists of *Carex rostrata*, *Scorpidium cossonii* and *Sphagnum subsecundum* and *S. compactum*, and few short hummocks are covered by *S. compactum* and *S.* sect. *acutifolia* and *Calluna vulgaris*. In the center of the peatland a small open pool is located, which acts as a buffer for the discharge after a

precipitation event. Close to this pond, birches (*Betula pendula*) and cotton deergrass (*Trichophorum alpinum)* can be found. The vegetation at plot 1, 2, 4, 5 and 6 are mainly dominated by *Molinia caerulea*. At Plot 4 *Trichophorum alpinum* has a high cover and plot 4 is the only plot where *Sphagnum* species are highly present (*Sphagnum subsecundum*). Apart from *M. caerulea* the other abundant occurring plant species are: At plot 1 *Calluna vulgaris*, *Trichophorum alpinum*; At plot 2 *Carex nigra*; At plot 5 *Aulacomnium palustre*, *Equisetum palustre*, *Tomentypnum nitens* and at plot 6: *Campylium stellatum*, *Carex rostrata*, *Scorpidium cossonii.* At the other plots, no *M. caerulea* is present, Plot 3 is dominated by *Carex nigra*, plot 7 is dominated by *C. rostrata* and *Valeriana dioica*, plot 8 by *Scorpidium cossonii* and plot 9 by *Calluna vulgaris*.

The water table of the complete catchment flows on deep impermeable morainic strata, which results into seepage into the fen (Cescatti et al. 1999). Seepage reaches the surface in the peatland at two ephemeral springs (defined as inflows, Figure 1b). This water flows through superficial streams to the lowest point of the peatland, where the water drains into a perennial stream, which flows down the mountain (defined as outflow, Figure 1b).

The average annual air temperature of 2012, 2014 and 2015, were close to the long-term average, while the temperature in 2013 was lower (Table 5-1). In the first three years, the precipitation was higher than the long-term average, with 2014 being an exceptional wet year, while in 2015, the precipitation was well below the long-term average (Table 5-1).

Table 5-1 Annual average temperature and annual precipitation at the Monte Bondone peatland over the period 2012-2015in combination with the long-term average.

	Long-term average (1958-2008, Eccel et al. 2012)	2012	2013	2014	2015
Average annual air temperature (°C)	5.4	5.1	4.3	5.0	5.0
Precipitation (mm)	1290	1650.4	1740.6	2082.6	964.8

5.3.2 Experimental setup

An eddy covariance instrumented tower was mounted in the center of the peatland in 2011 to measure water, carbon and energy fluxes and meteorological conditions. A shielded probe (Rotronic M103A, Bassersdorf, Germany) measured air temperature and relative humidity at 2 m height. Incoming Photosynthetically Active Radiation (PAR) was measured by a LICOR 190SZ sensor (Licor, Lincoln, NE, USA), while the incoming and outgoing short- and longwave-infrared radiation was measured by a CNR1 (Kipp & Zonen, Delft, the Netherlands). Both of these latter two sensors were installed on a horizontal bar at 3.5 meter above the soil surface. The volumetric soil water content was measured between tussocks of *Molinia caerulea* and under *Calluna vulgaris* at 5 cm depth with a CS616 water content reflectometer (Campbell Scientific, Logan, UT, USA). The distance between the locations, where these two sensors were installed is around 10 meters. The soil temperature was measured along a profile at 2, 5, 10, 20 and 50 cm depth with a STP01 sensor (Hukseflux Thermal Sensors B.V, Delft, the Netherlands) from the 1st July 2012. All data was collected once a minute on a CR3000 data logger (Campbell Scientific, Logan, UT, USA) with an AM16/32 multiplexer (Campbell Scientific, Logan, UT, USA) and averaged to half-hourly values. Wind speed, wind direction and sensible heat fluxes were measured at 20 Hz with a R3-100 3D sonic anemometer (Gill instruments, Lymington, Hampshire, UK).

The latent heat fluxes were measured with the eddy covariance system, consisting of two infrared gas analyzers (LI7500 and LI7200 (Licor, Lincoln, NE, USA)). The data of the gas analyzers and the anemometer was stored on an industrial computer (FX5507, Fabiatech, Taipei, Taiwan) located in the field (Pullens et al. 2016b).

On the 16th December 2013 a heated tipping bucket rain gauge (model 52202 Young, Traverse City, MI, USA) was installed. Before then, the precipitation data from a meteorological station, located 400 m away from the EC tower, was used (Meteo Trentino, station name: Giardino Botanico). In addition, the total snow height and the snow density of the freshly fallen snow were daily manually measured at this location by the provincial meteorological service, Meteo Trentino.

Missing meteorological data (20% of the half hourly data points, due to malfunctioning of the sensors or power shortage) were replaced by data from a nearby (500 meters horizontal distance) eddy covariance tower located in a grassland (Figure 5-1a) (Marcolla et al. 2011, Sakowska et al. 2014). For soil temperature, a dissimilarity was expected between the grassland and the peatland, but there was a highly significant relationship between the two sites for all depths ($R^2 > 0.95$, $T_{soil,peatland,5cm} = -0.46+0.94* T_{soil,grassland,5cm}$). The remaining gaps in the meteorological data (0.9%), caused by malfunction of both towers, were replaced by data from two nearby meteorological stations of Meteo Trentino (Figure 5-1a, Giardino Botanico and Viote, the latter 1 km away from the peatland tower). Soil temperature was not measured at the Meteo Trentino weather stations, therefore when missing, soil temperatures were replaced by linear interpolations. A more detailed overview of the site and the instruments is described in (Pullens et al., 2016b).

The measured soil water content data was not considered correct when the soil was covered by snow; under these conditions the temperature of the soil at the depth of the

soil water content probes (5 cm) was around zero degrees Celsius, which resulted in soil water content measurements dropping to unrealistic values (< 20%).

5.3.3 Soil properties

Soil samples were collected on 3-4 July 2014 for physical and chemical analyses under all nine main vegetation types occurring in the fen (Figure 5.1b). At each point, three soil samples replicates located at 1 m distance were collected at different depths (0-5, 50-55 and 100-105 cm). The samples at 0-5 cm were taken with Eijkelkamp soil core sampler rings (diameter 5 cm, height 5 cm, volume 98 cm^3), while at the depths of 50-55 and 100-105 cm the samples were collected with an Eijkelkamp split tube sampler (Eijkelkamp, Giesbeek, the Netherlands, same dimensions as the soil core sampler rings). The samples were not taken in plant tussocks.

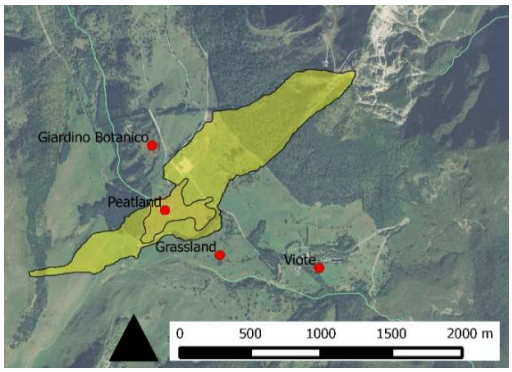

Figure 5-1a Catchment area (yellow shade, 93 ha) plotted over an aerial picture, with the four meteorology stations (in red). The "Viote" and "Giardino Botanico" meteorology stations are managed by MeteoTrentino. The "Peatland" and "Grassland" are eddy covariance towers. The turquois line is the stream outflow from the peatland. The outline of the peatland is drawn with a darker yellow inside the catchment area. Orthophoto from Autonomous Province of Trento.

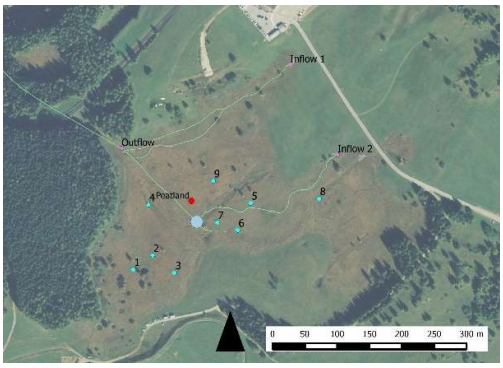

Figure 5.1b Overview of the peatland with the location of the eddy covariance tower (red), sampling points of the bulk density (light blue), measurement sites of stream flow and DOC at inflow 1,2 and the outflow (purple) and the streams/channels (blue-green). The location of the pool is indicated with a blue dot. Orthophoto from Autonomous Province of Trento.

Overall, 81 samples were collected from the 9 plots; samples that were too compacted due to compression were discarded as well as samples which were too wet, i.e. slurry. In total 50 soil samples were transported in closed plastic bags to the laboratory for analyses. The samples were composed of 27 samples from 0-5 cm, 15 samples from

50-55 cm and 8 samples from 100-105 cm depths. Each sample was weighed on the day of sampling before it was oven dried at 55°C until a stable mass was reached (after ~24 hours) to calculate the bulk density. The bulk density was sampled to explore the soil variability and to identify the plots for hydraulic conductivity measurements (Assouline 2006), where an increase in soil bulk density associated with compaction can impact on soil hydraulic properties (Laliberte et al. 1966).

After this step, the soil was grinded with a mortar and pestle, to break clumps of peat, before it was sieved (2 mm sieve) to remove leaves and roots. A subset of the sample was placed in a metal container with a metal ball and inserted in a Mixer Mill MM 200 (Retsch, Haan, Germany), which was run at the speed of 25 Hz for 5 minutes. The rest of the sample was placed in a 105°C oven to measure the remaining water content. A homogenous subsample (5 mg) from the ball-milled samples was inserted in tin caps and the amount of soil carbon and nitrogen was measured in a PerkinElmer 2400 Series II CHNS/O Elemental analyzer (PerkinElmer, Waltham, MA, USA).

Before statistical analysis was applied, the bulk density data was tested for normality. In this study all of the values were normally distributed (Shapiro-Wilk test, W=0.99, p=0.9). For the statistical analysis of the bulk density, the Tukey's HSD (honest significant difference) test was used using the R software (version: 3.1.2, (R Development Core Team. R Foundation for Statistical Computing 2017)).

5.3.4 Hydraulic conductivity

The saturated hydraulic conductivity of the peatland soil was measured by means of the adjusted Modified Cube Method presented in Lewis et al. (2012). In literature, different methods are used to measure the hydraulic conductivity, such as the standpipe technique (Hvorslev 1951) and Modified Cube Method (MCM, Beckwith et al. 2003). An advantage of the MCM over the standpipe technique is that with the

MCM both the horizontal and the vertical hydraulic conductivity can be measured. In August 2014 two soil samples from 5 of the 9 bulk density plots were sampled at 0-10 and 40-50 cm depths. These plots were chosen because they showed the biggest range of bulk density (see Results section) and therefore the extent of hydraulic conductivity in the peatland could be analyzed (Assouline 2006). A metal tube with a square section (12x12x100 cm) and a cutting edge was driven into the peat to a depth of 70 cm, after the vegetation was removed from the top soil to prevent damage to the peat core. The tube was extracted and due to suction, the sample stayed in the sampling tube during the retrieval. The saturated hydraulic conductivity was calculated by using Darcy's law (Darcy 1856):

$$K_{sat} = \frac{Q*L}{A*\Delta h} \quad (5.1)$$

in which, K_{sat} is the saturated hydraulic conductivity (m s^{-1}), Q is the discharge (m^3 s^{-1}), L is the length of the sample (m), A is the area of one open side of the cube (m^2), and Δh is the difference in head between the top and bottom of the sample (m). For each peat block, both the horizontal and vertical hydraulic conductivities were measured. For the horizontal hydraulic conductivity**,** the procedure was identical, only the blocks were rotated 90 degrees. The hydraulic conductivity was only measured on soil samples from the peatland. Due to lower volumetric water content in the surrounding soils, there was no suction of the soil to remain in the sampler. For these soils hydraulic conductivity values from literature are used.

5.3.5 Streamflow and dissolved organic carbon (DOC)

The stream heights at the two inflows and the outflow of the peatland were measured with pressure transducers (Dipper-PT, *SEBA* Hydrometrie GmbH & Co., Germany). The pressure transducers were installed in perforated pipes on the May 14 2014. The

water level was measured every half-hour and the data was stored on internal Flash memory cards and collected at regular intervals.

The streamflow was measured and water samples for dissolved organic carbon (DOC) were collected at the same locations as the stream height (Figure 1b). The streamflow was measured 10 times during 2014 and 2015 with a FP111 Global Flow Probe (College Station, Texas, USA) to convert the stream height measurement time series in discharge time series. The uncertainty of the device used for the flow measurements is 0.1 m/s. No weir was allowed to be installed at the in- and outflows since the site is a Natura 2000 protected area. Stream flow measurements were complicated due to the dynamic cross sections of the stream channels and the occurrence of dense vegetation in the stream.

During the streamflow measurements, stream water samples (around 500 ml) were collected. The samples were filtered in the laboratory with a Millipore System, using Isopore™ Membrane filters with 0.4 µm pore size (Merck Millipore, Billerica, MA, USA). After the filtration, the samples were frozen and stored at -20°C before shipment to the department of Agriculture of the University of Bologna. At the University of Bologna the samples were melted and well mixed. From each sample a 2 ml aliquot was taken, where 30µl of 2M HCl was added. To eliminate inorganic carbon the samples were sparged for 3 minutes. After this step, 50 µl of each sample was inserted in a TOC-V-RMN1 Shimadzu analyzer and combusted at a temperature of 720°C. At least three measurements of organic C and total N (mineral and organic dissolved N) were performed with the same sample (a minimum of three to a maximum of five in order to have the lowest coefficient of variation among three measurements).

5.3.6 GEOtop

GEOtop is a process-based distributed model of the water and energy budget (Rigon et al. 2006), that requires a digital elevation model (DEM), soil type, vegetation and river networks in distributed maps for the catchment. Also meteorological data is needed to calculate the water and energy balance of the given catchment: precipitation, air temperature, wind speed, wind direction, incoming short- and longwave radiation, which were all measured at an eddy covariance tower in the peatland (Pullens et al. 2016b). During this study, the GEOtop model was run with an hourly time step to calculate the water and energy balance over the complete catchment, therefore all input data was aggregated to hourly values. GEOtop incorporates precipitation to calculate evapotranspiration, runoff and seepage. To model the horizontal and vertical movement of the water in the soil, a fully three-dimensional description of the Richards' equation is used (Endrizzi et al. 2014). For this modelling exercise, the authors used the GEOtop version 2.0, which also simulates freezing soils (Dall'Amico et al. 2011) and a multi-layered snow cover (Endrizzi et al. 2014), which is necessary since the Monte Bondone site receives snow every winter.

The modeled period was October 1 2011 until January 1 2016 where the initial three months were used as a spin-up. The temperature and precipitation at higher altitudes than the tower were calculated using lapse-rates; for temperature 6.5 °C km^{-1} and a precipitation lapse rate of 0.2 mm km^{-1} (Gubler et al. 2013), which are the average lapse-rate values calculated for the complete Autonomous Province of Trento (Eccel et al. 2012). The air temperature threshold when the precipitation was considered as snow instead of rain was set to 0°C.

The soil and plant parameters are needed as input variables in GEOtop and are crucial for the water and energy dynamics (Table 5-2). All plant parameters are set constant

over the complete modelling period, as no detailed in-situ information was available over the complete modelling period on the dynamics of the vegetation in the complete catchment. The catchment was partitioned into four different soil types: bare rock and rock with a very shallow layer of soil (scree); peat; mineral soil and mineral soil with high hydraulic conductivity. A mineral soil with a high hydraulic conductivity, an artificial pathway, was added because GEOtop needed it to be able to model water flowing into the peatland.

An average of measured values of hydraulic conductivity was used for the peatland, more details of the field measurements are presented in the Results section. For the rocks and grassland the hydraulic conductivity values were initially taken from literature (Holden and Burt 2003, Xie et al. 2012, Lewis et al. 2012, Gubler et al. 2013, Cunliffe et al. 2013, Endrizzi et al. 2014, Chiesa et al. 2014), and were manually varied minimal (less than 10%) around those values, but within the measured ranges which are presented in the mentioned references (Table 5-3). The hydraulic conductivity values derived from literature were varied in such a way that the simulated discharge was behaving in a natural matter, thus no immediate peak runoff or stagnation of water was simulated. The depth of the bedrock/impermeable soil layer was set to the measured maximum depth of the peat of 4 m (Dalla Fior 1969), at this depth the hydraulic conductivity was set to 0 mm s^{-1}, to create an impervious boundary. The soils in the catchment were divided in 6 layers, with increasing depth from 0.1 to 1.5 m (0-0.1, 0.1-0.4, 0.4-0.5, 0.5-1.5, 1.5-2.5, 2.5-4 m). The soil depth of the "bare rock and rock with a very shallow layer of soil" was set to 0.5 m, while for the other sites a constant soil depth of 4 meter was used.

Table 5-2 Vegetation parameters used in the GEOtop simulations for the Monte Bondone catchment. Parameters not mentioned in this table are kept at the default value.

	Rock	Grassland	Peatland	Forest
Height of vegetation (mm)	200	300	300	3000
Depth of roots (mm)	100	300	300	1000
LAI (m/m)	1	1	2.5	4
Canopy fraction (%)	95	95	95	100
Vegetation reflectivity in the visible spectrum	0.15	0.15	0.4	0.15
Vegetation reflectivity in the near infrared spectrum	0.4	0.4	0.4	0.4
Vegetation transmissivity in the visible spectrum	0.07	0.07	0.07	0.07
Vegetation transmissivity in the near infrared spectrum	0.32	0.32	0.32	0.32

Table 5-3 Soil parameters used for simulating the water and energy balance of the Monte Bondone peatland. The values of the hydraulic conductivity of the peatland are the measured values in this study. Other values are derived from literature (Holden and Burt 2003, Xie et al. 2012, Lewis et al. 2012, Gubler et al. 2013, Cunliffe et al. 2013, Endrizzi et al. 2014, Chiesa et al. 2014)

	Symbol	Unit	Rocks	Mineral soil	Mineral soil with high hydraulic conductivity	Peat
Horizontal saturated hydraulic conductivity 0-40 cm depth	$Kh_{sat0-40}$	$m\ s^{-1}$	$1 \cdot 10^{-5}$	$2 \cdot 10^{-4}$	$1 \cdot 10^{-3}$	$3 \cdot 10^{-6}$
Vertical saturated hydraulic conductivity 0-40 cm depth	$Kv_{sat0-40}$	$m\ s^{-1}$	$1 \cdot 10^{-5}$	$2 \cdot 10^{-4}$	$5 \cdot 10^{-4}$	$1 \cdot 10^{-6}$
Horizontal saturated hydraulic conductivity 40-400 cm depth	$Kh_{sat40-400}$	$m\ s^{-1}$	$1 \cdot 10^{-5}$	$2 \cdot 10^{-6}$	$1 \cdot 10^{-3}$	$2 \cdot 10^{-6}$
Vertical saturated hydraulic conductivity 40-400 cm depth	$Kv_{sat40-400}$	$m\ s^{-1}$	$1 \cdot 10^{-5}$	$2 \cdot 10^{-6}$	$5 \cdot 10^{-4}$	$6 \cdot 10^{-7}$
Residual water content	Θ_{res}	-	0.05	0.25	0.05	0.2
Saturated water content	Θ_{sat}	-	0.3	0.5	0.3	0.9
Van Genuchten	n	-	2	2	2	1.8
Van Genuchten	α	cm^{-1}	0.01	0.1	0.5	0.05

GEOtop calculates the water and energy balance of each 25m side grid cell composing the catchment. To validate the model, the output of the grid cell where the eddy covariance tower is located was compared with the measured 5 cm depth soil temperature and water content, with snow depth, outgoing short- and longwave radiation, the latent and sensible heat fluxes and the stream discharge of the complete catchment.

5.4 Results

5.4.1 Bulk density

The bulk density of all samples ranged from 0.04 to 0.22 g/cm^3, while its averages were 0.10 (± 0.03), 0.14 (± 0.02) and 0.16 (± 0.05) g/cm^3 at 0-5, 50-55 and 100-105 cm depth respectively. No significant difference between the three replicates at each of the nine plots was found (data not shown, Tukey test, $\alpha = 0.05$). The bulk density of all the plots was significantly higher at 100-105 cm depth compared to 0-5 cm depth ($p = 0.002$), while there was no statistical difference between 50-55 cm depth and 100-105 cm depth and 0-5 cm depth and 50-55 cm depth. At the 0-5cm depth layer, the bulk density of two plots 3 and 7 (Figure 5-2a), both located close to the peatland edge and with some plant species common to grasslands (e.g. *Deschampsia cespitosa* and *Primula farinosa*), was statically higher than all the other samples at the same depth (Figure 5-2, Tukey test, $\alpha = 0.05$). No statistical difference between plots was found at deeper layers.

The mean soil carbon-to-nitrogen (C/N) ratios were 23.61 (± 8.98), 20.34 (± 4.68) and 20.13 (± 5.21) at 0-5, 50-55 and 100-105 cm depth respectively. The C/N ratio of the peat was only significantly higher at 0-5 cm depth under a *Calluna vulgaris*-dominated plot (plot 9, Figure 5-2b). There was no significant difference among the depths.

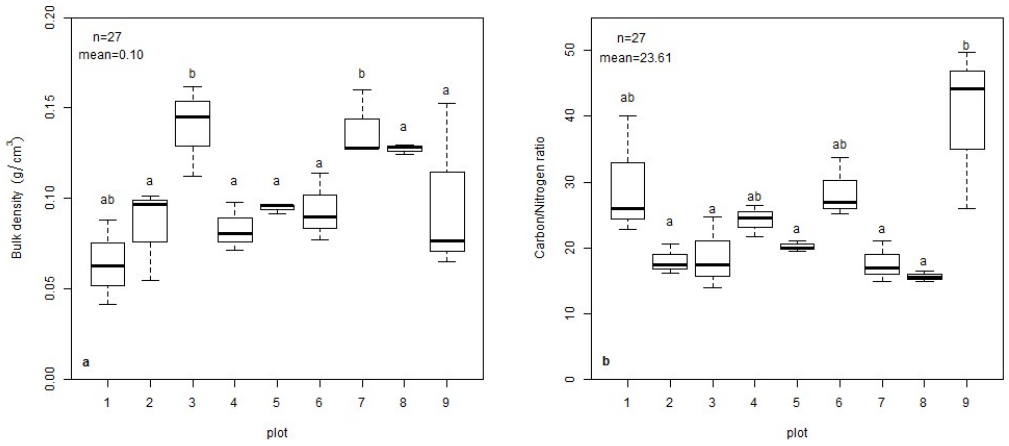

Figure 5-2a. Bulk density of soil samples collected at 0-5 cm depth. Samples with the same letter did not differ significantly based on Tukey HSD pair-wise comparison (α = 0.05). b. Carbon/nitrogen ratio of soil samples collected at 0-5 cm depth. Samples with the same letter did not differ significantly based on Tukey HSD pair-wise comparison (α = 0.05).

5.4.2 Hydraulic conductivity

Since the highest variation in bulk density was observed between sample plots 1, 3, 4, 7 and 9, the horizontal and vertical saturated hydraulic conductivity was measured at these plots. In general the hydraulic conductivity of the peatland was very low, but the variation between the plots was very high (Table 5-4). The horizontal saturated hydraulic conductivity, Kh_{sat}, at the surface (0-5 cm) ranged from $2.11 \cdot 10^{-6}$ m/s to $2.74 \cdot 10^{-4}$ m/s (a difference of two orders of magnitude), while at deeper depth (40-50 cm), the Kh_{sat} ranged from $9.0 \cdot 10^{-8}$ m/s to $1.51 \cdot 10^{-5}$ m/s (a difference of three orders of magnitude). The vertical saturated hydraulic conductivity showed the same variability: $Kv_{sat,}$ at the surface (0-5 cm) ranged from $2.35 \cdot 10^{-6}$ m/s to $2.24 \cdot 10^{-5}$ m/s, a difference of one order of magnitude and at deeper depth (40-50 cm), Kv_{sat} ranged from $4.0 \cdot 10^{-7}$ m/s to $1.55 \cdot 10^{-5}$ m/s (a difference of two orders of magnitude). At plot 3, dominated by *Carex nigra*, it was not possible to collect the sample at 40-50 cm depth because the soil was too wet, i.e. slurry. Interesting to note is that at plot 9, where there is mainly *C. vulgaris*, the water drains very fast, while at plot 4, where more *Sphagnum* spp. is located, the water has a tendency to drain slowly.

*Table 5-4 Hydraulic conductivity of different plots and at different depths. *at plot 3 it was not possible to collect samples at the depth of 40-50 cm. NOTE: at plot 9 the horizontal hydraulic conductivity at 0-10 cm depth was 10-100 times higher compared to the other samples at the same depth.*

Depth		Plot 1	Plot 3	Plot 4	Plot 7	Plot 9
0-10 cm	Kh_{sat} (m s^{-1})	$2.43 \cdot 10^{-6}$	$6.97 \cdot 10^{-6}$	$2.11 \cdot 10^{-6}$	$3.02 \cdot 10^{-6}$	$2.74 \cdot 10^{-4}$
	Kv_{sat} (m s^{-1})	$2.24 \cdot 10^{-5}$	$1.41 \cdot 10^{-5}$	$1.18 \cdot 10^{-5}$	$1.13 \cdot 10^{-5}$	$2.35 \cdot 10^{-6}$
40-50 cm	Kh_{sat} (m s^{-1})	$1.51 \cdot 10^{-5}$	NA*	$4.09 \cdot 10^{-6}$	$2.24 \cdot 10^{-6}$	$9.01 \cdot 10^{-8}$
	Kv_{sat} (m s^{-1})	$8.03 \cdot 10^{-6}$	NA*	$6.97 \cdot 10^{-6}$	$1.55 \cdot 10^{-5}$	$4.03 \cdot 10^{-7}$

5.4.3 Dissolved organic carbon

The DOC concentrations at both inflows were low, while the outflow showed higher values (Figure 5-3). The average amount of DOC over the 9-month period is 0.72 (± 0.26) mg/L, 1.34 (± 1.07) mg/L and 3.02 (± 0.76) mg/L for inflow 1, 2 and the outflow respectively. The average difference between the outflow and the sum of the inflows is 0.96 (± 1.34) mg/L, indicating a carbon loss. A peak in DOC concentrations was observed in inflow 3 in the autumn, when the vegetation was senescing. After snowmelt there was a peak in inflow 2 (Figure 5-3), indicating a source of DOC from vegetation located higher in the catchment.

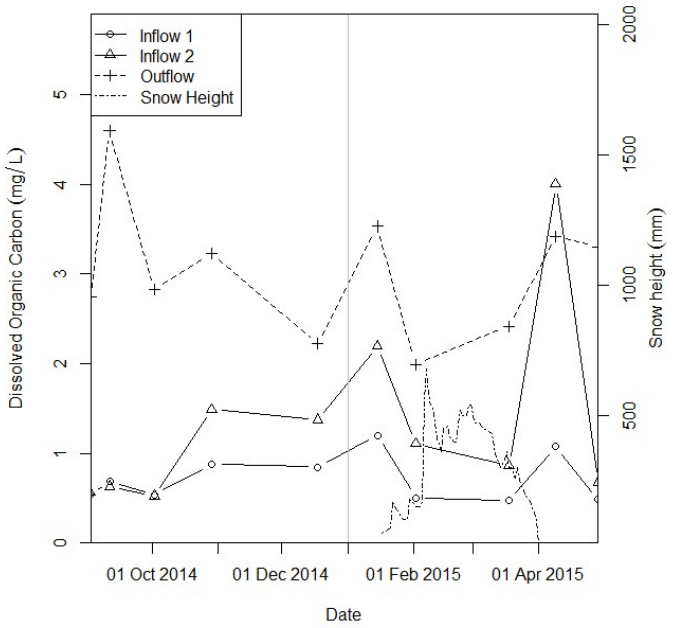

Figure 5-3 Dissolved organic carbon in water sampled during 2015 at two inflows/seepage (inflow 1 and 2) and one outflow (outflow). The snow height in mm is also indicated.

5.4.4 GEOtop

Over the four years (January 1 2012 until January 1 2016), GEOtop was able to simulate the soil temperature at 5 cm depth very accurately (Figure 5-4 and Table 5-6), even with a slight overestimation, in particular in the years 2012 and 2013. During the period of snow cover the model was performing worse than during the snow-free period (Table 5-6). Over the complete catchment, the peatland had the smallest amplitude in the soil temperature of all soil types, due to the higher soil water content.

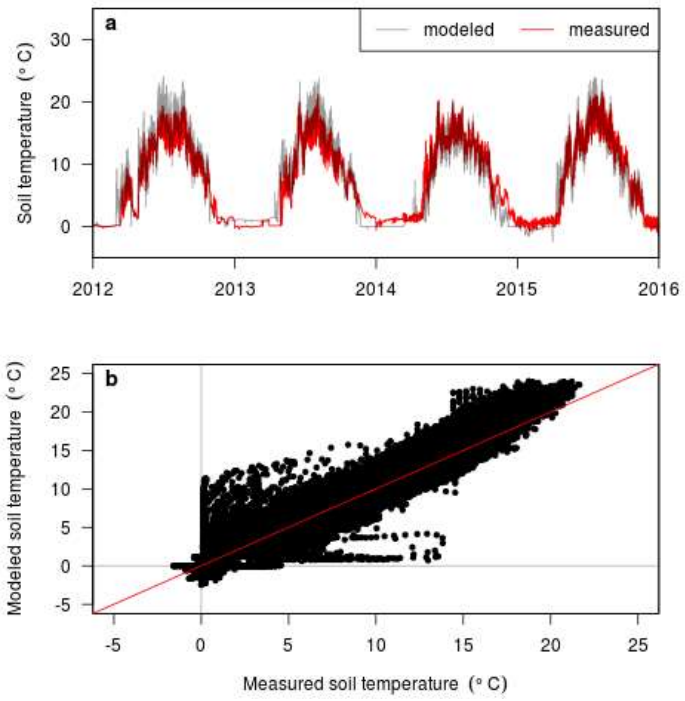

Figure 5-4 a. Time series and 1:1 regression plot (b) of the modeled and measured soil temperature at 5 cm depth over the period 2012-2015.

The outgoing shortwave radiation in winter is high due to the reflection of the light by the snow. During snowmelt, the values rapidly decrease when the soil and vegetation become visible again (Figure 5-5). The model slightly underestimated the measured outgoing shortwave radiation (Table 5-6, Figure 5-5), replicating measurements better during snow cover than in the snow-free period (Table 5-6).

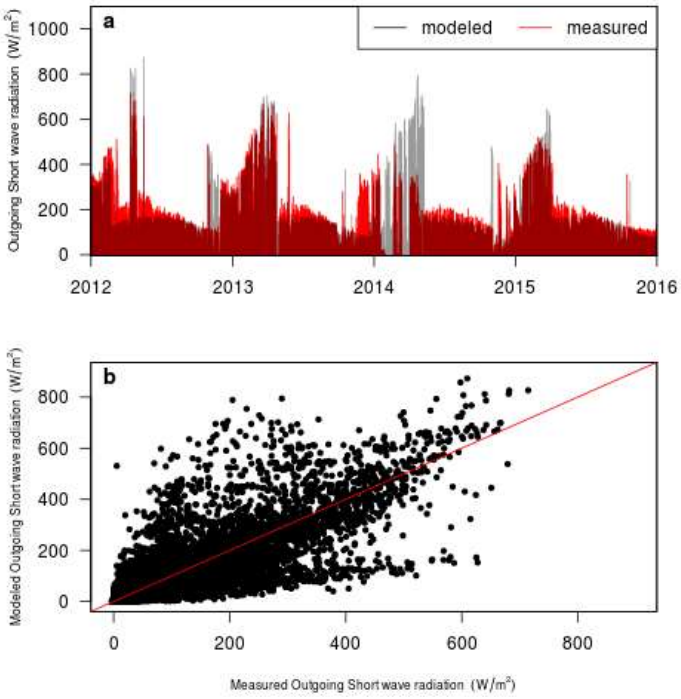

Figure 5-5 a. Time series and 1:1 regression plot (b) of the modeled and measured outgoing shortwave radiation over the period 2012-2015.

For outgoing longwave radiation the model performs overall better than for shortwave radiation (Table 5-6 and Figure 5-6). The model is following the measured seasonality and its outputs are in the same range as the measured values, particularly in the snow-free period (Table 5-6).

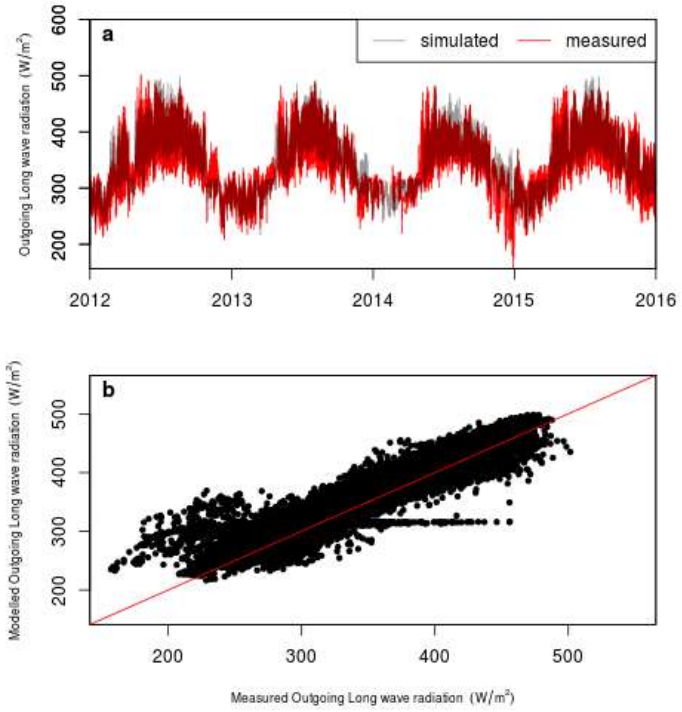

Figure 5-6 a. Time series and 1:1 regression plot (b) of the modeled and measured outgoing longwave radiation over the period 2012-2015.

The modeled soil water content of the catchment has a large spatial and temporal variability (Appendix 7.2). In the peatland, the measured soil water content during the snow-free period ranged between 25 and 90%. The model was able to follow the dynamics of the SWC over the years (Figure 5-7). The SWC measured under *Molinia caerulea* and *Calluna vulgaris* correlated well when no snow cover was present (R^2=0.75, RMSE=11.8, $swc_{Molinia}$ = 11.5 + 0.76 * $swc_{Calluna}$). The output of the model tracked the data from the sensor under *C. vulgaris* slightly better than the data from the sensor under *M. caerulea* (Figure 5-7 and Table 5-6). Overall, the model was able to follow the dynamics measured in the field, even the big drop in soil water content at the beginning of 2015. In 2014, which was the wettest year of the simulation, the model overestimated the soil water content during the summer months after the big rain events occurred. The model was representing the soil water content accurately in 2012 and 2013, with an overestimation of the SWC from the mid-2015.

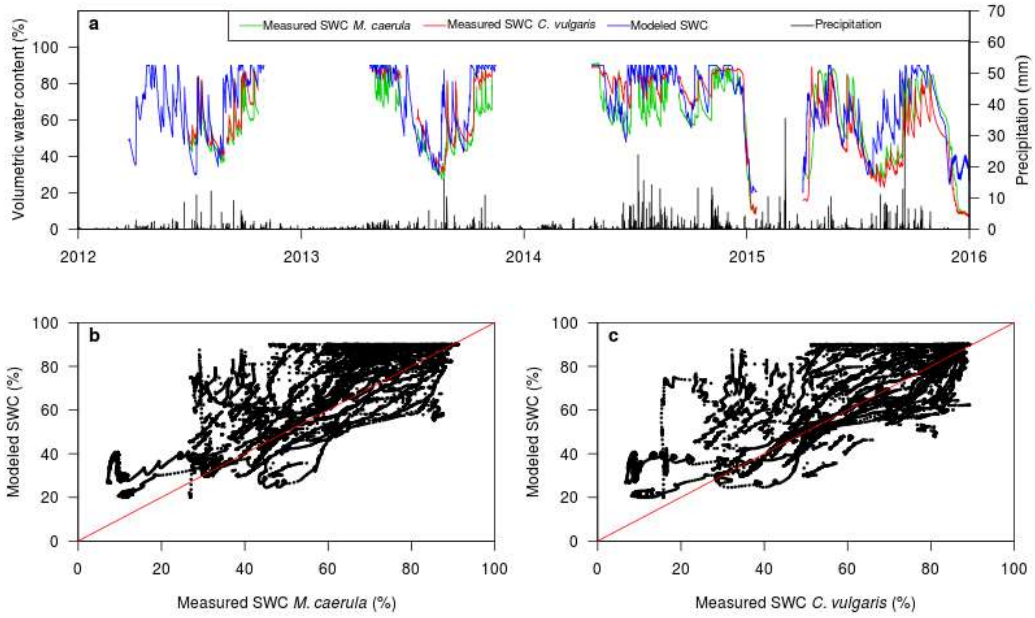

Figure 5-7 a. Time series of the modeled and measured soil water content at 5 cm depth and measured precipitation over the period 2012-2015. b and c. 1:1 regression plot of modeled soil water content and measured soil water content under Molinia caerulea (b) and Calluna vulgaris (c).

The modeled heat fluxes were compared with the measured, non-gap filled latent (Table 5-6, Figure 5-8) and sensible (Table 5-6 and Figure 5-9) heat fluxes measured with the eddy covariance system over the peatland (Pullens et al. 2016b). The modelled latent heat fluxes were overestimated (Figure 5-8), while the sensible heat fluxes were underestimated (Figure 5-9). The negative sensible heat fluxes occur when the air temperature is colder than the soil temperature and indicate a heat flux from the soil surface.

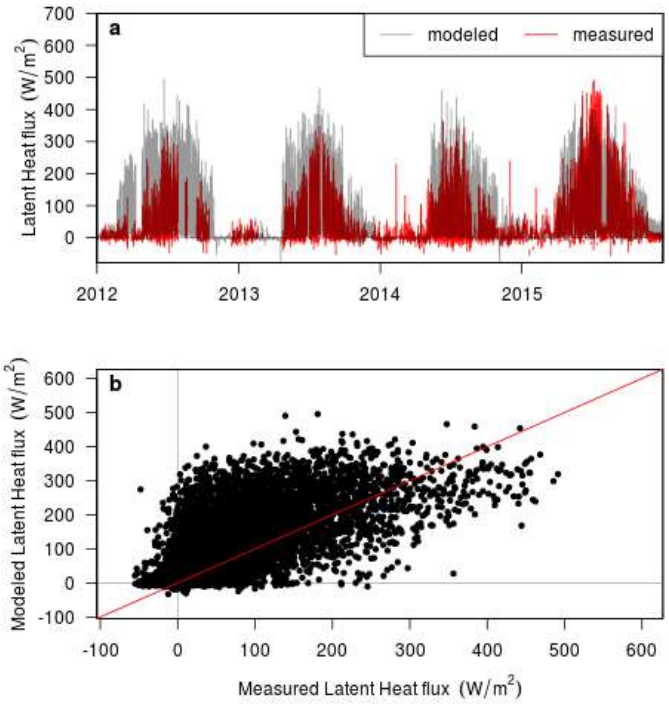

Figure 5-8 a. Time series and 1:1 regression plot (b) of the modeled and measured latent heat flux over the period 2012-2015.

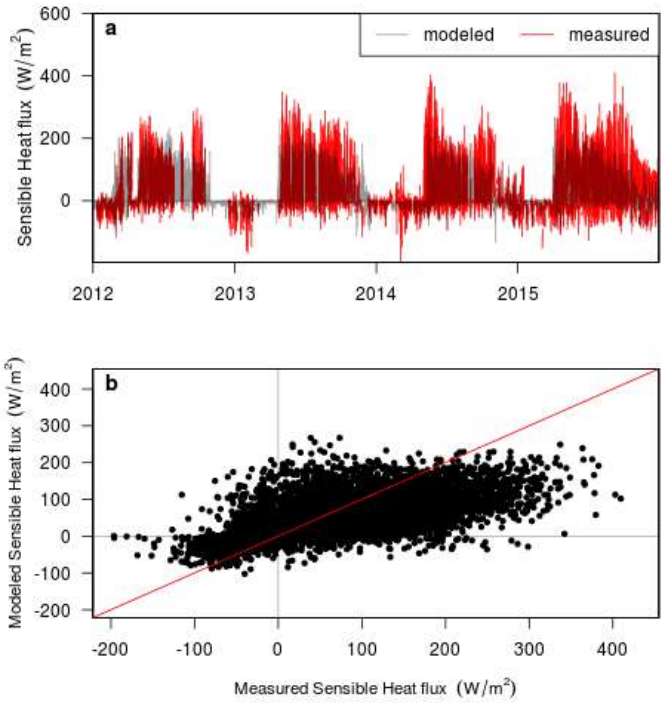

Figure 5-9 a. Time series and 1:1 regression plot (b) of the modeled and measured sensible heat flux over the period 2012-2015.

The simulated monthly energy balance of the peatland is illustrated in Figure 5-10. Most of the net radiation is converted by the system into latent heat flux (annual: 51%,

with a maximum of 65% in August). The energy balance is almost closed, with the total incoming energy being only slightly higher than the outgoing energy fluxes, the imbalance of the modelled energy balance closure was 9 % for each of the four years.

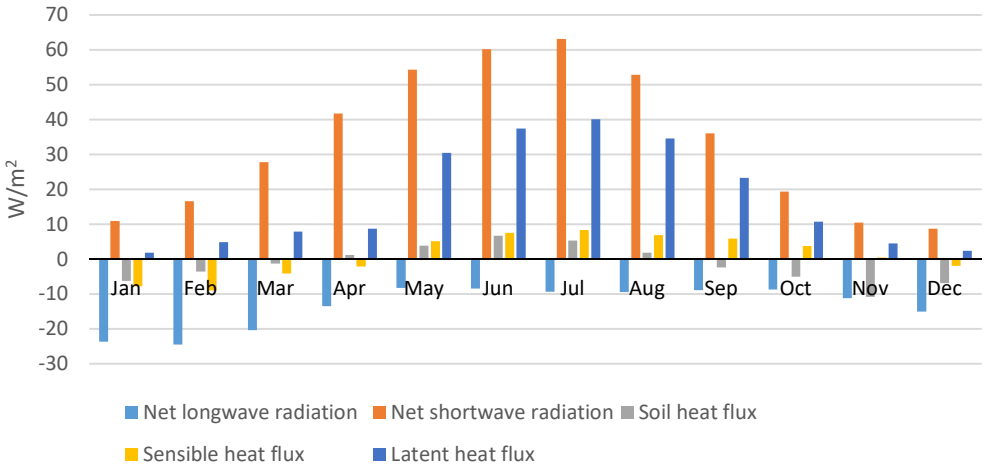

Figure 5-10 Modeled monthly energy balance at the Monte Bondone peatland averaged over 2012-2015.

The model is able to follow the interannual variability of the snow height correctly for the 4 years (Table 5-6 and Figure 5-11). The measured snow height ranged from 43 to 204 cm in 2012 and 2014. At the beginning of the 2014 - 2015 winter, the measured air temperature was below 0 °C, therefore the model simulated snow, while in the field no snow was present yet.

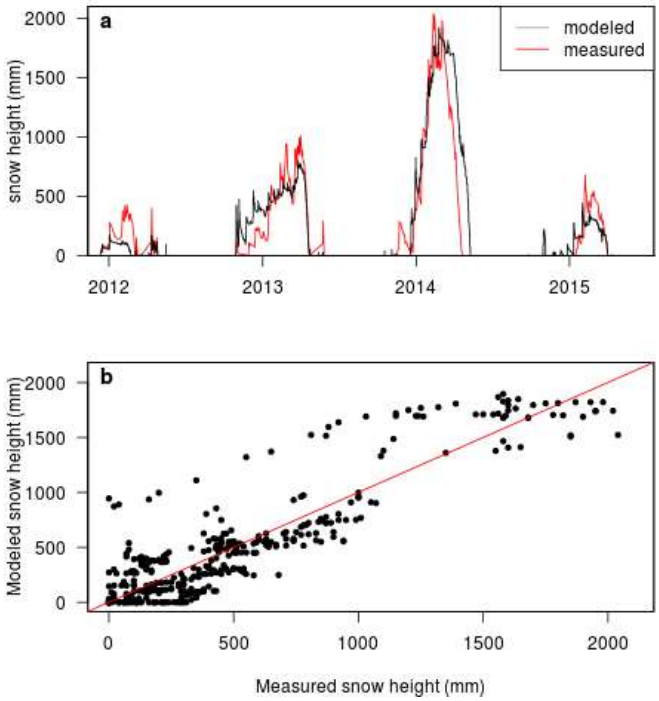

Figure 5-11 a. Time series and 1:1 regression plot (b) of the modeled and measured snow height over the period 2012-2015.

The modeled discharge is very spiky, as expected given the small catchment size (Figure 5-12 a and b). These spikes are not in the episodic measurements of the stream flow, since the flow was not measured immediately after a precipitation event. 2014 was the wettest year and the modeled discharge is higher than the episodic measurements. In 2015, the driest year, the model is much closer to the episodic measurements. The model simulated a mean annual flow of 29, 36, 50 and 20 L/s, for 2012, 2013, 2014 and 2015, respectively.

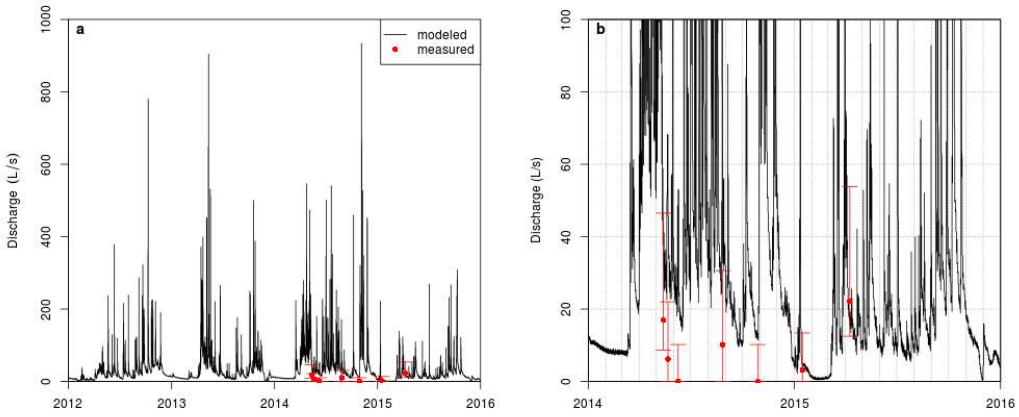

Figure 5-12 a. Modeled discharge over the period 2012-2015 in liters per second. The discharge measurements and their uncertainties are depicted in red. b Modeled discharge over the period 2014-2015 in liter per second. The discharge measurements and their uncertainties are depicted in red.

During 2012-2015, the average annual measured precipitation at the peatland was 1318 mm/year, the evapotranspiration was 214 mm/year (16% of precipitation) and the discharge 1148 was mm/year (84% of precipitation). The modelled monthly water balance is depicted in Figure 5-13. In winter, there was very low evapotranspiration. During spring (April and May) the snow melts, which results in a high discharge indicating that precipitation was stored as snowpack. While in November and December the precipitation is higher than the discharge indicating the arrival of snow.

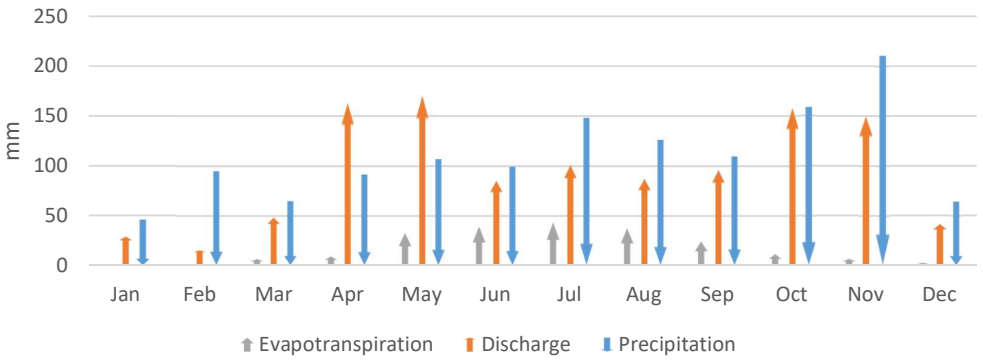

Figure 5-13 Monthly water balance at the Monte Bondone peatland averaged over 2012-2015.

The estimation of discharges was required to determine the DOC flux. The annual DOC export was calculated with the average concentration of DOC (0.96 ± 1.34

mg/L), and the modeled monthly stream flow (Table 5-5). The carbon balance of the peatland over the years 2012 – 2015 including CO_2, CH_4 and DOC fluxes was 168.3 ± 82.0 g C m^{-2} yr^{-1} (Table 5-5), indicating a loss of carbon.

Table 5-5 DOC export, percentage of NEE by the DOC export and the complete carbon balance of the peatland over four years (2012-2015).

	2012	2013	2014	2015
DOC export (g C m^{-2} yr^{-1})	7.7	12.3	13.8	8.0
Percentage of extra loss of DOC of the measured NEE	7.5 %	4.7 %	7.9 %	9.0 %
Complete carbon balance (CO_2, CH_4 and DOC fluxes, g C m^{-2} yr^{-1})	111.2	275.3	189.5	97.3

*Table 5-6 Spearman's correlation, root mean square error (RMSE) and linear regression of soil temperature, outgoing short- and longwave radiation, soil water content, latent and sensible heat fluxes between model outputs and measurements for the complete period of 2012-2015 and for the sub periods with or without snow cover. * The soil water content measurements are not considered reliable under snow cover. **The regression is formulated as "modeled=a+bx", in which x is the measured variable.*

		Soil temperature (°C)	Outgoing shortwave radiation (W/m^2)	Outgoing longwave radiation (W/m^2)	Soil water content *C. vulgaris**	Soil water content *M. caerulea**	Latent heat flux (W/m^2)	Sensible heat flux (W/m^2)
Complete period	R^2	0.92	0.74	0.86	-	-	0.53	0.52
	RMSE	1.90	48.13	20.06	-	-	67.89	55.10
	Regression**	-0.20+1.06x	3.40+0.90x	29.8+0.93x	-	-	28.4+0.96x	12.8+0.46x
Sow cover	R^2	0.15	0.78	0.63	-	-	0.27	0.24
	RMSE	2.23	61.25	16.61	-	-	17.49	29.70
	Regression**	0.28+0.52x	37.73+0.94x	81.4+0.72x	-	-	4.20+0.40x	-4.28+0.18x
No snow cover	R^2	0.83	0.67	0.83	0.60	0.56	0.47	0.09
	RMSE	1.25	40.66	21.50	15.36	16.39	60.10	90.61
	Regression**	-0.09+1.05x	4.690.85x	70.1+0.83x	2.10+0.88x	8.19+0.75x	16.01+0.3x	3.39+0.033x

5.5 Discussion

The vegetation in the peatland is heterogeneous, which results in differences in bulk densities and C/N ratios. The occurrence of some grassland plant species in two plots could suggest that the peatland is slowly being transformed into a grassland, via the encroachment of grassland and woody plant species surrounding the peatland (Gerdol et al. 2008, Stine et al. 2011, Holmgren et al. 2015). At the plot where *Calluna vulgaris* was located (plot 9), the bulk density did not differ significantly from the other plots, while the C/N ratio of the soil top layer was higher than any other plots. Due to the differences in vegetation and bulk densities, the hydraulic conductivity in the peatland was highly variable with differences of two-three orders of magnitude (plot 1, 3, 4, 7 and 9, Table 5-4). Differences of these orders of magnitude have been observed in other peatlands (Lewis et al. 2012, Cunliffe et al. 2013) and can arise from different humification and fibrosity of the peat (Hoag and Price 1995, Cunliffe et al. 2013).

The spatial variability of the hydraulic conductivity introduces a high uncertainty in the simulation of soil water content. For this study, the average of the hydraulic conductivity of the plots with the most abundant plant species was used (Table 5-4). The hydraulic conductivity of the rock and mineral soils in the catchment is based on a literature study and on model evaluations. The error introduced into the model by using literature values cannot be quantified, because no hydraulic conductivity have been measured in the other soil types. Due to the low moisture content of these soils there was no suction of the soil to remain in the sampler, and therefore no samples were taken. During first trial simulations, the water did not flow into the peatland, the water stagnated around the peatland, which indicates that the water in the field had quick preferential pathways. Possibly due the existence of macropores that make the soil drain faster through seepage and underground water flows, which are difficult to

simulate and quantify in the field (Nousiainen et al. 2015). In addition, the coarse model grid may have cancelled out the small-scale (sub-grid) variability. With the addition of a mineral soil with high hydraulic conductivity along water pathways, the model was able to simulate a superficial underground flow.

Overall, the model performs better during the snow-free period, the model simulated the soil water content and soil temperature well and was able to follow the interannual variability of the soil temperature for all the four years. For almost all outputs, a lower coefficient of determination was found for the period of snow cover, apart from sensible heat and outgoing short wave radiation where a higher coefficient of determination was found during the period of snow cover. Both these results could potentially be the result of a static, non-dynamic vegetation used in the model. Nevertheless, the low values of RMSE indicate a reasonable fit for all outputs under snow cover. The comparison between the data from the eddy covariance tower and the GEOtop simulation also indicates that the model reasonably represents the energy balance, even with the vegetation parameters as static, non-dynamic.

In the winter of 2014-2015 snow was modeled earlier than it was measured in the field, in GEOtop the snowfall is simulated based on the measured air temperature at 2 meters. The threshold for precipitation to fall as snow was set to 0 degrees Celsius. The mismatch between model outputs and measurements could indicate that the air temperature at 2 meter is not a good indicator of predicting snow, since the soil temperature could be too high, resulting in immediate snowmelt.

The relatively high latent heat flux, compared to the net radiation was comparable with the GEOtop simulation of the Rott catchment (Hingerl et al. 2016), supporting the suitability of GEOtop to model complex catchments containing peatland ecosystems. The Rott catchment is located in a pre-alpine region of Southern Germany (ranging

from 550 – 850 m asl) and the predominant land use types are pasture (44%), coniferous (37%) and mixed forest (18%). Overall, the energy balance and its components simulated by the model follow the expected pattern and are similar to the measured values of the heat fluxes (Figure 5-8 and 9). The imbalance of the modeled energy balance closure is much better (9%) than the typical imbalance of the measured energy balance closure by eddy covariance systems (25%, Wilson et al. 2002). The model simulates a low sensible heat and a high latent heat flux compared to the measurements, in the model the vegetation is set as a constant without any seasonal trends. This results in mismatches between the model outputs and the measurements, which have been seen in other simulations with GEOtop in complex mountainous terrains (Hingerl et al. 2016).

The model seems to overestimate the discharge and simulates high discharge peaks, which were not measured in the field but may have occurred due to the lack of continuous monitoring of discharge. Possible explanations for the differences between the measurements and the model output can be the lack of measurements just after heavy rain events, the spatial variability of the hydraulic conductivity, which can give high percentage errors in the water budget (Koerselman 1989) and/or the fact that after a precipitation event the runoff flows over the banks. Additionally to the flow overbanks, no stage-discharge relation could be established, because of the dynamic shape of the stream. During the field campaign, the measured streamflow velocity was between 0-0.1 m/s. This is within the accuracy of the instrument and could not be considered as reliable as desired.

In 1914 the top layer of some section of the peatland were harvested (Cescatti et al. 1999), which could have resulted in pathways where the water drains faster. Subsequently it could have introduced flat areas where water stagnates. The

occurrence of these pools in the catchment is not incorporated in GEOtop, while in the peatland there are some areas with standing water almost year round. The size of these pools vary significantly over the year, which indicate they could act as a buffer for the discharge, resulting in the modelled discharge being than the measured discharge.

Since the complete catchment is located on a deep impermeable morainic strata, there is seepage into the fen (Cescatti et al. 1999). The seep reaches the surface in the peatland in two places, where it forms two streams (inflows). Due to the complex topography of the catchment and the variation in soil depth and soil composition in the catchment, the flow in the unconfined aquifer is not quantifiable. The existence of a confined aquifer cannot be identified in the field: this could lead to an additional sink of water, not integrated in the model and therefore resulting in higher modeled stream flow (Holden and Burt 2002, Lowry et al. 2009, Lewis et al. 2012, Cunliffe et al. 2013). The depth of the soils in the complete catchment is variable; in the peatland the depth ranges from 0.8 m at the border to 4.4 m in the center (Dalla Fior 1969). These irregularities result in the variability in the amount of water that can be stored in this soil column, which are currently not integrated in GEOtop. In the model a constant soil thickness has been assumed, and due to the coarse grid size the variability in the soil was cancelled out. The average annual water balance shows that the highest amounts of discharge are at the end of the snow period. In these periods, the snow is melting which results in high runoff. The model is able to simulate the evapotranspiration clear seasonal trend with its very low values during the period of snow cover, which is also found in the measured data.

5.5.1 Dissolved Organic Carbon

Just before snowfall, the concentration of DOC has a small spike in all streams, which could be coming from the vegetated area higher up the mountain, where snow arrived

earlier in the year. During the first days after snowfall, the snow melts during daytime and the water drains into the soil. During this period, the water could have collected DOC in the forested area located above the peatland. Only after snowmelt, the DOC concentration in one of the two inflows (inflow 2) was higher than the outflow. For all the other samples, the DOC in the outflow was higher than the sum of the two inflows, indicating a carbon loss of the peatland via DOC. The monthly measurement of DOC used in this study was an adequate interval of sampling to calculate the annual flux of DOC, since the changes in flow are a bigger contribution to annual DOC export than changes in DOC concentration (Grünheid et al. 2005, Worrall et al. 2006, Nilsson et al. 2008, Koehler et al. 2009). The carbon emissions via DOC can have a big influence on the carbon balance of the ecosystem (Gielen et al. 2011). In pristine peatlands the DOC can account for 20% to 40% of the net ecosystem CO_2 exchange (Roulet et al. 2007, Nilsson et al. 2008, Koehler et al. 2011). Also in drained peatlands a big carbon loss through DOC has been measured (even up to 3.3 ± 1.5 kg DOC over several days after draining a 900 m^2 poor fen (Strack et al. 2008)). The concentration of DOC at the Monte Bondone peatland site is at the lower range of DOC measured at peatlands (Freeman et al. 2004, Munir et al. 2015). Due to the aerobic conditions in the soil, the dead organic matter was decomposed and mineralized to CO_2. The most abundant plant species is *M. caerulea*, which decomposing fast (Vuuren et al. 1993) and results in high ecosystem respiration (Pullens et al. 2016b)s. Also with a deep water table, the DOC values were expected to be high (Freeman et al. 2004, Worrall et al. 2006, Dieleman et al. 2016). The fact that the DOC values were low could indicate that most of the carbon is emitted via ecosystem respiration and that the main source of DOC were the partially decomposed recalcitrant carbon compounds in the soil, such as root exudates (Fenner and Freeman 2011, Hribljan et al. 2014, Dieleman et al. 2016). The modeled annual water balance indicates that 87 % of the precipitation leaves the

catchment as discharge, based on the average of the measured DOC concentrations and the monthly average modeled discharge values an initial estimate of the total DOC export can be calculated. It has to be taken into account that this method introduce high uncertainties in the total export, since it is a combination of the uncertainty of the measured water flow, the uncertainty in the model outcomes and the uncertainty of the DOC measurements. In this study the modeled discharge is likely to be overestimated, which could result in an overestimation of the DOC export. The small measured amount of DOC in combination with the modeled discharge results in a small export of DOC from the peatland. Over the four years the average of the loss of DOC is 10.2 (± 3.8) g C m^{-2} yr^{-1} (Table 5-5), this is comparable to a blanket bog peatland in Ireland (14.1 ± 1.5 g C m^{-2} yr^{-1} for 2007 (Koehler et al. 2009)), an upland peat catchment in England (9.4 g C m^{-2} yr^{-1} (Worrall et al. 2003)), a subarctic Atlantic blanket bog in Norway (7.2 ± 0.7 g C m^{-2} yr^{-1} (de Wit et al. 2016)), a mixed acid mire system in Sweden (17.8 ± 0.7 g C m^{-2} yr^{-1} (Nilsson et al. 2008)), a fen in Minnesota, United States (10.0 ± 3.0 g C m^{-2} yr^{-1} (Pastor et al. 2003)) and lower than a rich fen in Minnesota, United States (21.2 ± 6.9 g C m^{-2} yr^{-1} (Urban et al. 1989)). At a restored peatland, on former agricultural land, in the Netherlands, the DOC export is higher (20.6 ± 4.3 g C m^{-2} yr^{-1} (Hendriks et al. 2007)).

The combination of DOC and the previously presented carbon fluxes (CO_2 and CH_4 (Pullens et al. 2016b)) indicate that the peatland is acting as a carbon source for all four subsequent years with a carbon balance ranging from 95.3 to 273.8 g C m^{-2} yr^{-1}.

Following the simulation, it could be advocated that the use of a hydrological model could provide a better insight in the water and energy balance of any given catchment. In this study, the implementation of GEOtop indicated the need of the integration of a ‘mineral soil with high hydraulic conductivity’ as an artificial pathway. Even with an

extensive field campaign, this soil type and the possible existence of macropores could have not have been identified, since not the complete soil column could have been sampled. Possibly the application of a ground penetrating radar would have resulted in a better insight in the hydraulic pathways in the soil compared to an extensive field campaign. Nevertheless, the implementation of GEOtop, without this extensive soil data can provide very important insights in the water and energy balance of a complex mountainous catchment.

5.6 Conclusion

This study presents a study of a peatland on the Monte Bondone plateau, near Trento, in the Eastern Italian Alps conducted with the model GEOtop (v2.0), and an ad hoc field campaign. The peatland has a heterogeneous vegetation, which results in diverse soil bulk density and hydraulic conductivity. This introduces biases into the model outputs but overall GEOtop was able to simulate the water and energy dynamics of the peatland over four years comparable to the measured values.

The bulk density and hydraulic conductivity of the peatland were measured from in situ samples to investigate soil variability. The modeled streamflow has higher discharge peaks compared to the infrequent measured discharge. Nevertheless the model was able to simulate the interannual variability of the volumetric water content and soil temperature accurately. The comparison of the modeled energy fluxes and the measured values from the eddy covariance tower indicate that GEOtop is able to follow the seasonal patterns and is within the same range of the measured values. The model has a smaller misbalance of the energy balance compared to the measurements made by the on-site eddy covariance tower.

Based on the modeled discharge and the measured DOC values, an initial estimation of DOC export of the peatland through extrapolation was made. The DOC

concentration in the stream water was low, but the high stream flows lead to similar DOC losses compared to other peatlands.

The study shows that a process-based hydrological model can be used to study the water and energy dynamics of a peatland in a mountainous area, when some adjustments are made like the addition of an artificial pathway with high hydraulic conductivity. For the peatland at Monte Bondone this resulted in the estimate of four years of carbon balance (CO_2, CH_4 fluxes and DOC losses combined), which indicated that the peatland was a carbon source for all four subsequent years. The carbon balance was 111.2, 275.2, 189.5 and 97.3 g C m^{-2} yr^{-1} for 2012, 2013, 2014 and 2015 respectively.

5.7 Replicable Research

GEOtop model is freely available as indicated on the site htttp://www.geotop.org. The orthophoto and DEM data of the site are available from Autonomous Province of Trento, P.A.T, from http://www.urbanistica.provincia.tn.it/sez_siat/BancheDati/-RepertorioCartografico/pagina3.html. Data from the campaign and hydrometeorological data used in this paper are available (from the authors). A simplified test case of this study is online available at: https://github.com/jeroenpullens/geotop_monte_bondone_sample

5.8 Acknowledgements

The authors would like to thank the three anonymous reviewers for their useful suggestions and comments. The authors would also like to thank Pablo Torralba Rubio, Marilu Solas Obra, Lorenzo Frizzera, Roberto Zampedri and Mauro Cavagna for field assistance. The authors would also like to thank Paola Gioacchini of DIPSA, Bologna for the analysis of the DOC samples. The authors would also like to thank the GEOtop community for their help and support. The authors also like to thank

Cristina Bruno and Bruno Maiolini for lending the FP111 Global Flow Probe. One of the authors work (R. Rigon) was partially financed by the Trento University project CLIMAWARE.

6 The NUCOMBog R package for simulating vegetation, water, carbon and nitrogen dynamics in peatlands

J.W.M. Pullens [a,b,*], M. Bagnara [c], R. Silveyra González [c], D. Gianelle [a,d], M. Sottocornola [e] , M.M.P.D. Heijmans [f], G. Kiely [b], F. Hartig [c, g]

[a] Department of Sustainable Agro-ecosystems and Bioresources, Research and Innovation Centre, Fondazione Edmund Mach (FEM), Via E. Mach 1, 38010 San Michele all'Adige, Trento, Italy

[b] Hydromet, Department of Civil and Environmental Engineering and Environmental Research Institute, University College Cork, Cork, Ireland

[c] Department of Biometry and Environmental System Analysis, University of Freiburg, Freiburg, Germany

[d] Foxlab Joint CNR-FEM Initiative, Via E. Mach 1, 38010 San Michele all'Adige, Trento, Italy

[e] Department of Science, Waterford Institute of Technology, Waterford, Ireland

[f] Plant Ecology and Nature Conservation Group, Wageningen University & Research, Wageningen, the Netherlands

[g] Theoretical Ecology, Faculty of Biology and Pre-Clinical Medicine, University of Regensburg, Universitätsstraße 3, 93053 Regensburg, Germany

Published in Ecological Informatics (2017) 40, 35-39, doi: 10.1016/j.ecoinf.2017.05.001

6.1 Abstract

Since peatlands store up to 30% of the global soil organic carbon, it is important to understand how these ecosystems will react to a change in climate and management. Process-based ecosystem models have emerged as important tools for predicting long-term peatland dynamics, but their application is often challenging because they require programming skills. In this paper, we present NUCOMBog, an R package of the NUCOM-Bog model (Heijmans et al. 2008), which simulates the vegetation, carbon, nitrogen and water dynamics of peatlands in monthly time steps. The package complements the model with appropriate functions, such as the calculation of net ecosystem exchange, as well as parallel functionality. As a result, the NUCOMBog R package provides a user-friendly tool for simulating vegetation and biogeochemical cycles/fluxes in peatlands over years/decades, under different management strategies and climate change scenarios, with the option to use all the in-built model analysis capabilities of R, such as plotting, sensitivity analysis or optimization.

6.2 Introduction

Peatlands play an important role in the carbon cycle of the Earth. Although they cover only about 3% of the terrestrial global surface, they have stored up to 455–600 Petagrams (Pg, 10^{15} g) carbon during the postglacial period (Gorham 1991, Yu et al. 2010, Yu 2012), equivalent to about 30% of the global soil organic carbon (Gorham 1991). Peatland soils consist of dead organic matter, which is decomposed slowly due to the permanently water saturated soil. The presence of *Sphagnum* mosses makes the decomposition rates even lower due to their high recalcitrance to decomposition. Pristine peatlands commonly act as carbon sinks (e.g. Lund et al. 2010, Humphreys et al. 2014, McVeigh et al. 2014), while peatlands disturbed by human activities (e.g. such as peat harvesting) are mostly acting as carbon sources (e.g. Hendriks et al. 2007,

Harpenslager et al. 2015a, Moreno-Mateos et al. 2015, Pullens et al. 2016b). A major concern is that the immense soil carbon pool of peatlands is vulnerable to climate change, in particular to changes in precipitation, water table depth and temperature (Frolking et al. 2011, Van Der Kolk et al. 2016). Changes in precipitation regimes would likely have an effect on the plant species composition through changes in the water table depth (Sottocornola et al. 2009, Dieleman et al. 2015). Peatlands located in regions with a maritime climate are also threatened by invasions of shrubs and trees (Stine et al. 2011, Heijmans et al. 2013, Holmgren et al. 2015), which could potentially reverse their carbon footprint from a sink to a source (Dorrepaal et al. 2009, Bond-Lamberty and Thomson 2010, Frolking et al. 2011), resulting in a positive climate feedback. It is therefore vital to understand how the stored carbon in peatlands will respond to changes in climate and management.

The reaction of peatlands to climate change is a slow process (years/decades to centruries, Frolking et al. 2010), with complex interactions between different vegetation communities. The most widely used tool to understand these interactions and simulate the future of both the stored carbon and the vegetation are process-based models.

The application of these models, however, is often challenging for new users because they require specialized input formats and programming knowledge when tasks such as sensitivity analyses or parameter calibrations are needed. It would therefore be an advantage to have ecosystem models available in established environments for scientific computing, such as R or Python. In this paper, we describe the new NUCOMBog R package, which provides a user-friendly interface to the NUCOM-Bog ecosystem model, which simulates the dynamics of vegetation, carbon, nitrogen and water in peatlands.

6.3 Model description

The NUCOM-Bog model (NUtrient cycling and COmpetition Model (Berendse 1988, van Oene et al. 1999, Heijmans et al. 2008, 2013)), written in Delphi, simulates the carbon and nitrogen dynamics of five plant functional types (PFTs): graminoids, ericaceous shrubs and three groups of *Sphagnum* mosses (lawn, hollow and hummock mosses) in monthly time steps. The model simulates an area of one square meter with a flat moss surface. A schematic representation of the model is depicted in Figure 6-1. The model can be used to simulate the current state of the peatland and to assess the effects of climate change (e.g. temperature increase, changes in precipitation regime), or other global changes such as increasing atmospheric CO_2 levels and nitrogen deposition, as well as local nitrogen fertilization or different re-vegetation regimes, which can aid the design of management strategies.

Changes in vegetation composition are driven by competition for light and nitrogen among the five PFTs. Light is first available to the taller graminoids, then to the dwarf shrubs and finally to the mosses. For each time step (one month), NUCOMBog calculates the potential growth rate of each plant functional type (*Gpot*) based on the amount of intercepted light (*LI*), maximum growth rate (*Gmax*), the CO_2 concentration in the atmosphere, air temperature (*temp*) and water table depth (WTD) according to

$$G_{pot} = LI * G_{max} * f(CO_2) * f(temp) * f(WTD). \quad (1)$$

Each plant functional type has its own optimal range for temperature and water level depth. The model calculates the WTD based on precipitation, potential evapotranspiration (according to Penman, 1946) and drainage. The drainage in the model calculation considers surface run-off and lateral outflow through the living moss layer (Heijmans et al., 2008).

The only nutrient limiting growth of the plants in the model is nitrogen. When not enough nitrogen is available, the calculated potential growth rate (*Gpot*) for each PFT is reduced. The incoming nitrogen from wet and dry atmospheric depositions is first made available to the mosses (Heijmans et al. 2002). The remaining nitrogen leaches into the soil, where it becomes available for the ericaceous shrubs with their shallow roots (Figure 6-1). Deeper in the soil the nitrogen is available for the roots of the graminoids. Apart from light and nitrogen, the growth rate of each PFT depends on its optimal temperature and WTD range. For the carbon balance, plant growth (net primary production) and decomposition of soil organic matter (heterotrophic respiration) are simulated for each PFT. A detailed description of the model is provided in Heijmans et al. (2008).

Dead organic matter (DOM), which is critical for the development of peatlands, follows the same route to deeper soil layers as nitrogen: fresh DOM is first incorporated in the moss layer, before it enters the top soil (acrotelm). In the acrotelm the water table fluctuates, which results in both anaerobic and aerobic decomposition taking place. Below the acrotelm is the permanent waterlogged soil (catotelm), where decomposition rates are lower due to the lack of oxygen (Figure 6-1). In the model, the boundary between acrotelm and catotelm is defined as the yearly deepest mean WTD, calculated over the previous 10 years. The change of soil depth of the acrotelm and the catotelm is calculated from the incoming DOM and decomposition in the respective layer.

The model assumes that all PFTs are present at any time, with a minimum cover of 0.1 %. Thus, PFTs can always grow once their growing conditions are suitable (these assumptions correspond to a permanent seed bank). While the plant community develops, the original NUCOM-Bog model (Heijmans et al., 2008) calculates the

monthly net primary production (NPP). For this package, NUCOM-Bog has been modified in such a way that it also returns the monthly heterotrophic respiration. In this way, the net ecosystem exchange (NEE) can be calculated:

$$NEE = -(NPP - heterotrophic\ respiration) \quad (2)$$

The NUCOMBog R package follows the micro-meteorological sign convention, i.e. a negative NEE is a carbon uptake for the ecosystem. All fluxes are in grams of carbon per square meter per month (g C m^{-2} $month^{-1}$).

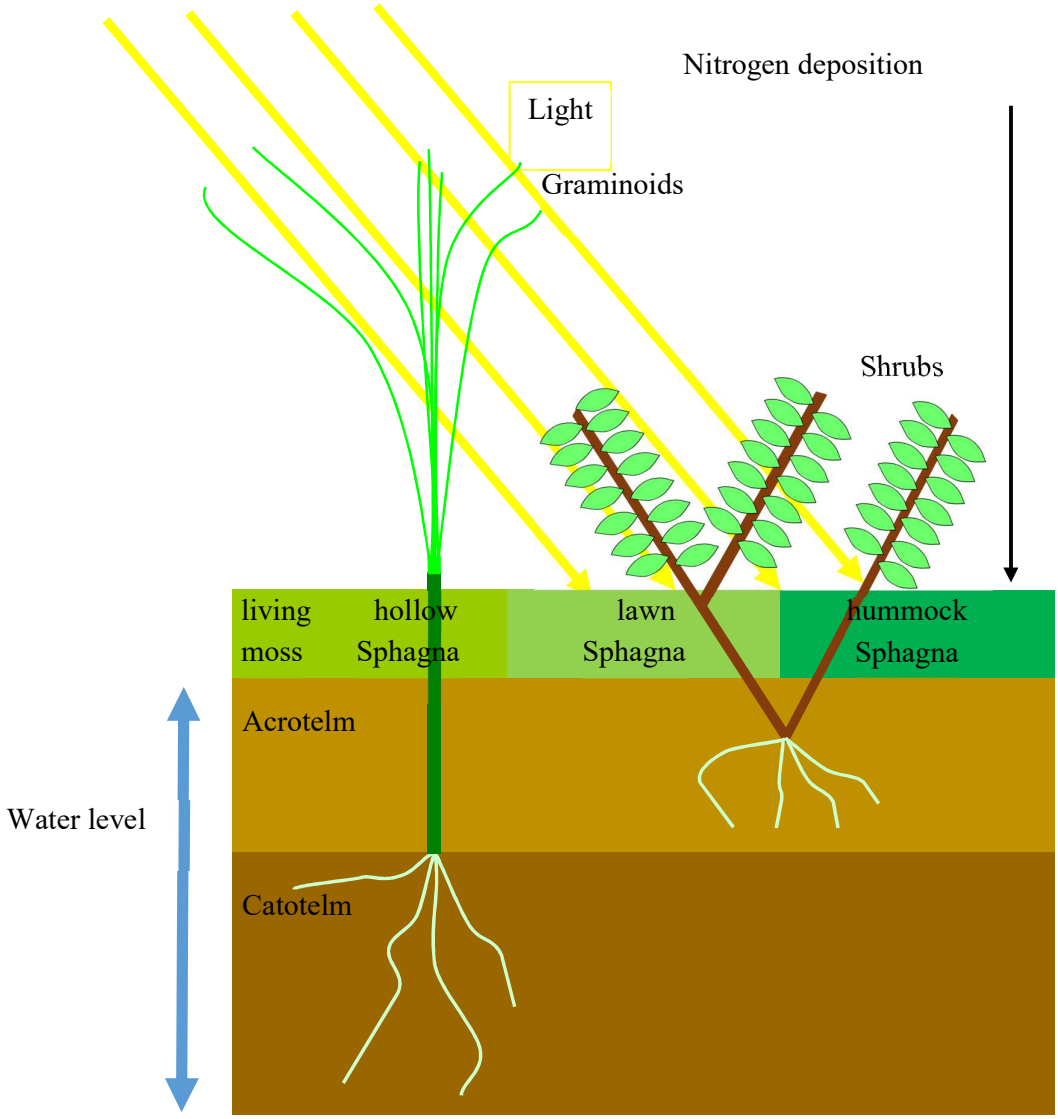

Figure 6-1 Schematic representation of NUCOM-Bog (Adapted from Heijmans et al. 2008)

NUCOM-Bog has been validated with paleo-ecological data, which showed that the model was able to simulate vegetation composition changes in response to climatic changes in the Little Ice Age (Heijmans et al. 2008). In addition, simulated year-to-year variations in water table position and the response of mosses and vascular plants to these changes compared well with observations (Heijmans et al. 2013).

6.4 R package

The NUCOMBog R package provides an interface to the statistical programing language R (R Development Core Team. R Foundation for Statistical Computing 2017), which is available under the terms of the Free Software Foundation's GNU General Public License in source code form for Windows, MacOS and Linux. The NUCOMBog package is available on the Comprehensive R Archive Network (CRAN) and was first released in April 2016. The R package relies on an external executable, which is freely available at: https://github.com/jeroenpullens/NUCOMBog as model source code, as well as a precompiled executable. To run the model in R, the user first has to provide the bulk density and the initial biomass values per PFT separated into grams of carbon and nitrogen per plant tissue (shoot/leaf, stem and root), soil carbon and nitrogen content and the bulk density of the acrotelm and catotelm, as well as environmental and climatic data (Figure 6-2). The environmental data consists of the annual atmospheric CO_2 concentration in parts per million (ppm) and the sum of both wet and dry annual nitrogen deposition in kg N per hectare (kg N ha^{-1} yr^{-1}). The climatic data consists of monthly air temperature (°C), precipitation (mm), and the calculated Penman potential evapotranspiration (mm, Penman 1948). The R package also includes some test data (data from Heijmans et al. 2008), that needs to be copied into a user defined folder prior to use. The function *copytestdata* allows the user to copy the data and test the model.

To initialize a model run, the function *setupNUCOM* is called. The user must specify the file paths of the input data as well as the output directory (Figure 6-2). In addition, the starting and end year of the simulation need to be specified. The model simulates full years, starting in January and ending in December. When not all the initial biomass values are available (e.g. root biomass is unavailable because destructive measurement are not allowed on site), the user can decide to perform a spin-up run to reach a stable equilibrium (so-called “steady state”). When the data from the spin-up is not needed for subsequent analysis, the parameter "*Startval*" in the function *setupNUCOM* can be used. The “*Startval*” value should be set to the number of months used for the spin-up, and the function *getData* will only load the requested data into the R environment.

The *setupNUCOM* function also allows specifying the output variables; the function *getData* is implemented to retrieve the desired output variables and for the period requested. While the NUCOMBog model returns net primary production (NPP), the R package NUCOMBog also returns the monthly heterotrophic respiration (R_h). From these two values the net ecosystem exchange (NEE) is calculated, so that the model outputs can be compared to sites where carbon fluxes are measured by eddy covariance towers or flux chambers. The model also predicts the water table depth (m), where positive values indicate water table depths below ground surface. The output is directly loaded in R via the function *getData*, so it can be used for further analyses. A schematic representation of the workflow of the R package is depicted in Figure 6-2.

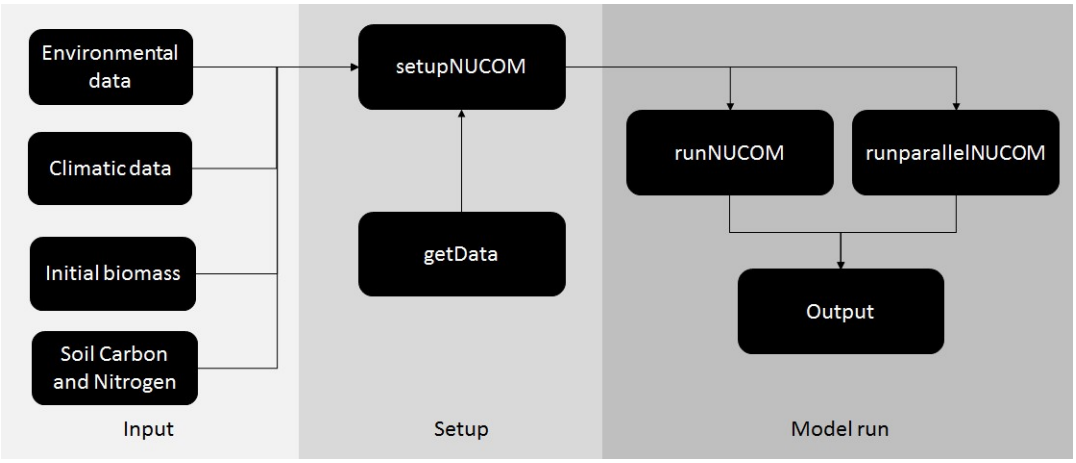

Figure 6-2 Schematic representation of the workflow of the R package NUCOMBog.

The model can be run with either the default parameter values from Heijmans et al. (2008), or user-defined parameters, via the *runNUCOM* function. Parameter values not provided by the user are automatically set to their default values. To facilitate the swift calculation of a large number of model evaluations, for example for sensitivity analysis or model calibration, the package provides support for parallel runs on multiple processors via the *runparallelNUCOM* function. The *runparallelNUCOM* function will run the model for a list of parameter combinations, and save the outputs in separate folders. These functionalities, together with the integration of the model in R, open the possibility to use the model together with one of the many algorithms for model calibration and analysis that are implemented in R, for example sensitivity analysis (Saltelli et al. 2008), parameter calibration via optimization, and Bayesian inference (Hartig et al. 2012). The possibility to make use of such sophisticated algorithms will help to improve the model, and identify gaps in the present knowledge about the functioning of peatlands in general and specifically under stress of climate change or management regimes.

6.5 Case study: Walton Moss, England

As a case study, we show a simulation with NUCOMBog for historic data from the Walton Moss site in England (Heijmans et al. 2008). The data for this simulation is

included in the test data of the NUCOMBog R package. To run the simulations, first the data is copied from the R package to a user-defined folder

```
copytestdata(new_folder = "/home/jeroen/test_data/")
```

After this step, the executable of the model is copied into the folder. The folder structure has to be kept intact. When the executable is copied, the model can be run by using the following commands.

```
test_setup_singlecore <- setupNUCOM(mainDir = "/home/jeroen/test_data/",
    climate = "ClimWLMhis.txt", environment = "EnvWLMhis.txt",
    inival = "inivalWLMhis.txt", start = 1766, end = 1999, type = c("NEE",
        "WTD", "NPP", "hetero_resp"), parallel = F)
output <- runNUCOM(setup = test_setup_singlecore, parameters = NULL)
```

This command runs the model with the input data from 1766 to 1999, and requests the outputs NEE, WTD, NPP and heterotrophic respiration. Outputs are stored in the variable “output”, which can subsequently be used for further analysis in R, for example to produce figures (Figure 6-3), compare model outputs to data, perform sensitivity analysis and parameter calibration (for which several packages already exist within the R environment).

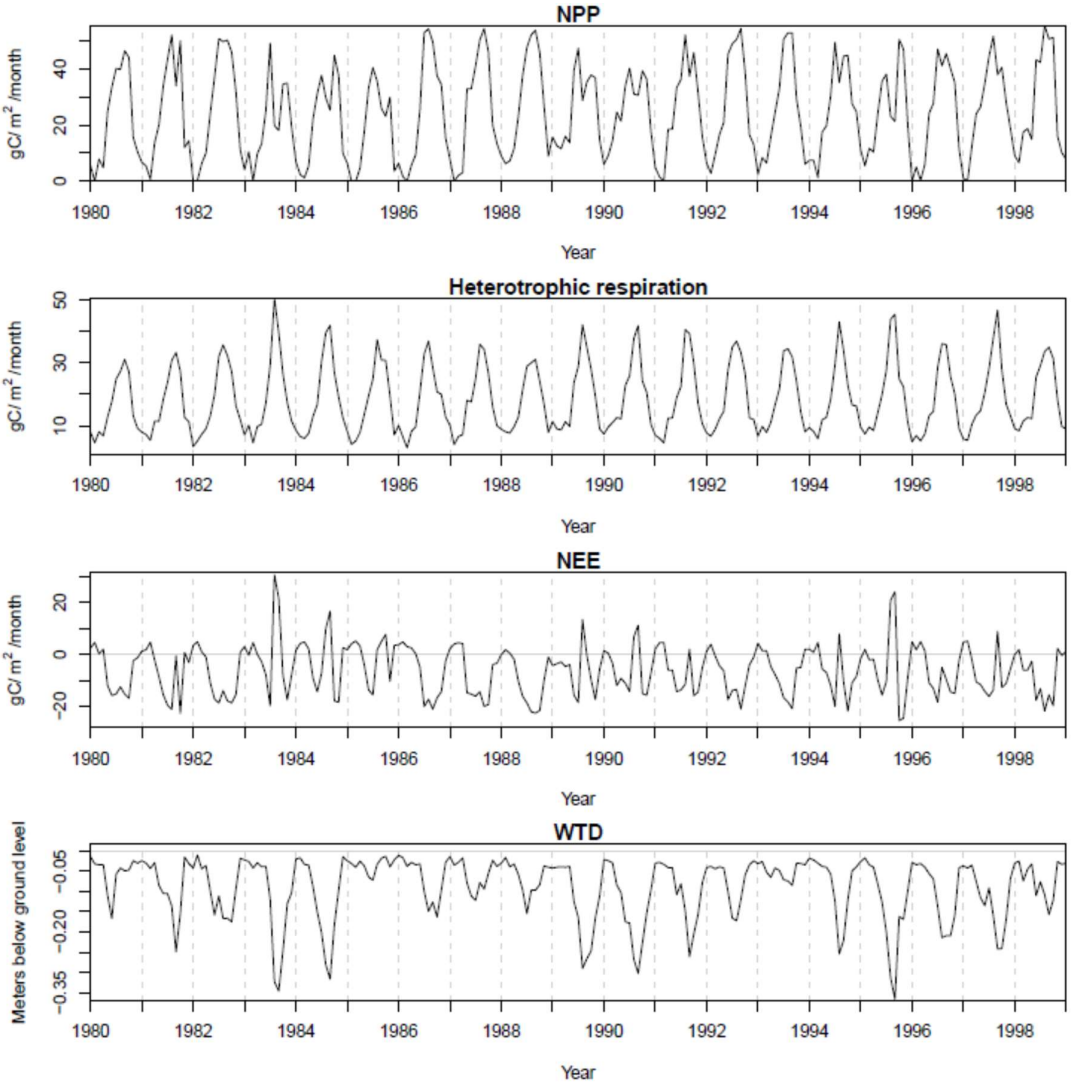

Figure 6-3 Simulated monthly NPP, NEE, heterotrophic respiration and WTD from 1980 until 1999 for Walton Moss, England.

6.6 Conclusion

Some of the most important uses of models are to correctly represent physical processes, to predict the future and to understand the past. With the presented NUCOMBog R package, the vegetation, carbon and water balance of peatlands can be easily simulated from within the R environment. The ease of running the model, together with various options of analysis, provides many possibilities for investigating the stability of peatland vegetation, as well as facilitate its use for educational purposes.

The addition of heterotrophic respiration and net ecosystem exchange as outputs provides better possibilities to investigate processes in peatlands that are equipped with eddy covariance towers, or where flux chamber measurements are being taken. In particular, when data over many years are available, the model outputs could be evaluated against the measured data. The possibility to perform sensitivity analysis and model calibration can give precious insights on the relative importance and uncertainty of parameters, which will in turn lead to a better understanding of the ecosystem functioning. Because the package allows running the model in parallel, the computational time of such tasks is significantly reduced.

In conclusion, the integration of NUCOMBog into the R environment streamlines the process of model application and opens up many new options of model analysis. We hope that these possibilities will eventually lead to new insights about peatland dynamics, thus making NUCOMBog an even more valuable tool to investigate the vegetation, carbon, nitrogen and water dynamics of peatlands over time and to identify possible threats for the modelled peatlands.

6.7 Acknowledgements

The authors would like to thank Alessio Gianelle for his help with the Delphi code.

This work was supported by a STSM grant to JWMP from COST Action FP1304 (Profound, http://cost-profound.eu/site/). MB acknowledges funding by the DFG Priority Program 1374 "Infrastructure-Biodiversity-Exploratories" (Ref-No DO 786/8-1).

Author contributions: JWMP, DG, MB, FH, MS and GK designed the research; JWMP, MB and FH performed the research; MB, FH, MMPDH and RSG contributed

with model coding and gave conceptual advice; JWMP wrote the paper. All authors discussed the results and implications and commented on the manuscript at all stages.

6.8 Data accessibility

The NUCOMBOG R package is available on the Comprehensive R Archive Network (CRAN), test data is incorporated in the package and the source code of the executable and the executable of the model are available on GitHub (https://github.com/jeroenpullens/NUCOMBog). All functions in the NUCOMBog R package have documented help files and more information about running the package is provided in the vignette of the package.

7 Site-specific and multi-site calibration of vegetation and carbon model on three different peatlands

7.1 Abstract

Peatlands store a vast amount of carbon in their soils and therefore play an important role in the earth's carbon cycle. The NUtrient cycling and COMpetition Model (NUCOM-Bog) was applied for three different sites to investigate how peatlands in different climates and locations around the world function and to understand which are the main factors that drive the different ecosystems. A site-specific and a multi-site Bayesian calibration was performed and compared using net ecosystem exchange and water table depth from three sites (Canada, Ireland and Italy). The peatlands are a raised bog (Mer Bleue), a blanket bog (Glencar) and a fen (Monte Bondone). The multi-site calibration was comparable to the site-specific calibration. The model has difficulties to represent the respiration in winter at all sites, both at the site-specific and the multi-site calibration, and in simulating the water table depth at sites where the water drains via streams (Glencar and Monte Bondone). A comparison of the marginal parameter uncertainty of the multi-site calibration and the site-specific calibrations indicate that with the multi-site calibration the parameter uncertainty can be reduced by using information from multiple sites.

7.2 Introduction

Peatlands play a very important role in the carbon cycle of the Earth (Gorham 1991, Yu 2012), they cover only 3% of the land surface, mainly in the northern hemisphere (IPCC 2007, 2013, Parish et al. 2008, Yu et al. 2010, Schuur et al. 2015). Yet they have stored up to 455–600 petagram (Pg, 10^{15} g) carbon during the postglacial period (Gorham 1991, Yu et al. 2010, Yu 2012, Charman et al. 2013), equivalent to 20-30% of the global soil organic carbon (Gorham 1991, Yu 2012). Peatland soils contain

approximately half the amount of carbon dioxide in the atmosphere in the form of carbon (Rydin and Jeglum 2015). Due to the waterlogged soils, there is an imbalance between the decomposition, that is limited, and the biomass production. Consequently, in peatlands the dead organic matter (DOM) is accumulating, which over centuries/millennia resulted in layers of peat ranging from centimetres to meters.

Peatlands occur in different types, with bogs and fens as the main types. The main difference between these two types of peatlands is the origin of the water. For bogs the main source of water is precipitation (ombrotrophic), while for fens the water comes from surface- and groundwater (minerotrophic) (Wheeler and Proctor 2000). This results in differences in nutrients and minerals in the peatland and therefore influences the vegetation composition (Sottocornola et al. 2009). In bogs, the vegetation is dominated by *Sphagnum* mosses, which make the water more acidic by taking up cations and secreting H^+ ions (Clymo 1964). This acidification results in slowing down the decomposition of plant material even further. While fens are mainly dominated by grasses, sedges and reeds, and are due to their water source and its dissolved minerals more alkaline.

Millennia have passed to arrive at the state in which the peatlands are now and due to human disturbances and climate change the future of natural peatlands and therefore their carbon pools are under pressure (Frolking et al. 2011, Petrescu et al. 2015, Kamocki et al. 2016). Following the stages of peatland formation (Gorham 1957), the vegetation of peatlands has changed over time (Chambers et al. 2017). The understanding of these transitions in the vegetation are important to understand how peatlands are working and cope with climate change.

In this paper, we investigate how peatlands in different climates and locations around the world differ from each other, by implementing the NUCOM-Bog (NUtrient

cycling and COmpetition Model (Chapter 6 and Heijmans et al. 2008)) on the different peatlands.

The objectives of this study are i) to calibrate NUCOM-Bog for different sites. With the calibration of the model for each site specific, we want to understand whether the differences in parameter values have an ecological meaning or can they be explained by other factors, such as climate or location. After the model has been calibrated, ii) a multi-site calibration will be performed to get a more general parameter set and in this way to get more information about the ecosystem functioning. With a multi-site calibration a global set of parameters can be found, which might perform worse compared to site-specific calibration, but might result to parameters, which are generalizable. For sites with a low amount of data, the multi-site calibration could result in a better calibration, since information from the other sites is used.

7.3 Materials and Methods

7.3.1 Sites

In this paper three sites will be compared, all located in the Northern Hemisphere. The sites are located on different continents and have all different climates, and are therefore different types of peatlands. The peatlands are located in Canada, Ireland and Italy.

7.3.1.1 Mer Bleue

The Mer Bleue peatland is a 2,800 ha ombrotrophic raised bog located in the Ottawa River Valley, 10 km east of Ottawa, Ontario, Canada (45.40° N longitude, 75.50° W latitude, 69 m asl). The mean annual temperature is 6.3 °C and ranges from –10.5 °C in January to 21.0 °C in July. The mean annual precipitation is 943 mm, of which 268 mm falls during the summer months (Bubier et al. 2006). During winter the snow cover usually lasts from December to March with a maximum height of 0.6 and 0.8 m

(Lafleur et al. 2003). The total nitrogen deposition at this site is around 8 kg N/ha/yr (Turunen et al. 2004).

The dominant vegetation of Mer Bleue are mosses, *Sphagnum angustifolium*, *S. rubellum*, *S. magellanicum*, sedges, *Eriophorum vaginatum*, and shrubs, *Chamaedaphne calyculata*, *Ledum groenlandicum*, *Kalmia angustifolia*, and *Vaccinium myrtillodes*. On the site is a small fraction of trees (*Larix laricina*, *Betula papyrifera*, and *Picea glauca*) (Lafleur et al. 2001, Letts et al. 2005). At the Mer Bleue site, an eddy covariance tower has been operational since 1999. For more information about the Mer Bleue site, see Roulet et al. (2007).

For this exercise, monthly meteorological and eddy covariance data from the site from 1999-2013 is used, and meteorological data from a nearby meteorological station at Ottawa International Airport (15 km south-west of the site, Environmental Canada) from 1939 - 1999 is used.

7.3.1.2 Glencar

The Glencar site is an Atlantic blanket bog located in the Southwest of Ireland (51°55' N latitude, 9°55' W longitude, 150 m asl) (Sottocornola and Kiely 2010b). The mean annual temperature is 10.5°C and the mean annual precipitation is 2571 mm, where the summers are drier than the winters (McVeigh et al. 2014). The total nitrogen at this site is around 5 kg N/ha/yr (Henry and Aherne 2014, Johnson et al. 2016). The site is divided into four microforms based on their relative elevation: hummocks, high lawns, low lawns, and hollows. The distribution of the microform composition inside the eddy-covariance footprint was estimated as 6% hummocks, 62% high lawns, 21% low lawns, and 11% hollows (Laine et al. 2006). Vascular plants cover about 30% of the bog surface, with the most common species being *Molinia caerulea*, *Calluna vulgaris*, *Erica tetralix*, *Narthecium ossifragum*, *Rhynchospora alba*, *Eriophorum*

angustifolium, *Schoenus nigricans*, and *Menyanthes trifoliata*. The bryophyte component is not widespread, about 25% of the bog surface, and the principal species include a brown moss, *Racomitrium lanuginosum*, and *Sphagnum* mosses, covering about 10% each, so that large areas of the peatland are covered by bare soil (Sottocornola et al. 2009, McVeigh et al. 2014). At the Glencar site, an eddy covariance tower has been operational since 2003. For more information about the Glencar wetland, see McVeigh et al. (2014).

For this exercise, monthly meteorological and eddy covariance data from the site from 2003-2012 is used, and meteorological data from a nearby meteorological station at Valentia (30 km west of the site, Met Éireann) from 1939 - 2003 is used.

7.3.1.3 Monte Bondone

Monte Bondone peatland is a 10 hectares minerotrophic relatively nutrient-poor fen located on the Monte Bondone plateau in the Italian Alps (46°01'03 N latitude, 11°02'27 E longitude, 1563 m a.s.l.) (Pullens et al. 2016b). Mean annual temperature is 5.4°C and mean annual precipitation is 1290 mm (Eccel et al. 2012), with a typical snow cover lasting from October-November until early May. The total nitrogen at this site is around 20 kg N/ha/yr (Sutton et al. 2011). The vegetation of the area is very heterogeneous, but is mainly dominated by *Molinia caerulea* forming big tussocks, while in the depressions the main vegetation consists of *Carex rostrata*, *Valeriana dioica*, *Scorpidium cossonii* and scattered *Sphagnum* spp. The southwestern area of the peatland is dominated by *Eriophorum vaginatum*, with high tussocks of *Carex nigra* covering the lower areas. *Sphagnum* spp. as well as *Trichophorum alpinum* and *Drosera rotundifolia* occur close to the outflow stream. In the eastern part of the peatland, there are some short hummocks with *Calluna vulgaris* and *Sphagnum section acutifolia.* In 1914, 0.35 ha of the peatland was harvested, for burning, by

removing the peat top layer (Cescatti et al. 1999). At the Monte Bondone peatland site, an eddy covariance tower has been operational since 2012. For more information about the Monte Bondone peatland, see Pullens et al. (2016b).

For this exercise, monthly meteorological and eddy covariance data from the site from 2012-2016 is used, and meteorological data from a nearby meteorological station at Monte Bondone (1 km from the site, Meteo Trentino) from 1926 - 2012 is used.

7.3.2 NUCOM-Bog

In this paper the R package entitled NUCOMBog (Chapter 6 and Pullens et al. 2016a) is used, which incorporates the NUCOM-Bog (NUtrient cycling and COmpetition Model (Heijmans et al. 2008)) and calculates the monthly net ecosystem exchange, heterotrophic respiration, net primary production and water table depth. The NUCOM-Bog model is derived from earlier NUCOM models (Berendse 1988, van Oene et al. 1999) and simulates the vegetation, water and carbon dynamics in peat bogs on a monthly time step. In the model, five plant functional types (PFTs) are represented: graminoids, shrubs, hummock, lawn and hollow mosses, where all PFTs compete for light and nitrogen. The incoming light is first available for the graminoids, the fraction of light that is not absorbed is available for the shrubs, and finally for the mosses (Figure 7-1). The mosses are the only PFT that are able to bind the nitrogen deposition, the uptake of nitrogen by the canopy of vascular plants is assumed negligible (Heijmans et al. 2008). The deposited nitrogen, which is not taken up by the mosses, leaches into the soil. The roots of the vascular plants are not evenly distributed in the soil, the roots of the shrubs are shallower than the roots of the graminoids (Figure 7-1). Leached nitrogen is, therefore, firstly available for the shrubs, and later for the graminoids. Hence the nitrogen and light follow the opposite order of availability for the PFTs.

When the mosses die, the nitrogen is incorporated into the soil. The soil is composed of three layers, the living moss layer, the acrotelm and the catotelm (Figure 7-1). Both the acrotelm and the catotelm are composed of dead organic material. The catotelm is always water saturated; therefore, all biological processes are slower in the catotelm compared to the acrotelm (Heijmans et al. 2008). In the acrotelm, the roots of the shrubs are present, while in the catotelm the roots of the graminoids are located. The dead plant material is first incorporated in the acrotelm, where it is partially decomposed, and subsequently passed on to the catotelm when the water table level rises.

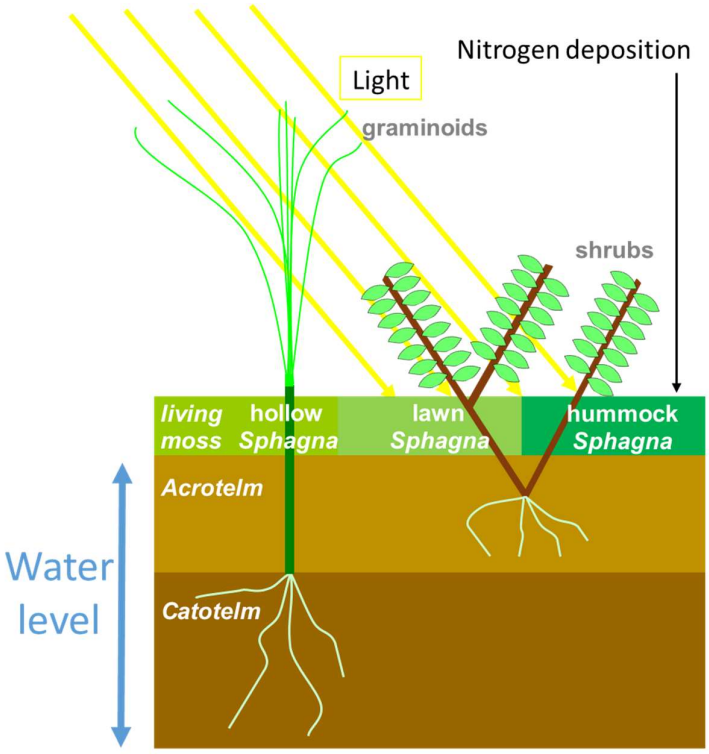

Figure 7-1 Schematic representation of NUCOM-Bog (adapted from Heijmans et al. 2008)

Since two out of three sites are covered in snow during winter, an adaptation to the model has been made. In the original model the decomposition of the DOM is calculated by using the air temperature, but previous research has shown that the respiration is better calculated by using soil temperature (Wohlfahrt and Galvagno

2017). This has also been seen at each used site: Mer Bleue (Lafleur et al. 2005), Glencar (McVeigh et al. 2014) and Monte Bondone (Pullens et al. 2016b).

The formula that calculates the decomposition per soil layer, the air temperature is changed with soil temperature:

$$Decomposition\ rate = Carbon\ dead\ mass * relative\ decay\ rates *\ f_D(T) \quad (7.1)$$

in which the relative decay rates are specific for the acrotelm and catotelm and differ among the PFTs and the organs of the PFTs, the temperature dependent function is defined by Kirschbaum (1995) as:

$$f_D(T) = \exp(-3.764 + 0.204 * T * (1 - 0.5 * \frac{T}{36.9}) \quad (7.2)$$

where T is changed from air temperature to soil temperature. For the catotelm half the temperature dependency is used because fluctuations are reduced (Heijmans et al. 2008).

7.3.3 Data processing

For each model run a stabilization period was used, for each site the model was run starting from 1766 till 2012 (Ireland), 2013 (Mer Bleue) and 2016 (Italy). A historical dataset was made by assembling all available climate data into monthly minimum and maximum values. Repetition and trends in the meteorological data were avoided set by copying the data back to 1766. For each month, a value was taken randomly between the measured minimum and maximum of that specific month over the complete data set.

To get a data set of nitrogen deposition for the period from 1766 - present, measured data for each individual site was used and organised following the dynamics of nitrogen deposition published in Heijmans et al. (2008) and matching modelled values for the past and future (Dentener 2006).

7.3.4 Sensitivity analysis

The total number of parameters in the model is too big to be used in the calibration (>150 parameters, see supplementary material of (Heijmans et al. 2008)), therefore prior to calibration a sensitivity analysis was performed. A sensitivity analysis indicates which parameters are the most sensitive, i.e. the parameters whose variation around the set values causes the biggest changes in the model output. This information is needed to know which parameters are the most important and allows to focus the calibration effort on them. The Morris function of the R-package "sensitivity" (Saltelli et al. 2008) which implements the Morris's elementary effects screening method (Morris 1991, Campolongo et al. 2007) was used. This Morris function 'walks' through the complete parameter range for each parameter specified, changing one factor at a time (OAT-method) and creates a Latin Hypercube with all the parameter combinations. The function subsequently starts running the model with all precalculated parameter value sets. From the outputs of the model runs, the sensitivity of the model to different parameters are derived.

The sensitivity analysis was carried out for all sites individually and the minimum and maximum values are provided for each parameter, corresponding to the parameter space of the prior distribution used during the Bayesian calibration.

7.3.5 Bayesian calibration

A Bayesian algorithm was used to find the parameter distribution for which the model has the lowest mismatch with the data. The data that was used to calibrate the model against is the net ecosystem exchange (NEE) and the water table depth (WTD), for both these measurements, the standard deviation was included as two extra parameters in the calibration. In this study, the DE-zs algorithm was used, which stands for Differential Evolution Markov Chain with a snooker updater (Ter Braak and Vrugt

2008). The algorithm starts with a set of parameters taken from the predefined prior distribution for each parameter. Since some parameters in the model are empirical and without physiological meaning, the prior distributions was set uniform. The prior distributions were not set too wide, since the values might not have a biological significance and might not result in convergence of parameters (Gelman and Rubin 1992). The initial set of parameter values were the starting point of the Bayesian calibration. This method searches through the parameter distribution of all parameters, which returns the highest negative log likelihood:

$$\mathcal{L}(\theta|D) \propto p(D|\theta) \quad (3)$$

in which $\mathcal{L}$ is the likelihood of a set of parameters (θ), given outcome (D) is equal to the probability (p) of the observed outcome (D) given the parameter values (θ).

The DE-zs algorithm runs a set number of parallel chains and during the run shares information among the parallel chains so that the proposal densities of randomised jumps are adjusted, resulting in accelerated movement of the MCMC chains towards an equilibrium (Ter Braak and Vrugt 2008). This equilibrium has the smallest log likelihood, i.e. the smallest error between the model and the data.

The DE-zs algorithm is implemented in the R package "BayesianTools", which is available on CRAN (Hartig et al. 2017). In this paper all analyses are done with R (version: 3.2.0 (R Development Core Team. R Foundation for Statistical Computing 2017)), NUCOMBog (version: 1.0.2.1) and BayesianTools (version: 0.0.10.0).

For each site, the NUCOMBog model was calibrated on the complete available data set of net ecosystem exchange and water table depth. Each calibration was run for 10^6 iterations, before the Gelman-Rubin index (Gelman and Rubin 1992) was calculated. After each site was calibrated individually, a multi-site calibration was started. The multi-site calibration is performed by running the model for all the three sites in

parallel and summing up the likelihood values. This has as an advantage that the variability of the climate is wider and that potential measurement or systematic errors are cancelled out in respect to site-specific calibration (Minunno et al. 2016).

The predictive power of the model was assessed by calculating the coefficient of regression and the Nash-Sutcliffe efficiency (Nash and Sutcliffe 1970), also known as the modelling efficiency (Janssen and Heuberger 1995) for the maximum a posteriori parameter distribution. The confidence interval of the Bayesian calibration was addressed by randomly selecting 200 parameter sets from the posterior distribution.

7.4 Results

7.4.1 Sensitivity analysis

The Morris sensitivity analysis returns two metrics, μ* and σ, which represent the mean and the standard deviation of the output in respect to the original values (Morris 1991). In total 33 parameters are found to be the most sensitive for the model, for all sites the parameter set was identical. The growth and the mortality parameters are the most sensitive parameters for all the PFTs, see Appendix 7.1. The sensitivity analysis gives an insight in where the model is the most sensitive and where potentially more research has to be done. In the original model the growth and mortality parameters in the model are based on field measurement and on literature values.

7.4.2 Site-specific calibration

7.4.2.1 Mer Bleue

For the Mer Bleue site, the most amount of data is available and for the calibration the complete dataset is used. After the calibration, the modelled net ecosystem exchange (Figure 7-2) and water table depth data (Figure 7-3) were compared with the measured data. The Gelman-Rubin diagnostics (1.12, (Gelman and Rubin 1992)) indicate that the model parameters reached convergence after 10^6 iterations. For both the net

ecosystem exchange and the water table depth, the model results after calibration are in the range of the measurements. The maximum a posteriori values indicate that the model has problems with simulating the respiration in winter. Nevertheless for net ecosystem exchange the model performs reasonable compared to the measured data (R^2 = 0.60, NSE = 0.55).

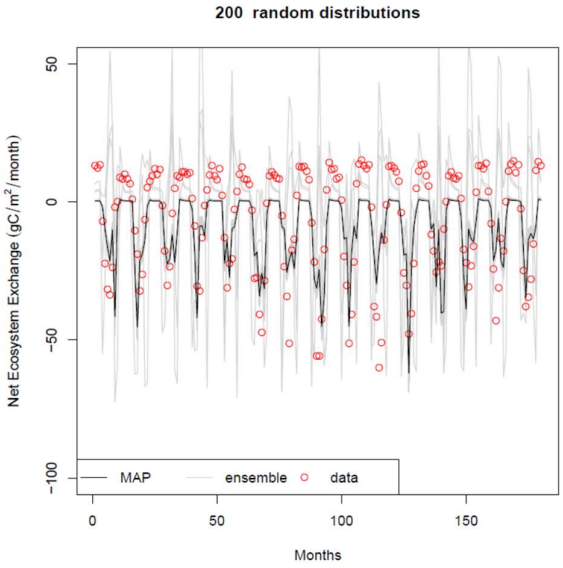

Figure 7-2 Net ecosystem exchange at Mer Bleue. In grey, the result of 200 randomly taken parameter set from the posterior distribution (ensemble), in red the measured values and in black, the NEE calculated with the maximum a posteriori (MAP) values.

The calibrated model is simulating the water table depth poor (R^2 = 0.24, NSE= 0.14), nevertheless the modelled values are in the range of the measured values and the model is following the trend of the data (Figure 7-3). Interesting to see is that the model simulates (at one time step) a water table level slightly above the surface level, while the measured data is around 30 cm deep. This mismatch in water table data does not seem to have a big impact on the NEE values. Over the complete period, the modelled water table depth is in the upper region of the measured data.

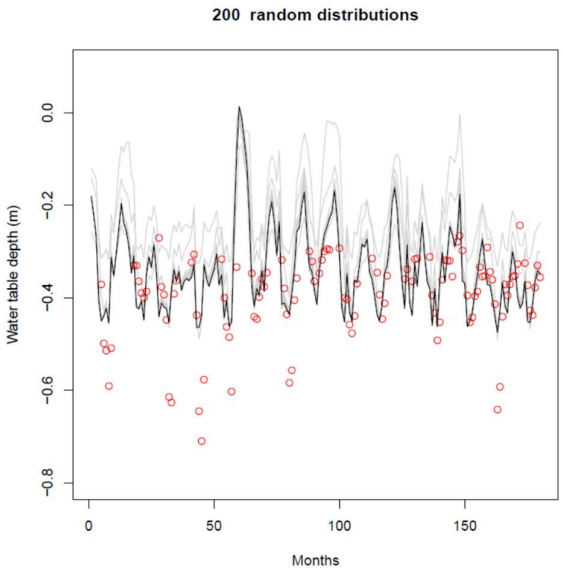

Figure 7-3 Water table depth at Mer Bleue. In grey, the result of 200 randomly taken parameter set from the posterior distribution, in red the measured values and in black, the water table depth calculated with the maximum a posteriori values.

7.4.2.2 Glencar

For Glencar the model has difficulties to reach convergence, after 10^6 iterations the Gelman-Rubin index is 1.92. This indicates that the calibration has problems with finding the posterior distribution for the parameters, an increase of the number of iterations not decrease the Gelman-Rubin parameter (data not shown). Nevertheless, the parameters for this site are the most restricted after calibration (Appendix 7.2). The maximum a posteriori distribution of the parameters shows that the calibrated model is not able to simulate respiration data in winter (Figure 7-4), as previously seen for Mer Bleue. However, the model is following the trend (Figure 7-4) of the measurements and is able to reach the maximum uptake values (R^2= 0.44, NSE= 0.44). With the random 200 posterior distributions, the model is able to simulate the respiration values better, but not as close as the model was able at the Mer Bleue site.

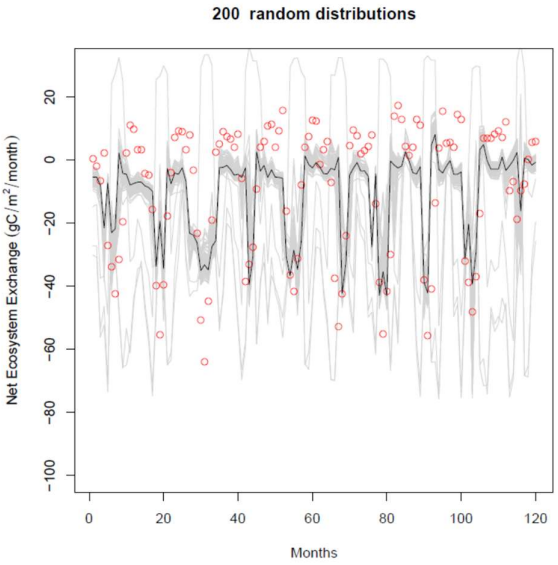

Figure 7-4 Net Ecosystem Exchange at Glencar. In grey, the result of 200 randomly taken parameter set from the posterior distribution, in red the measured values and in black, the NEE calculated with the maximum a posteriori values.

The model has difficulties in following the dynamics of the water table at Glencar (Figure 7-5). Overall the model is in the same range, but the model is does not follow the dynamics of the measurements (R^2=0.03, NSE= -3.21). Also the model seems to simulate the water table depths above the surface that are not measured in the field.

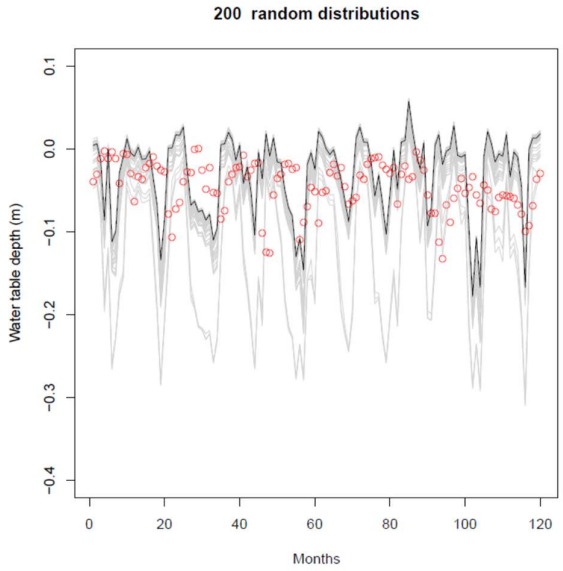

Figure 7-5 Water table depth at Glencar. In grey, the result of 200 randomly taken parameter set from the posterior distribution, in red the measured values and in black, the water table depth calculated with the maximum a posteriori values.

7.4.2.3 Monte Bondone

The Monte Bondone site is the only fen and is the site with the amount number of data. Also at this site the simulation with the maximum a posteriori parameters results in no respiration in winter, while the model is able to reach the levels of uptake (R^2 = 0.30, NSE= 0.20). The Gelman-Rubin diagnostics (1.13, (Gelman and Rubin 1992)) indicate that the model parameters reached convergence after 10^6 iterations. When the ensemble of 200 parameter sets randomly taken from the prior distributions is used, the model is able to reach the respiration values (Figure 7-6).

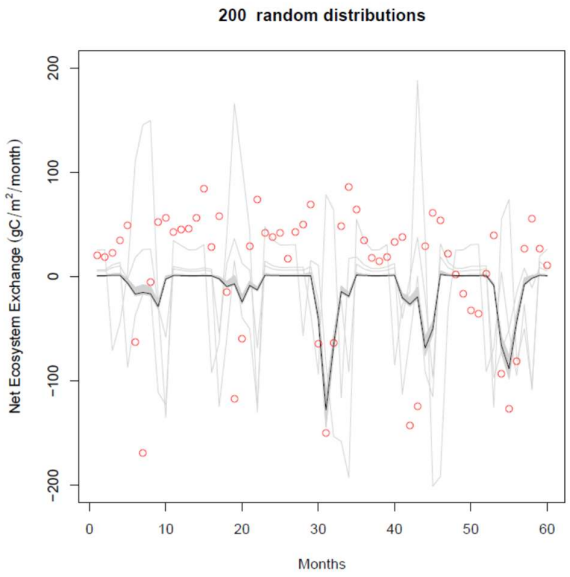

Figure 7-6 Net Ecosystem Exchange at Monte Bondone. In grey, the result of 200 randomly taken parameter set from the posterior distribution, in red the measured values and in black, the NEE calculated with the maximum a posteriori values.

For the first years, no water table depth data was available; nevertheless, the model is in the range of the measured values (Figure 7-7). The model is simulating two peaks, where the water is above the soil surface. This is not measured in the field and results to a big mismatch (R^2= 0.04, NSE= -2.31), since there is a small amount of data.

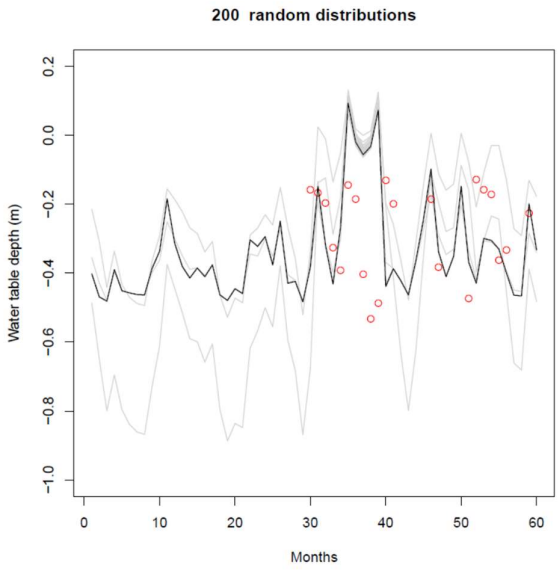

Figure 7-7 Water table depth at Monte Bondone. In grey, the result of 200 randomly taken parameter set from the posterior distribution, in red the measured values and in black, the water table depth calculated with the maximum a posteriori values.

7.4.3 Multi-site calibration

During the multi-site calibration all data from the three sites was used to calculate one common likelihood and to calculate a global parameter set. The multi-site calibration performs comparable to the site-specific calibration for each individual site, both the R^2 and the NSE are similar (Table 7-1). The Gelman-Rubin index for the multi-site calibration was the highest in this study (2.4), indicating convergence problems. For the water table depth simulations of Mer Bleue the same peak can be identified, and the same trend of water table depth for Monte Bondone can be seen (Figure 7-8). For Glencar the calibration is simulating a lower water table depth than measured, also compared to the site-specific calibration.

Also after the multi-site calibration, the simulated net ecosystem exchange for Mer Bleue and Monte Bondone show no respiration in winter, while for Glencar the winter values are closer to the measured values, but a bigger mismatch is introduced in the uptake values.

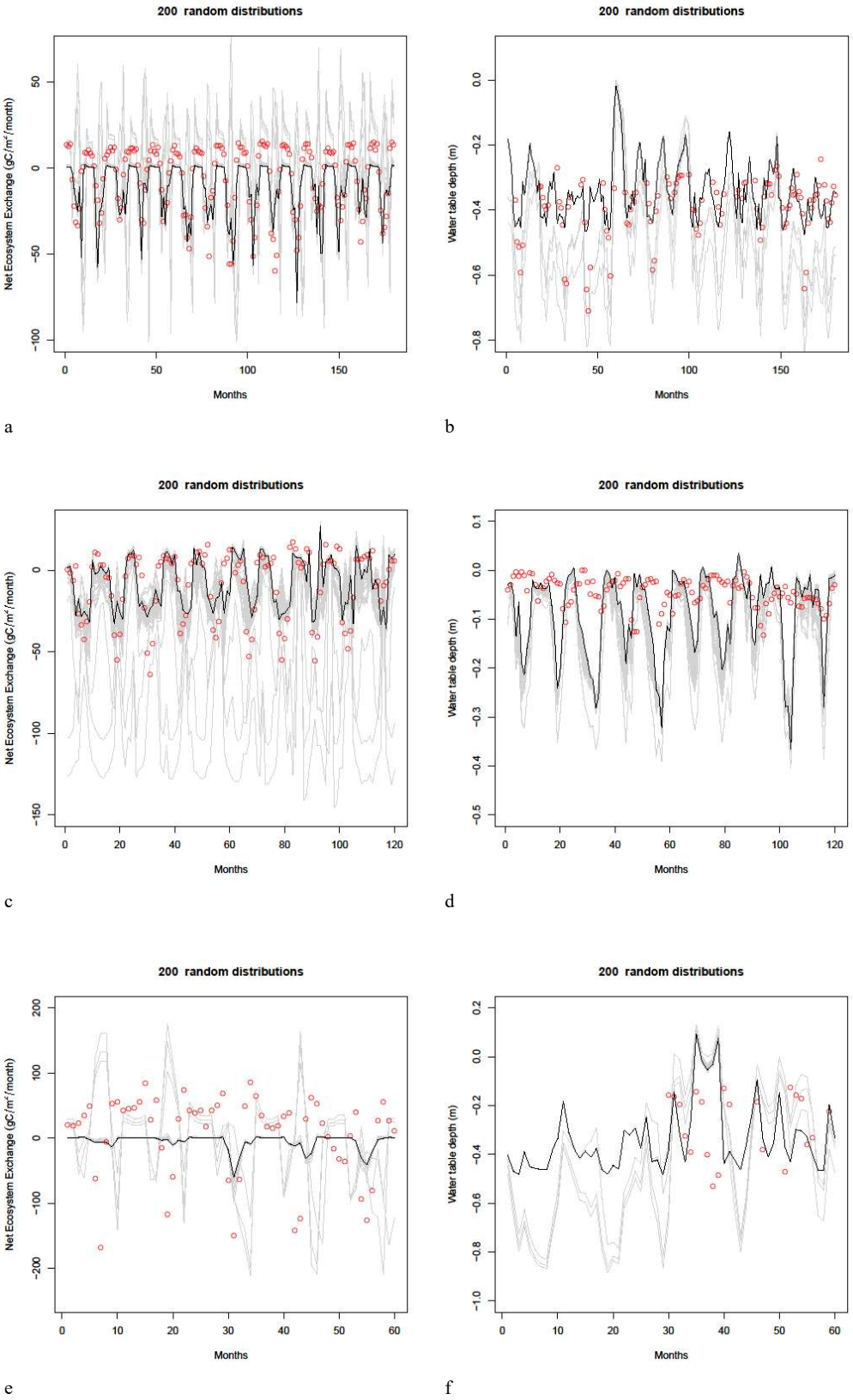

Figure 7-8 Net ecosystem Exchange at Mer Bleue, Glencar and Monte Bondone (a, c, e, respectively) and the water table depth at the same sites (b, d, f). In grey, the result of 200 randomly taken parameter set from the posterior distribution, in red the measured values and in black, the NEE/WTD calculated with the maximum a posteriori values.

The marginal parameter uncertainty of the multi-site calibration is narrower than the site-specific calibration for both Mer Bleue and Monte Bondone, and comparable with the marginal parameter uncertainty of Glencar (Appendix 7.2).

Table 7-1 Coefficient of determination (R^2) and Nash Sutcliffe (NSE) for the net ecosystem exchange (NEE) and water table depth (WTD) of all three sites calculated based on the maximum a posteriori values from the multi-site comparison.

		R^2	NSE
Mer Bleue	NEE	0.58	0.51
	WTD	0.24	0.14
Glencar	NEE	0.41	0.41
	WTD	0.01	-10.51
Monte Bondone	NEE	0.29	0.14
	WTD	0.04	-2.32

7.5 Discussion

Before this model exercise, the NUCOM-Bog model has not been used to analyse the monthly and year-to-year variation. The model has been proven successful in simulation over a long period of time (Heijmans et al. 2008), by focussing at the vegetation changes and the stored carbon pool in the peat.

The original parameter values in the model are based on field measurements and on literature reviews, but it has to be kept in mind that these parameters are difficult to measure. The potential growth rate of a plant can only be guessed and not measured, a plant never grows on its maximum potential growth rate, since there are always limiting factors. Nevertheless the model was able to simulate the uptake values reasonably well. The mortality rate of the plants in the model are defined as monthly values, this is a significant simplification of the reality, where the mortality is following a seasonal trend. The graminoids die off when the air temperature goes

below a certain limit (Taylor et al. 2001), this is not incorporated in the model and could explain the difficulties in modelling winter decomposition. The model does not compute ecosystem respiration, but only net primary production and heterotrophic respiration; these values are not measured by the eddy covariance towers.

7.5.1 Site-specific calibration

The calibration has been performed on three sites individually and on all the sites together. The site-specific calibrations indicate that the model has problems with the simulation of respiration in winter. At Mer Bleue and Monte Bondone in winter the peatland is covered by a layer of snow, this snow cover isolates the soil and can store CO_2 in the snow pack (Monson et al. 2006, Larsen et al. 2007). Since NUCOM-Bog does not compute a snow cover and calculates the respiration values based on air temperature, the decision to use the soil temperature for respiration was made (Lafleur et al. 2005, McVeigh et al. 2014, Pullens et al. 2016b, Wohlfahrt and Galvagno 2017). The model has a basic function to calculate the respiration of the DOM in both layers of the soil (equation 7.1), this function is based on a literature review (Kirschbaum 1995). The relation Kirschbaum (1995) (equation 7.2) found with the data derived from literature had a coefficient of determination of 0.500. The shape of the formula implies that there is no decomposition when the air temperature is below zero degrees (equation 7.2). Apart from the snow cover that is present at Mer Bleue and Monte Bondone, the maximum a posteriori parameter values also indicate no winter respiration at Glencar. Different empirical function of respiration curves, such as the Q10 formula and the Arrhenius function (Arrhenius 1898), as well as equations proposed by Lloyd and Taylor (1994) and Jenkinson (1990) have been tested in the model, but none of them led to reasonable results in winter.

In both Glencar and Monte Bondone the model simulates water table levels above the soil surface. In both sites the water drains via streams (Chapter 5 and Lewis et al. 2013), this process is not incorporated in NUCOM-Bog and therefore high water table levels are simulated. In the model, the whole water balance is calculated four times a month by dividing the monthly precipitation into four equal portions. This procedure speeds up drainage and the response of evapotranspiration to water level (Heijmans et al. 2008), but also creates a bias, by assuming that the precipitation is uniform during the month. Despite the model is not able to simulate lower water table levels at these specific months, for the other months the model is in the range of the measurements.

The fact that the model runs on a monthly time step has as consequence that sub monthly or daily fluctuations, which might be present in the data are averaged out in the model. The model does not seem to be able to simulate the extremes in the data, probably because there are more data points around the mean values. It also has to be kept in mind that the data is measured via the eddy covariance technique and subsequently gap filled, which is known to introduce high uncertainties. The range of uncertainties in the measurements at these sites are in the range of 20-30% (Roulet et al. 2007, McVeigh et al. 2014, Pullens et al. 2016b). These uncertainties are considered during this model exercise, but it has to be taken into account when comparing the model with the measurements.

For all model simulations the run started at the year 1766, in this way the vegetation could establish and the ecosystem could stabilize. The methods used to make a data set starting in 1766 could have introduced a bias of which the range is not quantifiable. Nevertheless, the model performs well for the Mer Bleue site, with only a minor change to the model by using the soil temperature in the decomposition formula.

For Monte Bondone the smallest dataset was available and this results in less power of the calibration. For sites with a low amount of data a multi-site calibration could result in a better calibration.

7.5.2 Multisite calibration

The multi-site calibration did not perform better than the single-site calibration; overall, the model efficiency and the coefficient of determination were similar (Table 7-1). The same has been found by Minunno et al. (2016), who calibrated a simple ecosystem model, with 12 parameters, to estimate carbon and water fluxes of boreal forests on 10 sites. The sites of the present study are located on different continents and are different types of peatland, which result in difficulties for calibration. Nevertheless, the multi-site calibration results in a narrower marginal parameter uncertainty of parameters for Monte Bondone and Mer Bleue, based on the information provided by the Glencar site (Appendix 7.2). As Mäkelä et al. (2008) found for their model, most likely the parameters in the model are highly correlated and the processes in the model can be equally well represented by a generic parameterisation. The fact that the single-site and the multi-site calibration result in the same mismatch between the data and the model would suggest that the error to be predominantly the model's rather than that of the data. (Van Oijen et al. 2011).

7.6 Conclusion

The presented study indicates that the NUCOM-Bog model is able to simulate the summer uptakes reasonably well, but the model has difficulties in simulating the respiration values in winter. Nevertheless, the model is following for all sites the measured trends and the modelled ranges of the uptakes are in the range of the measured uptakes. The model has difficulties in simulating the water table depth for sites where the peatland is drained via streams. An improvement in the water table

depth simulations and the winter respiration should be considered vital for the model to be able to simulate the carbon and water dynamics accurately at monthly time steps. Compared to the site-specific calibration, the multi-site calibration performed similar, but the multi-site calibration result in a narrower marginal parameter uncertainty indicating the strength of multi-site calibration by using the information from all sites.

7.7 Acknowledgements

This work was supported by a STSM grant to JWMP from COST Action FP1304 (Profound, http://cost-profound.eu/site/).

The authors would like to thank Dr. Alessio Gianelle for helping with making modifications to the code.

7.8 Appendixes

Appendix 7.1 List of parameters used in the calibration.

Plant functional type	Description (unit)	Default value (Heijmans et al. 2008)	Minimum	Maximum
Graminoids	Light extinction coefficient (-)	0.5	0.05	1
	Maximum growth rate (g C/m^2/month)	70	7	350
	Mortality rate of leaves (month^{-1})	0.08	0.008	0.4
	Specific Leaf Area (m^2 g C)	0.012	0.0012	0.024
	Minimum temperature for optimal growth (˚C)	12	1.2	4.8
	Maximum temperature for optimal growth (˚C)	20	2	34
	Temperature for optimal growth (˚C)	25	2.5	35
Ericaceous	Light extinction coefficient (-)	0.8	0.08	1
	Maximum growth rate (g C/ m^2/month)	60	6	300
	Mortality rate of leaves (month^{-1})	0.04	0.004	0.2
	Specific Leaf Area (m^2/g C)	0.012	0.0012	0.024
	Minimum temperature for optimal growth (˚C)	5	0.5	2
	Maximum temperature for optimal growth (˚C)	14	1.4	30.8
	Temperature for optimal growth (˚C)	25	2.5	35
	Minimum water table level for optimal growth (mm)	100	10	167
Hummock mosses	Carbon allocation factor (-)	1	0.1	5
	Maximum growth rate (g C/m^2/month)	45	4.5	225
	Mortality rate of leaves (month^{-1})	0.04	0.004	0.2
	Minimum temperature for optimal growth (˚C)	25	2.5	35
	Maximum temperature for optimal growth (˚C)	14	1.4	19.6
	Temperature for optimal growth (˚C)	18	1.8	39.6
Lawn mosses	Carbon allocation factor (-)	1	0.1	5
	Maximum growth rate (g C/m^2/month)	50	5	250
	Mortality rate of leaves (month^{-1})	0.04	0.004	0.2
	Minimum temperature for optimal growth (˚C)	25	2.5	35
	Maximum temperature for optimal growth (˚C)	14	1.4	19.6
	Temperature for optimal growth (˚C)	18	1.8	39.6
Hollow mosses	Carbon allocation factor (-)	1	0.1	5
	Maximum growth rate (g C/m^2/month)	60	6	300
	Mortality rate of leaves (month^{-1})	0.08	0.008	0.4
	Minimum temperature for optimal growth (˚C)	25	2.5	35
	Maximum temperature for optimal growth (˚C)	10	1	14
	Temperature for optimal growth (˚C)	18	1.8	39.6
Generic parameters	Standard deviation of net ecosystem exchange measurements	1	0.1	10
	Standard deviation of water table measurements	0.1	0.01	0.1

Appendix 7.2 Marginal parameter uncertainty of parameters after calibration scaled to the prior provided minimum and maximum values.

In this appendix, the marginal parameter uncertainty of parameters after calibration scaled to the minimum and maximum values provided are presented for the three site-specific calibration and the multi-site calibration. The order of the parameters on the y axis is the inverse order of the parameters in Appendix 1, but the number correlate with the parameters in Appendix 1.

Mer Bleue

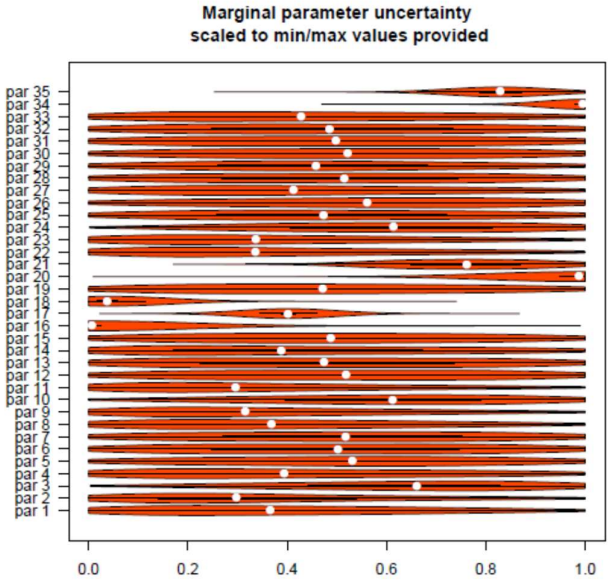

Glencar

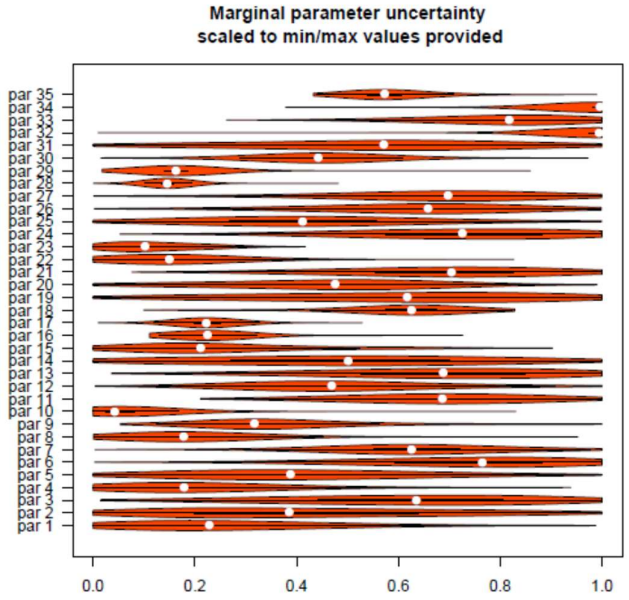

Monte Bondone

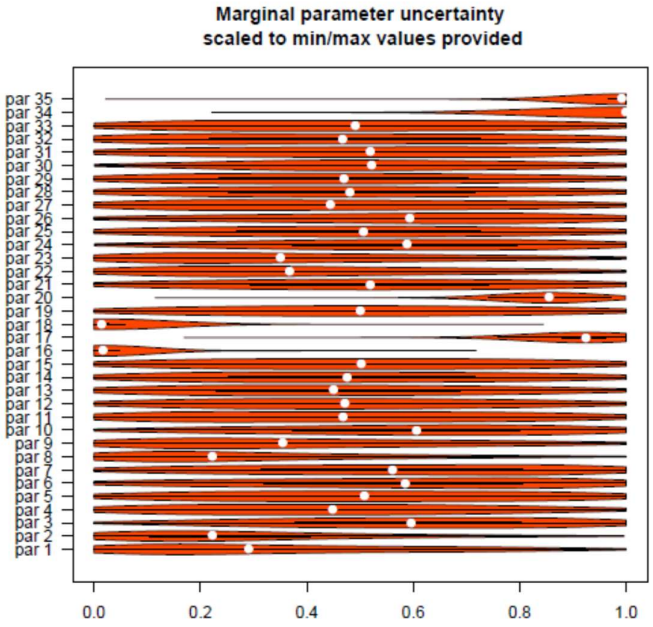

Multi-site calibration

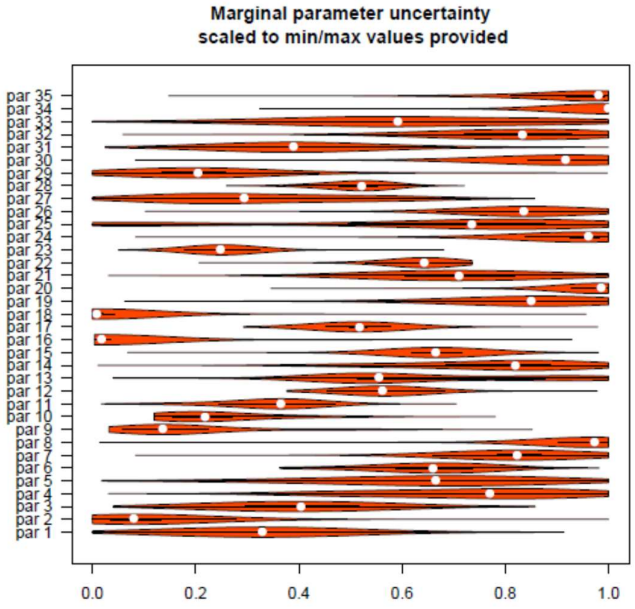

8 Discussion

8.1 Carbon fluxes

At the Monte Bondone peatland the CO_2 fluxes were continuously measured with an eddy covariance system for a four-year period (2012-2015), during a 10-month measurement campaign in 2014 also the methane fluxes were measured. Based on the CO_2 fluxes the peatlands was acting as a carbon source with a net ecosystem exchange (NEE) of 103.5, 262.9, 175.7, 89.2 g C-CO_2 m^{-2} yr^{-1} for 2012, 2013, 2014 and 2015 respectively. With the addition of the methane fluxes the peatland was a bigger source, even though the methane fluxes were small (3.2 g C/m^2) compared to other peatlands: 3.7 to 32 g C- CH_4 m^{-2} yr^{-1}, (Hendriks et al. 2007, Roulet et al. 2007, Nilsson et al. 2008, Aurela et al. 2009, Lund et al. 2009, 2010, Bäckstrand et al. 2010, Sonnentag et al. 2010, Beetz et al. 2013, Wu et al. 2013, McVeigh et al. 2014). The peatland is a carbon source due to the short growing season (carbon uptake period: 73 ± 7 days) and the presence of a snow cover during winter. Under the snow cover, the soil does not reach sub-zero temperatures and therefore the decomposition was considered ongoing (Morgner et al. 2010). The locked-up CO_2 in the snow was released during snow melt and results in a high ecosystem respiration (R_{eco}) after winter. In spite of the short carbon uptake period, the annual growth primary production (GPP) was very high due to the abundance of the highly productive *Molinia caerulea*. These high GPP values during the growing season were not high enough to compensate for the even higher loss of carbon via ecosystem respiration (R_{eco}) during the year and in particular the winter period.

The interannual variability in NEE was very big, in 2013 the loss of carbon was more than twice as big as the loss of carbon in 2015. The biggest drivers of this variability were air temperature, soil water content and photosynthetic active radiation. Due to

climate change it is expected that the air temperature will rise and changes in the precipitation regime will happen at high elevation (Beniston et al. 1997, IPCC 2007, 2013, Im et al. 2010, Eccel et al. 2012, Steger et al. 2013, Pepin et al. 2015, Tudoroiu et al. 2016). The predicted changes in precipitation can be opposite of sign and different in magnitude. These effects of the climate change can lead to a higher R_{eco} and therefore a bigger carbon loss of the peatland over time, or a higher GPP and changing the peatland from a carbon source to a carbon sink, but the scale and the range these effects are still unknown.

8.2 Hydrological modelling

The Monte Bondone peatland is located in the lowest area of the Viote plateau, and thereby receives all the precipitation of the catchment, either via runoff or via seepage. To study the hydrology of the catchment the process-based hydrological model GEOtop in combination with an appropriate set of in situ measurements were used. Due to the highly heterogeneous vegetation, differences in the bulk density and hence the hydraulic conductivity of the soil occurred (Assouline 2006). In the peatland, differences of two-three orders of magnitude for hydraulic conductivity have been measured, which are in range with measurements taken at other peatlands (van Breemen 1995, Beckwith et al. 2003, Holden and Burt 2003, Lewis et al. 2012). The spatial variability of the hydraulic conductivity introduces a high uncertainty in the simulation of soil water content. The values for the hydraulic conductivity of the other soils, a grassland, forest and bare rock, in the catchment are based on a literature study.

The model seems to overestimate the discharge and simulates high discharge peaks, which are not measured in the field. Since the peatland is a Natura 2000 protected area, no weir could be installed and the overflow could not be quantified. Possible explanations for the differences between the measurements and the model output can

be the lack of measurements immediately after heavy rain events, the spatial variability of the hydraulic conductivity and/or the fact that after a precipitation event the runoff flows over the banks. Nevertheless did the model simulated the soil water content and soil temperature well and was it able to follow the interannual variability of the soil temperature for all the four years. Based on the energy balance, the model is able to follow the energy fluxes of the peatland. Overall the GEOtop model performed reasonably well and is able to provide valuable information to assess a water, energy and carbon budget of the system.

With the modelled discharge and the measured dissolved organic carbon (DOC) concentration, an estimate of the DOC fluxes can be calculated. Over the 10 month sampling period a DOC loss of 0.96 mg/L was measured and combined with the modelled discharge, this resulted in an average loss of DOC 10.2 ± 3.8 g C m^{-2} yr^{-1} over the four years. The loss of carbon due to DOC was an extra loss of 7.0 ± 1.8 % of the NEE over the four years, which is lower than what is measured in pristine peatlands, where DOC can account for 20% to 40% of the net ecosystem CO_2 exchange (Roulet et al. 2007, Koehler et al. 2011). Over the four years the average of the loss of DOC at the Monte Bondone site is comparable to a blanket bog peatland in Ireland (14.1 ± 1.5 g C m^{-2} yr^{-1} for 2007 (Koehler et al. 2009)), an upland peat catchment in England (9.4 g C m^{-2} yr^{-1} (Worrall et al. 2003)), a subarctic Atlantic blanket bog in Norway (7.2 ± 0.7 g C m^{-2} yr^{-1} (de Wit et al. 2016)). a fen in Minnesota, United States (10.0 ± 3.0 g C m^{-2} yr^{-1} (Pastor et al. 2003)) and is lower than a rich fen in Minnesota, United States (21.2 ± 6.9 g C m^{-2} yr^{-1} (Urban et al. 1989)).

With the estimation of DOC loss, four years of carbon balance (CO_2, CH_4 fluxes and DOC losses combined) could be calculated, which indicated that the peatland was a carbon source for all four subsequent years. The carbon balance was 112.3, 273.8,

190.8 and 95.3 g C m^{-2} yr^{-1} for 2012, 2013, 2014 and 2015 respectively. This study shows that a process-based hydrological model can be used to study the water and energy dynamics of a peatland in a mountainous area.

8.3 Carbon modelling

Carbon models are generally applied to simulate one particular site, but in this study, three study sites are simulated with the same model. The model has been calibrated for each of the three sites individually and on all the sites together (multi-site calibration). The strength of a multi-site calibration, compared to site-specific calibrations is that the parameter values can provide more information about the ecosystem functioning in general. This global set of parameters, which might perform worse compared to site-specific calibrations, are more generic. This means that the model can be potentially used for more sites, without calibrating for each site specifically (Minunno et al. 2016). The calibration with the help of Bayesian framework is a useful tool since this method also calculates the uncertainty in the posterior distributions of the parameters. For the calibration, only little prior knowledge for the parameter ranges is needed. Some parameters in the model are empirical and without physiological meaning, for these parameters no prior knowledge is available, therefore uniform prior distributions are used.

In this study, it has been show that the multi-site calibration has comparable results with the site-specific calibration. The three different sites used in this study do not only differ in type of peatland (raised bog, blanket bog and fen), but also differ in climate, nevertheless does the multi-site calibration result in a narrower marginal parameter uncertainty of parameters for Monte Bondone and Mer Bleue, based on the information provided by the Glencar site. The broad marginal parameter uncertainties for Mer Bleue and Monte Bondone indicate that most likely the parameters in the

model are highly correlated and the processes in the model can be equally well represented by a generic parameterisation (Mäkelä et al. 2008, Yuan et al. 2014).

The fact that the single-site and the multi-site calibration result in the same mismatch between the data and the model would suggest that the error to be predominantly the model's rather than that of the data (Van Oijen et al. 2011). Nevertheless is the model for all sites following the measured trends and are the modelled ranges of the carbon uptake in the range of the measured uptakes. The model has difficulties in simulating the water table depth for sites where the peatland is drained via streams and in simulating winter respiration for all three sites. An improvement in the water table depth simulations and the winter respiration should be considered vital for the model to be able to simulate the carbon and water dynamics accurately at monthly time steps.

Recommendations for future research

The research conducted at the Monte Bondone peatland since 2012 raises some issues and questions that I would like to recommend for future investigations.

- The carbon balance of the peatland was measured over a four year period in which the site was a pertinent carbon source. The hypothesis is that this is due to the snow cover in winter. A snow removal experiment could provide more information on the winter fluxes without snow cover. Since this experiment is not applicable on ecosystem scale multiple chambers has to be installed to measure the winter fluxes.
- The interannual variability in the four years measurement was high, interesting would be to continue the measurements for a longer period, to capture the interannual variability of both the carbon fluxes as the meteorological conditions.
- To get an idea about how much carbon is stored in this specific peatland, better peat depth measurements have to be taken. The proposed method is a ground penetrating radar; in this case, both the depth of the bedrock and potential natural drainage pipes can be measured. The results could be used for better hydrologic modelling and as a validation for carbon accumulation models.
- Remote sensing techniques could be used to identify and quantify the number of peatlands in the Alps, in this way an estimate of the extent of peatlands in the Alps can be made.
- Since the Monte Bondone peatland is the first alpine peatland for which a carbon balance is made, the addition of other sites could result in better insights in the carbon storage in alpine peatlands.

- The pools/ponds in the wetland can play a big role in the carbon balance of the peatland; more research has to be done to identify the contribution of ebullition (gas emission via bubbling) to the greenhouse gas balance.
- The influence of the peat harvesting in 1914 on the carbon balance is not known, potentially with chamber measurements, the pristine parts can be measured. A comparison between these measurements and the eddy covariance technique can possibly indicate the effect of the harvesting.
- The climate change in mountainous areas is expected to push plant species out of their climate envelope. Longer time series of eddy covariance measurements in combination with reoccurring intensive vegetation surveys can provide detailed information in the effects of climate change.

References

Abdalla, M., A. Hastings, J. Truu, M. Espenberg, Ü. Mander, and P. Smith. 2016. Emissions of methane from northern peatlands: a review of management impacts and implications for future management options. Ecology and Evolution 6:7080–7102.

Aerts, R., and F. Berendse. 1989. Above-Ground Nutrient Turnover and Net Primary Production of an Evergreen and a Deciduous Species in a Heathland Ecosystem. Source Journal of Ecology 77:343–356.

Ammann, B., H. E. Wright, V. Stefanova, J. F. N. Van Leeuwen, W. O. Van Der Knaap, D. Colombaroli, and W. Tinner. 2013. The role of peat decomposition in patterned mires: A case study from the central Swiss Alps. Preslia 85:317–332.

Andersen, R., R. Pouliot, and L. Rochefort. 2013. Above-ground net primary production from vascular plants shifts the balance towards organic matter accumulation in restored sphagnum bogs. Wetlands 33:811–821.

Arrhenius, S. 1898. The effect of constant influences upon physiological relationships. Scandinavian Archives of Physiology 8:367–415.

Aslan-Sungur, G., X. Lee, F. Evrendilek, and N. Karakaya. 2016. Large interannual variability in net ecosystem carbon dioxide exchange of a disturbed temperate peatland. Science of the Total Environment 554–555:192–202.

Assouline, S. 2006. Modeling the Relationship between Soil Bulk Density and the Hydraulic Conductivity Function. Vadose Zone Journal 5:697.

Aubinet, M., C. Feigenwinter, B. Heinesch, Q. Laffineur, D. Papale, M. Reichstein, J. Rinne, and E. Van Gorsel. 2012. Nighttime Flux Correction. Pages 133–157Eddy Covariance: A Practical Guide to Measurement and Data Analysis. Springer Netherlands, Dordrecht.

Aurela, M., T. Laurila, and J. P. Tuovinen. 2002. Annual CO2 balance of a subarctic fen in northern Europe: Importance of the wintertime efflux. Journal of Geophysical Research Atmospheres 107.

Aurela, M., T. Laurila, and J. P. Tuovinen. 2004. The timing of snow melt controls the annual CO_2 balance in a subarctic fen. Geophysical Research Letters 31.

Aurela, M., A. Lohila, J. P. Tuovinen, J. Hatakka, T. Riutta, and T. Laurila. 2009. Carbon dioxide exchange on a northern boreal fen. Boreal Environment Research 14:699–710.

Bäckstrand, K., P. M. Crill, M. Jackowicz-Korczyñski, M. Mastepanov, T. R. Christensen, and D. Bastviken. 2010. Annual carbon gas budget for a subarctic peatland, Northern.pdf. Biogeosciences 7:95–108.

Baldocchi, D. D. 2003. Assessing the eddy covariance technique for evaluating carbon dioxide exchange rates of ecosystems: Past, present and future. Global Change Biology 9:479–492.

Baldocchi, D., M. Detto, O. Sonnentag, J. Verfaillie, Y. A. Teh, W. Silver, and N. M. Kelly. 2012. The challenges of measuring methane fluxes and concentrations over a peatland pasture. Agricultural and Forest Meteorology 153:177–187.

Baldocchi, D., E. Falge, L. Gu, R. Olson, D. Hollinger, S. Running, P. Anthoni, C. Bernhofer, K. Davis, R. Evans, J. Fuentes, A. Goldstein, G. Katul, B. Law, X. Lee, Y. Malhi, T. Meyers, W. Munger, W. Oechel, U. K. T. Paw, K. Pilegaard, H. P. Schmid, R. Valentini, S. Verma, T. Vesala, K. Wilson, and S. Wofsy. 2001. FLUXNET: A New Tool to Study the Temporal and Spatial Variability of Ecosystem-Scale Carbon Dioxide, Water Vapor, and Energy Flux Densities. Bulletin of the American Meteorological Society 82:2415–2434.

Bart, D., T. Davenport, and A. Yantes. 2016. Environmental predictors of woody plant encroachment in calcareous fens are modified by biotic and abiotic land-use legacies. Journal of Applied Ecology 53:541–549.

Bauer, I. E., D. Tirlea, J. S. Bhatti, and R. C. Errington. 2007. Environmental and biotic controls on bryophyte productivity along forest to peatland ecotones. Canadian Journal of Botany 85:463–475.

Beckwith, C. W., A. J. Baird, and A. L. Heathwaite. 2003. Anisotropy and depth-related heterogeneity of hydraulic conductivity in a bog peat. II: Modelling the effects on groundwater flow. Hydrological Processes 17:103–113.

Beer, J., and C. Blodau. 2007. Transport and thermodynamics constrain belowground carbon turnover in a northern peatland. Geochimica et Cosmochimica Acta 71:2989–3002.

Beetz, S., H. Liebersbach, S. Glatzel, G. Jurasinski, U. Buczko, and H. Höper. 2013. Effects of land use intensity on the full greenhouse gas balance in an Atlantic peat bog. Biogeosciences 10:1067–1082.

Bellamy, P. E., L. Stephen, I. S. Maclean, and M. C. Grant. 2012. Response of blanket bog vegetation to drain-blocking. Applied Vegetation Science 15:129–135.

Beniston, M. 2006. Mountain weather and climate: A general overview and a focus on climatic change in the Alps. Hydrobiologia 562:3–16.

Beniston, M., H. F. Diaz, and R. S. Bradley. 1997. Climatic change at high elevation sites: an Overview. Climatic Change 36:233–251.

Berendse, F. 1988. Een simulatiemodel als hulpmiddel bij het beheer van vochtige heidevelden. CABO, Wageningen, NL (In Dutch), Wageningen.

Bertoldi, G., S. Della Chiesa, C. Notarnicola, L. Pasolli, G. Niedrist, and U. Tappeiner. 2014. Estimation of soil moisture patterns in mountain grasslands by means of SAR RADARSAT2 images andhydrological modeling. Journal of Hydrology 516:245–257.

Bertoldi, G., C. Notarnicola, G. Leitinger, S. Endrizzi, M. Zebisch, S. Della Chiesa, and U. Tappeiner. 2010. Topographical and ecohydrological controls on land surface temperature in an alpine catchment. Ecohydrology 3:189–204.

Bertoldi, G., R. Rigon, and T. M. Over. 2006. Impact of Watershed Geomorphic Characteristics on the Energy and Water Budgets. Journal of Hydrometeorology 7:389–403.

Beven, K. J., and M. J. Kirkby. 1979. A physically based, variable contributing area model of basin hydrology / Un modèle à base physique de zone d'appel variable de l'hydrologie du bassin versant. Hydrological Sciences Bulletin 24:43–69.

Beyer, C., and H. Höper. 2015. Greenhouse gas exchange of rewetted bog peat extraction sites and a Sphagnum cultivation site in northwest Germany. Biogeosciences 12:2101–2117.

Biester, H., K. H. Knorr, J. Schellekens, A. Basler, and Y. M. Hermanns. 2014. Comparison of different methods to determine the degree of peat decomposition in peat bogs. Biogeosciences 11:2691–2707.

Blok, D., B. Elberling, and A. Michelsen. 2016. Initial Stages of Tundra Shrub Litter Decomposition May Be Accelerated by Deeper Winter Snow But Slowed Down by Spring Warming. Ecosystems 19:155–169.

Blok, D., U. Sass-Klaassen, G. Schaepman-Strub, M. M. P. D. Heijmans, P. Sauren, and F. Berendse. 2011. What are the main climate drivers for shrub growth in Northeastern Siberian tundra? Biogeosciences 8:1169–1179.

Bohn, T. J., E. Podest, R. Schroeder, N. Pinto, K. C. McDonald, M. Glagolev, I. Filippov, S. Maksyutov, M. Heimann, X. Chen, and D. P. Lettenmaier. 2013. Modeling the large-scale effects of surface moisture heterogeneity on wetland carbon fluxes in the West Siberian Lowland. Biogeosciences 10:6559–6576.

Bond-Lamberty, B., and A. Thomson. 2010. Temperature-associated increases in the global soil respiration record. Nature 464:579–582.

Bowling, D. R., and W. J. Massman. 2011. Persistent wind-induced enhancement of diffusive CO_2 transport in a mountain forest snowpack. Journal of Geophysical Research: Biogeosciences 116.

Ter Braak, C. J. F., and J. A. Vrugt. 2008. Differential Evolution Markov Chain with snooker updater and fewer chains. Statistics and Computing 18:435–446.

Bragazza, L., A. Buttler, B. J. M. Robroek, R. Albrecht, C. Zaccone, V. E. J. Jassey, and C. Signarbieux. 2016. Persistent high temperature and low precipitation reduce peat carbon accumulation. Global Change Biology 22:4114–4123.

van Breemen, N. 1995. How Sphagnum bogs down other plants. Trends in Ecology & Evolution 10:270–275.

Bridgham, S. D., J. P. Megonigal, J. K. Keller, N. B. Bliss, and C. Trettin. 2006. The Carbon Balance of North American Wetlands. Wetlands 26:889–916.

Bu, Z., J. Hans, H. Li, G. Zhao, X. Zheng, J. Ma, and J. Zeng. 2011. The response of peatlands to climate warming: A review. Acta Ecologica Sinica 31:157–162.

Bubier, J. L., T. R. Moore, and G. Crosby. 2006. Fine-scale vegetation distribution in a cool temperate peatland. Canadian Journal of Botany 84:910–923.

Burba, G. 2013. Eddy Covariance Method. Lincoln, Nebraska.

Burba, G. G., D. K. McDermitt, A. Grelle, D. J. Anderson, and L. Xu. 2008. Addressing the influence of instrument surface heat exchange on the measurements of CO_2 flux from open-path gas analyzers. Global Change Biology 14:1854–1876.

Burba, G., A. Schmidt, R. L. Scott, T. Nakai, J. Kathilankal, G. Fratini, C. Hanson, B. Law, D. K. Mcdermitt, R. Eckles, M. Furtaw, and M. Velgersdyk. 2012. Calculating CO_2 and H_2O eddy covariance fluxes from an enclosed gas analyzer using an instantaneous mixing ratio. Global Change Biology 18:385–399.

Camill, P. 2005. Permafrost thaw accelerates in boreal peatlands during late-20th century climate warming. Climatic Change 68:135–152.

Campolongo, F., J. Cariboni, and A. Saltelli. 2007. An effective screening design for sensitivity analysis of large models. Environmental Modelling and Software 22:1509–1518.

Carmichael, M. J., E. S. Bernhardt, S. L. Bräuer, and W. K. Smith. 2014. The role of vegetation in methane flux to the atmosphere: Should vegetation be included as a distinct category in the global methane budget? Biogeochemistry 119:1–24.

Cescatti, A., C. Chemini, C. De Siena, D. Gianelle, G. Nicolini, and G. Wohlfahrt. 1999. Monte Bondone composite landscape, Italy. Pages 35–94*in* A. Cernusca, U. Tappeiner, and N. Bayfield, editors.Land-Use in European Mountian Ecosystems, ECOMONT - Concepts and results. Wissenschafts-Verlag, Berlin.

Chambers, F., A. Crowle, J. Daniell, D. Mauquoy, J. McCarroll, N. Sanderson, T. Thom, P. Toms, and J. Webb. 2017. Ascertaining the nature and timing of mire

degradation: using palaeoecology to assist future conservation management in Northern England. AIMS Environmental Science 4:54–82.

Charman, D. J., D. W. Beilman, M. Blaauw, R. K. Booth, S. Brewer, F. M. Chambers, J. A. Christen, A. Gallego-Sala, S. P. Harrison, P. D. M. Hughes, S. T. Jackson, A. Korhola, D. Mauquoy, F. J. G. Mitchell, I. C. Prentice, M. Van Der Linden, F. De Vleeschouwer, Z. C. Yu, J. Alm, I. E. Bauer, Y. M. C. Corish, M. Garneau, V. Hohl, Y. Huang, E. Karofeld, G. Le Roux, J. Loisel, R. Moschen, J. E. Nichols, T. M. Nieminen, G. M. MacDonald, N. R. Phadtare, N. Rausch, U. Sillasoo, G. T. Swindles, E. S. Tuittila, L. Ukonmaanaho, M. Väliranta, S. Van Bellen, B. Van Geel, D. H. Vitt, and Y. Zhao. 2013. Climate-related changes in peatland carbon accumulation during the last millennium. Biogeosciences 10:929–944.

Chiesa, D. D., G. Bertoldi, G. Niedrist, N. Obojes, S. Endrizzi, J. D. Albertson, G. Wohlfahrt, L. Hörtnagl, and U. Tappeiner. 2014. Modelling changes in grassland hydrological cycling along an elevational gradient in the Alps. Ecohydrology 7:1453–1473.

Clein, J. S., and J. P. Schimel. 1995. Microbial activity of tundra and taiga soils at sub-zero temperatures. Soil Biology and Biochemistry 27:1231–1234.

Clymo, R. S. 1964. The Origin of Acidity in Sphagnum Bogs. Source: The Bryologist 67:427–431.

Clymo, R. S. 1984. The Limits to Peat Bog Growth. Philosophical Transactions of the Royal Society B: Biological Sciences 303:605–654.

Clymo, R. S. 2004. Hydraulic conductivity of peat at Ellergower Moss, Scotland. Hydrological Processes 18:261–274.

Clymo, R. S., and P. M. Hayward. 1982. The Ecology of Sphagnum. Pages 229–289Bryophyte Ecology. Springer Netherlands, Dordrecht.

Couwenberg, J., R. Dommain, and H. Joosten. 2010. Greenhouse gas fluxes from tropical peatlands in south-east Asia. Global Change Biology 16:1715–1732.

Cunliffe, A. M., A. J. Baird, and J. Holden. 2013. Hydrological hotspots in blanket peatlands: Spatial variation in peat permeability around a natural soil pipe. Water Resources Research 49:5342–5354.

Dall'Amico, M., S. Endrizzi, S. Gruber, and R. Rigon. 2011. A robust and energy-conserving model of freezing variably-saturated soil. Cryosphere 5:469–484.

Dalla Fior, G. 1969. Analisi polliniche di torbe e depositi lacustri della Venezia Tridentina. TEMI, Trento.

Darcy, H. 1856. Les fontaines publiques de la ville de Dijon : exposition et application des principes à suivre et des formules à employer dans les questions de distribution d'eau. Recherche:647.

Dengel, S., D. Zona, T. Sachs, M. Aurela, M. Jammet, F. J. W. Parmentier, W. Oechel, and T. Vesala. 2013. Testing the applicability of neural networks as a gap-filling method using CH_4 flux data from high latitude wetlands. Biogeosciences 10:8185–8200.

Dentener, F. J. 2006. Global maps of atmospheric nitrogen deposition, 1860, 1993, and 2050.

Devia, G. K., B. P. Ganasri, and G. S. Dwarakish. 2015. A Review on Hydrological Models. Aquatic Procedia 4:1001–1007.

Dieleman, C. M., B. A. Branfireun, J. W. Mclaughlin, and Z. Lindo. 2015. Climate change drives a shift in peatland ecosystem plant community: Implications for ecosystem function and stability. Global Change Biology 21:388–395.

Dieleman, C. M., Z. Lindo, J. W. McLaughlin, A. E. Craig, and B. A. Branfireun. 2016. Climate change effects on peatland decomposition and porewater dissolved organic carbon biogeochemistry. Biogeochemistry 128:385–396.

Donat, M. G., A. L. Lowry, L. V. Alexander, P. A. O'Gorman, and N. Maher. 2017. Addendum: More extreme precipitation in the world's dry and wet regions. Nature Climate Change 7:154–158.

Dorrepaal, E., S. Toet, R. S. P. van Logtestijn, E. Swart, M. J. van de Weg, T. V. Callaghan, and R. Aerts. 2009. Carbon respiration from subsurface peat accelerated by climate warming in the subarctic. Nature 460:616–619.

Drösler, M., A. Freibauer, T. R. Christensen, and T. Friborg. 2008. The Continental-Scale Greenhouse Gas Balance of Europe. Page *in* A. J. Dolman, R. Valentini, and A. Freibauer, editors. The Continental-Scale Greenhouse Gas Balance of Europe. Springer New York, New York, NY.

Eccel, E., P. Cau, and R. Ranzi. 2012. Data reconstruction and homogenization for reducing uncertainties in high-resolution climate analysis in Alpine regions. Theoretical and Applied Climatology 110:345–358.

Endrizzi, S., S. Gruber, M. Dall'Amico, and R. Rigon. 2014. GEOtop 2.0: Simulating the combined energy and water balance at and below the land surface accounting for soil freezing, snow cover and terrain effects. Geoscientific Model Development 7:2831–2857.

Evans, C. D., S. E. Page, T. Jones, S. Moore, V. Gauci, R. Laiho, J. Hruška, T. E. H. Allott, M. F. Billett, E. Tipping, C. Freeman, and M. H. Garnett. 2014. Contrasting vulnerability of drained tropical and high-latitude peatlands to fluvial loss of stored carbon. Global Biogeochemical Cycles 28:1215–1234.

Ewen, J., G. Parkin, and P. E. O'Conell. 2000. SHETRAN : Distributed River Basin Flow Modeling System. Journal of Hydrologic Engineering 5:250–258.

Falge, E., D. Baldocchi, R. Olson, P. Anthoni, M. Aubinet, C. Bernhofer, G. Burba, R. Ceulemans, R. Clement, H. Dolman, A. Granier, P. Gross, T. Grünwald, D. Hollinger, N.-O. Jensen, G. Katul, P. Keronen, A. Kowalski, C. T. Lai, B. E. Law, T. Meyers, J. Moncrieff, E. Moors, J. W. Munger, K. Pilegaard, Ü. Rannik, C. Rebmann, A. Suyker, J. Tenhunen, K. Tu, S. Verma, T. Vesala, K. Wilson, and S. Wofsy. 2001. Gap filling strategies for defensible annual sums of net ecosystem exchange. Agricultural and Forest Meteorology 107:43–69.

Fatichi, S., E. R. Vivoni, F. L. Ogden, V. Y. Ivanov, B. Mirus, D. Gochis, C. W. Downer, M. Camporese, J. H. Davison, B. Ebel, N. Jones, J. Kim, G. Mascaro, R. Niswonger, P. Restrepo, R. Rigon, C. Shen, M. Sulis, and D. Tarboton. 2016. An overview of current applications, challenges, and future trends in distributed process-based models in hydrology. Journal of Hydrology 537:45–60.

Fenner, N., and C. Freeman. 2011. Drought-induced carbon loss in peatlands. Nature Geoscience 4:895–900.

Foken, T., M. Göockede, M. Mauder, L. Mahrt, B. Amiro, and W. Munger. 2004. Post-Field Data Quality Control. Pages 181–208Handbook of Micrometeorology. Kluwer Academic Publishers, Dordrecht.

Freeman, C., N. Fenner, N. J. Ostle, H. Kang, D. J. Dowrick, B. Reynolds, M. A. Lock, D. Sleep, S. Hughes, and J. Hudson. 2004. Export of dissolved organic carbon from peatlands under elevated carbon dioxide levels. Nature 430:195–198.

Fritsch, S., F. Guenther, M. Suling, and S. M. Mueller. 2016. Training of Neural Networks [R package neuralnet version 1.33]. Comprehensive R Archive Network (CRAN).

Frolking, S. E., J. L. Bubier, T. R. Moore, T. Ball, L. M. Bellisario, A. Bhardwaj, P. Carroll, P. M. Crill, P. M. Lafleur, J. H. McCaughey, N. T. Roulet, A. E. Suyker, S. B. Verma, J. M. Waddington, and G. J. Whiting. 1998. Relationship between ecosystem productivity and photosynthetically active radiation for northern peatlands. Global Biogeochemical Cycles 12:115–126.

Frolking, S., N. T. Roulet, T. R. Moore, P. J. H. Richard, M. Lavoie, and S. D. Muller. 2001. Modeling northern peatland decomposition and peat accumulation. Ecosystems 4:479–498.

Frolking, S., N. T. Roulet, E. Tuittila, J. L. Bubier, A. Quillet, J. Talbot, and P. J. H. Richard. 2010. A new model of Holocene peatland net primary production, decomposition, water balance, and peat accumulation. Earth System Dynamics 1:1–21.

Frolking, S., J. Talbot, M. C. Jones, C. C. Treat, J. B. Kauffman, E.-S. Tuittila, and N. Roulet. 2011. Peatlands in the Earth's 21st century climate system. Environmental Reviews 19:371–396.

Gao, J., J. Holden, and M. Kirkby. 2016. The impact of land-cover change on flood peaks in peatland basins. Water Resources Research 52:3477–3492.

Gatis, N., D. J. Luscombe, E. Grand-Clement, I. P. Hartley, K. Anderson, D. Smith, and R. E. Brazier. 2016. The effect of drainage ditches on vegetation diversity and CO_2 fluxes in a *Molinia caerulea*-dominated peatland. Ecohydrology 9:407–420.

Gebauer, R. L. E., J. F. Reynolds, and J. D. Tenhunen. 1995. Growth and allocation of the arctic sedges *Eriohorum angustifolium* and *E. vaginatum*: effects of variable soil oxygen and nutrient availability. Oecologia 104:330–339.

Gelman, A., and D. B. Rubin. 1992. Itsim. Statistical Science 7:457–511.

Gerdol, R., L. Bragazza, and L. Brancaleoni. 2008. Heatwave 2003: High summer temperature, rather than experimental fertilization, affects vegetation and CO_2 exchange in an alpine bog. New Phytologist 179:142–154.

Gielen, B., J. Neirynck, S. Luyssaert, and I. A. Janssens. 2011. The importance of dissolved organic carbon fluxes for the carbon balance of a temperate Scots pine forest. Agricultural and Forest Meteorology 151:270–278.

Gilmanov, T. G., D. A. Johnson, and N. Z. Saliendra. 2003. Growing season CO2 fluxes in a sagebrush-steppe ecosystem in Idaho: bowen ratio/energy balance measurements and modeling. Basic and Applied Ecology 4:167–183.

Giorgi, F., J. W. Hurrell, M. R. Marinucci, and M. Beniston. 1997. Elevation dependency of the surface climate change signal: A model study. Journal of Climate 10:288–296.

Gong, J., S. Kellomäki, K. Wang, C. Zhang, N. Shurpali, and P. J. Martikainen. 2013. Modeling CO_2 and CH_4 flux changes in pristine peatlands of Finland under changing climate conditions. Ecological Modelling 263:64–80.

Gore, A. J. P. 1983. Ecosystems of the World 4A. Mires: Swamps, Bog, Fen and Moor. Page (A. J. P. Gore and D. W. Goodall, Eds.).

Gorham, E. 1957. The Development of Peat Lands. The Quarterly Review of Biology 32:145–166.

Gorham, E. 1991. Northern peatlands: role in the carbon cycle and probable responses to climatic warming. Ecological Applications 1:182–195.

Gregory, D., R. N. B. Smith, and P. M. Cox. 1996. Canopy, surface and soil hydrology. Unified Model documentation Paper 25.

Grünheid, S., G. Amy, and M. Jekel. 2005. Removal of bulk dissolved organic carbon (DOC) and trace organic compounds by bank filtration and artificial recharge. Water Research 39:3219–3228.

Gubler, S., S. Endrizzi, S. Gruber, and R. S. Purves. 2013. Sensitivities and uncertainties of modeled ground temperatures in mountain environments. Geoscientific Model Development 6:1319–1336.

Haahti, K., L. Warsta, T. Kokkonen, B. A. Younis, and H. Koivusalo. 2016. Distributed hydrological modeling with channel network flow of a forestry drained peatland site. Water Resources Research 52:246–263.

Hammond, R. F. 1978. The Peatlands of Ireland. Page Soil Survey Bulletin No. 35.

Harpenslager, S. F., G. Van Dijk, S. Kosten, J. G. M. Roelofs, A. J. P. Smolders, and L. P. M. Lamers. 2015a. Simultaneous high C fixation and high C emissions in Sphagnum mires. Biogeosciences 12:4739–4749.

Harpenslager, S. F., E. van den Elzen, M. A. R. Kox, A. J. P. Smolders, K. F. Ettwig, and L. P. M. Lamers. 2015b. Rewetting former agricultural peatlands: Topsoil removal as a prerequisite to avoid strong nutrient and greenhouse gas emissions. Ecological Engineering 84:159–168.

Hartig, F., J. Dyke, T. Hickler, S. I. Higgins, R. B. O'Hara, S. Scheiter, and A. Huth. 2012. Connecting dynamic vegetation models to data - an inverse perspective. Journal of Biogeography 39:2240–2252.

Hartig, F., F. Minunno, S. Paul, and D. Cameron. 2017. BayesianTools: General-Purpose MCMC and SMC Samplers and Tools for Bayesian Statistics.

Hatala, J. A., M. Detto, O. Sonnentag, S. J. Deverel, J. Verfaillie, and D. D. Baldocchi. 2012. Greenhouse gas (CO_2, CH_4, H_2O) fluxes from drained and flooded agricultural peatlands in the Sacramento-San Joaquin Delta. Agriculture, Ecosystems and Environment 150:1–18.

Heijmans, M. M. P. D., H. Klees, W. De Visser, and F. Berendse. 2002. Response of a Sphagnum bog plant community to elevated CO_2 and N supply. Plant Ecology 162:123–134.

Heijmans, M. M. P. D., Y. A. M. Van der Knaap, M. Holmgren, and J. Limpens. 2013. Persistent versus transient tree encroachment of temperate peat bogs: Effects of climate warming and drought events. Global Change Biology 19:2240–2250.

Heijmans, M. M. P. D., D. Mauquoy, B. van Geel, and F. Berendse. 2008. Long-term effects of climate change on vegetation and carbon dynamics in peat bogs. Journal of Vegetation Science 19:307–320.

Hendriks, D. M. D., J. van Huissteden, A. J. Dolman, and M. K. van der Molen. 2007. The full greenhouse gas balance of an abandoned peat meadow. Biogeosciences 4:411–424.

Henry, J., and J. Aherne. 2014. Nitrogen deposition and exceedance of critical loads for nutrient nitrogen in Irish grasslands. Science of the Total Environment 470–471:216–223.

Hingerl, L., H. Kunstmann, S. Wagner, M. Mauder, J. Bliefernicht, and R. Rigon. 2016. Spatio-temporal variability of water and energy fluxes – a case study for a mesoscale catchment in pre-alpine environment. Hydrological Processes 30:3804–3823.

Hoag, R. S., and J. S. Price. 1995. A field-scale, natural gradient solute transport experiment in peat at a Newfoundland blanket bog. Journal of Hydrology 172:171–184.

Hobbie, S. E. 1996. Temperature and plant species control over litter decomposition in Alaska Tundra. Ecological Monographs 66:502–522.

Holden, J., and T. P. Burt. 2002. Piping and pipeflow in a deep peat catchment. Catena 48:163–199.

Holden, J., and T. P. Burt. 2003. Hydraulic conductivity in upland blanket peat: Measurement and variability. Hydrological Processes 17:1227–1237.

Holmgren, M., C. Y. Lin, J. E. Murillo, A. Nieuwenhuis, J. Penninkhof, N. Sanders, T. van Bart, H. van Veen, H. Vasander, M. E. Vollebregt, and J. Limpens. 2015. Positive shrub-tree interactions facilitate woody encroachment in boreal peatlands. Journal of Ecology 103:58–66.

Hribljan, J. A., E. S. Kane, T. G. Pypker, and R. C. Chimner. 2014. The effect of long-term water table manipulations on dissolved organic carbon dynamics in a poor fen peatland. Journal of Geophysical Research: Biogeosciences 119:1–19.

Humphreys, E. R., C. Charron, M. Brown, and R. Jones. 2014. Two Bogs in the Canadian Hudson Bay Lowlands and a Temperate Bog Reveal Similar Annual Net Ecosystem Exchange of CO2. Arctic, Antarctic, and Alpine Research 46:103–113.

Humphreys, E. R., and P. M. Lafleur. 2011. Does earlier snowmelt lead to greater CO 2 sequestration in two low Arctic tundra ecosystems? Geophysical Research Letters 38.

Hvorslev, M. J. 1951. Time Lag and Soil Permeability in Ground-Water Observations.

Im, E. S., E. Coppola, F. Giorgi, and X. Bi. 2010. Local effects of climate change over the Alpine region: A study with a high resolution regional climate model with a surrogate climate change scenario. Geophysical Research Letters 37.

IPCC. 2007. Climate Change 2007: The Physical Science Basis. Contribution of Working group I to the Fourth Assessment Report of Intergovernmental Panel on Climate Change. Cambridge University Press, New York.

IPCC. 2013. The physical science basis. Contribution of working group I to the fifth assessment report of the intergovernmental panel on climate change. Page (T. F. Stocker, D. Qin, G.-K. Plattner, M. Tignor, S. K. Allen, J. Boschung, A. Nauels, Y. Xia, V. Bex, and P. M. Midgley, Eds.) K., Tignor, M., Allen, SK, Boschung, J., Nauels, A., Xia, Y., Bex, V., Midgley, PM, Eds. Cambridge University Press, Cambridge, United Kingdom and New York, NY, USA.

IRRI. 2012. The Eddy Covariance Method. Pages 1–19Eddy Covariance. Springer Netherlands, Dordrecht.

Ise, T., A. L. Dunn, S. C. Wofsy, and P. R. Moorcroft. 2008. High sensitivity of peat decomposition to climate change through water-table feedback. Nature Geoscience 1:763–766.

Janssen, P. H. M., and P. S. C. Heuberger. 1995. Calibration of process-oriented models. Ecological Modelling 83:55–66.

Jarosz, N., Y. Brunet, E. Lamaud, M. Irvine, J. M. Bonnefond, and D. Loustau. 2008. Carbon dioxide and energy flux partitioning between the understorey and the overstorey of a maritime pine forest during a year with reduced soil water availability. Agricultural and Forest Meteorology 148:1508–1523.

Järveoja, J., M. Peichl, M. Maddison, K. Soosaar, K. Vellak, E. Karofeld, A. Teemusk, and Ü. Mander. 2016. Impact of water table level on annual carbon and greenhouse gas balances of a restored peat extraction area. Biogeosciences 13:2637–2651.

Jenkinson, D. S. 1990. The turnover of organic carbon and nitrogen in soil. Philosophical Transactions: Biological Sciences 329:361–368.

Johnson, J., T. Cummins, and J. Aherne. 2016. Critical loads and nitrogen availability under deposition and harvest scenarios for conifer forests in Ireland. Science of the Total Environment 541:319–328.

Joosten, H., Clarke, D. 2002. Wise Use of Mires and Peatlands - and Including F Ramework for D Ecision - Making. International mire conservation group.

Jungkunst, H. F., H. Flessa, C. Scherber, and S. Fiedler. 2008. Groundwater level controls CO_2, N_2O and CH_4 fluxes of three different hydromorphic soil types of a temperate forest ecosystem. Soil Biology and Biochemistry 40:2047–2054.

Juszczak, R., M. Acosta, and J. Olejnik. 2012. Comparison of daytime and nighttime ecosystem respiration measured by the closed chamber technique on a temperate mire in Poland. Polish Journal of Environmental Studies 21:643–658.

Juszczak, R., E. Humphreys, M. Acosta, M. Michalak-Galczewska, D. Kayzer, and J. Olejnik. 2013. Ecosystem respiration in a heterogeneous temperate peatland and its sensitivity to peat temperature and water table depth. Plant and Soil 366:505–520.

Kamocki, A. K., A. Kołos, and P. Banaszuk. 2016. Can we effectively stop the expansion of trees on wetlands? Results of a birch removal experiment. Wetlands Ecology and Management:1–9.

Kirschbaum, M. U. F. 1995. The temperature dependence of soil organic matter decomposition, and the effect of global warming on soil organic C storage. Soil Biology and Biochemistry 27:753–760.

Kljun, N., P. Calanca, M. W. Rotach, and H. P. Schmid. 2004. A simple parameterisation for flux footprint predictions. Boundary-Layer Meteorology 112:503–523.

van der Knaap, W. O., M. Lamentowicz, J. F. N. van Leeuwen, S. Hangartner, M. Leuenberger, D. Mauquoy, T. Goslar, E. A. D. Mitchell, T. Lamentowicz, and C. Kamenik. 2011. A multi-proxy, high-resolution record of peatland development and its drivers during the last millennium from the subalpine Swiss Alps. Quaternary Science Reviews 30:3467–3480.

Koebsch, F., G. Jurasinski, M. Koch, J. Hofmann, and S. Glatzel. 2015. Controls for multi-scale temporal variation in ecosystem methane exchange during the growing season of a permanently inundated fen. Agricultural and Forest Meteorology 204:94–105.

Koehler, A. K., K. Murphy, G. Kiely, and M. Sottocornola. 2009. Seasonal variation of DOC concentration and annual loss of DOC from an Atlantic blanket bog in South Western Ireland. Biogeochemistry 95:231–242.

Koehler, A. K., M. Sottocornola, and G. Kiely. 2011. How strong is the current carbon sequestration of an Atlantic blanket bog? Global Change Biology 17:309–319.

Koerselman, W. 1989. Groundwater and surface water hydrology of a small groundwater-fed fen. Wetlands Ecology and Management 1:31–43.

Van Der Kolk, H. J., M. M. P. D. Heijmans, J. Van Huissteden, J. W. M. Pullens, and F. Berendse. 2016. Potential Arctic tundra vegetation shifts in response to changing temperature, precipitation and permafrost thaw. Biogeosciences 13:6229–6245.

Lafleur, P. M., T. R. Moore, N. T. Roulet, and S. Frolking. 2005. Ecosystem respiration in a cool temperate bog depends on peat temperature but not water table. Ecosystems 8:619–629.

Lafleur, P. M., N. T. Roulet, and S. W. Admiral. 2001. Annual cycle of CO_2 exchange at a bog peatland. Journal of Geophysical Research 106:3071.

Lafleur, P. M., N. T. Roulet, J. L. Bubier, S. Frolking, and T. R. Moore. 2003. Interannual variability in the peatland-atmosphere carbon dioxide exchange at an ombrotrophic bog. Global Biogeochemical Cycles 17.

Laine, A. M., M. Sottocornola, G. Kiely, K. A. Byrne, D. Wilson, and E. S. Tuittila. 2006. Estimating net ecosystem exchange in a patterned ecosystem: Example from blanket bog. Agricultural and Forest Meteorology 138:231–243.

Laine, A. M., D. Wilson, G. Kiely, and K. A. Byrne. 2007. Methane flux dynamics in an Irish lowland blanket bog. Plant and Soil 299:181–193.

Laitinen, J., S. Rehell, A. Huttunen, T. Tahvanainen, R. Heikkilä, and T. Lindholm. 2007. Mire systems in Finland - Special view to aapa mires and their water-flow pattern. Suo 58:1–26.

Laliberte, G. E., A. T. Corey, and R. H. Brooks. 1966. Properties of Unsaturated Porous Media. Page Hydrology Papers. Hydrology. Colorado State University.

Lang, S. I., J. H. C. Cornelissen, T. Klahn, R. S. P. Van Logtestijn, R. Broekman, W. Schweikert, and R. Aerts. 2009. An experimental comparison of chemical traits and litter decomposition rates in a diverse range of subarctic bryophyte, lichen and vascular plant species. Journal of Ecology 97:886–900.

Larsen, K. S., P. Grogan, S. Jonasson, and A. Michelsen. 2007. Respiration and Microbial Dynamics in Two Subarctic Ecosystems during Winter and Spring Thaw: Effects of Increased Snow Depth. Arctic, Antarctic, and Alpine Research 39:268–276.

Lasslop, G., M. Reichstein, D. Papale, A. D. Richardson, A. Arneth, A. BARR, P. Stoy, and G. Wohlfahrt. 2010. Separation of net ecosystem exchange into assimilation and respiration using a light response curve approach: critical issues and global evaluation. Global Change Biology 16:187–208.

Lavoie, R., J. Deslandes, and F. Proulx. 2016. Assessing the ecological value of wetlands using the MACBETH approach in Quebec City. Journal for Nature Conservation 30:67–75.

Lawrence, B. A., R. D. Jackson, and C. J. Kucharik. 2013. Testing the stability of carbon pools stored in tussock sedge meadows. Applied Soil Ecology 71:48–57.

Letts, M. G., P. M. Lafleur, and N. T. Roulet. 2005. On the relationship between cloudiness and net ecosystem carbon dioxide exchange in a peatland ecosystem. Ecoscience 12:53–59.

Lewis, C. 2011. Measurement and modelling of soil hydrological properties for use in the distributed rainfall runoff model – GEOtop.

Lewis, C., J. Albertson, X. Xu, and G. Kiely. 2012. Spatial variability of hydraulic conductivity and bulk density along a blanket peatland hillslope. Hydrological Processes 26:1527–1537.

Lewis, C., J. Albertson, T. Zi, X. Xu, and G. Kiely. 2013. How does afforestation affect the hydrology of a blanket peatland? A modelling study. Hydrological Processes 27:3577–3588.

Li, W., R. E. Dickinson, R. Fu, G. Y. Niu, Z. L. Yang, and J. G. Canadell. 2007. Future precipitation changes and their implications for tropical peatlands. Geophysical Research Letters 34.

Lloyd, J., and J. Taylor. 1994. On the temperature dependence of soil respiration. Functional ecology 8:315–323.

Lowry, C. S., D. Fratta, and M. P. Anderson. 2009. Ground penetrating radar and spring formation in a groundwater dominated peat wetland. Journal of Hydrology 373:68–79.

Lund, M., P. M. Lafleur, N. T. Roulet, A. Lindroth, T. R. Christensen, M. Aurela, B. H. Chojnicki, L. B. Flanagan, E. R. Humphreys, T. Laurila, W. C. Oechel, J. Olejnik, J. Rinne, P. Schubert, and M. Nilsson. 2010. Variability in exchange of CO_2 across 12 northern peatland and tundra sites. Global Change Biology 16:2436–2448.

Lund, M., A. Lindroth, T. R. Christensen, and L. Ström. 2009. Annual CO_2 balance of a temperate bog. Meddelanden fran Lunds Universitets Geografiska Institutioner, Avhandlingar 59:804–811.

Mäkelä, A., M. Pulkkinen, P. Kolari, F. Lagergren, P. Berbigier, A. Lindroth, D. Loustau, E. Nikinmaa, T. Vesala, and P. Hari. 2008. Developing an empirical model of stand GPP with the LUE approach: Analysis of eddy covariance data at five contrasting conifer sites in Europe. Global Change Biology 14:92–108.

Mäkilä, M., M. Saarnisto, and T. Kankainen. 2001. Aapa mires as a carbon sink and source during the Holocene. Journal of Ecology 89:589–599.

Marcolla, B., A. Cescatti, G. Manca, R. Zorer, M. Cavagna, A. Fiora, D. Gianelle, M. Rodeghiero, M. Sottocornola, and R. Zampedri. 2011. Climatic controls and ecosystem responses drive the inter-annual variability of the net ecosystem exchange of an alpine meadow. Agricultural and Forest Meteorology 151:1233–1243.

Massman, W. J., and X. Lee. 2002. Eddy covariance flux corrections and uncertainties in long-term studies of carbon and energy exchanges. Agricultural and Forest Meteorology 113:121–144.

Massman, W. J., R. A. Sommerfeld, A. R. Mosier, K. F. Zeller, T. J. Hehn, and S. G. Rochelle. 1997. A model investigation of turbulence-driven pressure-pumping effects on the rate of diffusion of CO_2 , N_2O, and CH_4 through layered snowpacks. Journal of Geophysical Research 102:18851.

Mast, M. A., K. P. Wickl, R. T. Striegl, and D. W. Clow. 1998. Winter fluxes of CO_2 and CH_4 from subalpine soils in Rocky Mountain National Park, Colorado. Global Biogeochemical Cycles 12:607–620.

McVeigh, P., M. Sottocornola, N. Foley, P. Leahy, and G. Kiely. 2014. Meteorological and functional response partitioning to explain interannual variability of CO_2 exchange at an Irish Atlantic blanket bog. Agricultural and Forest Meteorology 194:8–19.

Miller, C. A., B. W. Benscoter, and M. R. Turetsky. 2015. The effect of long-term drying associated with experimental drainage and road construction on vegetation composition and productivity in boreal fens. Wetlands Ecology and Management 23:845–854.

Minkkinen, K., K. A. Byrne, and C. Trettin. 2008. Climate impacts of peatland forestry. Page Peatlands and Climate Change.

Minunno, F., M. Peltoniemi, S. Launiainen, M. Aurela, A. Lindroth, A. Lohila, I. Mammarella, K. Minkkinen, and A. Mäkelä. 2016. Calibration and validation of a semi-empirical flux ecosystem model for coniferous forests in the Boreal region. Ecological Modelling 341:37–52.

Mitsch, W. J., B. Bernal, A. M. Nahlik, Ü. Mander, L. Zhang, C. J. Anderson, S. E. Jørgensen, and H. Brix. 2013. Wetlands, carbon, and climate change. Landscape Ecology 28:583–597.

Moffat, A. M., D. Papale, M. Reichstein, D. Y. Hollinger, A. D. Richardson, A. G. Barr, C. Beckstein, B. H. Braswell, G. Churkina, A. R. Desai, E. Falge, J. H. Gove, M. Heimann, D. Hui, A. J. Jarvis, J. Kattge, A. Noormets, and V. J. Stauch. 2007. Comprehensive comparison of gap-filling techniques for eddy covariance net carbon fluxes. Agricultural and Forest Meteorology 147:209–232.

van der Molen, M. K., J. van Huissteden, F. J. W. Parmentier, A. M. R. Petrescu, A. J. Dolman, T. C. Maximov, A. V. Kononov, S. V. Karsanaev, and D. A. Suzdalov. 2007. The growing season greenhouse gas balance of a continental tundra site in the Indigirka lowlands, NE Siberia. Biogeosciences 4:985–1003.

Moncrieff, J. B., J. M. Massheder, H. De Bruin, J. Elbers, T. Friborg, B. Heusinkveld, P. Kabat, S. Scott, H. Soegaard, and A. Verhoef. 1997. A system to measure surface fluxes of momentum, sensible heat, water vapour and carbon dioxide. Journal of Hydrology 188–189:589–611.

Moncrieff, J., R. Clement, J. Finnigan, and T. Meyers. 2004. Averaging, Detrending, and Filtering of Eddy Covariance Time Series. Pages 7–31*in* X. Lee, W. J. Massman, and B. E. Law, editors.Handbook of Micrometeorology. Kluwer Academic Publishers, Dordrecht.

Monson, R. K., S. P. Burns, M. W. Williams, A. C. Delany, M. Weintraub, and D. A. Lipson. 2006. The contribution of beneath-snow soil respiration to total ecosystem respiration in a high-elevation, subalpine forest. Global Biogeochemical Cycles 20.

Moore, P. A., T. G. Pypker, and J. M. Waddington. 2013. Effect of long-term water table manipulation on peatland evapotranspiration. Agricultural and Forest Meteorology 178–179:106–119.

Moore, T. R., N. T. Roulet, and J. M. Waddington. 1998. Uncertainty in predicting the effect of climatic change on the carbon cycling of Canadian peatlands. Climatic Change 40:229–245.

Moreno-Mateos, D., P. Meli, M. I. Vara-Rodríguez, and J. Aronson. 2015. Ecosystem response to interventions: Lessons from restored and created wetland ecosystems. Journal of Applied Ecology 52:1528–1537.

Morgner, E., B. Elberling, D. Strebel, and E. J. Cooper. 2010. The importance of winter in annual ecosystem respiration in the High Arctic: effects of snow depth in two vegetation types. Polar Research 29:58–74.

Morris, M. D. 1991. Factorial Sampling Plans for Preliminary Computational Experiments. Technometrics 33:161.

Munir, T. M., M. Perkins, E. Kaing, and M. Strack. 2015. Carbon dioxide flux and net primary production of a boreal treed bog: Responses to warming and water-table-lowering simulations of climate change. Biogeosciences 12:1091–1111.

Murphy, M. T., A. McKinley, and T. R. Moore. 2009. Variations in above- and below-ground vascular plant biomass and water table on a temperate ombrotrophic peatland. Botany 87:845–853.

Murray, K. R., A. K. Borkenhagen, D. J. Cooper, and M. Strack. 2017. Growing season carbon gas exchange from peatlands used as a source of vegetation donor material for restoration. Wetlands Ecology and Management:1–15.

Nakai, T., and K. Shimoyama. 2012. Ultrasonic anemometer angle of attack errors under turbulent conditions. Agricultural and Forest Meteorology 162–163:14–26.

Nash, J. E., and J. V. Sutcliffe. 1970. River flow forecasting through conceptual models part I - A discussion of principles. Journal of Hydrology 10:282–290.

Nilsson, M., J. Sagerfors, I. Buffam, H. Laudon, T. Eriksson, A. Grelle, L. Klemedtsson, P. Weslien, and A. Lindroth. 2008. Contemporary carbon accumulation in a boreal oligotrophic minerogenic mire - A significant sink after accounting for all C-fluxes. Global Change Biology 14:2317–2332.

Nousiainen, R., L. Warsta, M. Turunen, H. Huitu, H. Koivusalo, and L. Pesonen. 2015. Analyzing subsurface drain network performance in an agricultural monitoring site with a three-dimensional hydrological model. Journal of Hydrology 529:82–93.

van Oene, H., F. Berendse, C. G. F. de Kovel, N. Conservation, and P. E. Group. 1999. Model analysis of the effects of historic CO_2 levels and nitrogen inputs on vegetation succession. Ecological Applications 9:920–935.

Van Oijen, M., D. R. Cameron, K. Butterbach-Bahl, N. Farahbakhshazad, P. E. Jansson, R. Kiese, K. H. Rahn, C. Werner, and J. B. Yeluripati. 2011. A Bayesian framework for model calibration, comparison and analysis: Application to four models for the biogeochemistry of a Norway spruce forest. Agricultural and Forest Meteorology 151:1609–1621.

Oren, R., J. S. Sperry, G. G. Katul, D. E. Pataki, B. E. Ewers, N. Phillips, and K. V. R. Schäfer. 1999. Survey and synthesis of intra- and interspecific variation in stomatal sensitivity to vapour pressure deficit. Plant, Cell and Environment 22:1515–1526.

Page, S. E., J. O. Rieley, and C. J. Banks. 2011. Global and regional importance of the tropical peatland carbon pool. Global Change Biology 17:798–818.

Papale, D., M. Reichstein, M. Aubinet, E. Canfora, C. Bernhofer, W. Kutsch, B. Longdoz, S. Rambal, R. Valentini, T. Vesala, and D. Yakir. 2006. Towards a standardized processing of Net Ecosystem Exchange measured with eddy covariance technique: algorithms and uncertainty estimation. Biogeosciences 3:571–583.

Parish, F., A. Sirin, D. Charman, H. Joosten, T. Minayeva, M. Silvius, and L. Stringer. 2008. Assessment on Peatlands, Biodiversity and Climate Change: Main Report. Page (K. L. and W. I. W. Global Environment Centre, Ed.). Global Environment Centre, Kuala Lumpur and Wetlands International, Wageningen.

Pastor, J., J. Solin, S. D. Bridgham, K. Updegraff, C. Harth, P. Weishampel, and B. Dewey. 2003. Global warming and the export of dissolved organic carbon from boreal peatlands. Oikos 100:380–386.

Penman, H. L. 1948. Natural Evaporation from Open Water, Bare Soil and Grass. Proceedings of the Royal Society A: Mathematical, Physical and Engineering Sciences 193:120–145.

Pepin, N., R. S. Bradley, H. F. Diaz, M. Baraer, E. B. Caceres, N. Forsythe, H. Fowler, G. Greenwood, M. Z. Hashmi, X. D. Liu, J. R. Miller, L. Ning, A. Ohmura, E. Palazzi, I. Rangwala, W. Schöner, I. Severskiy, M. Shahgedanova, M. B. Wang, S. N. Williamson, and D. Q. Yang. 2015. Elevation-dependent warming in mountain regions of the world. Nature Climate Change 5:424–430.

Perucco, F., D. A. Petraglia, and D. M. Carbognani. 2013. Flussi di CO_2 in differenti comunità vegetali di una torbiera alpina. Univeristà degli studi di Parma.

Petrescu, A. M. R., A. Lohila, J.-P. Tuovinen, D. D. Baldocchi, A. R. Desai, N. T. Roulet, T. Vesala, A. J. Dolman, W. C. Oechel, B. Marcolla, T. Friborg, J. Rinne, J. H. Matthes, L. Merbold, A. Meijide, G. Kiely, M. Sottocornola, T. Sachs, D. Zona, A. Varlagin, D. Y. F. Lai, E. Veenendaal, F.-J. W. Parmentier, U. Skiba, M. Lund, A. Hensen, J. van Huissteden, L. B. Flanagan, N. J. Shurpali, T. Grünwald, E. R. Humphreys, M. Jackowicz-Korczyński, M. A. Aurela, T. Laurila, C. Grüning, C. A. R. Corradi, A. P. Schrier-Uijl, T. R. Christensen, M. P. Tamstorf, M. Mastepanov, P. J. Martikainen, S. B. Verma, C. Bernhofer, and A. Cescatti. 2015. The uncertain climate footprint of wetlands under human pressure. Proceedings of the National Academy of Sciences 112:4594–4599.

Van Den Pol-Van Dasselaar, A., M. L. Van Beusichem, and O. Oenema. 1999. Determinants of spatial variability of methane emissions from wet grasslands on peat soil. Biogeochemistry 44:221–237.

Potvin, L. R., E. S. Kane, R. A. Chimner, R. K. Kolka, and E. A. Lilleskov. 2014. Effects of water table position and plant functional group on plant community, aboveground production, and peat properties in a peatland mesocosm experiment (PEATcosm). Plant and Soil 387:277–294.

Pullens, J. W. M., R. Silveyra Gonzalez, M. Bagnara, and F. Hartig. 2016a. NUCOMBog: NUtrient Cycling and COMpetition Model Undisturbed Open Bog Ecosystems in a Temperate to Sub-Boreal Climate [R package].

Pullens, J. W. M., M. Sottocornola, G. Kiely, P. Toscano, and D. Gianelle. 2016b. Carbon fluxes of an alpine peatland in Northern Italy. Agricultural and Forest Meteorology 220:69–82.

Quinty, F., and L. Rochefort. 2003. Peatland restoration guide. Page Peatland restoration guide. Canadian And, Sphagnum Peat Moss Association and New Brunswick Department of Natural Resources Energy. Québec, Québec.

R Development Core Team. R Foundation for Statistical Computing. 2017. A language and environment for statistical computing. R Foundation for Statistical Computing, Vienna, Austria.

Reichstein, M., E. Falge, D. Baldocchi, D. Papale, M. Aubinet, P. Berbigier, C. Bernhofer, N. Buchmann, T. Gilmanov, A. Granier, T. Grünwald, K. Havránková, H. Ilvesniemi, D. Janous, A. Knohl, T. Laurila, A. Lohila, D. Loustau, G. Matteucci, T. Meyers, F. Miglietta, J. M. Ourcival, J. Pumpanen, S. Rambal, E. Rotenberg, M. Sanz, J. Tenhunen, G. Seufert, F. Vaccari, T. Vesala, D. Yakir, and R. Valentini. 2005. On the separation of net ecosystem exchange into assimilation and ecosystem respiration: Review and improved algorithm. Global Change Biology 11:1424–1439.

Rempel, A. W. 2007. Formation of ice lenses and frost heave. Journal of Geophysical Research: Earth Surface 112.

Richardson, A. D., M. D. Mahecha, E. Falge, J. Kattge, A. M. Moffat, D. Papale, M. Reichstein, V. J. Stauch, B. H. Braswell, G. Churkina, B. Kruijt, and D. Y. Hollinger. 2008. Statistical properties of random CO_2 flux measurement uncertainty inferred from model residuals. Agricultural and Forest Meteorology 148:38–50.

Rigon, R., M. Bancheri, G. Formetta, and A. deLavenne. 2016. The geomorphological unit hydrograph from a historical-critical perspective. Earth Surface Processes and Landforms 41:27–37.

Rigon, R., G. Bertoldi, and T. M. Over. 2006. GEOtop: A Distributed Hydrological Model with Coupled Water and Energy Budgets. Journal of Hydrometeorology 7:371–388.

Rinaldo, A., and I. Rodriguez-Iturbe. 1996. Geomorphological Theory of the Hydrological Response. Hydrological Processes 10:803–829.

Rinne, J., T. Riutta, M. Pihlatie, M. Aurela, S. Haapanala, J. P. Tuovinen, E. S. Tuittila, and T. Vesala. 2007. Annual cycle of methane emission from a boreal fen measured by the eddy covariance technique. Tellus, Series B: Chemical and Physical Meteorology 59:449–457.

Roulet, N., T. Moore, J. Bubier, and P. Lafleur. 1992. Northern fens: methan flux and climatic change. Tellus Series B 44:100–105.

Roulet, N. T., P. M. Lafleur, P. J. H. Richard, T. R. Moore, E. R. Humphreys, and J. Bubier. 2007. Contemporary carbon balance and late Holocene carbon accumulation in a northern peatland. Global Change Biology 13:397–411.

Ruimy, A., P. G. Jarvis, D. D. Baldocchi, and B. Saugier. 1995. CO_2 Fluxes over Plant Canopies and Solar Radiation: A Review. Advances in Ecological Research 26:1–68.

Rydin, H., and J. K. Jeglum. 2015. The Biology of Peatlands. Page The Biology of Peatlands. Oxford University Press, Oxford.

Sakowska, K., D. Gianelle, A. Zaldei, A. Macarthur, F. Carotenuto, F. Miglietta, R. Zampedri, M. Cavagna, and L. Vescovo. 2015. WhiteRef: A new tower-based

hyperspectral system for continuous reflectance measurements. Sensors (Switzerland) 15:1088–1105.

Sakowska, K., L. Vescovo, B. Marcolla, R. Juszczak, J. Olejnik, and D. Gianelle. 2014. Monitoring of carbon dioxide fluxes in a subalpine grassland ecosystem of the Italian Alps using a multispectral sensor. Biogeosciences 11:4695–4712.

Saltelli, A., K. Chan, and E. Scott. 2008. Sensitivity Analysis. Wiley, New York.

Scherrer, S. C., P. Ceppi, M. Croci-Maspoli, and C. Appenzeller. 2012. Snow-albedo feedback and Swiss spring temperature trends. Theoretical and Applied Climatology 110:509–516.

Schuur, E. A. G., A. D. McGuire, C. Schädel, G. Grosse, J. W. Harden, D. J. Hayes, G. Hugelius, C. D. Koven, P. Kuhry, D. M. Lawrence, S. M. Natali, D. Olefeldt, V. E. Romanovsky, K. Schaefer, M. R. Turetsky, C. C. Treat, and J. E. Vonk. 2015. Climate change and the permafrost carbon feedback. Nature 520:171–179.

Schwalm, M., and J. Zeitz. 2014. Dissolved organic carbon concentrations vary with season and land use – investigations from two fens in Northeastern Germany over two years. Biogeosciences Discussions 11:7079–7111.

Smith, P., and C. Fang. 2010. A warm response by soils. Nature 464:499.

Smith, T. A. 1970. in Higher Plants. Pages 5302–5307*in* H. W. Woolhouse, editor.Advances in Botanical Research. Volume 7. Academic Press, Cambridge.

Sonnentag, O., G. van der Kamp, A. G. Barr, and J. M. Chen. 2010. On the relationship between water table depth and water vapor and carbon dioxide fluxes in a minerotrophic fen. Global Change Biology 16:1762–1776.

Sottocornola, M. 2007. Four years of observations of carbon dioxide fluxes, water and energy budgets, and vegetation patterns in an Irish Atlantic blanket bog. University College Cork.

Sottocornola, M., and G. Kiely. 2010a. Hydro-meteorological controls on the CO_2 exchange variation in an Irish blanket bog. Agricultural and Forest Meteorology 150:287–297.

Sottocornola, M., and G. Kiely. 2010b. Energy fluxes and evaporation mechanisms in an Atlantic blanket bog in southwestern Ireland. Water Resources Research 46.

Sottocornola, M., A. M. Laine, G. Kiely, K. A. Byrne, and E. S. Tuittila. 2009. Vegetation and environmental variation in an Atlantic blanket bog in South-western Ireland. Plant Ecology 203:69–81.

St-Hilaire, F., J. Wu, N. T. Roulet, S. Frolking, P. M. Lafleur, E. R. Humphreys, and V. Arora. 2010. McGill wetland model: Evaluation of a peatland carbon simulator developed for global assessments. Biogeosciences 7:3517–3530.

Steger, C., S. Kotlarski, T. Jonas, and C. Schär. 2013. Alpine snow cover in a changing climate: A regional climate model perspective. Climate Dynamics 41:735–754.

Stine, M. B., L. M. Resler, and J. B. Campbell. 2011. Ecotone characteristics of a southern Appalachian Mountain wetland. Catena 86:57–65.

Stoy, P. C., G. G. Katul, M. B. S. S. Siqueira, J.-Y. Y. Juang, K. A. Novick, J. M. Uebelherr, and R. Oren. 2006. An evaluation of models for partitioning eddy covariance-measured net ecosystem exchange into photosynthesis and respiration. Agricultural and Forest Meteorology 141:2–18.

Strachan, I. B., L. Pelletier, and M.-C. Bonneville. 2016. Inter-annual variability in water table depth controls net ecosystem carbon dioxide exchange in a boreal bog. Biogeochemistry 127:99–111.

Strack, M., J. M. Waddington, R. A. Bourbonniere, E. L. Buckton, K. Shaw, P. Whittington, and J. S. Price. 2008. Effect of water table drawdown on peatland dissolved organic carbon export and dynamics. Hydrological Processes 22:3373–3385.

Strack, M., Y. Zuback, C. McCarter, and J. Price. 2015. Changes in dissolved organic carbon quality in soils and discharge 10 years after peatland restoration. Journal of Hydrology 527:345–354.

Sutton, M. A., C. M. Howard, J. W. Erisman, G. Billen, A. Bleeker, P. Grennfelt, H. van Grinsven, and B. Grizzetti. 2011. The European Nitrogen Assessment - Sources, Effects and Policy Perspectives, Cambridge University Press, ISBN:9781107006126, 664 pp. Cambridge University Press, Cambridge.

Tahvanainen, T. 2011. Abrupt ombrotrophication of a boreal aapa mire triggered by hydrological disturbance in the catchment. Journal of Ecology 99:404–415.

Talbot, J., N. T. Roulet, O. Sonnentag, and T. R. Moore. 2014. Increases in aboveground biomass and leaf area 85 years after drainage in a bog. Botany 92:713–721.

Tallis, J. 1998. Growth and degradation of British and Irish blanket mires. Environmental Reviews 6:81–122.

Taylor, K., A. P. Rowland, and H. E. Jones. 2001. *Molinia caerulea* (L.) Moench. Journal of Ecology 89:126–144.

Taylor, N., J. Price, and M. Strack. 2016. Hydrological controls on productivity of regenerating Sphagnum in a cutover peatland. Ecohydrology 9:1017–1027.

Todini, E. 2007. Hydrological catchment modelling: past, present and future. Hydrol. Earth Syst. Sci. 11:468–482.

Tokida, T., T. Miyazaki, M. Mizoguchi, O. Nagata, F. Takakai, A. Kagemoto, and R. Hatano. 2007. Falling atmospheric pressure as a trigger for methane ebullition from peatland. Global Biogeochemical Cycles 21.

Tudoroiu, M., E. Eccel, B. Gioli, D. Gianelle, H. Schume, L. Genesio, and F. Miglietta. 2016. Negative elevation-dependent warming trend in the Eastern Alps. Environmental Research Letters 11:44021.

Turetsky, M. R., A. Kotowska, J. Bubier, N. B. Dise, P. Crill, E. R. C. Hornibrook, K. Minkkinen, T. R. Moore, I. H. Myers-Smith, H. Nykänen, D. Olefeldt, J. Rinne, S. Saarnio, N. Shurpali, E. S. Tuittila, J. M. Waddington, J. R. White, K. P. Wickland, and M. Wilmking. 2014. A synthesis of methane emissions from 71 northern, temperate, and subtropical wetlands. Global Change Biology 20:2183–2197.

Turunen, J., N. T. Roulet, T. R. Moore, and P. J. H. Richard. 2004. Nitrogen deposition and increased carbon accumulation in ombrotrophic peatlands in eastern Canada. Global Biogeochemical Cycles 18.

Urban, N. R., S. E. Bayley, and S. J. Eisenreich. 1989. Export of dissolved organic carbon and acidity from peatlands. Water Resources Research 25:1619–1628.

Vanselow-Algan, M., S. R. Schmidt, M. Greven, C. Fiencke, L. Kutzbach, and E. M. Pfeiffer. 2015. High methane emissions dominated annual greenhouse gas balances 30 years after bog rewetting. Biogeosciences 12:4361–4371.

Vivoni, E. R., V. Y. Ivanov, R. L. Bras, and D. Entekhabi. 2004. Generation of Triangulated Irregular Networks Based on Hydrological Similarity. Journal of Hydrologic Engineering 9:288–302.

Vrugt, J. A., C. J. F. ter Braak, H. V. Gupta, and B. A. Robinson. 2009. Equifinality of formal (DREAM) and informal (GLUE) Bayesian approaches in hydrologic modeling? Stochastic Environmental Research and Risk Assessment 23:1011–1026.

Vuuren, M. M. I. Van, F. Berendse, and W. De Visser. 1993. Species and site differences in the decomposition of litters and roots from wet heathlands. Canadian Journal of Botany 71:167–173.

Waddington, J. M., P. J. Morris, N. Kettridge, G. Granath, D. K. Thompson, and P. A. Moore. 2015. Hydrological feedbacks in northern peatlands. Ecohydrology 8:113–127.

Wagner, D., S. Kobabe, E. M. Pfeiffer, and H. W. Hubberten. 2003. Microbial controls on methane fluxes from a polygonal tundra of the Lena Delta, Siberia. Permafrost and Periglacial Processes 14:173–185.

Wang, J. M., J. G. Murphy, J. A. Geddes, C. L. Winsborough, N. Basiliko, and S. C. Thomas. 2013. Methane fluxes measured by eddy covariance and static chamber techniques at a temperate forest in central Ontario, Canada. Biogeosciences 10:4371–4382.

Webb, E. K., G. I. Pearman, and R. Leuning. 1980. Correction of flux measurements for density effects due to heat and water vapour transfer. Quarterly Journal of the Royal Meteorological Society 106:85–100.

Weissert, L. F., and M. Disney. 2013. Carbon storage in peatlands: A case study on the Isle of Man. Geoderma 204–205:111–119.

Wheeler, B. D., and M. C. F. Proctor. 2000. Ecological gradients, subdivisions and terminology of north-west European mires. Journal of Ecology 88:187–203.

Wilson, D., E.-S. Tuittila, J. Alm, J. Laine, E. P. Farrell, and K. A. Byrne. 2007. Carbon dioxide dynamics of a restored maritime peatland. Ecoscience 14:71–80.

Wilson, K., A. Goldstein, E. Falge, M. Aubinet, D. Baldocchi, P. Berbigier, C. Bernhofer, R. Ceulemans, H. Dolman, C. Field, A. Grelle, A. Ibrom, B. E. Law, A. Kowalski, T. Meyers, J. Moncrieff, R. Monson, W. Oechel, J. Tenhunen, R. Valentini, and S. Verma. 2002. Energy balance closure at FLUXNET sites. Agricultural and Forest Meteorology 113:223–243.

Wilson, R. M., A. M. Hopple, M. M. Tfaily, S. D. Sebestyen, C. W. Schadt, L. Pfeifer-Meister, C. Medvedeff, K. J. McFarlane, J. E. Kostka, M. Kolton, R. K. Kolka, L. A. Kluber, J. K. Keller, T. P. Guilderson, N. A. Griffiths, J. P. Chanton, S. D. Bridgham, and P. J. Hanson. 2016. Stability of peatland carbon to rising temperatures. Nature Communications 7:13723.

de Wit, H. A., J. L. J. Ledesma, and M. N. Futter. 2016. Aquatic DOC export from subarctic Atlantic blanket bog in Norway is controlled by seasalt deposition, temperature and precipitation. Biogeochemistry 127:305–321.

Wohlfahrt, G., and M. Galvagno. 2017. Revisiting the choice of the driving temperature for eddy covariance CO_2 flux partitioning. Agricultural and Forest Meteorology 237–238:135–142.

Worrall, F., T. P. Burt, and J. K. Adamson. 2006. Trends in drought frequency - The fate of DOC export from British peatlands. Climatic Change 76:339–359.

Worrall, F., M. Reed, J. Warburton, and T. Burt. 2003. Carbon budget for a British upland peat catchment. Science of the Total Environment 312:133–146.

Woziwoda, B., and D. Kopeć. 2014. Afforestation or natural succession? Looking for the best way to manage abandoned cut-over peatlands for biodiversity conservation. Ecological Engineering 63:143–152.

Wu, J., N. T. Roulet, J. Sagerfors, and M. Nilsson. 2013. Simulation of six years of carbon fluxes for a sedge-dominated oligotrophic minerogenic peatland in Northern Sweden using the McGill Wetland Model (MWM). Journal of Geophysical Research: Biogeosciences 118:795–807.

Wu, Y., and C. Blodau. 2013. PEATBOG: A biogeochemical model for analyzing coupled carbon and nitrogen dynamics in northern peatlands. Geoscientific Model Development 6:1173–1207.

Xie, Z., Z. Di, Z. Luo, and Q. Ma. 2012. A Quasi-Three-Dimensional Variably Saturated Groundwater Flow Model for Climate Modeling. Journal of Hydrometeorology 13:27–46.

Yu, Z. C. 2012. Northern peatland carbon stocks and dynamics: A review. Biogeosciences 9:4071–4085.

Yu, Z., J. Loisel, D. P. Brosseau, D. W. Beilman, and S. J. Hunt. 2010. Global peatland dynamics since the Last Glacial Maximum. Geophysical Research Letters 37.

Yuan, W., W. Cai, S. Liu, W. Dong, J. Chen, M. A. Arain, P. D. Blanken, A. Cescatti, G. Wohlfahrt, T. Georgiadis, L. Genesio, D. Gianelle, A. Grelle, G. Kiely, A. Knohl, D. Liu, M. V. Marek, L. Merbold, L. Montagnani, O. Panferov, M. Peltoniemi, S. Rambal, A. Raschi, A. Varlagin, and J. Xia. 2014. Vegetation-specific model parameters are not required for estimating gross primary production. Ecological Modelling 292:1–10.

Zanella, A., M. Tomasi, C. De Siena, L. Frizzera, B. Jabiol, and G. Nicolini. 2001. Humus Forestali - Manuale di ecologia per il riconoscimento e l'interpretazione - Applicazione alle faggete. Centro di Ecologia Alpina, Trento.

Zanello, F., P. Teatini, M. Putti, and G. Gambolati. 2011. Long term peatland subsidence: Experimental study and modeling scenarios in the Venice coastland. Journal of Geophysical Research: Earth Surface 116.

Zeileis, A., and G. Grothendieck. 2005. zoo: S3 Infrastructure for Regular and Irregular Time Series. Journal of Statistical Software 14:1–27.

Zhao, X., and Y. Huang. 2015. A comparison of three gap filling techniques for eddy covariance net carbon fluxes in short vegetation ecosystems. Advances in Meteorology 2015:1–12.

Appendices

Appendix 1: **Pullens, J. W. M.**, M. Sottocornola, G. Kiely, P. Toscano, and D. Gianelle. 2016b. Carbon fluxes of an alpine peatland in Northern Italy. Agricultural and Forest Meteorology 220:69–82

Appendix 2: **Pullens, J. W. M.**, M. Bagnara, R. Silveyra González, D. Gianelle, M. Sottocornola, M. M. P. D. Heijmans, G. Kiely, F. Hartig. 2017. The NUCOMBog R package for simulating vegetation, water, carbon and nitrogen dynamics in peatlands. Ecological Informatics 40:35-39.

Appendix 3: van der Kolk, H.-J., M. M. P. D. Heijmans, J. van Huissteden, **J. W. M. Pullens**, and F. Berendse. 2016. Potential Arctic tundra vegetation shifts in response to changing temperature, precipitation and permafrost thaw. Biogeosciences 13:6229–6245.

Appendix 4: Vignette/manual of **Pullens, J. W. M**., R. Silveyra Gonzalez, M. Bagnara, and F. Hartig. 2016a. NUCOMBog: NUtrient Cycling and COMpetition Model Undisturbed Open Bog Ecosystems in a Temperate to Sub-Boreal Climate.

Agricultural and Forest Meteorology 220 (2016) 69–82

Contents lists available at ScienceDirect

Agricultural and Forest Meteorology

journal homepage: www.elsevier.com/locate/agrformet

Carbon fluxes of an alpine peatland in Northern Italy

J.W.M. Pullens[a,c,*], M. Sottocornola[b], G. Kiely[c], P. Toscano[d], D. Gianelle[a,e]

[a] Department of Sustainable Agro-ecosystems and Bioresources, Research and Innovation Centre, Fondazione Edmund Mach (FEM), Via E. Mach 1, San Michele all'Adige, Trento 38010, Italy
[b] Department of Science, Waterford Institute of Technology, Waterford, Ireland
[c] Hydromet, Department of Civil and Environmental Engineering and Environmental Research Institute, University College Cork, Cork, Ireland
[d] National Research Council—Institute for Biometeorology (CNR—IBIMET), Florence, Italy
[e] Foxlab Joint CNR-FEM Initiative, Via E. Mach 1, San Michele all'Adige, Trento 38010, Italy

ARTICLE INFO

Article history:
Received 11 September 2015
Received in revised form 8 January 2016
Accepted 11 January 2016

Keywords:
Alpine peatland
Carbon dioxide
Methane
Eddy covariance
Minerotrophic fen
Water table depth

ABSTRACT

It is widely known that peatlands are a significant carbon (C) stock. Most peatlands are located in boreal and subarctic regions of the northern hemisphere but some occur also at high altitude and, contrary to the first; their contribution in terms of carbon sequestration is far less studied. In the Alps, there are numerous small peatlands, which are threatened by increasing temperatures and an alteration of their water balance. The aim of this study was to investigate the carbon fluxes of a small-scale fen in the Alps over three years (2012–2014).

During the study period, the peatland experienced a high interannual variation in weather conditions while it acted as a carbon source based on CO_2 emissions (NEE: 180.7 ± 65.2 g C—CO_2 m^{-2} yr^{-1}) for all three years. This was mainly due to the short net C uptake period (73 ± 7 days) and high respiration. Ecosystem respiration and summer gross primary production were both very high compared to other peatlands around the world and compared to a nearby low productive grassland. In wintertime, the soil did not freeze, resulting in a slow decomposition of the organic matter. Low methane fluxes were recorded during a 10-month measurement campaign, for a total of 3.2 g C—CH_4 m^{-2} over the December 2013–September 2014 period. Our findings suggest that the interannual variability of temperature and soil water content exert a strong influence on the carbon balance of peatlands of the Alps and that could further worsen depending upon the magnitude of climate change.

1. Introduction

Peatlands contain the largest terrestrial soil carbon (C) pool in the world (Gorham, 1991). Northern peatlands store an estimated 547 (473–621) PgC (Yu et al., 2010), which is around 20% of the total amount of global soil organic carbon (IPCC, 2007), despite covering only about 3% of the land surface. Peatlands occur globally; however the biggest and most studied areas are located in the northern hemisphere (Parish et al., 2008; Schuur et al., 2015; Yu et al., 2010). Most of researched peatlands are in high latitude regions and these peatlands are studied for the vulnerability of their carbon storage, the effects of climate change and permafrost degradation (Camill, 2005; Dorrepaal et al., 2009; Frolking et al., 2001). Peatlands have been accumulating carbon for thousands of years. The decomposition of plant material is very slow due to the waterlogged soils and high recalcitrance of present *Sphagnum* mosses. The carbon can be released as the greenhouse gasses carbon dioxide (CO_2), methane (CH_4), or as Dissolved Organic Carbon (DOC) in waterbodies. Methane is only produced under anaerobic conditions (Wang et al., 2013). The emission of CH_4 in peatlands is has been linked to the presence of plants with aerenchyma, a tissue that can conduct methane from the soil to the atmosphere (Carmichael et al., 2014; Van Den Pol-Van Dasselaar et al., 1999). Aerenchyma tissue can be found mainly in sedges, so a high sedge abundance could potentially be an indicator of high methane emission (Armstrong, 1979; Gebauer et al., 1995). It is estimated that peatlands contribute to around 33% of the annual global methane efflux (ca 645 Tg CH_4 $year^{-1}$, (Carmichael et al., 2014)).

Due to climate change, pristine peatlands can be potential carbon sources (Bond-Lamberty and Thomson, 2010; Dorrepaal et al., 2009; Drösler et al., 2008; Frolking et al., 2011; Lawrence et al., 2013). The general global response of peatlands to climate change is hard to predict due to the uneven distribution of peatlands over the world, in addition to this only the most accessible peatlands are

* Corresponding author at: Fondazione Edmund Mach, Sustainable Ecosystems & Bioresources, Via Mach 1, San Michele All'Adige, 38010 Trento, Italy.
Tel.: +39 (0) 461 615 675.
E-mail address: johannes.pullens@fmach.it (J.W.M. Pullens).

http://dx.doi.org/10.1016/j.agrformet.2016.01.012
0168-1923/

studied (Frolking et al., 2011). Warmer temperatures could lead to an increase in plant growth (net primary production, NPP) and an increase in ecosystem respiration (R_{eco}) (Beer and Blodau, 2007; Smith and Fang, 2010; Gong et al., 2013). The different magnitudes of these two contrasting fluxes could change peatlands from a carbon sink to a carbon source (Bond-Lamberty and Thomson, 2010; Dorrepaal et al., 2009; Lawrence et al., 2013). A difference in annual precipitation could result in a drop in the water table depth which will trigger faster decomposition of stored carbon, since more peat can be decomposed under aerobic conditions and simultaneously a reduction in CH_4 emissions (Andersen et al., 2013; Couwenberg et al., 2010; Gong et al., 2013; Jungkunst et al., 2008; Mitsch et al., 2012). On the contrary a rise in water table depth can reduce the decomposition (Murphy et al., 2009), increase the NPP (Sonnentag et al., 2010), with a positive effect on carbon accumulation, but with a negative effect in terms of increased CH_4 emissions (Lawrence et al., 2013; Petrescu et al., 2015; Vanselow-Algan et al., 2015).

To measure the net ecosystem CO_2 exchange (NEE) at an ecosystem level, the eddy covariance (EC) micrometeorological technique is typically used. This technique allows to measure turbulent fluxes, which are exchanged between vegetation canopy and the atmosphere (Baldocchi, 2003). The advantage of this method is that it continuously measures the fluxes over a long period of time (years or even decades) and in a non-destructive way. In this way, the dynamics of ecosystems can be investigated and followed over time. NEE can then be partitioned to calculate the gross primary production (GPP) and ecosystem respiration (R_{eco}).

As highlighted by Drösler et al. (2008) measurements need to be done at different peatland ecosystems, to reach a better understanding of, and to upscale the greenhouse gas balance of peatlands regionally and/or globally. The difficulty with upscaling is that peatlands occur in different types: e.g. fen, aapa mire, blanket bog and raised bog, which are reliant on different water and nutrient sources, ombrotrophic (rainwater fed) vs minerotrophic (groundwater fed) (Wheeler and Proctor, 2000). The differences in water sources, the dissolved minerals and nutrients can lead to different plant communities and therefore a different greenhouse gas balance. Measurements on pristine peatlands indicate that these untouched peatlands are mainly acting as a CO_2 sink (34.9 to 329 g C—CO_2 m^{-2} yr^{-1}) and as a methane source (3.2 to 32 g C—CH_4 m^{-2} yr^{-1}) (Aurela et al., 2009; Bäckstrand et al., 2010; Beetz et al., 2013; Koehler et al., 2011; Lund et al., 2010, 2007; McVeigh et al., 2014; Nilsson et al., 2008; Petrescu et al., 2015; Roulet et al., 2007; Sonnentag et al., 2010; Sottocornola and Kiely, 2010; Wu et al., 2013). On the contrary drained and managed wetlands often act as a CO_2 source (Beyer and Höper, 2015; Hatala et al., 2012). Many factors are influencing the carbon balance, such as: vegetation, hydrology, ground water level (Murphy et al., 2009), human disturbance (Hendriks et al., 2007) and climatic variability (McVeigh et al., 2014). Peatlands with a high cover of bryophytes and a low cover of vascular plants, show lower GPP than peatlands with a high vascular plant cover (Beetz et al., 2013). Since peatlands are rather widespread, the climatic conditions are very important. A comparison of different peatlands can provide more information why some peatlands are bigger carbon sources than others (Drösler et al., 2008).

In the Alpine area, numerous small peatland fens are present. In the Alps the climatic conditions for these fens to develop into raised bogs are rare. This results in an infilling of non-peatland plant species (trees and grasses) into the peatland. The peatland fens in the Alps are being threatened by rising temperatures and changes in their precipitation regime (Beniston et al., 1997; Eccel et al., 2012; Im et al., 2010; IPCC, 2013, 2007; Pepin et al., 2015; Steger et al., 2012). The predicted changes in precipitation can be opposite of sign and different in magnitude. Alpine fens are already experiencing modifications due to climate change with an acceleration of the infilling with trees (Stine et al., 2011). This is leading to the invasion of non-peatland plants typical of drier ecosystems that are turning the peatlands into grasslands and forests, with a consequent loss of both their stored soil carbon and their biodiversity (Stine et al., 2011). Tree encroachment for example is more persistent with global warming than it is with summer drought, while a combination of the two results in tree-dominated peatlands (Heijmans et al., 2013; Holmgren et al., 2015). Despite the risks and the regular occurrence of peatlands in the Alps, their carbon and water cycle has been poorly studied because peatlands represent a small part of the dominant ecosystems in the Alps (Parish et al., 2008). To our knowledge the only research on Alpine peatlands focused on their restoration and management (Ammann et al., 2013; Van Der Knaap et al., 2011) while no attempt was taken to measure the carbon fluxes with an eddy covariance system.

The objectives of this paper are (i) to investigate three years of carbon and methane fluxes of a peatland in the Italian Alps, (ii) to study the inter annual variability of the carbon fluxes and (iii) to compare the fluxes of this alpine peatland with other peatlands.

We hypothesize that the peatland will be a small carbon sink, since the vegetation of the peatland grows very fast during the growing season. We assume that the carbon taken up during this period is more than the carbon released over the rest of the year, particularly when the peatland is covered with snow and all biological processes are slowed down or stopped. We also think that the peatland will have high methane fluxes, since the peatland has a high coverage of sedges.

2. Materials and methods

2.1. Site

The study site is a 10 hectares minerotrophic relatively nutrient poor fen located at 1563 m a.s.l. on the Monte Bondone plateau (Fig. 1), near Trento, in the Italian Alps (latitude 46°01′03N, longitude 11°02′27E). The peatland is placed in a relict glacial lakebed, that was formed during the last ice age (Cescatti et al., 1999), in a saddle shaped valley with a mountain top on the eastside (Palon, 2090 m a.s.l., Fig. 1a). The runoff of the complete watershed flows on deep impermeable morainic strata, which result into seepage into the fen (Cescatti et al., 1999). This seepage enters the peatland through two inflow streams; from the fen the water discharges in a stream (Fig. 1). The average annual precipitation during 1958–2008 was 1290 mm yr^{-1} with an average air temperature of 5.4 °C (Eccel et al., 2012). The snow-free period typically lasts from early May to late October-beginning November.

The vegetation of the area is very heterogeneous: the areas closest to the tower are mainly dominated by *Molinia caerula* forming big tussocks, while in the depressions the main vegetation consists of *Carex rostrata*, *Valeriana dioica, Scorpidium cossonii* and scattered *Sphagnum* spp. The southwestern area of the peatland is dominated by *Eriophorum vaginatum*, with high tussocks of *Carex nigra* covering the lower areas. *Sphagnum* spp. as well as *Trichophorum alpinum* and *Drosera rotundifolia* occur close to the outflow stream. In the eastern part of the peatland, between the two inflow streams, there are some short hummocks with *Calluna vulgaris* and *Sphagnum* section *acutifolia*. At this part of the peatland, there is no influence from the incoming streams.

In 1914, 0.35 ha of the peatland was harvested for burning by removing the peat top layer (Cescatti et al., 1999), this is still visible today (Fig. 1b). This area is mainly covered by *Campylium stellatum*, *S. cossonii* and *C. rostrata* today. The depth of the peat ranges from 0.82 m at the border (Cescatti et al., 1999; Zanella et al., 2001) to 4.3 m in the centre (Dalla Fior, 1969).

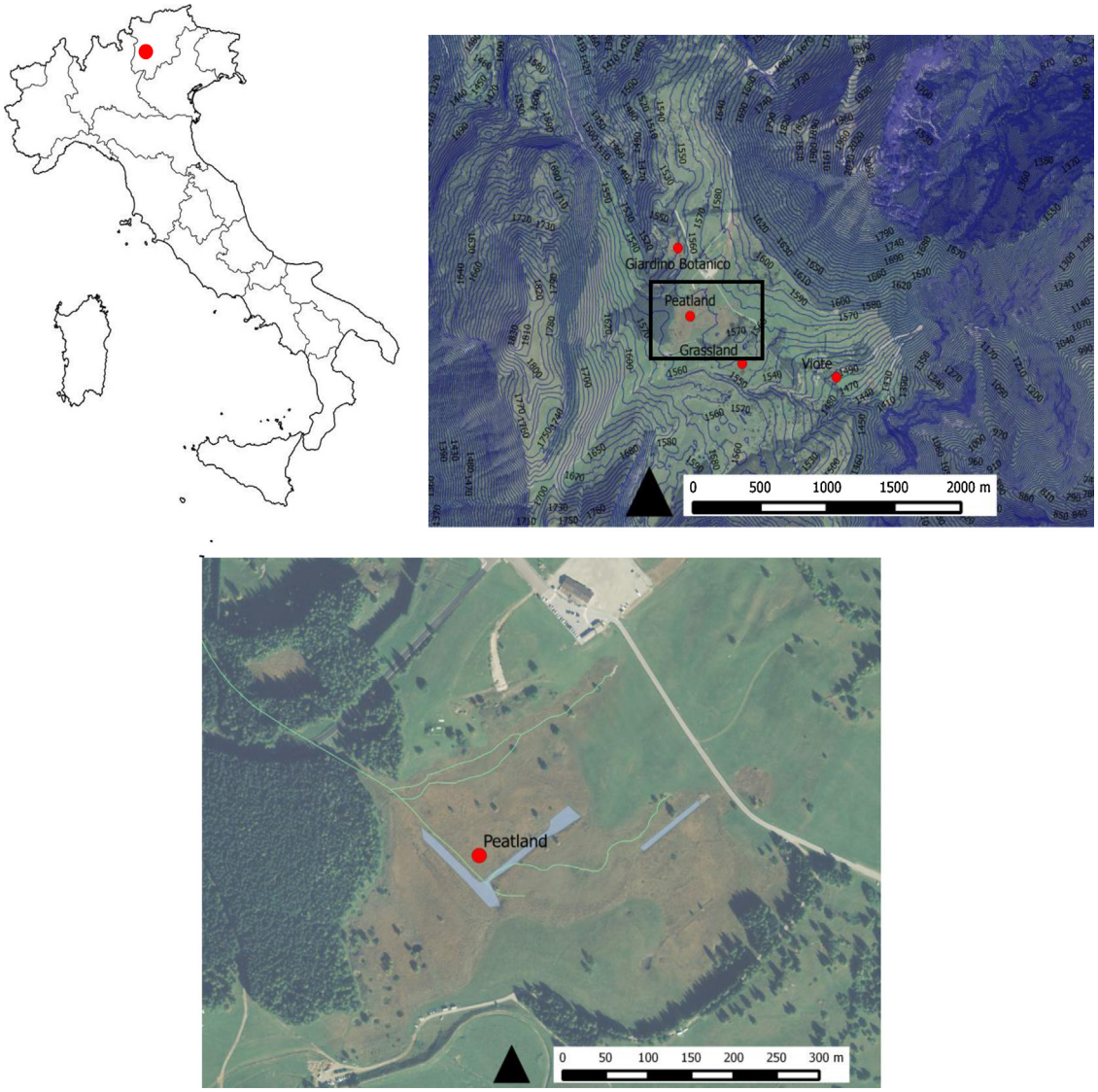

Fig. 1. (Top left) The location of the peatland in respect to the topography of Italy, (top right) An overview of Monte Bondone site. The names refer to the sites of which data has been used. Giardino Botanico and Viote are two meteorological towers of Meteo Trentino. Grassland is an eddy covariance tower located at an alpine grassland (Marcolla et al., 2011; Sakowska et al., 2015); peatland is the location of the eddy covariance tower at the peatland. The plotted contour lines have an interval of 10 m. (Bottom) aerial view of the peatland site, with in blue the areas where peat extraction has taken place in 1914. The highlighted area is 0.35 ha. the turquoise line is a stream running through the peatland. (For interpretation of the references to color in this figure legend, the reader is referred to the web version of this article.)

2.2. Meteorological data

A four-meter tower was installed in the summer of 2011 at the centre of the peatland. The tower was equipped with multiple meteorological sensors. A shielded probe (Rotronic M103A, Bassersdorf, Germany) measured air temperature and relative humidity at 2 m height. The incoming and outgoing, shortwave and far-infrared radiation were measured by a CNR1 (Kipp & Zonen, Delft, the Netherland), while the incoming Photosynthetically Active Radiation (PAR) was measured by a LICOR 190SZ sensor (Licor, Lincoln, NE, USA). All radiometers were positioned on a horizontal side arm of the tower at a height of 3.5 m above the soil surface.

The soil temperature was measured along a profile at 2, 5, 10, 20 and 50 cm depth below the surface with a STP01 sensor (Hukseflux Thermal Sensors B.V, Delft, the Netherlands) from the 1st of July 2012. Soil temperature was also measured with four T107 temperature probes at 2 and 5 cm depth (Campbell Scientific, Logan, UT, USA), under a tussock of *M. caerula* and under a *C. vulgaris* shrub. In the same locations as the T107, two volumetric water content probes (CS616, Campbell Scientific, Logan, UT, USA) were also buried at a depth of 5 cm.

A heated tipping bucket rain gauge (model 52202 from Young, Traverse City, MI, USA) measured precipitation. This instrument was installed on the 16th of December 2013. Before then, the data from a meteorological station, located 400 meters away, was used (Meteo Trentino, station name: Giardino Botanico (46°01′18N, 11°02′23E)). The snow height and density were measured at another Meteo Trentino weather station (Monte Bondone–Viote 46°00′49N, 11°03′17E) on the same plateau as the peatland.

All meteorological data was collected once a minute on a data logger (CR3000, Campbell Scientific, Logan, UT, USA) with a multiplexer (AM16/32, Campbell Scientific, Logan, UT, USA) and averaged or summed to half-hourly values. Missing meteorological data (26% of the total, due to malfunctioning of the sensors or power shortage) were replaced by data from a nearby (500 m horizontal distance) meteorological and eddy covariance tower located in a nutrient poor grassland (Marcolla et al., 2011; Sakowska et al.,

2014). Since the towers were very close to each other, no significant differences in temperature, PAR and relative humidity were found (data not shown). Since the grassland tower is located on a different slope the precipitation data of the grassland was not used. For soil temperature a difference was expected between the grassland and the peatland, but there was a highly significant correlation between the half-hourly values from the two sites for all depths ($R^2 > 0.95$). If data were missing from the grassland site too (0.9%), they were replaced by data from the two close Meteo Trentino meteorological stations (Giardino Botanico and Viote, Fig. 1a). The Giardino Botanico station is located on the same slope as the eddy covariance tower and therefore the precipitation data of the Giardino Botanico station was used to fill the gaps in the precipitation data. Soil temperature was not measured at these stations, but since no gap exceed 5 h, gaps in the peatland timeseries were filled with linear interpolation.

The water table depth of the peatland was measured at 3 m distance from the tower with a pressure transducer (Dipper-PT, SEBA Hydrometrie GmbH & Co., Germany). The pressure transducer was installed inside a perforated pipe on the 14th of May 2014. The water level was measured every half-hour. The data of the pressure transducer was collected on an internal Flash memory card and downloaded at regular intervals.

2.3. Carbon and methane fluxes measurements

Besides the meteorological sensors, the tower was equipped with an eddy covariance system mounted at 1.6 m above the soil surface. The system, consisting of a LI7500 open path CO_2/H_2O gas analyser, a LI7200 enclosed path CO_2/H_2O gas analyser (both from Licor, Lincoln, NE, USA) and a R3-100 3D sonic anemometer (Gill instruments, Lymington, Hampshire, UK), all operating at 20 Hz. In December 2013, a LI7700 open path CH_4 analyser (Licor, Lincoln, NE, USA) was also installed at the same height. The data from both the LI7200 and LI7700 was collected and stored in an Analyser Interface Unit (LI7550); the data from the LI7500 was collected by Scanemone software (University of Tuscia, Italy) and stored on an industrial PC. Because both the LI7500 and the LI7200 were simultaneously operational, the signal from the anemometer was split into a digital and an analogue signal: the digital signal was collected by the LI7550, where the data was combined with the data from the LI7200 and LI7700. The analogue signal was transferred to an indoor PCI unit of Gill, where it was computed with the data from the LI7500.

The intake tube of the enclosed path analyser (LI7200) was 98.7 cm long, with an internal diameter of 9 mm. The flow rate to suck air into the analyser was set to 15 L min^{-1}. To prevent condensation, the inlet tube was heated by a spiral resistor wire and insulated. Moreover, the intake tube was slightly tilted down, to avoid water entering the sensor cell. To prevent insects or other debris being drawn into the cell, a fine screen was added at the inlet of the intake tube.

All fluxes were analysed using the EddyPro Software (version 5.1.1, LICOR, Lincoln, NE, USA), applying a 2-D rotation and with the following corrections: (1) angle of attack for wind components for the Gill anemometer (Nakai and Shimoyama, 2012); (2) a WPL 'Burba correction' was implemented on the data from the LI7500 to compensate for the density fluctuations of the gases because of the heating effect of this instrument (Burba et al., 2012); (3) the low-pass frequency response correction (Moncrieff et al., 1997).

Consecutive the fluxes were removed when: (1) their quality flag was different from 0 or 1 ("0" means high quality fluxes, "1" means fluxes are suitable for carbon budget analysis) (Moncrieff et al., 2004); (2) u^* was lower than 0.2 m s^{-1} during night-time (PAR < 20 μmol m^{-2} s^{-1}) (Papale et al., 2006); (3) the CO_2 mixing ratio was smaller than 250 or bigger than 500 μmol mol^{-1}; (4) the CO_2 fluxes were above or below seasonal thresholds (Supplement Table 1); (5) less than 70% of the fluxes originated from inside the peatland (the footprint was calculated by using the footprint model of Kljun et al. (2004)). After these filters the percentage of data gaps increased from 34% to 65% of gaps for the LI7200 and for the LI7500 from 53% to 74%. The former gap figures were due to system malfunctioning or power outage.

After the filters were applied, the relationship between the CO_2 fluxes computed from the data of the two infrared gas analysers was significant ($p < 0.05$, $R^2 > 0.92$, LI7200 = 0.09 + 0.99 × LI7500, $n = 7524$). During the winter the R^2 value (0.2713) was lower than in the summer (0.8985), but R^2 was significant in all seasons.

Therefore, CO_2 fluxes computed with the LI7200 are presented here and gaps in this time series were filled with data computed from the open path sensor (LI7500). When both time series were missing or removed, (53% of the data), the CO_2 fluxes were gap filled with the online Reichstein tool (Reichstein et al., 2005; URL: http://www.bgc-jena.mpg.de/bgi/index.php/Services/REddyProcWeb). The same tool was used to partition the measured NEE into GPP and R_{eco}. The environmental factors used for the gap filling were: Global radiation, Soil temperature at 5 cm, relative humidity, Vapour pressure deficit (VPD) and u^* (friction velocity). The tool made a look up table where gaps in the NEE data were filled with NEE with similar climatic conditions. The window in which the method is looking for similar results is 7 days, if there are no similar conditions found the method increased the window with steps of 7 days.

The methane sensor (LI7700) was active at this site from December 2013 until September 2014 and during this period there were minor problems with the data acquisition. Since the sensor has an open path the quality and availability of the data was susceptible to meteorological conditions (in total 66% of data gaps). The data was collected by a LI7550 and analysed with EddyPro. Only the fluxes with a quality flag of 0 and 1 were used (Moncrieff et al., 2004). Nevertheless, the data was very noisy and hard filters were applied: all fluxes outside the range of −0.04 to 0.05 μmol s^{-1} m^{-2} were discarded. After the filters, 30% of the data was considered good. The CH_4 fluxes were gap filled using the online Reichstein tool (Reichstein et al., 2005).

Due to the high amount of snow during the winter of 2013–2014 (up to 204 cm), on the 11th of March 2014 the complete LICOR setup was raised 1.5 m above the snow level (3.1 m above soil surface). During the snowmelt in the early spring (the 29th of April 2014), the LICOR setup was lowered to its original position (1.6 m above soil surface).

An error analysis was performed by estimating uncertainties separately for the different error sources (Aurela, 2002). By combining these errors, an uncertainty of 23%, 21% and 30% for 2012, 2013 and 2014 was calculated for the annual balance. These values are in the same range as presented for eddy covariance measurements (Aurela, 2002; Lafleur et al., 2001; Richardson et al., 2008; Sottocornola and Kiely, 2010).

All analyses of the data were done with the half-hourly values of the fluxes and meteorological parameters, unless otherwise indicated. The data was analysed by using the R software version 3.2.1 (R Core Team, 2013) with the zoo package (Zeileis and Grothendieck, 2005). For the analysis the growing season is defined as the period where the cumulative NEE is declining, indicating an uptake of carbon. The micrometeorological sign convention is used in this paper, e.g. a negative sign means carbon sequestration.

A correlation coefficient analysis was performed to understand the main drivers of the measured carbon fluxes. Apart from the NEE, GPP and R_{eco} daily average values of air temperature, PAR, soil water content (SWC), VPD and daily sum of precipitation were used for this analysis. The Spearman correlations were calculated over three complete years and over each quarter of the years

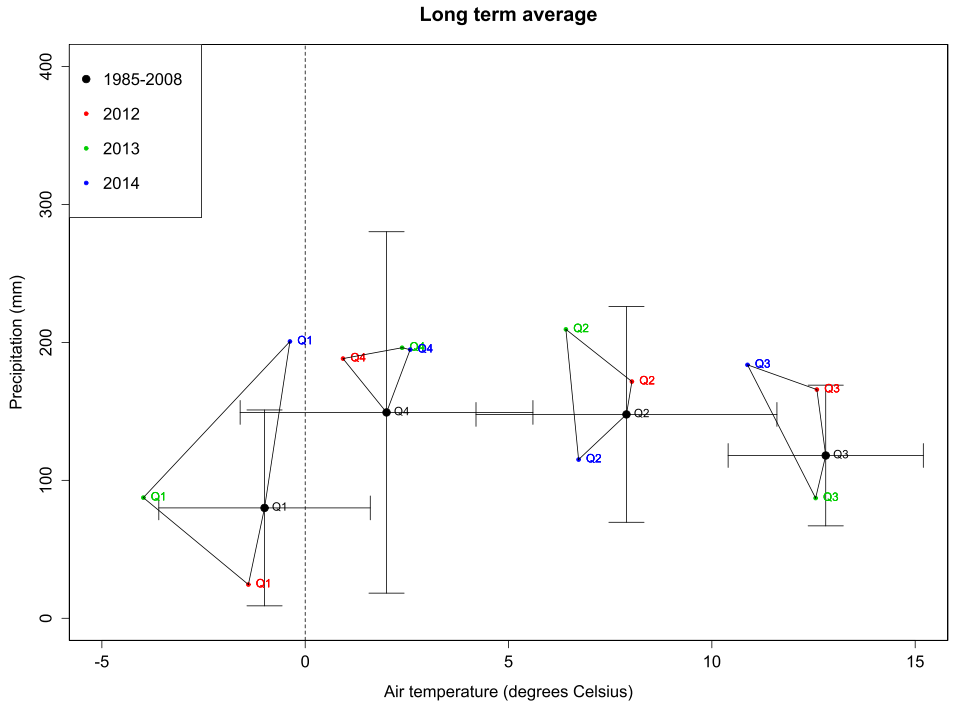

Fig. 2. Quarterly average air temperature and precipitation for 2012, 2013 and 2014 compared with the long-term average and their variation (1985–2008, Eccel et al., 2012).

3. Results

3.1. Meteorological data

The 2012 and 2014 annual temperatures of 5.1 °C and 5.0 °C, respectively, were close to the long-term average (1985–2008: 5.4 °C, Eccel et al., 2012), while in 2013 the temperature was lower (4.3 °C). The seasonal temperatures in 2012 were close to the averages apart from higher temperatures in May and lower temperatures in December (Figs. 2 and 3). In 2014 the spring and summer temperatures were colder, while in winter and autumn were warmer than the long-term average. The colder 2013 annual temperature was caused by colder temperatures in all seasons except in autumn, in particular in winter. The precipitation variation in the three years was also very pronounced, with annual values of 1650.4, 1740.6, and 2082.6 mm (for 2012, 2013 and 2014, respectively), all well above the long-term average of 1290 mm per year (Eccel et al., 2012). The first and third quarter of 2014 was wetter than the long-term average (Fig. 2). 2014 had particularly high precipitation in January and February and in July compared to the other years, while May and September were dryer (Fig. 3). 2012 had a dry winter with little snowfall compared to the other two years and then regular precipitation throughout the year. 2013 had little precipitation in the winter, but a very wet spring. In July and August 2014, the radiation was consistent with the high amount of precipitation, with lower radiation than the other years (Fig. 3). The annual daytime average PAR was 318 (2012), 290 (2013) and 287 (2014) $\mu mol\ m^{-2}\ s^{-1}$, while the average daytime PAR during the growing season was 1006 (2012), 948 (2013) and 942 (2014) $\mu mol\ m^{-2}\ s^{-1}$. During the very wet summer 2014 the water table was around 17 cm below soil level, while in autumn it dropped to 60 cm deep following a very dry September and start of October (Fig. 4). The mean water table depth was 27 cm below the surface over the measured period.

During the winter, neither the soil temperature at 5 cm depth under *M. caerula* and *C. vulgaris* dropped below 0 °C, because the snow cover and the layer of dead *M. caerula* leaves were acting as insulators (Fig. 3 and Fig. 5). In all years the soil temperature at 5 cm depth was above 5 °C when the first snow fell, then it decreased to near 0 °C in the following two months under the snow pack. The date at which the snow arrived was very variable with a range of 16 to 43 days difference. In 2011, the snow arrived the on 13th December; in 2012 it arrived on the 31st October, in 2013 on the 15th November and in 2014 the snow did not arrive (it arrived the 16th of January 2015). The maximum snow height in the three winters, was very variable and ranged from 43 cm (2012), 101 cm (2013) to 204 cm (2014) (Fig. 5). During the winters of 2011–2012 and 2013–2014, the snow density showed an increasing trend; while in the winter 2012–2013, there was a drop in snow density in the middle of the snow covered period. The peatland was covered with snow for 101, 173 and 157 days during the winter of 2012, 2013 and 2014, respectively. The long-term snow cover period average and the maximum snow height from 1985–2015 is 140 ± 29 days and 95 ± 52 cm, respectively (Meteotrentino). The difference in the snow water equivalent and amount of precipitation was responsible for the difference in SWC, which was higher in winter 2014 (above 80%) than in the other winters. During the summer season the SWC of the peatland never dropped below 31%, which was measured during the summer of 2013 (Fig. 3). Conversely, in 2014, the wettest year, the SWC did not drop beneath 66% during the summer. Under the snow cover the SWC dropped to 60% in 2013 compared to more than 80% in 2014, the annual average of the SWC was 74% over the three years.

3.2. Carbon and methane fluxes measurements

In all three years, the peatland was a source of CO_2 (Fig. 6). The peatland acted as a carbon sink for only four months a year, June to September (Fig. 6). The annual NEE measured at the Monte Bondone fen was 103.5, 262.9, 175.7 g C—CO_2 m^{-2} in the calendar years 2012, cooler 2013 and wettest 2014 respectively (Fig. 6). In total, the net CO_2 uptake period (the period where NEE < 0) was 64, 75 and 81 days for 2012, 2013 and 2014, respectively. During this period, the uptake was 4.2, 2.8 and 3.5 g C—CO_2 m^{-2} per day. In 2013, the CO_2 uptake period started later than in 2014 (Fig. 6 and Fig. 7), because of the long period of snow cover. The quarterly inter-annual variations

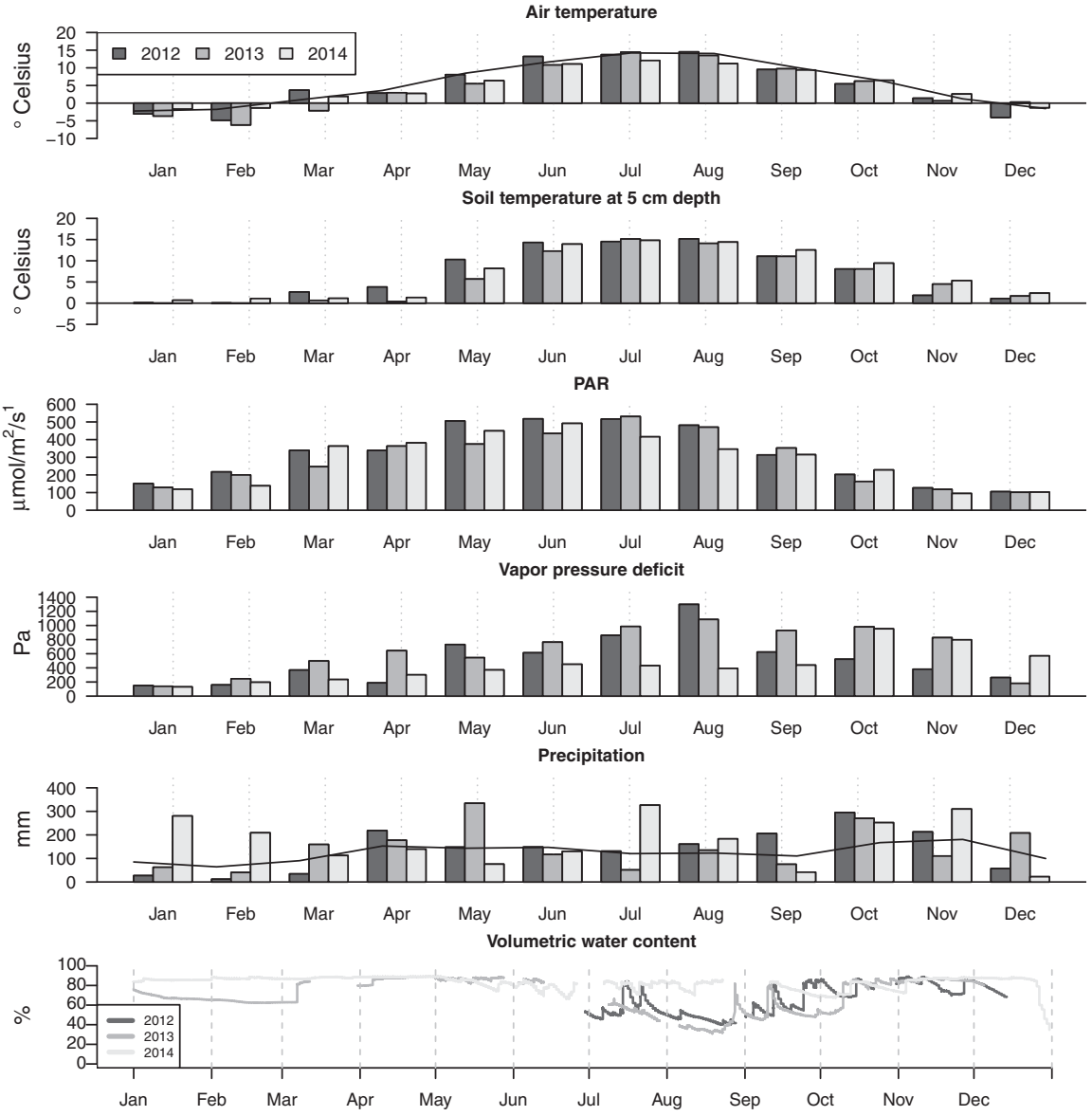

Fig. 3. Monthly values for meteorological variables across 3 years: average air temperature with the long-term average (Eccel et al., 2012) as a solid line, average soil temperature at 5 cm depth, total photosynthetic active radiation (PAR), mean vapour pressure deficit, total precipitation, and volumetric water content under *Calluna vulgaris* at 5 cm depth.

showed that all seasons have the same trends, apart from higher daily emissions in the first quarter of 2014, compared to the other years (Fig. 8). This could have been driven by high SWC, which was higher than in the other years (Table 1). Interesting to see is that the lower annual NEE of 2012 can be explained by the shorter C uptake period, due to an increase in ecosystem respiration.

The gross primary production (GPP) was high between June and September for all years, with the highest production in

Table 1
Spearman's correlations between Net Ecosystem Exchange (g C—CO_2 m^{-2} s^{-1}), Gross Primary Production (g C—CO_2 m^{-2} s^{-1}) and ecosystem respiration (g C—CO_2 m^{-2} s^{-1}) and air temperature (°C), photosynthetic active radiation (µmol m^{-2} s^{-1}), vapor pressure deficit (Pa), soil water content (%) and precipitation (mm) over three complete years and over each quarter of the years. All values are daily averages, apart from precipitation, which is a daily sum.

	NEE					GPP					Reco				
	Air temp	PAR	VPD	SWC	Prec	Air temp	PAR	VPD	SWC	Prec	Air temp	PAR	VPD	SWC	Prec
Yearly	−0.34	−0.40	−0.00	0.18	0.07	0.82	0.65	0.57	−0.45	0.05	0.82	0.56	0.61	−0.56	0.06
Q1	−0.07	0.10	0.40	−0.70	0.08	0.23	0.34	0.46	0.06	0.16	0.03	0.23	0.46	−0.59	0.11
Q2	−0.33	−0.15	−0.20	0.34	0.09	0.74	0.29	0.42	−0.84	−0.18	0.82	0.29	0.38	−0.79	−0.15
Q3	−0.52	−0.63	−0.04	−0.11	−0.04	0.65	0.63	0.09	0.07	0.06	0.63	0.34	0.15	−0.14	0.13
Q4	0.67	0.29	0.64	−0.30	0.19	0.55	0.26	0.66	−0.09	0.24	0.68	0.24	0.72	−0.22	0.25

Light gray: $p < 0.05$.
Dark gray: $p < 0.10$.
White: $p > 0.1$.

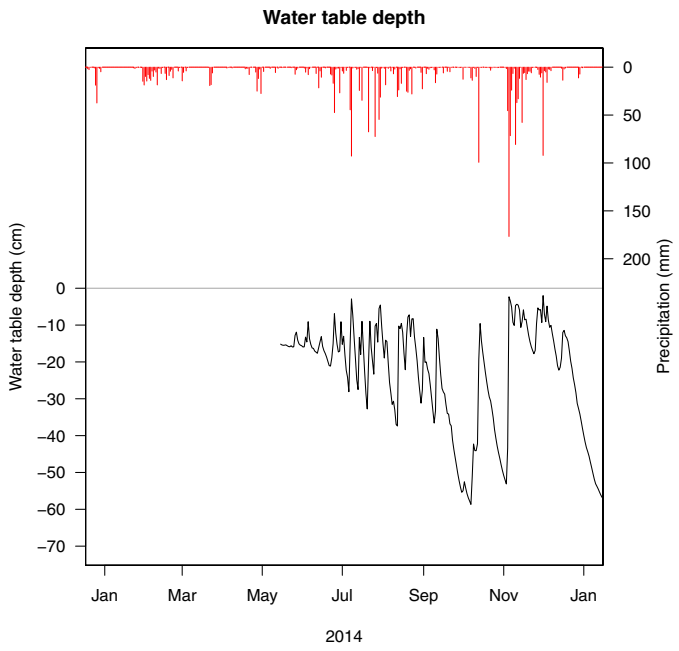

Fig. 4. Daily water table depth (in black) and daily precipitation (in red) from 14th of May 2014.

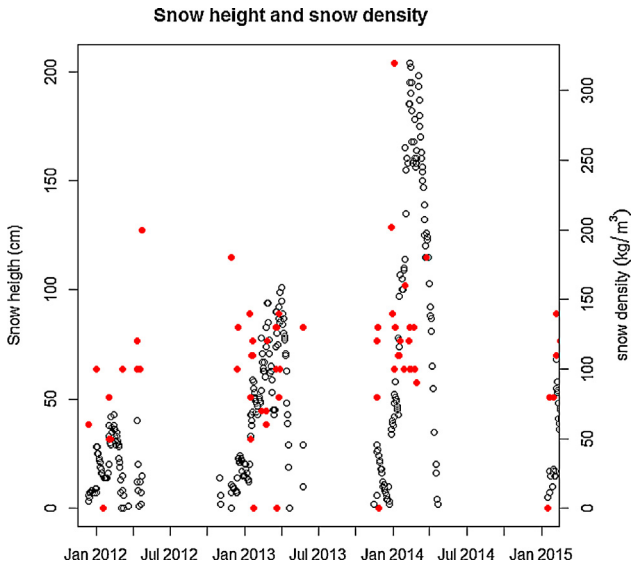

Fig. 5. Measured snow height and snow density during the years 2012, 2013 and 2014. The snow height (cm) is depicted by the black dots and the snow density (kg/m^3) by the red points. The values are not measured on site but at nearby a meteorological site.

July (168.7, 117.0 and 150.1 g C—CO_2 m^{-2} for 2012, 2013 and 2014, respectively). During May, the GPP was still very low, due to the late snowmelt. The annual GPP was 999.1, 1133.6 and 1248.2 g C—CO_2 m^{-2} for 2012, 2013 and 2014, respectively.

During the three winters there was a slight variation in the NEE, where 2013 had the highest emissions despite having the coldest air temperature (Fig. 8). Through the winter of 2012 and 2014 the ecosystem respiration was low, compared to the ecosystem respiration of the winter of 2013 (Fig. 7). During the winter of 2012–2013 the peatland was a big source of CO_2 and showed an elevated R_{eco} (compared to the other years) over the first three months of the year with a maximum monthly emission of 118.2 g C—CO_2 m^{-2} (March 2013). During the summer months of all years (Fig. 8), the R_{eco} increased and showed the characteristic bell shape. In 2012, the R_{eco} was lower in all months, apart from May and December, compared to the other years. In wettest 2014, the R_{eco} was higher in June, September, October and November, compared to the same months of the other years. The annual ecosystem respiration (R_{eco}) was 1102.4, 1396.4 and 1423.8 g C—CO_2 m^{-2} in the calendar years 2012, 2013 and 2014.

Based on the three years of carbon fluxes and meteorological measurements the correlation between the half-hourly values of NEE, R_{eco}, GPP and meteorological parameters were analysed. Frolking et al. (1998) described a correlation between NEE of peatlands and incoming radiation:

$$\mathrm{NEE} = \frac{\alpha \times \mathrm{PAR} \times \mathrm{GPP_{max}}}{\alpha \times \mathrm{PAR} + \mathrm{GPP_{max}}} - R$$

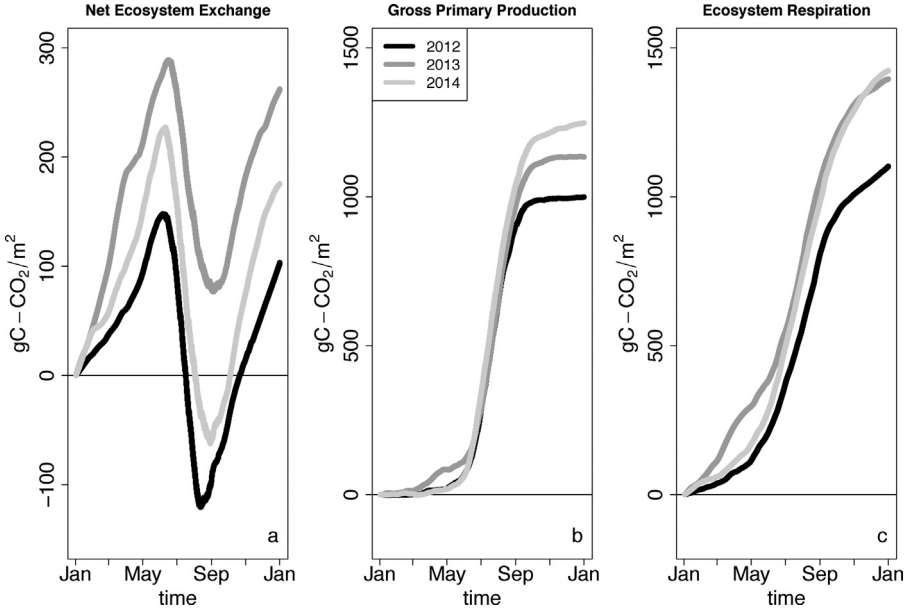

Fig. 6. (a) Cumulative NEE flux for each year (b) Cumulative GPP flux for each year (c) cumulative R_{eco} flux for each year.

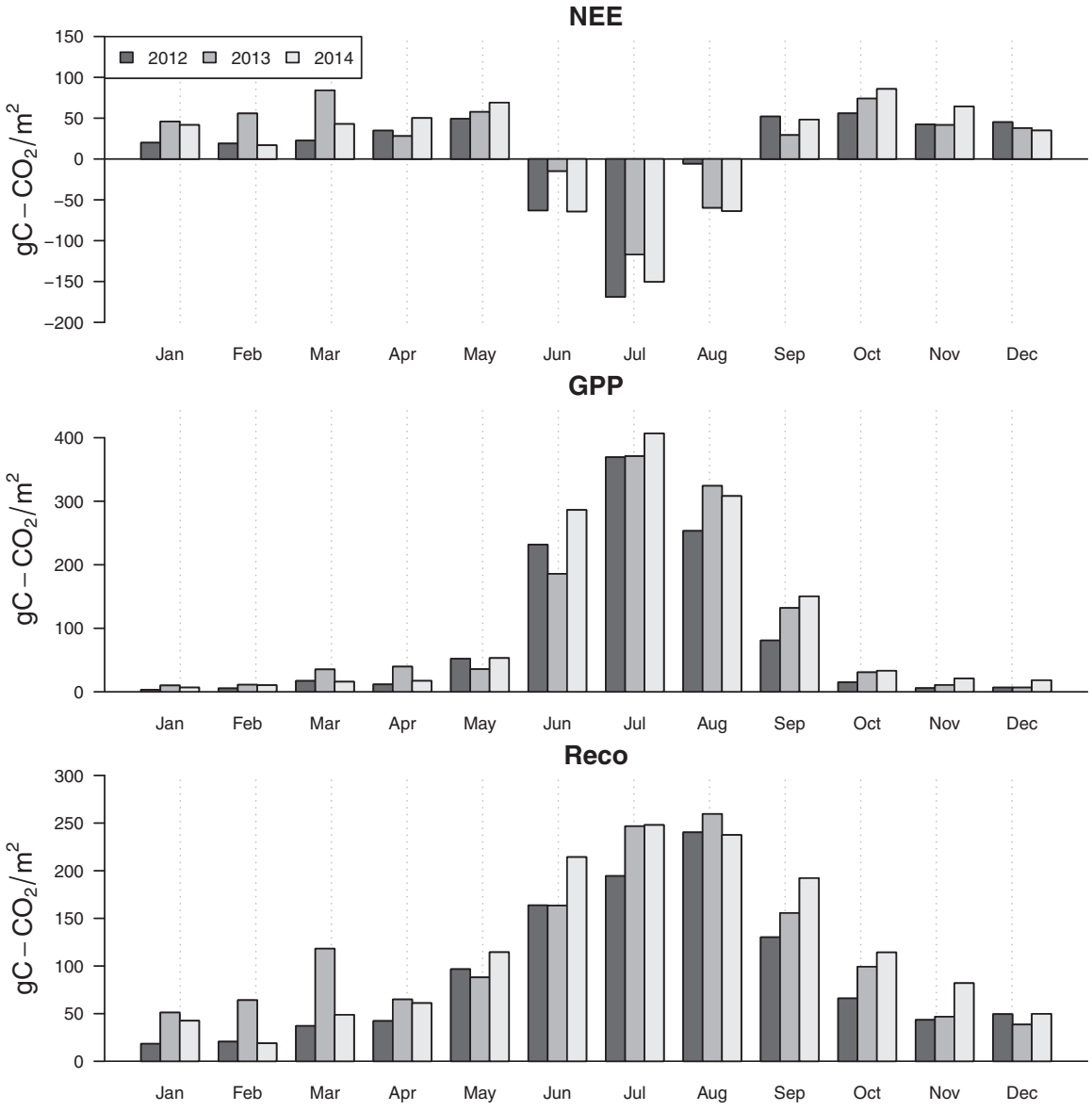

Fig. 7. Monthly values for CO_2 exchange variable across 3 years: sums of Net Ecosystem Exchange (NEE), sums of Gross Primary Production (GPP) and sums of ecosystem respiration (R_{eco}).

where α is the initial slope of the rectangular hyperbola and R is the dark respiration value. For this analysis, only the data from the summer was used, where the midday uptake was higher than 5 μmol m^{-2} s^{-1}. Over the data a rectangular hyperbola was fitted, since NEE becomes light saturated.

$$NEE = \frac{0.05 \times PAR \times GPP_{max}}{0.05 \times PAR + GPP_{max}} - 6.4 \quad R^2 = 0.83, p < 0.01$$

Over the complete years and all half-hourly data points, the GPP was linearly correlated to NEE.

$$GPP = 3.66 - 1.09 \times NEE \quad R^2 = 0.85, p < 0.01$$

While R_{eco} was exponentially correlated with the air temperature. $R_{eco} = e^{0.1029 \times Tair} + 1.2656$ $R^2 = 0.58$, $p < 0.01$

No comparison with soil temperature at 5 cm depth has been made since this variable was used to gap fill the data.

Over the three years, the daily values of NEE, GPP and R_{eco} are significantly correlated with Air temperature, PAR, VPD, soil water content and precipitation (Table 1). NEE is significantly correlated with air temperature, PAR and SWC. Interesting is that SWC has a negative relation with GPP and R_{eco}, which means that a decrease of SWC will increase the GPP and R_{eco}. Over the years, during all seasons the SWC had a significant correlation with inter-annual variability of NEE, but in the second quarter of the year (months: April, May, June) there was a positive correlation between NEE and SWC. During these months the soil was very wet, due to the snow melt (Figs. 3 and 5). Overall an increase in NEE is correlated with an increase of air temperature and PAR and a decrease in NEE with an increase in SWC.

Methane fluxes measured over 10 month showed small emissions, generally not higher than 0.035 μmol CH_4 m^{-2} s^{-1} (Fig. 9). Over this 10-month period, the total emission of the peatland was 3.2 g C—CH_4 m^{-2}. No relation between water table depth and methane fluxes at half hourly, nor daily time steps was found. In addition, air pressure as a proxy for ebullition of methane bubbles did not explain the methane flux (data not shown, $R^2 < 0.001$, $p > 0.25$). The CH_4 fluxes also show no daily or monthly trend or relationship with any measured meteorological parameters (data not shown, $p > 0.10$).

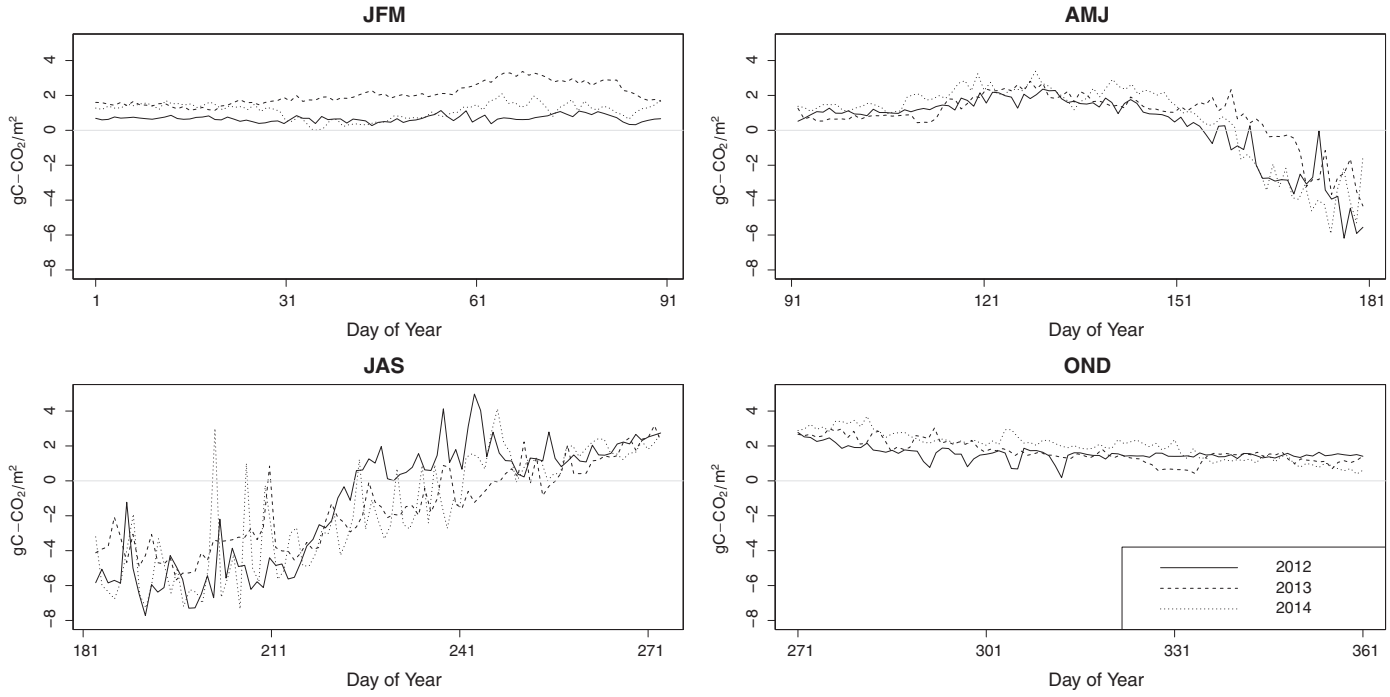

Fig. 8. Quarterly daily NEE fluxes over three years. JFM = January February March, APJ = April May June, JAS; July, August, September, OND = October, November, December.

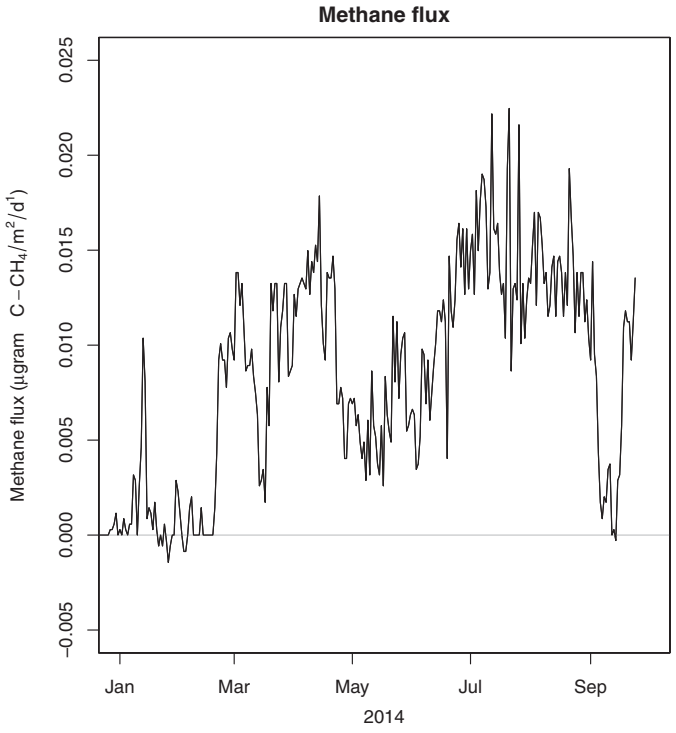

Fig. 9. Half-hourly data points of measured CH_4 fluxes.

4. Discussion

The observed CO_2 emissions of this Alpine peatland were much higher than in all of the other untouched peatlands monitored with an eddy covariance system (Aurela et al. 2015; Aurela et al., 2009; Bäckstrand et al., 2010; Beetz et al., 2013; Hendriks et al., 2007; Lund et al., 2007; McVeigh et al., 2014; Roulet et al., 2007; Sonnentag et al., 2010), since most of the low altitude northern latitude, pristine peatlands act as a carbon sink. The range of annual NEE (-329 to $-9\,g\,C{-}CO_2\,m^{-2}$), GPP (288 to $1215\,g\,C{-}CO_2\,m^{-2}$) and R_{eco} (232 to $1307\,g\,C{-}CO_2\,m^{-2}$) over different types of peatlands and altitudes are presented in Table 2; all peatlands are either untouched (by anthropogenic disturbances), or these activities were minor and occurred more than 30 years ago, apart from The Horstermeer site which is a wetland restored around 20 years ago from an abandoned agricultural peat meadow (Hendriks et al., 2007). Compared to the peatlands presented in Table 2, which are all carbon sinks, the peatland at Monte Bondone had a significantly shorter active carbon uptake period (ANOVA, $p < 0.01$). In spite of this short carbon uptake period, the annual GPP was very high. Only in one of the peatlands where fluxes are measured with an EC system (Horstermeer, NL), such a high annual GPP was measured. At the Horstermeer-site the annual GPP was high because of the long growing season (around 165 days) and the relatively eutrophic soil conditions (Hendriks et al., 2007). The GPP in other fens was less than half of the GPP measured at Monte Bondone. At these other sites more mosses and less vascular plants are present compared to the Monte Bondone peatland (Aurela et al., 2009; Beetz et al., 2013; Nilsson et al., 2008; Sonnentag et al., 2010; Wu et al., 2013). At our site, the abundant presence of *M. caerula* was possibly resulting in high values of GPP (Aerts and Berendse, 1989; Jarosz et al., 2008; Vanselow-Algan et al., 2015).

The R_{eco} of the Monte Bondone peatland is the highest value seen in Table 2; most of the sites have an ecosystem respiration of about $200–500\,g\,C{-}CO_2\,m^{-2}\,yr^{-1}$. The great root biomass of *M. caerula* when it is as widespread and developed as in Monte Bondone probably results in an increased root respiration and microbial respiration of root exudates compared to other plant communities (Gatis et al., 2015). The high R_{eco} during winter, with low air temperatures, was the effect of the snow insulation (Morgner et al., 2010), so the soil temperatures were still high enough to support decomposition even though the temperatures were close to zero degrees Celsius (Clein and Schimel, 1995).

The fitted rectangular hyperbola on the NEE of the peatland at Monte Bondone shows a clear difference with other peatlands (Frolking et al., 1998). Frolking et al. (1998) found an average of 0.024 ± 0.008 for the initial slope of the rectangular hyperbola (α)

Table 2
Comparison of Monte Bondone peatland with other peatlands of different types and locations, with the standard deviation in brackets (±).

Site	Glencar (McVeigh et al., 2014)	Fäjemyr (Lund et al., 2007, 2010)	Mer Bleue (Roulet et al., 2007)	Stordalen (Bäckstrand et al., 2010)	Horstermeer (Hendriks et al., 2007)	Sandhill fen (Sonnentag et al., 2010)	Friesinger Moos (Beetz et al., 2013)	Lompolojänkkä (Aurela et al., 2009; Aurela et al. 2015)	Degerö Stormyr (Nilsson et al., 2008; Wu et al., 2013)	Monte Bondone peatland (this study)
Latitude	51.55N	56.15N	45.41N	55.78N	52.25N	53.80N	53.68N	67.03N	64.18N	46.02N
Longitude	9.55E	13.33E	75.48W	3.23W	5.04E	104.62E	8.82E	24.49E	19.55E	11.03E
Type	Blanket bog	Eccentric bog	Raised bog	Mixed Mire	Restored peatland	Fen	Fen	Fen	Poor fen	Fen
Elevation (m a.s.l.)	145–170	96	69	267	0	494	0	180	270	1563
Duration (years)	9	1	6	11	3	4	2	3	5	3
Length growing season (days)	Around 130	214	171 ± 22	169	163 ± 26	Around 180	218	119	153	73 ± 7
NEE (g C—CO_2 m^{-2} yr^{-1})	−55.7 ± 18.9	−80	−40.2 ± 40.5	−34.9 ± 4	−329 ± 88	−129.7 ± 74.7	−14 ± 75	−117 ± 83.4	−54 ± 5.6	180.7 ± 65.2
GPP (g C—CO_2 m^{-2} yr^{-1})	288 ± 17	Around 250	259 ± 52	Around 200	1215 ± 70	421.8 ± 69.2	630 ± 64	n.a.	448 ± 83	1191.0 ± 42.9
R_{eco} (g C—CO_2 m^{-2} yr^{-1})	232 ± 7	Around 250	230 ± 40	Around 150	886 ± 27	301.5 ± 30.0	617 ± 38	n.a.	404 ± 76	1307.7 ± 25.4
CH4 (g C—CH_4 m^{-2} yr^{-1})	6.2[a]	n.a.	3.7 ± 0.5	11 ± 12	32 ± 21	n.a.	4.7 ± 0.6	n.a.	11.5 ± 2.2	3.2[*]
Water table depth[b] (cm)	−4.4 ± 1.4	−3.3 ± 7.8	−40 ± 10	−5 ± 10	−20 ± 25	−15 ± 10	−59 ± 20	2.5 ± 2.3	−10 ± 5	−27.6 ± 18

[*] For the methane fluxes of the Monte Bondone peatland no uncertainty can be given, since this value is derived from the 10 and a half-month data-period.
[a] Chamber measurements (Laine et al., 2007).
[b] Negative values of water table depth are below soil level.

and −2.38 ± 2.45 for the dark respiration (R) for peatlands, while at Monte Bondone the values were: 0.05 and −6.4, respectively. The higher value for the dark respiration could explain the high values of R_{eco}, while the higher value for α indicates a productive system. These high values are found at C3 crops or at grasslands (Ruimy et al., 1995).

The fluxes measured at the Bondone peatland were very different from those measured at the same time in a nearby managed poor grassland (*Sieversio-Nardetum strictae*), since the grassland was close to being CO_2 neutral (9.14 ± 75.21 g C—CO_2 m^{-2} (Marcolla et al., 2011)). The different NEE between the two sites are due to the higher winter ecosystem respiration in the peatland compared to the grassland. The high winter ecosystem respiration at the peatland, under the snow cover indicates that the microbes in the soil are still actively decomposing the high amount of stored soil carbon (Clein and Schimel, 1995). The GPP of the peatland was also higher than the GPP of the grassland (Marcolla et al., 2011) possibly because of the higher productivity of the peatland plants (as *M. caerulea*) compared to the less productive (*Festuca rubra* and *Nardus stricta*) Monte Bondone grassland plants (Marcolla et al., 2011; Sakowska et al., 2014) and to the management of the grassland. Each year around mid-July, the vegetation is cut and the biomass is removed, reducing the GPP and the R_{eco}.

During the three years the GPP as well as the duration of the net CO_2 uptake period increased; the same trend is not visible in NEE (Fig. 8). The high GPP in 2014 can be explained by the fact that the soil water content was high (Table 1), due to the high amount of precipitation. The plants could therefore keep their stomata open longer without having to cope with water stress (Oren et al., 1999).

The NEE and R_{eco} in February and March of 2013 were higher than in the same months of the other years (Fig. 7). During this period the SWC was lower than in the winter of 2013–2014, which might indicate that the WTL was also lower. As a consequence, this could have resulted in a faster decomposition under aerobic condition of soil organic carbon.

Possible errors in the measured fluxes at the Monte Bondone site consist of high data loss due to unstable situations, rain, power failure and due to the snowfall. The total amount of data gaps for the open path analyser (74%) was higher than the enclosed path analyser (65%). The open path is much more susceptible to external influences, e.g. when it rains the laser path is blocked and no fluxes can be measured. In total 53% of the data consisted of gaps, since not all the gaps of both analysers did not overlap. Another source of error can be the snowfall, when the snow fell the EC system should be lifted to maintain a constant height above the soil surface. In 2014 the EC system was raised, on the date that the EC system was raised the snow was close to the EC system. The snow height in 2014 increased very fast, which could have resulted in an underestimation of fluxes due to a decrease of the footprint. At sites were snow is present during the winter, the height of the EC system should be increased according to the snow height. The methane open path sensor was more susceptible to influences, since the open path was longer, 50 cm compared to 12.5 cm of the open path CO_2 analyser, hence the low amount of data available from this sensor (30%).

In February and March 2013, the average air temperature was lower than in the other years. The combination of low air temperatures and snowfall leads to a snow pack with a low density, e.g. presence of macro pores (Bowling and Massman, 2011; Massman et al., 1997). The increase in snow depth in February and March 2013 (Fig. 5), possibly caused air to be trapped in the newly fallen snow pack. During daytime, the occasionally positive air temperature and the high level of incoming radiation resulted in snowmelt. Due to the high porosity of the snow the water migrated down and accumulated (Rempel, 2007). During the nights, the air temperature dropped below zero again. This unfreezing and re-freezing process could have led to the formation of ice lenses in the snow

pack. Ice lenses have the capability to trap the air underneath it (Mast et al., 1998), so that the CO_2 produced during the decomposition was being stored in the snow pack (Larsen et al., 2007). During the snowmelt the ice lenses melted and the stored gasses was released in pulses, measured as peaks of ecosystem respiration in February and March 2013 (Fig. 7) (Larsen et al., 2007; Monson et al., 2006). Soil respiration in winter could be as much as 7–10% of the annual ecosystem respiration (Monson et al., 2006), in March 2013, during snow melt, the ecosystem respiration was 8.5% of the annual ecosystem respiration.

The methane fluxes were not measured for a complete year and no correlation between methane fluxes and meteorological variables was found. Nevertheless, it is plausible that the methane fluxes at this site do not play a major role in the carbon balance due to the low water table. During the measurements in 2014, the release of methane was a continuous diffusion process, even though the data showed many spikes. In our data there was no diurnal trend, which was also found by Rinne et al. (2007) at a peatland in Finland. It is difficult to measure methane fluxes with an eddy covariance setup, the micrometeorology plays a big role in the production of methane and the microbes which produce methane are not uniformly spread in the soil (Baldocchi et al., 2012; Bohn et al., 2013; Koebsch et al., 2015). The gap filling of methane is much more difficult compared to CO_2 data, therefore no consensus about the best method to gap fill methane data has been found in literature (Dengel et al., 2013). Methane can be released in bursts, which happens when there is a drop in the air pressure. This drop in pressure results in an over pressure of methane gas in the soil, which can result in the ebullition of methane gas (Tokida et al., 2007). After the snowmelt, the emission of methane increased a little, but overall the fluxes were at the lower range (3.2 g C—CH_4 m^{-2} over the 10-month study period), compared to other peatlands: 3.7 to 32 g C—CH_4 m^{-2} yr^{-1}, Table 2). This is remarkable since most of the peatland is covered by *M. caerula*, which is known to be able to conduct methane through its aerenchyma (Carmichael et al., 2014; Turetsky et al., 2014; Van Den Pol-Van Dasselaar et al., 1999). The high cover of *M. caerula* in this peatland does not directly link with high emissions of methane, while this relation was found in other peatlands (e.g. Couwenberg et al., 2010; Turetsky et al., 2014; Vanselow-Algan et al., 2015). During the measurement of the CH_4 fluxes, the measured water table was deep, up to 17 cm in summer and even to 60 cm in autumn. Methane is only produced under anaerobic conditions and emitted with a shallow water table; with a deep water table the methane is oxidized in the upper aerobic soil layers (Jungkunst et al., 2008; Wagner et al., 2003). At Mer Bleue and the Friesinger Moor the amount of methane emitted is more or less the same and also the water table level has the same depth (Beetz et al., 2013; Roulet et al., 2007, Table 2). This coincides with the findings that the methane emissions with a water table level of more than 20 cm below soil level is close to zero (Couwenberg et al., 2010; Jungkunst et al., 2008; Turetsky et al., 2014; Wagner et al., 2003). At Stordalen and Glencar the water table level was much shallower and therefore the methane emission was much higher (Bäckstrand et al., 2010; Koehler et al., 2011; Turetsky et al., 2014). At Horstermeer the methane fluxes were very high and not comparable with other sites where methane fluxes were measured, since it is a restored peatland and the eutrophic soil was not excavated (Hendriks et al., 2007). It has to be stated that the methane fluxes and the water table depth at Monte Bondone were only measured during the wettest year (2014) and not for the complete year.

5. Conclusion

The study of carbon fluxes of an alpine peatland for 2012–2014 shows that the peatland at Monte Bondone acted as a significant carbon source, based on its CO_2 emissions. This is a major contrast to all other pristine peatlands studied to date, most of which are at elevations below 300 m a.s.l, which are sinks for carbon. The methane emissions of this site were very low, due to a low water table. Despite being very high, the GPP of the peatland during the growing season was not high enough to compensate for the even higher loss of carbon (R_{eco}) during the winter period. During the snow cover, the decomposition of organic matter was an ongoing process. The active carbon uptake period of the peatland was 73 ± 7 days. The start of the growing season was induced by the melt of the snow, so changes in the date of snowmelt could result in differences in the carbon balance of the peatland.

With climate change, the period with snow cover will be shorter, which can possibly result in a longer growing season (Aurela et al., 2004; Humphreys and Lafleur, 2011). With a decrease of precipitation, part of the peatland will likely dry up, which will lead to an overall increase in *M. caerula* and will even make it possible for other species to colonize it. The surrounding area of the peatland is covered by grasses (*Sieversio-Nardetum strictae* association), which can invade the peatland when the water table drops (Stine et al., 2011). The increase in *M. caerula* could result in a higher carbon uptake, while the eventual transition to grassland will have unknown consequences. However, the first years to decades the grassland might act as a carbon source, since the carbon in the soil will become unstable (Schwalm and Zeitz, 2014). To gain a better insight in the effect of climate change on alpine peatlands, a longer time series of carbon measurements is needed as well as studies on changes in the hydrology and the vegetation of the peatland.

Acknowledgments

The authors would like to thank Roberto Zampedri and Mauro Cavagna, from Fondazione Edmund Mach, for the maintenance of the eddy covariance tower and for the collection of the data. The authors thank Dr. Beniamino Gioli from the National Research Council—Institute for Biometeorology, Florence for lending the open path methane sensor (LI7700). The authors also want to thank the Associate Editor Eva Falge and the two anonymous reviewers for their useful suggestions and comments.

Appendix A. Supplementary data

Supplementary data associated with this article can be found, in the online version, at http://dx.doi.org/10.1016/j.agrformet.2016.01.012.

References

Aerts, R., Berendse, F., 1989. Above-ground nutrient turnover and net primary production of an evergreen and a deciduous species in a heathland ecosystem. J. Ecol. 77, 343–356, http://dx.doi.org/10.2307/2260754.

Ammann, B., Wright, H.E., Stefanova, V., Van Leeuwen, J.F.N., Van Der Knaap, W.O., Colombaroli, D., Tinner, W., 2013. The role of peat decomposition in patterned mires: a case study from the central Swiss Alps. Preslia 85, 317–332.

Andersen, R., Pouliot, R., Rochefort, L., 2013. Above-ground net primary production from vascular plants shifts the balance towards organic matter accumulation in restored *Sphagnum* bogs. Wetlands 33, 811–821, http://dx.doi.org/10.1007/s13157-013-0438-5.

Armstrong, W., 1979. Aeration in higher plants. In: Woolhouse, H.W. (Ed.), Advances in Botanical Research. Academic Press, Cambridge, p. p332.

Aurela, M., 2002. Annual CO_2 balance of a subarctic fen in northern Europe: importance of the wintertime efflux. J. Geophys. Res. 107, 4607, http://dx.doi.org/10.1029/2002JD002055.

Aurela, M., Laurila, T., Tuovinen, J.-P., 2004. The timing of snow melt controls the annual CO_2 balance in a subarctic fen. Geophys. Res. Lett. 31, L16119, http://dx.doi.org/10.1029/2004GL020315.

Aurela, M., Lohila, A., Tuovinen, J., 2009. Carbon dioxide exchange on a northern boreal fen. Boreal Environ. Res. 14, 699–710.

Aurela, M., Lohila, A., Tuovinen, J.-P., Hatakka, J., Penttilä, T., Laurila, T., 2015. Carbon dioxide and energy flux measurements in four northern-boreal ecosystems at Pallas. Boreal Environ. Res. 20, 455–473.

Bäckstrand, K., Crill, P.M., Jackowicz-Korczyñski, M., Mastepanov, M., Christensen, T.R., Bastviken, D., 2010. Annual carbon gas budget for a subarctic peatland, Northern Sweden. Biogeosciences 7, 95–108, http://dx.doi.org/10.5194/bg-7-95-2010.

Baldocchi, D.D., 2003. Assessing the eddy covariance technique for evaluating carbon dioxide exchange rates of ecosystems: past, present and future. Glob. Chang. Biol. 9, 479–492, http://dx.doi.org/10.1046/j.1365-2486.2003.00629.x.

Baldocchi, D.D., Detto, M., Sonnentag, O., Verfaillie, J., Teh, Y.A., Silver, W., Kelly, N.M., 2012. The challenges of measuring methane fluxes and concentrations over a peatland pasture. Agric. For. Meteorol. 153, 177–187 (10.1016/j.agrformet.2011.04.013 LB—electronic format).

Beer, J., Blodau, C., 2007. Transport and thermodynamics constrain belowground carbon turnover in a northern peatland. Geochim. Cosmochim. Acta 71, 2989–3002, http://dx.doi.org/10.1016/j.gca.2007.03.010.

Beetz, S., Liebersbach, H., Glatzel, S., Jurasinski, G., Buczko, U., Höper, H., 2013. Effects of land use intensity on the full greenhouse gas balance in an Atlantic peat bog. Biogeosciences 10, 1067–1082, http://dx.doi.org/10.5194/bg-10-1067-2013.

Beniston, M., Diaz, H.F., Bradley, R.S., 1997. Climatic change at high elevation sites: an overview. Clim. Change 36, 233–251, http://dx.doi.org/10.1023/A: 1005380714349.

Beyer, C., Höper, H., 2015. Greenhouse gas exchange of rewetted bog peat extraction sites and a *Sphagnum* cultivation site in northwest Germany. Biogeosciences 12, 2101–2117, http://dx.doi.org/10.5194/bg-12-2101-2015.

Bohn, T.J., Podest, E., Schroeder, R., Pinto, N., McDonald, K.C., Glagolev, M., Filippov, I., Maksyutov, S., Heimann, M., Chen, X., Lettenmaier, D.P., 2013. Modeling the large-scale effects of surface moisture heterogeneity on wetland carbon fluxes in the West Siberian Lowland. Biogeosciences 10, 6559–6576, http://dx.doi.org/10.5194/bg-10-6559-2013.

Bond-Lamberty, B., Thomson, A., 2010. Temperature-associated increases in the global soil respiration record. Nature 464, 579–582, http://dx.doi.org/10.1038/nature08930.

Bowling, D.R., Massman, W.J., 2011. Persistent wind-induced enhancement of diffusive CO_2 transport in a mountain forest snowpack. J. Geophys. Res. 116, G04006, http://dx.doi.org/10.1029/2011JG001722.

Burba, G., Schmidt, A., Scott, R.L., Nakai, T., Kathilankal, J., Fratini, G., Hanson, C., Law, B., McDermitt, D.K., Eckles, R., Furtaw, M., Velgersdyk, M., 2012. Calculating CO_2 and H_2O eddy covariance fluxes from an enclosed gas analyzer using an instantaneous mixing ratio. Glob. Chang. Biol. 18, 385–399, http://dx.doi.org/10.1111/j.1365-2486.2011.02536.x.

Camill, P., 2005. Permafrost thaw accelerates in boreal peatlands during late-20th century climate warming. Clim. Change 68, 135–152.

Carmichael, M.J., Bernhardt, E.S., Bräuer, S.L., Smith, W.K., 2014. The role of vegetation in methane flux to the atmosphere: should vegetation be included as a distinct category in the global methane budget? Biogeochemistry 119, 1–24, http://dx.doi.org/10.1007/s10533-014-9974-1.

Cescatti, A., Chemini, C., De Siena, C., Gianelle, D., Nicolini, G., Wohlfahrt, G., 1999. Monte bondone composite landscape, Italy. In: Cernusca, A., Tappeiner, U., Bayfield, N. (Eds.), Land-Use in European Mountian Ecosystems, ECOMONT—Concepts and Results. Wissenschafts-Verlag, Berlin, pp. 35–94.

Clein, J.S., Schimel, J.P., 1995. Microbial activity of tundra and taiga soils at sub-zero temperatures. Soil Biol. Biochem. 27, 1231–1234.

Couwenberg, J., Dommain, R., Joosten, H., 2010. Greenhouse gas fluxes from tropical peatlands in south-east Asia. Glob. Chang. Biol. 16, 1715–1732, http://dx.doi.org/10.1111/j.1365-2486.2009.02016.x.

Dalla Fior, G., 1969. Analisi polliniche di torbe e depositi lacustri della Venezia Tridentina, Trento. TEMI, Trento (Italy).

Dengel, S., Zona, D., Sachs, T., Aurela, M., Jammet, M., Parmentier, F.-J.W., Oechel, W.C., Vesala, T., 2013. Testing the applicability of neural networks as a gap-filling method using CH4 flux data from high latitude wetlands. Biogeosciences 10, 8185–8200, http://dx.doi.org/10.5194/bg-10-8185-2013.

Dorrepaal, E., Toet, S., van Logtestijn, R.S.P., Swart, E., van de Weg, M.J., Callaghan, T.V., Aerts, R., 2009. Carbon respiration from subsurface peat accelerated by climate warming in the subarctic. Nature 460, http://dx.doi.org/10.1038/nature08216, 616-U79.

Drösler, M., Freibauer, A., Christensen, T.R., Friborg, T., 2008. Observations and status of peatland greenhouse gas emissions in Europe. In: Dolman, A.J., Valentini, R., Freibauer, A. (Eds.), The Continental-Scale Greenhouse Gas Balance of Europe, Ecological Studies. Springer, New York, NY, http://dx.doi.org/10.1007/978-0-387-76570-9.

Eccel, E., Cau, P., Ranzi, R., 2012. Data reconstruction and homogenization for reducing uncertainties in high-resolution climate analysis in Alpine regions. Theor. Appl. Climatol. 110, 345–358, http://dx.doi.org/10.1007/s00704-012-0624-z.

Frolking, S., Bubier, J.L., Moore, T.R., Ball, T., Bellisario, L.M., Bhardwaj, A., Carroll, P., Crill, P.M., Lafleur, P.M., McCaughey, J.H., Roulet, N.T., Suyker, A.E., Verma, S.B., Waddington, J.M., Whiting, G.J., 1998. Relationship between ecosystem productivity and photosynthetically active radiation for Northern peatlands. Global Biogeochem. Cycles 12, 115–126, http://dx.doi.org/10.1029/97GB03367.

Frolking, S., Roulet, N.T., Moore, T.R., Richard, P.J.H., Lavoie, M., Muller, S., 2001. Modeling northern peatland decomposition and peat accumulation. Ecosystems 4, 479–498, http://dx.doi.org/10.1007/s10021-001-0105-1.

Frolking, S., Talbot, J., Jones, M.C., Treat, C.C., Kauffman, J.B., Tuittila, E., Roulet, N.T., 2011. Peatlands in the Earth's 21st century climate system. Environ. Rev. 19, 371–396, http://dx.doi.org/10.1139/a11-014.

Gatis, N., Luscombe, D.J., Grand-Clement, E., Hartley, I.P., Anderson, K., Smith, D., Brazier, R.E., 2015. The effect of drainage ditches on vegetation diversity and CO_2 fluxes in a Molinia caerulea dominated peatland. Ecohydrology, http://dx.doi.org/10.1002/eco.1643 (n/a–n/a).

Gebauer, R.L.E., Reynolds, J.F., Tenhunen, J., 1995. Growth and allocation of the arctic sedges eriophorum angustifolium and *E. vaginatum*: effects of variable soil oxygen and nutrient availability. Oecologia 104, 330–339.

Gong, J., Kellomäki, S., Wang, K., Zhang, C., Shurpali, N., Martikainen, P.J., 2013. Modeling CO_2 and CH_4 flux changes in pristine peatlands of Finland under changing climate conditions. Ecol. Modell. 263, 64–80, http://dx.doi.org/10.1016/j.ecolmodel.2013.04.018.

Gorham, E., 1991. Northern Peatlands: role in the carbon cycle and probable responses to climatic warming. Ecol. Appl. 1, 182–195, http://dx.doi.org/10.2307/1941811.

Hatala, J.A., Detto, M., Sonnentag, O., Deverel, S.J., Verfaillie, J., Baldocchi, D.D., 2012. Greenhouse gas (CO_2, CH_4, H_2O) fluxes from drained and flooded agricultural peatlands in the Sacramento-San Joaquin Delta. Agric. Ecosyst. Environ. 150, 1–18, http://dx.doi.org/10.1016/j.agee.2012.01.009.

Heijmans, M., van der Knaap, Y.A.M., Holmgren, M., Limpens, J., 2013. Persistent versus transient tree encroachment of temperate peat bogs: effects of climate warming and drought events. Glob. Change Biol. 19, 2240–2250, http://dx.doi.org/10.1111/gcb.12202.

Hendriks, D.M.D., van Huissteden, J., Dolman, A.J., van der Molen, M.K., 2007. The full greenhouse gas balance of an abandoned peat meadow. Biogeosciences 4, 411–424.

Holmgren, M., Lin, C.-Y., Murillo, J.E., Nieuwenhuis, A., Penninkhof, J., Sanders, N., van Bart, T., van Veen, H., Vasander, H., Vollebregt, M.E., Limpens, J., 2015. Positive shrub-tree interactions facilitate woody encroachment in boreal peatlands. J. Ecol. 103, 58–66, http://dx.doi.org/10.1111/1365-2745.12331.

Humphreys, E.R., Lafleur, P.M., 2011. Does earlier snowmelt lead to greater CO_2 sequestration in two low Arctic tundra ecosystems? Geophys. Res. Lett. 38, http://dx.doi.org/10.1029/2011GL047339 (n/a–n/a).

Im, E.-S., Coppola, E., Giorgi, F., Bi, X., 2010. Local effects of climate change over the Alpine region: a study with a high resolution regional climate model with a surrogate climate change scenario. Geophys. Res. Lett. 37, http://dx.doi.org/10.1029/2009GL041801.

IPCC, 2013. Climate Change 2013—The Physical Science Basis. Contribution of Working Group I to the Fifth Assessment Report of the Intergovernmental Panel on Climate Change. Cambridge University Press, Cambridge, United Kingdom and New York, NY, USA.

IPCC, 2007. Climate Change 2007: The Physical Science Basis. Contribution of Working Group I to the Fourth Assessment Report of Intergovernmental Panel on Climate Change. Cambridge University Press, New York, NY.

Jarosz, N., Brunet, Y., Lamaud, E., Irvine, M., Bonnefond, J.-M., Loustau, D., 2008. Carbon dioxide and energy flux partitioning between the understorey and the overstorey of a maritime pine forest during a year with reduced soil water availability. Agric. For. Meteorol. 148, 1508–1523, http://dx.doi.org/10.1016/j.agrformet.2008.05.001.

Jungkunst, H.F., Flessa, H., Scherber, C., Fiedler, S., 2008. Groundwater level controls CO_2, N_2O and CH_4 fluxes of three different hydromorphic soil types of a temperate forest ecosystem. Soil Biol. Biochem. 40, 2047–2054, http://dx.doi.org/10.1016/j.soilbio.2008.04.015.

Kljun, N., Calanca, P., Rotach, M.W., Schmid, H.P., 2004. A simple parameterisation for flux footprint predictions. Boundary-Layer Meteorol. 112, 503–523, http://dx.doi.org/10.1023/B:BOUN. 0000030653.71031.96.

Koebsch, F., Jurasinski, G., Koch, M., Hofmann, J., Glatzel, S., 2015. Controls for multi-scale temporal variation in ecosystem methane exchange during the growing season of a permanently inundated fen. Agric. For. Meteorol. 204, 94–105, http://dx.doi.org/10.1016/j.agrformet.2015.02.002.

Koehler, A.-K., Sottocornola, M., Kiely, G., 2011. How strong is the current carbon sequestration of an Atlantic blanket bog? Glob. Change Biol. 17, 309–319, http://dx.doi.org/10.1111/j.1365-2486.2010.02180.x.

Lafleur, P.M., Roulet, N.T., Admiral, S.W., 2001. Annual cycle of CO_2 exchange at a bog peatland. J. Geophys. Res. 106, 3071, http://dx.doi.org/10.1029/2000JD900588.

Laine, A., Wilson, D., Kiely, G., Byrne, K.A., 2007. Methane flux dynamics in an Irish lowland blanket bog. Plant Soil 299, 181–193, http://dx.doi.org/10.1007/s11104-007-9374-6.

Larsen, K.S., Grogan, P., Jonasson, S., Michelsen, A., 2007. Respiration and microbial dynamics in two subarctic ecosystems during winter and spring thaw: effects of increased snow depth. Arctic Antarct. Alp. Res. 39, 268–276, http://dx.doi.org/10.1657/1523-0430(2007)39[268:RAMDIT]2.0.CO;2.

Lawrence, B.A., Jackson, R.D., Kucharik, C.J., 2013. Testing the stability of carbon pools stored in tussock sedge meadows. Appl. Soil Ecol. 71, 48–57, http://dx.doi.org/10.1016/j.apsoil.2013.05.007.

Lund, M., Lafleur, P.M., Roulet, N.T., Lindroth, A., Christensen, T.R., Aurela, M., Chojnicki, B.H., Flanagan, L.B., Humphreys, E.R., Laurila, T., Oechel, W.C., Olejnik, J., Rinne, J., Schubert, P., Nilsson, M., 2010. Variability in exchange of CO_2 across 12 northern peatland and tundra sites. Glob. Change Biol. 16, 2436–2448, http://dx.doi.org/10.1111/j.1365-2486.2009.02104.x.

Lund, M., Lindroth, A., Christensen, T.R., Ström, L., 2007. Annual CO_2 balance of a temperate bog. Tellus B 59, http://dx.doi.org/10.3402/tellusb.v59i5.17060.
Marcolla, B., Cescatti, A., Manca, G., Zorer, R., Cavagna, M., Fiora, A., Gianelle, D., Rodeghiero, M., Sottocornola, M., Zampedri, R., 2011. Climatic controls and ecosystem responses drive the inter-annual variability of the net ecosystem exchange of an alpine meadow. Agric. For. Meteorol. 151, 1233–1243, http://dx.doi.org/10.1016/j.agrformet.2011.04.015.
Massman, W.J., Sommerfeld, R.A., Mosier, A.R., Zeller, K.F., Hehn, T.J., Rochelle, S.G., 1997. A model investigation of turbulence-driven pressure-pumping effects on the rate of diffusion of CO_2, N_2O, and CH_4 through layered snowpacks. J. Geophys. Res. 102, 18851, http://dx.doi.org/10.1029/97JD00844.
Mast, M.A., Wickland, K.P., Striegl, R.T., Clow, D.W., 1998. Winter fluxes of CO_2 and CH_4 from subalpine soils in Rocky Mountain National Park, Colorado. Global Biogeochem. Cycles 12, 607–620, http://dx.doi.org/10.1029/98GB02313.
McVeigh, P., Sottocornola, M., Foley, N., Leahy, P., Kiely, G., 2014. Meteorological and functional response partitioning to explain interannual variability of CO_2 exchange at an Irish Atlantic blanket bog. Agric. For. Meteorol. 194, 8–19, http://dx.doi.org/10.1016/j.agrformet.2014.01.017.
Mitsch, W.J., Bernal, B., Nahlik, A.M., Mander, Ü., Zhang, L., Anderson, C.J., Jørgensen, S.E., Brix, H., 2012. Wetlands, carbon, and climate change. Landsc. Ecol. 28, 583–597, http://dx.doi.org/10.1007/s10980-012-9758-8.
Moncrieff, J.B., Clement, R., Finnigan, J., Meyers, T., 2004. Averaging, detrending, and filtering of eddy covariance time series. In: Lee, X., Massman, W.J., Law, B.E. (Eds.), Handbook of Micrometeorology: A Guide for Surface Flux Measurements. Kluwer Academic Publishers, Dordrecht, pp. 7–31.
Moncrieff, J.B., Massheder, J.M., de Bruin, H., Elbers, J.A., Friborg, T., Heusinkveld, B., Kabat, P., Scott, S., Soegaard, H., Verhoef, A., 1997. A system to measure surface fluxes of momentum, sensible heat, water vapour and carbon dioxide. J. Hydrol. 188–189, 589–611, http://dx.doi.org/10.1016/S0022-1694(96)03194-0.
Monson, R., Burns, S.P., Williams, M.W., Delany, A.C., Weintraub, M., Lipson, D.A., 2006. The contribution of beneath-snow soil respiration to total ecosystem respiration in a high-elevation, subalpine forest. Global Biogeochem. Cycles 20, http://dx.doi.org/10.1029/2005GB002684 (n/a–n/a).
Morgner, E., Elberling, B., Strebel, D., Cooper, E.J., 2010. The importance of winter in annual ecosystem respiration in the High Arctic: effects of snow depth in two vegetation types. Polar Res. 29, 58–74, http://dx.doi.org/10.3402/polar.v29i1.6052.
Murphy, M.T., McKinley, a., Moore, T.R., 2009. Variations in above- and below-ground vascular plant biomass and water table on a temperate ombrotrophic peatland. Botany 87, 845–853, http://dx.doi.org/10.1139/B09-052.
Nakai, T., Shimoyama, K., 2012. Ultrasonic anemometer angle of attack errors under turbulent conditions. Agric. For. Meteorol. 162, 14–26, http://dx.doi.org/10.1016/j.agrformet.2012.04.004.
Nilsson, M., Sagerfors, J., Buffam, I., Laudon, H., Eriksson, T., Grelle, A., Klemedtsson, L., Weslein, P., Lindroth, A., 2008. Contemporary carbon accumulation in a boreal oligotrophic minerogenic mire—a significant sink after accounting for all C-fluxes. Glob. Chang. Biol. 14, 2317–2332, http://dx.doi.org/10.1111/j.1365-2486.2008.01654.x.
Oren, R., Sperry, J.S., Katul, G.G., Pataki, D.E., Ewers, B.E., Phillips, N., Schäfer, K.V.R., 1999. Survey and synthesis of intra- and interspecific variation in stomatal sensitivity to vapour pressure deficit. Plant Cell Environ. 22, 1515–1526, http://dx.doi.org/10.1046/j.1365-3040.1999.00513.x.
Papale, D., Reichstein, M., Aubinet, M., Canfora, E., Bernhofer, C., Kutsch, W., Longdoz, B., Rambal, S., Valentini, R., Vesala, T., Yakir, D., 2006. Towards a standardized processing of Net Ecosystem Exchange measured with eddy covariance technique: algorithms and uncertainty estimation. Biogeosciences 3, 571–583.
Parish, F., Sirin, A., Charman, D., Joosten, H., Minayeva, T., Silvius, M., Stringer, L., 2008. Assessment on Peatlands, Biodiversity and Climate Change: Main Report. Global Environment Centre, Kuala Lumpur and Wetlands International, Wageningen.
Pepin, N., Bradley, R.S., Diaz, H.F., Baraer, M., Caceres, E.B., Forsythe, N., Fowler, H., Greenwood, G., Hashmi, M.Z., Liu, X.D., Miller, J.R., Ning, L., Ohmura, A., Palazzi, E., Rangwala, I., Schöner, W., Severskiy, I., Shahgedanova, M., Wang, M.B., Williamson, S.N., Yang, D.Q., 2015. Elevation-dependent warming in mountain regions of the world. Nat. Clim. Chang. 5, 424–430, http://dx.doi.org/10.1038/nclimate2563.
Petrescu, A.M.R., Lohila, A., Tuovinen, J.-P., Baldocchi, D.D., Desai, A.R., Roulet, N.T., Vesala, T., Dolman, H., Oechel, W.C., Marcolla, B., Friborg, T., Rinne, J., Matthes, J.H., Merbold, L., Meijide, A., Kiely, G., Sottocornola, M., Sachs, T., Zona, D., Varlagin, A., Lai, D.Y.F., Veenendaal, E., Parmentier, F.-J.W., Skiba, U., Lund, M., Hensen, A., van Huissteden, J., Flanagan, L.B., Shurpali, N.J., Grünwald, T., Humphreys, E.R., Jackowicz-Korczyński, M., Aurela, M., Laurila, T., Grüning, C., Corradi, C.A.R., Schrier-Uijl, A.P., Christensen, T.R., Tamstorf, M.P., Mastepanov, M., Martikainen, P.J., Verma, S.B., Bernhofer, C., Cescatti, A., 2015. The uncertain climate footprint of wetlands under human pressure. Proc. Natl. Acad. Sci. U.S.A. 112, 4594–4599, http://dx.doi.org/10.1073/pnas.1416267112.
R Core Team, 2013. R: A Language and Environment for Statistical Computing. R Core Team.
Reichstein, M., Falge, E., Baldocchi, D.D., Papale, D., Aubinet, M., Berbigier, P., Bernhofer, C., Buchmann, N., Gilmanov, T., Granier, A., Grunwald, T., Havrankova, K., Ilvesniemi, H., Janous, D., Knohl, A., Laurila, T., Lohila, A., Loustau, D., Matteucci, G., Meyers, T., Miglietta, F., Ourcival, J.-M., Pumpanen, J., Rambal, S., Rotenberg, E., Sanz, M., Tenhunen, J., Seufert, G., Vaccari, F., Vesala, T., Yakir, D., Valentini, R., 2005. On the separation of net ecosystem exchange into assimilation and ecosystem respiration: review and improved algorithm. Glob. Change Biol. 11, 1424–1439, http://dx.doi.org/10.1111/j.1365-2486.2005.001002.x.
Rempel, A.W., 2007. Formation of ice lenses and frost heave. J. Geophys. Res. 112, F02S21, http://dx.doi.org/10.1029/2006JF000525.
Richardson, A.D., Mahecha, M.D., Falge, E., Kattge, J., Moffat, A.M., Papale, D., Reichstein, M., Stauch, V.J., Braswell, B.H., Churkina, G., Kruijt, B., Hollinger, D.Y., 2008. Statistical properties of random CO_2 flux measurement uncertainty inferred from model residuals. Agric. For. Meteorol. 148, 38–50, http://dx.doi.org/10.1016/j.agrformet.2007.09.001.
Rinne, J., Riutta, T., Pihlatie, M., Aurela, M., Haapanala, S., Tuovinen, J.-P., Tuittila, E.-S., Vesala, T., 2007. Annual cycle of methane emission from a boreal fen measured by the eddy covariance technique. Tellus B 59, http://dx.doi.org/10.3402/tellusb.v59i3.17009.
Roulet, N.T., Lafleur, P.M., Richard, P.J.H., Moore, T.R., Humphreys, E.R., Bubier, J.L., 2007. Contemporary carbon balance and late Holocene carbon accumulation in a northern peatland. Glob. Change Biol. 13, 397–411, http://dx.doi.org/10.1111/j.1365-2486.2006.01292.x.
Ruimy, A., Jarvis, P.G., Baldocchi, D.D., Saugier, B., 1995. CO_2 fluxes over plant canopies and solar radiation: a review. Adv. Ecol. Res. 26, 1–68, doi: http://dx.doi.org/10.1016/S0065-2504(08)60063-X.
Sakowska, K., Gianelle, D., Zaldei, A., MacArthur, A., Carotenuto, F., Miglietta, F., Zampedri, R., Cavagna, M., Vescovo, L., 2015. WhiteRef: a new tower-based hyperspectral system for continuous reflectance measurements. Sensors (Basel) 15, 1088–1105, http://dx.doi.org/10.3390/s150101088.
Sakowska, K., Vescovo, L., Marcolla, B., Juszczak, R., Olejnik, J., Gianelle, D., 2014. Monitoring of carbon dioxide fluxes in a subalpine grassland ecosystem of the Italian Alps using a multispectral sensor. Biogeosciences 11, 4695–4712, http://dx.doi.org/10.5194/bg-11-4695-2014.
Schuur, E.A.G., McGuire, A.D., Schädel, C., Grosse, G., Harden, J.W., Hayes, D.J., Hugelius, G., Koven, C.D., Kuhry, P., Lawrence, D.M., Natali, S.M., Olefeldt, D., Romanovsky, V.E., Schaefer, K., Turetsky, M.R., Treat, C.C., Vonk, J.E., 2015. Climate change and the permafrost carbon feedback. Nature 520, 171–179, http://dx.doi.org/10.1038/nature14338.
Schwalm, M., Zeitz, J., 2014. Dissolved organic carbon concentrations vary with season and land use – investigations from two fens in Northeastern Germany over two years. Biogeosci. Discuss. 11, 7079–7111, http://dx.doi.org/10.5194/bgd-11-7079-2014.
Smith, P., Fang, C., 2010. Carbon cylce: a warm response by soils. Nature 464, 24–25.
Sonnentag, O., Van Der Kamp, G., Barr, A.G., Chen, J.M., 2010. On the relationship between water table depth and water vapor and carbon dioxide fluxes in a minerotrophic fen. Glob. Change Biol. 16, 1762–1776, http://dx.doi.org/10.1111/j.1365-2486.2009.02032.x.
Sottocornola, M., Kiely, G., 2010. Hydro-meteorological controls on the CO_2 exchange variation in an Irish blanket bog. Agric. For. Meteorol. 150, 287–297, http://dx.doi.org/10.1016/j.agrformet.2009.11.013.
Steger, C., Kotlarski, S., Jonas, T., Schär, C., 2012. Alpine snow cover in a changing climate: a regional climate model perspective. Clim. Dyn. 41, 735–754, http://dx.doi.org/10.1007/s00382-012-1545-3.
Stine, M.B., Resler, L.M., Campbell, J.B., 2011. Ecotone characteristics of a southern Appalachian Mountain wetland. Catena 86, 57–65, http://dx.doi.org/10.1016/j.catena.2011.02.006.
Tokida, T., Miyazaki, T., Mizoguchi, M., Nagata, O., Takakai, F., Kagemoto, A., Hatano, R., 2007. Falling atmospheric pressure as a trigger for methane ebullition from peatland. Global Biogeochem. Cycles 21, http://dx.doi.org/10.1029/2006GB002790.
Turetsky, M.R., Kotowska, A., Bubier, J., Dise, N.B., Crill, P., Hornibrook, E.R.C., Minkkinen, K., Moore, T.R., Myers-Smith, I.H., Nykänen, H., Olefeldt, D., Rinne, J., Saarnio, S., Shurpali, N., Tuittila, E.-S., Waddington, J.M., White, J.R., Wickland, K.P., Wilmking, M., 2014. A synthesis of methane emissions from 71 northern, temperate, and subtropical wetlands. Glob. Change Biol. 20, 2183–2197, http://dx.doi.org/10.1111/gcb.12580.
Van Den Pol-Van Dasselaar, A., Van Beusichem, M.L., Oenema, O., 1999. Methane emissions from wet grasslands on peat soil in a nature preserve. Biogeochemistry 44, 205–220, http://dx.doi.org/10.1007/BF00992979.
Van Der Knaap, W.O., Lamentowicz, M., Van Leeuwen, J.F.N., Hangartner, S., Leuenberger, M., Mauquoy, D., Goslar, T., Mitchell, E.A.D., Lamentowicz, Ł., Kamenik, C., Lamentowicz, T., Kamenik, C., 2011. A multi-proxy, high-resolution record of peatland development and its drivers during the last millennium from the subalpine Swiss Alps. Quat. Sci. Rev. 30, 3467–3480, http://dx.doi.org/10.1016/j.quascirev.2011.06.017.
Vanselow-Algan, M., Schmidt, S.R., Greven, M., Fiencke, C., Kutzbach, L., Pfeiffer, E.-M., 2015. High methane emissions dominated annual greenhouse gas balances 30 years after bog rewetting. Biogeosciences 12, 4361–4371, http://dx.doi.org/10.5194/bg-12-4361-2015.
Wagner, D., Kobabe, S., Pfeiffer, E.-M., Hubberten, H.-W., 2003. Microbial controls on methane fluxes from a polygonal tundra of the Lena Delta. Siberia. Permafr. Periglac. Process. 14, 173–185, http://dx.doi.org/10.1002/ppp.443.
Wang, J.M., Murphy, J.G., Geddes, J.A., Winsborough, C.L., Basiliko, N., Thomas, S.C., 2013. Methane fluxes measured by eddy covariance and static chamber techniques at a temperate forest in central Ontario, Canada. Biogeosciences 10, 4371–4382, http://dx.doi.org/10.5194/bg-10-4371-2013.
Wheeler, B.D., Proctor, M.C.F., 2000. Ecological gradients, subdivisions and terminology of north-west European mires. J. Ecol. 88, 187–203, http://dx.doi.org/10.1046/j.1365-2745.2000.00455.x.

Wu, J., Roulet, N.T., Sagerfors, J., Nilsson, M., 2013. Simulation of six years of carbon fluxes for a sedge-dominated oligotrophic minerogenic peatland in Northern Sweden using the McGill Wetland Model (MWM). J. Geophys. Res. Biogeosci. 118, 795–807, http://dx.doi.org/10.1002/jgrg.20045.

Yu, Z., Loisel, J., Brosseau, D.P., Beilman, D.W., Hunt, S.J., 2010. Global peatland dynamics since the Last Glacial Maximum. Geophys. Res. Lett. 37, http://dx.doi.org/10.1029/2010GL043584.

Zanella, A., Tomasi, M., De Siena, C., Frizzera, L., Jabiol, B., Nicolini, G., 2001. Humus Forestali—manuale de ecologia per il riconoscimento e l'interpretazione. Centro di Ecologia Alpina, Trento.

Zeileis, A., Grothendieck, G., 2005. Zoo: S3 infrastructure for regular and irregular time series. J. Stat. Softw. 14, 1–27.

Ecological Informatics 40 (2017) 35–39

Contents lists available at ScienceDirect

Ecological Informatics

journal homepage: www.elsevier.com/locate/ecolinf

The NUCOMBog R package for simulating vegetation, water, carbon and nitrogen dynamics in peatlands

J.W.M. Pullens[a,b,*], M. Bagnara[c], R. Silveyra González[c], D. Gianelle[a,d], M. Sottocornola[e], M.M.P.D. Heijmans[f], G. Kiely[b], F. Hartig[g]

[a] Department of Sustainable Agro-ecosystems and Bioresources, Research and Innovation Centre, Fondazione Edmund Mach (FEM), Via E. Mach 1, 38010 San Michele all'Adige, Trento, Italy
[b] Hydromet, Department of Civil and Environmental Engineering and Environmental Research Institute, University College Cork, Cork, Ireland
[c] Department of Biometry and Environmental System Analysis, University of Freiburg, Freiburg, Germany
[d] Foxlab Joint CNR-FEM Initiative, Via E. Mach 1, 38010 San Michele all'Adige, Trento, Italy
[e] Department of Science, Waterford Institute of Technology, Waterford, Ireland
[f] Plant Ecology and Nature Conservation Group, Wageningen University & Research, Wageningen, The Netherlands
[g] Theoretical Ecology, Faculty of Biology and Pre-Clinical Medicine, University of Regensburg, Universitätsstraße 3, 93053 Regensburg, Germany

ARTICLE INFO

Keywords:
Competition
Net ecosystem exchange
NUCOMBOG
Peatland
R package
Vegetation

ABSTRACT

Since peatlands store up to 30% of the global soil organic carbon, it is important to understand how these ecosystems will react to a change in climate and management. Process-based ecosystem models have emerged as important tools for predicting long-term peatland dynamics, but their application is often challenging because they require programming skills. In this paper, we present NUCOMBog, an R package of the NUCOM-Bog model (Heijmans et al. 2008), which simulates the vegetation, carbon, nitrogen and water dynamics of peatlands in monthly time steps. The package complements the model with appropriate functions, such as the calculation of net ecosystem exchange, as well as parallel functionality. As a result, the NUCOMBog R package provides a user-friendly tool for simulating vegetation and biogeochemical cycles/fluxes in peatlands over years/decades, under different management strategies and climate change scenarios, with the option to use all the in-built model analysis capabilities of R, such as plotting, sensitivity analysis or optimization.

1. Introduction

Peatlands play an important role in the carbon cycle of the Earth. Although they cover only about 3% of the terrestrial global surface, they have stored up to 455–600 Petagrams (Pg, 10^{15} g) carbon during the postglacial period (Gorham, 1991; Yu, 2012; Yu et al., 2010), equivalent to about 30% of the global soil organic carbon (Gorham, 1991). Peatland soils consist of dead organic matter, which is decomposed slowly due to the permanently water saturated soil. The presence of *Sphagnum* mosses makes the decomposition rates even lower due to their high recalcitrance to decomposition. Pristine peatlands commonly act as carbon sinks (e.g. Humphreys et al., 2014; Lund et al., 2010; McVeigh et al., 2014), while peatlands disturbed by human activities (e.g. such as peat harvesting) are mostly acting as carbon sources (e.g. Harpenslager et al., 2015; Hendriks et al., 2007; Moreno-Mateos et al., 2015; Pullens et al., 2016). A major concern is that the immense soil carbon pool of peatlands is vulnerable to climate change, in particular to changes in precipitation, water table depth and temperature (Frolking et al., 2011; van der Kolk et al., 2016). Changes in precipitation regimes would likely have an effect on the plant species composition through changes in the water table depth (Dieleman et al., 2015; Sottocornola et al., 2009). Peatlands located in regions with a maritime climate are also threatened by invasions of shrubs and trees (Heijmans et al., 2013; Holmgren et al., 2015; Stine et al., 2011), which could potentially reverse their carbon footprint from a sink to a source (Bond-Lamberty and Thomson, 2010; Dorrepaal et al., 2009; Frolking et al., 2011), resulting in a positive climate feedback. It is therefore vital to understand how the stored carbon in peatlands will respond to changes in climate and management.

The reaction of peatlands to climate change is a slow process (years/decades to centruries, Frolking et al., 2010), with complex interactions between different vegetation communities. The most widely used tool to understand these interactions and simulate the future of both the stored carbon and the vegetation are process-based models.

The application of these models, however, is often challenging for new users because they require specialized input formats and program-

* Corresponding author at: Fondazione Edmund Mach, Sustainable Agro-ecosystems and Bioresources, Via Mach 1, 38010 San Michele All'Adige, Trento, Italy.
E-mail address: johannes.pullens@fmach.it (J.W.M. Pullens).

http://dx.doi.org/10.1016/j.ecoinf.2017.05.001
Received 10 August 2016; Received in revised form 4 May 2017; Accepted 6 May 2017
Available online 15 May 2017
1574-9541/

ming knowledge when tasks such as sensitivity analyses or parameter calibrations are needed. It would therefore be an advantage to have ecosystem models available in established environments for scientific computing, such as R or Python. In this paper, we describe the new NUCOMBog R package, which provides a user-friendly interface to the NUCOM-Bog ecosystem model, which simulates the dynamics of vegetation, carbon, nitrogen and water in peatlands.

2. Model description

The NUCOM-Bog model (NUtrient cycling and COmpetition Model (Berendse, 1988, Heijmans et al., 2008, 2013, van Oene et al., 1999)), written in Delphi, simulates the carbon and nitrogen dynamics of five plant functional types (PFTs): graminoids, ericaceous shrubs and three groups of *Sphagnum* mosses (lawn, hollow and hummock mosses) in monthly time steps. The model simulates an area of one square meter with a flat moss surface. A schematic representation of the model is depicted in Fig. 2. The model can be used to simulate the current state of the peatland and to assess the effects of climate change (e.g. temperature increase, changes in precipitation regime), or other global changes such as increasing atmospheric CO_2 levels and nitrogen deposition, as well as local nitrogen fertilization or different re-vegetation regimes, which can aid the design of management strategies.

Changes in vegetation composition are driven by competition for light and nitrogen among the five PFTs. Light is first available to the taller graminoids, then to the dwarf shrubs and finally to the mosses. For each time step (one month), NUCOMBog calculates the potential growth rate of each plant functional type (G_{pot}) based on the amount of intercepted light (*LI*), maximum growth rate (G_{max}), the CO_2 concentration in the atmosphere, air temperature (*temp*) and water table depth (WTD) according to

$$G_{pot} = LI^{*}G_{max}{}^{*} f\,(\mathrm{CO_2})^{*} f\,(temp)^{*} f\,(\mathrm{WTD}). \quad (1)$$

Each plant functional type has its own optimal range for temperature and water level depth. The model calculates the WTD based on precipitation, potential evapotranspiration (according to Penman, 1946) and drainage. The drainage in the model calculation considers surface run-off and lateral outflow through the living moss layer (Heijmans et al., 2008).

The only nutrient limiting growth of the plants in the model is nitrogen. When not enough nitrogen is available, the calculated potential growth rate (G_{pot}) for each PFT is reduced. The incoming nitrogen from wet and dry atmospheric depositions is first made available to the mosses (Heijmans et al., 2002). The remaining nitrogen leaches into the soil, where it becomes available for the ericaceous shrubs with their shallow roots (Fig. 1). Deeper in the soil the nitrogen is available for the roots of the graminoids. Apart from light and nitrogen, the growth rate of each PFT depends on its optimal temperature and WTD range. For the carbon balance, plant growth (net primary production) and decomposition of soil organic matter (heterotrophic respiration) are simulated for each PFT. A detailed description of the model is provided in Heijmans et al. (2008).

Dead organic matter (DOM), which is critical for the development of peatlands, follows the same route to deeper soil layers as nitrogen: fresh DOM is first incorporated in the moss layer, before it enters the top soil (acrotelm). In the acrotelm the water table fluctuates, which results in both anaerobic and aerobic decomposition taking place. Below the acrotelm is the permanent waterlogged soil (catotelm), where decomposition rates are lower due to the lack of oxygen (Fig. 1). In the model, the boundary between acrotelm and catotelm is defined as the yearly deepest mean WTD, calculated over the previous 10 years. The change of soil depth of the acrotelm and the catotelm is calculated from the incoming DOM and decomposition in the respective layer.

The model assumes that all PFTs are present at any time, with a minimum cover of 0.1%. Thus, PFTs can always grow once their growing conditions are suitable (these assumptions correspond to a

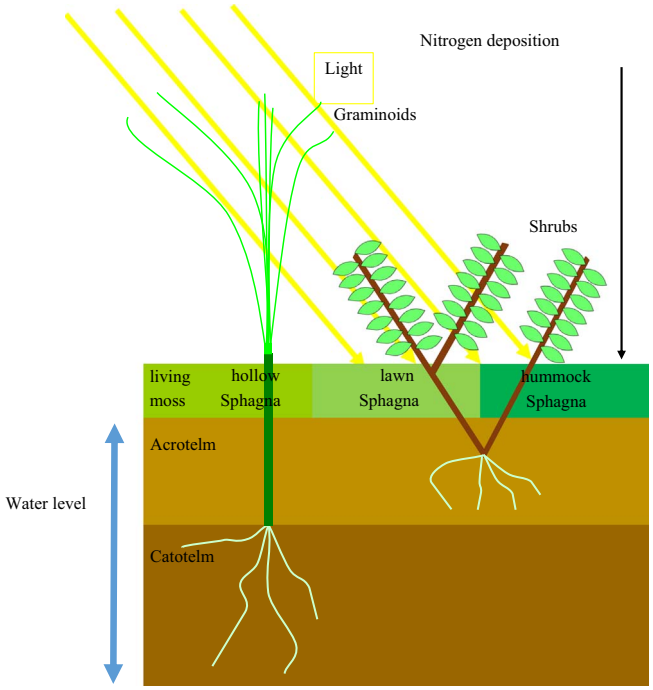

Fig. 1. Schematic representation of NUCOM-Bog. (Adapted from Heijmans et al., 2008)

permanent seed bank). While the plant community develops, the original NUCOM-Bog model (Heijmans et al., 2008) calculates the monthly net primary production (NPP). For this package, NUCOM-Bog has been modified in such a way that it also returns the monthly heterotrophic respiration. In this way, the net ecosystem exchange (NEE) can be calculated:

$$\mathrm{NEE} = -(\mathrm{NPP} - \text{heterotrophic respiration}) \quad (2)$$

The NUCOMBog R package follows the micro-meteorological sign convention, i.e. a negative NEE is a carbon uptake for the ecosystem. All fluxes are in grams of carbon per square meter per month ($g\ C\ m^{-2}\ month^{-1}$).

NUCOMBog has been validated with paleo-ecological data, which showed that the model was able to simulate vegetation composition changes in response to climatic changes in the Little Ice Age (Heijmans et al., 2008). In addition, simulated year-to-year variations in water table position and the response of mosses and vascular plants to these changes compared well with observations (Heijmans et al., 2013).

3. R package

The NUCOMBog R package provides an interface to the statistical programing language R (R Core Team, 2017), which is available under the terms of the Free Software Foundation's GNU General Public License in source code form for Windows, MacOS and Linux. The NUCOMBog package is available on the Comprehensive R Archive Network (CRAN) and was first released in April 2016. The R package relies on an external executable, which is freely available at: https://github.com/jeroenpullens/NUCOMBog as model source code, as well as a precompiled executable. To run the model in R, the user first has to provide the bulk density and the initial biomass values per PFT separated into grams of carbon and nitrogen per plant tissue (shoot/leaf, stem and root), soil carbon and nitrogen content and the bulk density of the acrotelm and catotelm, as well as environmental and climatic data (Fig. 2). The environmental data consists of the annual atmospheric CO_2 concentration in parts per million (ppm) and the sum of both wet and dry annual nitrogen deposition in kg N per hectare ($kg\ N\ ha^{-1}\ yr^{-1}$). The climatic data consists of monthly air tempera-

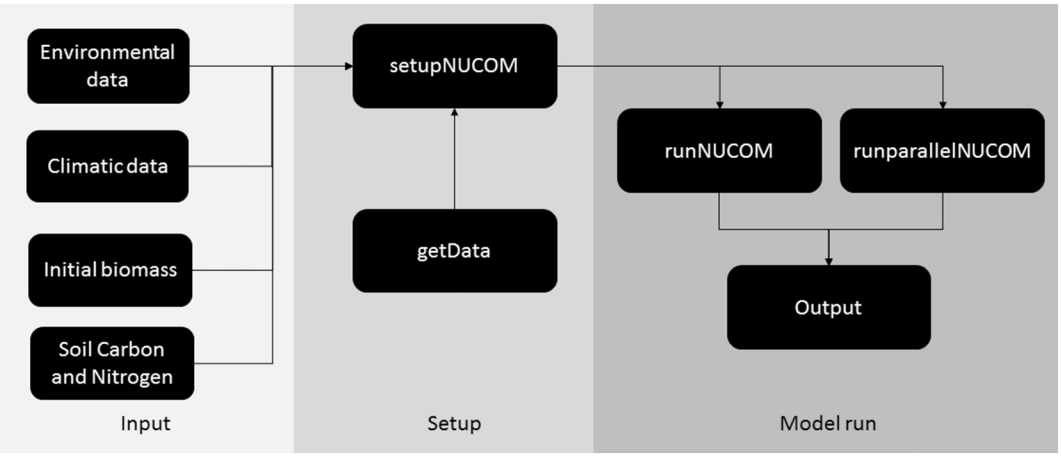

Fig. 2. Schematic representation of the workflow of the R package NUCOMBog.

ture (°C), precipitation (mm), and the calculated Penman potential evapotranspiration (mm, Penman, 1946). The R package also includes some test data (data from Heijmans et al., 2008), that needs to be copied into a user defined folder prior to use. The function *copytestdata* allows the user to copy the data and test the model.

To initialize a model run, the function *setupNUCOM* is called. The user must specify the file paths of the input data as well as the output directory (Fig. 2). In addition, the starting and end year of the simulation need to be specified. The model simulates full years, starting in January and ending in December. When not all the initial biomass values are available (e.g. root biomass is unavailable because destructive measurement are not allowed on site), the user can decide to perform a spin-up run to reach a stable equilibrium (so-called "steady state"). When the data from the spin-up is not needed for subsequent analysis, the parameter "*Startval*" in the function *setupNUCOM* can be used. The "*Startval*" value should be set to the number of months used for the spin-up, and the function *getData* will only load the requested data into the R environment.

The *setupNUCOM* function also allows specifying the output variables; the function *getData* is implemented to retrieve the desired output variables and for the period requested. While the NUCOMBog model returns net primary production (NPP), the R package NUCOMBog also returns the monthly heterotrophic respiration (R_h). From these two values the net ecosystem exchange (NEE) is calculated, so that the model outputs can be compared to sites where carbon fluxes are measured by eddy covariance towers or flux chambers. The model also predicts the water table depth (m), where positive values indicate water table depths below ground surface. The output is directly loaded in R via the function *getData*, so it can be used for further analyses. A schematic representation of the workflow of the R package is depicted in Fig. 2.

The model can be run with either the default parameter values from Heijmans et al. (2008), or user-defined parameters, via the *runNUCOM* function. Parameter values not provided by the user are automatically set to their default values. To facilitate the swift calculation of a large number of model evaluations, for example for sensitivity analysis or model calibration, the package provides support for parallel runs on multiple processors via the *runparallelNUCOM* function. The *runparallelNUCOM* function will run the model for a list of parameter combinations, and save the outputs in separate folders. These functionalities, together with the integration of the model in R, open the possibility to use the model together with one of the many algorithms for model calibration and analysis that are implemented in R, for example sensitivity analysis (Saltelli et al., 2000), parameter calibration via optimization, and Bayesian inference (Hartig et al., 2012). The possibility to make use of such sophisticated algorithms will help to improve the model, and identify gaps in the present knowledge about the functioning of peatlands in general and specifically under stress of climate change or management regimes.

4. Case study: Walton Moss, England

As a case study, we show a simulation with NUCOMBog for historic data from the Walton Moss site in England (Heijmans et al., 2008). The data for this simulation is included in the test data of the NUCOMBog R package. To run the simulations, first the data is copied from the R package to a user-defined folder.

```
copytestdata(new_folder = "/home/jeroen/test_data/")
```

After this step, the executable of the model is copied into the folder. The folder structure has to be kept intact. When the executable is copied, the model can be run by using the following commands.

```
test_setup_singlecore <- setupNUCOM(mainDir = "/home/jeroen/test_data/",
    climate = "ClimWLMhis.txt", environment = "EnvWLMhis.txt",
    inival = "inivalWLMhis.txt", start = 1766, end = 1999, type = c("NEE",
        "WTD", "NPP", "hetero_resp"), parallel = F)
output <- runNUCOM(setup = test_setup_singlecore, parameters = NULL)
```

This command runs the model with the input data from 1766 to 1999, and requests the outputs NEE, WTD, NPP and heterotrophic respiration. Outputs are stored in the variable "output", which can subsequently be used for further analysis in R, for example to produce figures (Fig. 3), compare model outputs to data, perform sensitivity analysis and parameter calibration (for which several packages already exist within the R environment).

5. Conclusion

Some of the most important uses of models are to correctly represent physical processes, to predict the future and to understand

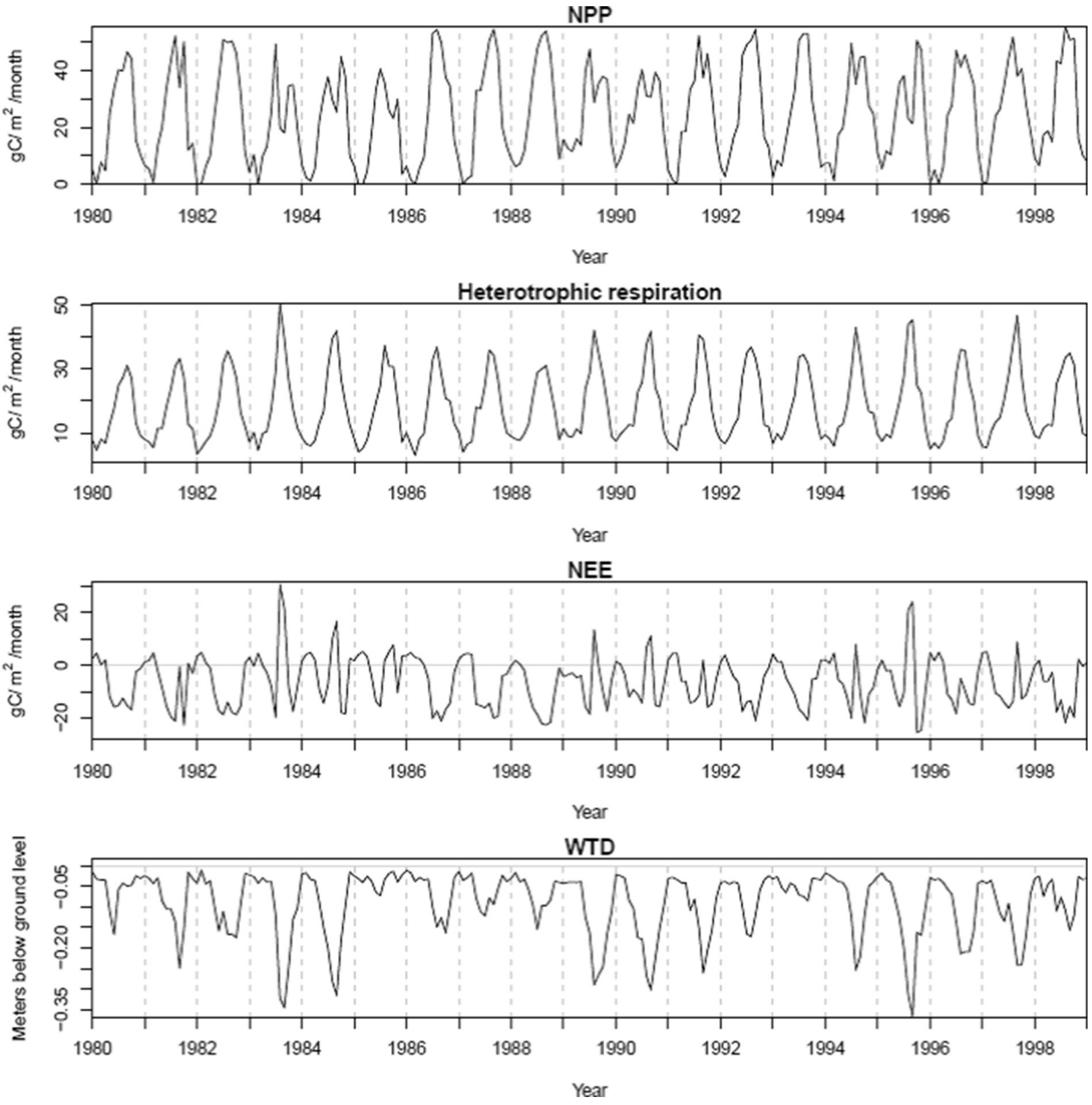

Fig. 3. Simulated monthly NPP, NEE, heterotrophic respiration and WTD from 1980 until 1999 for Walton Moss, England.

the past. With the presented NUCOMBog R package, the vegetation, carbon and water balance of peatlands can be easily simulated from within the R environment. The ease of running the model, together with various options of analysis, provides many possibilities for investigating the stability of peatland vegetation, as well as facilitate its use for educational purposes.

The addition of heterotrophic respiration and net ecosystem exchange as outputs provides better possibilities to investigate processes in peatlands that are equipped with eddy covariance towers, or where flux chamber measurements are being taken. In particular, when data over many years are available, the model outputs could be evaluated against the measured data. The possibility to perform sensitivity analysis and model calibration can give precious insights on the relative importance and uncertainty of parameters, which will in turn lead to a better understanding of the ecosystem functioning. Because the package allows running the model in parallel, the computational time of such tasks is significantly reduced.

In conclusion, the integration of NUCOMBog into the R environment streamlines the process of model application and opens up many new options of model analysis. We hope that these possibilities will eventually lead to new insights about peatland dynamics, thus making NUCOMBog an even more valuable tool to investigate the vegetation, carbon, nitrogen and water dynamics of peatlands over time and to identify possible threats for the modelled peatlands.

Author contributions

JWMP, DG, MB, FH, MS and GK designed the research; JWMP, MB and FH performed the research; MB, FH, MMPDH and RSG contributed with model coding and gave conceptual advice; JWMP wrote the paper. All authors discussed the results and implications and commented on the manuscript at all stages.

Data accessibility

The NUCOMBOG R package is available on the Comprehensive R Archive Network (CRAN), test data is incorporated in the package and the source code of the executable and the executable of the model are

available on GitHub (https://github.com/jeroenpullens/NUCOMBog). All functions in the NUCOMBog R package have documented help files and more information about running the package is provided in the vignette of the package.

Acknowledgements

The authors would like to thank Alessio Gianelle for his help with the Delphi code.

This work was supported by a STSM grant to JWMP from COST Action FP1304 (profound, http://cost-profound.eu/site/). MB acknowledges funding by the DFG Priority Program 1374 “Infrastructure-Biodiversity-Exploratories” (ref. no. DO 786/8-1).

References

Berendse, F., 1988. Een simulatiemodel als hulpmiddel bij het beheer van vochtige heidevelden. CABO, Wageningen, NL (In Dutch), Wageningen.

Bond-Lamberty, B., Thomson, A., 2010. Temperature-associated increases in the global soil respiration record. Nature 464, 579–582.

Dieleman, C.M., Branfireun, B.A., McLaughlin, J.W., Lindo, Z., 2015. Climate change drives a shift in peatland ecosystem plant community: implications for ecosystem function and stability. Glob. Chang. Biol. 21, 388–395.

Dorrepaal, E., Toet, S., van Logtestijn, R.S.P., Swart, E., van de Weg, M.J., Callaghan, T.V., Aerts, R., 2009. Carbon respiration from subsurface peat accelerated by climate warming in the subarctic. Nature 460, 616–619.

Frolking, S., Rotman, D., Tuittila, E., Bubier, J.L., Quillet, A., Talbot, J., Richard, P.J.H., 2010. A new model of Holocene peatland net primary production, decomposition, water balance, and peat accumulation. Earth Syst. Dynam. 1, 1–21.

Frolking, S., Talbot, J., Jones, M.C., Treat, C.C., Kauffman, J.B., Tuittila, E., Roulet, N.T., 2011. Peatlands in the Earth's 21st century climate system. Environ. Rev. 19, 371–396.

Gorham, E., 1991. Northern Peatlands: role in the carbon cycle and probable responses to climatic warming. Ecol. Appl. 1, 182–195.

Harpenslager, S.F., van Dijk, G., Kosten, S., Roelofs, J.G.M., Smolders, A.J.P., Lamers, L.P.M., 2015. Simultaneous high C fixation and high C emissions in *Sphagnum* mires. Biogeosciences 12, 4739–4749.

Hartig, F., Dyke, J., Hickler, T., Higgins, S.I., O'Hara, R.B., Scheiter, S., Huth, A., 2012. Connecting dynamic vegetation models to data - an inverse perspective. J. Biogeogr. 39, 2240–2252.

Heijmans, M.M.P.D., Klees, H., De Visser, W., Berendse, F., 2002. Response of a Sphagnum bog plant community to elevated CO_2 and N supply. Plant Ecol. 162, 123–134.

Heijmans, M.M.P.D., Mauquoy, D., Van Geel, B., Berendse, F., 2008. Long-term effects of climate change on vegetation and carbon dynamics in peat bogs. J. Veg. Sci. 19, 307–320.

Heijmans, M.M.P.D., van der Knaap, Y.A.M., Holmgren, M., Limpens, J., 2013. Persistent versus transient tree encroachment of temperate peat bogs: effects of climate warming and drought events. Glob. Chang. Biol. 19, 2240–2250.

Hendriks, D.M.D., van Huissteden, J., Dolman, A.J., van der Molen, M.K., 2007. The full greenhouse gas balance of an abandoned peat meadow. Biogeosciences 4, 411–424.

Holmgren, M., Lin, C.-Y., Murillo, J.E., Nieuwenhuis, A., Penninkhof, J., Sanders, N., van Bart, T., van Veen, H., Vasander, H., Vollebregt, M.E., Limpens, J., 2015. Positive shrub-tree interactions facilitate woody encroachment in boreal peatlands. J. Ecol. 103, 58–66.

Humphreys, E.R., Charron, C., Brown, M., Jones, R., 2014. Two bogs in the Canadian Hudson Bay lowlands and a temperate bog reveal similar annual net ecosystem exchange of CO_2. Arct. Antarct. Alp. Res. 46, 103–113.

van der Kolk, H.-J., Heijmans, M.M.P.D., van Huissteden, J., Pullens, J.W.M., Berendse, F., 2016. Simulating the effects of temperature and precipitation change on vegetation composition in Arctic tundra ecosystems. Biogeosci. Discuss. 1–32.

Lund, M., Lafleur, P.M., Roulet, N.T., Lindroth, A., Christensen, T.R., Aurela, M., Chojnicki, B.H., Flanagan, L.B., Humphreys, E.R., Laurila, T., Oechel, W.C., Olejnik, J., Rinne, J., Schubert, P., Nilsson, M., 2010. Variability in exchange of CO_2 across 12 northern peatland and tundra sites. Glob. Chang. Biol. 16, 2436–2448.

McVeigh, P., Sottocornola, M., Foley, N., Leahy, P., Kiely, G., 2014. Meteorological and functional response partitioning to explain interannual variability of CO_2 exchange at an Irish Atlantic blanket bog. Agric. For. Meteorol. 194, 8–19.

Moreno-Mateos, D., Meli, P., Vara-Rodríguez, M.I., Aronson, J., 2015. Ecosystem response to interventions: lessons from restored and created wetland ecosystems. J. Appl. Ecol. 52, 1528–1537.

van Oene, H., Berendse, F., de Kovel, C., 1999. Model analyses of the effects of the historic CO_2 levels and nitrogen inputs on vegetation succession. Ecol. Appl. 9, 920–935.

Penman, H.L., 1946. Natural evaporation from open water, bare soil and grass. Proc. R. Soc. Lond. A Math. Phys. Sci. 193, 120–145.

Pullens, J.W.M., Sottocornola, M., Kiely, G., Toscano, P., Gianelle, D., 2016. Carbon fluxes of an alpine peatland in northern Italy. Agric. For. Meteorol. 220, 69–82.

R Core Team, 2017. R: A Language and Environment for Statistical Computing. R Foundation for Statistical Computing, Vienna, Austria.

Saltelli, A., Chan, K., Scott, E.M., 2000. Sensitivity Analysis, first ed. Wiley, New York.

Sottocornola, M., Laine, A., Kiely, G., Byrne, K.a., Tuittila, E., 2009. Vegetation and environmental variation in an Atlantic blanket bog in South-western Ireland. Plant Ecol. 203, 69–81.

Stine, M.B., Resler, L.M., Campbell, J.B., 2011. Ecotone characteristics of a southern Appalachian Mountain wetland. Catena 86, 57–65.

Yu, Z.C., 2012. Northern peatland carbon stocks and dynamics: a review. Biogeosciences 9, 4071–4085.

Yu, Z., Loisel, J., Brosseau, D.P., Beilman, D.W., Hunt, S.J., 2010. Global peatland dynamics since the Last Glacial Maximum. Geophys. Res. Lett. 37.

Biogeosciences, 13, 6229–6245, 2016
www.biogeosciences.net/13/6229/2016/
doi:10.5194/bg-13-6229-2016

Biogeosciences Open Access EGU

Potential Arctic tundra vegetation shifts in response to changing temperature, precipitation and permafrost thaw

Henk-Jan van der Kolk[1], Monique M. P. D. Heijmans[1], Jacobus van Huissteden[2], Jeroen W. M. Pullens[1,3,4], and Frank Berendse[1]

[1]Plant Ecology and Nature Conservation Group, Wageningen University & Research, Wageningen, the Netherlands
[2]Earth and Climate Cluster, Vrije Universiteit Amsterdam, Amsterdam, the Netherlands
[3]Sustainable Ecosystems and Bioresources Department, Research and Innovation Centre, Fondazione Edmund Mach, San Michele all'Adige, Italy
[4]Hydromet, Department of Civil and Environmental Engineering and Environmental Research Institute, University College Cork, Cork, Ireland

Correspondence to: Monique M. P. D. Heijmans (monique.heijmans@wur.nl)

Received: 16 March 2016 – Published in Biogeosciences Discuss.: 21 March 2016
Revised: 3 October 2016 – Accepted: 27 October 2016 – Published: 18 November 2016

Abstract. Over the past decades, vegetation and climate have changed significantly in the Arctic. Deciduous shrub cover is often assumed to expand in tundra landscapes, but more frequent abrupt permafrost thaw resulting in formation of thaw ponds could lead to vegetation shifts towards graminoid-dominated wetland. Which factors drive vegetation changes in the tundra ecosystem are still not sufficiently clear. In this study, the dynamic tundra vegetation model, NUCOM-tundra (NUtrient and COMpetition), was used to evaluate the consequences of climate change scenarios of warming and increasing precipitation for future tundra vegetation change. The model includes three plant functional types (moss, graminoids and shrubs), carbon and nitrogen cycling, water and permafrost dynamics and a simple thaw pond module. Climate scenario simulations were performed for 16 combinations of temperature and precipitation increases in five vegetation types representing a gradient from dry shrub-dominated to moist mixed and wet graminoid-dominated sites. Vegetation composition dynamics in currently mixed vegetation sites were dependent on both temperature and precipitation changes, with warming favouring shrub dominance and increased precipitation favouring graminoid abundance. Climate change simulations based on greenhouse gas emission scenarios in which temperature and precipitation increases were combined showed increases in biomass of both graminoids and shrubs, with graminoids increasing in abundance. The simulations suggest that shrub growth can be limited by very wet soil conditions and low nutrient supply, whereas graminoids have the advantage of being able to grow in a wide range of soil moisture conditions and have access to nutrients in deeper soil layers. Abrupt permafrost thaw initiating thaw pond formation led to complete domination of graminoids. However, due to increased drainage, shrubs could profit from such changes in adjacent areas. Both climate and thaw pond formation simulations suggest that a wetter tundra can be responsible for local shrub decline instead of shrub expansion.

1 Introduction

Tundra ecosystems in the Arctic are shaped by strong interactions between biological, hydrological and climatological factors (Hinzman et al., 2005). An important feature of the Arctic ecosystem is permafrost, which is the soil that is persistently frozen for at least two years. For the near future, global climate models project a further increase in temperature and precipitation, with pronounced changes in the Arctic region (Johannessen et al., 2004; Vavrus et al., 2012; IPCC, 2014). Rising temperatures potentially result in increased seasonal thawing of the permafrost, and thus in an increased thickness of the active layer (the soil layer that thaws during the growing season) and drawback of near surface permafrost (Anisimov et al., 1997; Lawrence and Slater, 2005; Zhang et

al., 2005). Given the large soil organic carbon stocks in permafrost (Zimov et al., 2006a; Tarnocai et al., 2009), there is a major concern that these stocks get decomposed and subsequently released as CO_2 and CH_4 to the atmosphere (Dutta et al., 2006; McGuire et al., 2009). An increase in greenhouse gas release, including CO_2 and CH_4 (Christensen et al., 2004; Walter et al., 2006; Nauta et al., 2015; Schuur et al., 2015), from thawing permafrost could stimulate further warming and result in a positive feedback loop between temperature increase and greenhouse gas emission (Zimov et al., 2006b; Schuur et al., 2008; MacDougall et al., 2012; van Huissteden and Dolman, 2012; Schuur et al., 2015).

Climate change in the Arctic region affects tundra vegetation composition. The northernmost tundra is dominated by mosses and lichens due to the extremely low summer temperatures. Southwards, with increasing summer temperatures, graminoids and dwarf shrubs increase in abundance (Walker et al., 2005). Climate change influences the tundra vegetation in multiple ways. Warming experiments in tundra ecosystems showed an increase in graminoids and deciduous shrubs in response to raised temperatures, while mosses and lichens and the overall species diversity decreased (Walker et al., 2006). Shrubs have been observed to expand with ongoing temperature increase, presumably due to the increased availability of nutrients in the warmer soil (Tape et al., 2006; Myers-Smith et al., 2011). Several tree and shrub species, including dwarf birches (*Betula glandulosa* and *Betula nana*), willows (*Salix* spp.), juniper (*Juniperus nana*) and green alder (*Alnus viridis*), have expanded and increased in abundance in the Arctic as a response to climatic warming (Sturm et al., 2001; Tape et al., 2006; Hallinger et al., 2010; Elmendorf et al., 2012). However, besides climate, other factors such as herbivory, soil moisture and soil nutrient availability affect shrub growth as well, and it is therefore complex predicting the expansion of shrubs in the Arctic region (Myers-Smith et al., 2011, 2015). Increased abundance of shrubs might have important consequences for permafrost feedbacks. For example, an increase in low shrubs might slow down permafrost thaw as a result of the shadow they cast on the soil (Blok et al., 2010). However, tall shrubs may increase atmospheric heating and permafrost thawing due to their lower albedo (Bonfils et al., 2012)

Another mechanism by which climate change affects tundra vegetation is abrupt thaw resulting in local collapse of the permafrost. Thawing of underground ice masses results in a collapse of the ground, by which water-filled thermokarst ponds are formed. These ponds are first colonised by sedges and later by mosses (Jorgenson et al., 2006). Due to thaw pond formation, changes in northern permafrost landscapes from dry birch forests or shrub-dominated vegetation towards ponds or wetlands dominated by graminoids may occur with climatic change in both discontinuous and continuous permafrost regions (Jorgenson et al., 2001, 2006; Turetsky et al., 2002; Christensen et al., 2004; Nauta et al., 2015). In the continuous permafrost region, permafrost collapse can change the vegetation from shrub-dominated towards a wet graminoid-dominated stage within less than one decade. The thermokarst ponds might stimulate further soil collapse and as a consequence drastically alter hydrological and soil processes, as well as in adjacent areas (Osterkamp et al., 2009; Nauta et al., 2015; Schuur et al., 2015).

The factors that drive the observed tundra vegetation composition changes, especially shrub expansion, and their consequences are not yet well understood. Increased air temperatures lead to higher soil temperatures, especially in the shallow layers, and may thus promote microbial activity, thereby increasing nutrient availability in the soil. In tundra vegetation, shrubs are hypothesised to be best able to respond to such increased nutrient availability (Tape et al., 2006). It is, however, not known to what extent this and other shrub growth factors, including precipitation, growing season length and disturbances (Myers-Smith et al., 2011), will affect the competition between different plant functional types in the Arctic. As shrub expansion has important implications for land surface albedo and consequently climate feedbacks (Chapin et al., 2005; Pearson et al., 2013), it is crucial that we understand and are able to predict further vegetation change in the tundra.

One approach to better understand the interactions between plants in tundra landscapes is to use a dynamic vegetation model to analyse developments in vegetation composition in response to climatic changes. Tundra vegetation models that aim to predict the impacts of climate change on vegetation–substrate interactions should at least include the most important plant functional types, competition and permafrost feedbacks. Although several tundra vegetation models exist, these models do not take into account hydrological feedbacks, the formation of thaw ponds and vegetation–permafrost feedbacks or do not include mosses as separate plant functional type (e.g. Epstein et al., 2000; Wolf et al., 2008; Euskirchen et al., 2009). Therefore, in this study, the effects of climate change, including both temperature and precipitation change, on plant competition and vegetation composition were studied by developing a new model named NUCOM-tundra, based on earlier NUCOM (NUtrient and COMpetition) models for other ecosystems (Berendse, 1994a, b; van Oene et al., 1999; Heijmans et al., 2008, 2013). The new tundra vegetation model includes mosses, graminoids, dwarf shrubs, hydrological and soil processes, and permafrost dynamics. In this study, we simulated tundra vegetation changes under different climate change scenarios in order to (1) analyse the effects of future temperature and precipitation scenarios on tundra vegetation composition, and (2) explore the impacts of thaw pond formation due to local permafrost collapse.

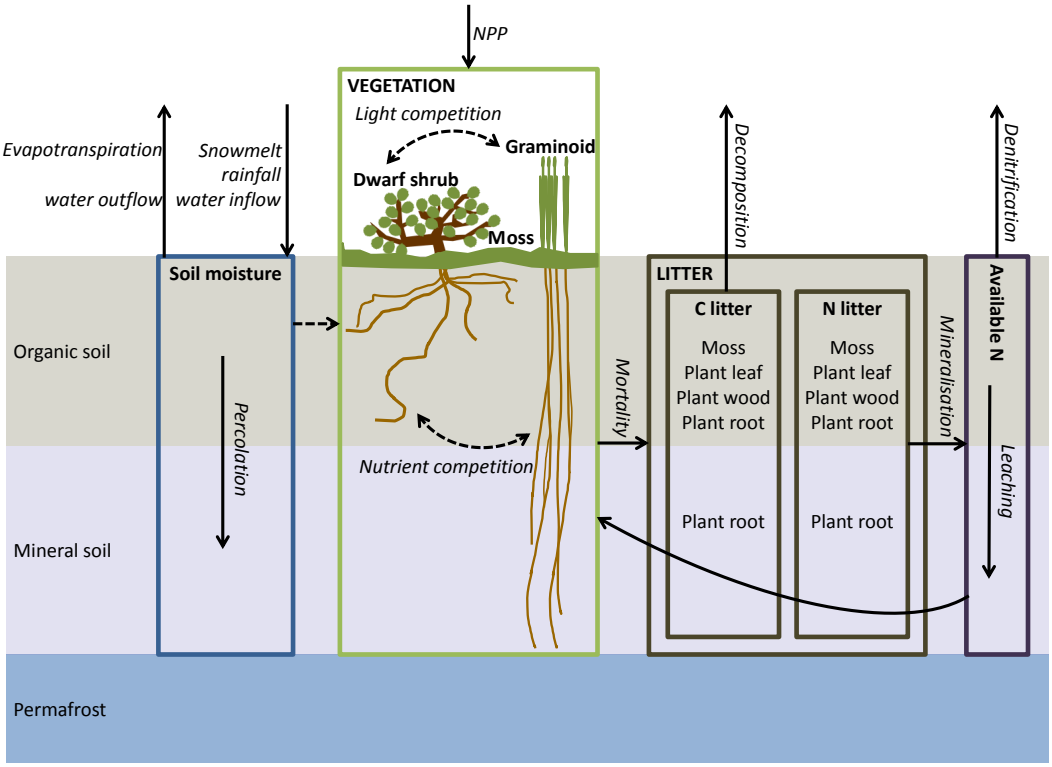

Figure 1. Schematic presentation of NUCOM-tundra, including the main processes simulated in organic and mineral soil layers and the effects of moisture and available nitrogen on vegetation. Air temperature influences many of these processes, including active layer depth, plant growth, evapotranspiration, snowmelt, decomposition, mineralisation and denitrification. The mineral soil is divided into 10 layers, each 10 cm in height.

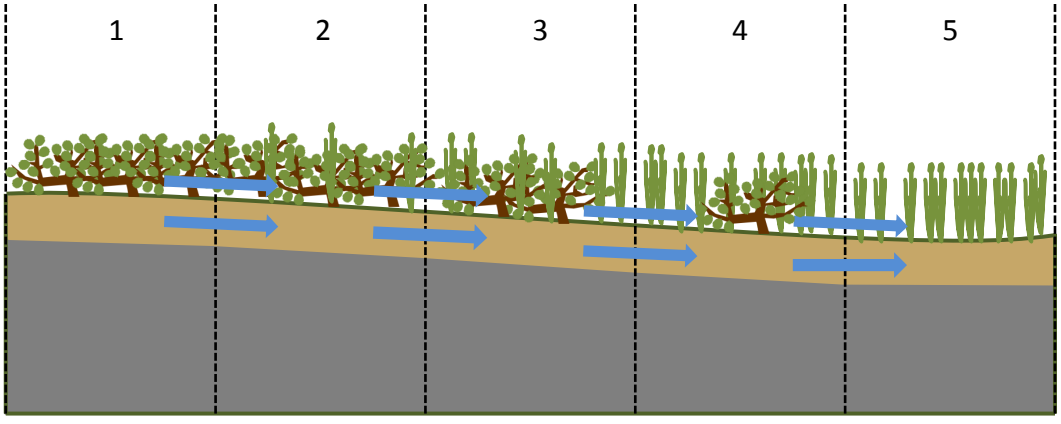

Figure 2. Vegetation types used in simulations of NUCOM-tundra. The vegetation types represent landscape positions, ranging from relatively dry shrub-dominated (1) to wet graminoid-dominated (5) vegetation. Blue arrows indicate water flows.

2 Methods

2.1 Brief model description

NUCOM-tundra has been developed to simulate long-term dynamics of vegetation composition in tundra landscapes for analysis of vegetation–permafrost–carbon feedbacks in relation to climate change and includes nitrogen and carbon cycling, permafrost and water dynamics (Fig. 1). An extensive model description and all equations are provided in the Supplement, Sect. S1.

NUCOM-tundra simulates the dynamics of three plant functional types (PFTs), moss, graminoids (e.g. *Eriophorum vaginatum*) and deciduous dwarf shrubs (e.g. *Betula nana*),

on a local scale and in the decadal timescale using a daily time step. NUCOM-tundra represents tundra landscapes, which are an alternation of shrub-dominated, graminoid-dominated and mixed vegetation types. The model is based on an area of 1 m^2. The biomass and nitrogen content of the vascular PFTs is separated into fine roots, woody plant parts (for shrubs) or rhizomes (for graminoids), and leaves. Mosses form a layer on top of the soil surface, with a thickness up to 4.5 cm. The soil profile is divided into an organic top soil layer with a variable height and 10 deeper mineral soil layers each with a thickness of 10 cm. The fine roots of vascular plants are distributed throughout the active soil profile, with graminoids rooting deeper in comparison to dwarf shrubs (Shaver and Cutler, 1979; Nadelhoffer et al., 1996; Iversen et al., 2015). The thickness of the active layer depends on the soil temperature profile (Sect. S1). The thickness of the organic layer, which consists solely of moss, leaf, stem and root litter, generally increases over time, depending on the balance between litter input and litter decomposition. The mineral soil layers contain initial soil organic carbon and nitrogen pools as well. During the simulations, only fine root litter is added to the mineral soil layers and decomposed there. The other litter types become part of the soil organic layer. Decomposition rates depend on soil temperature and differ among PFTs and plant organs (leaves, stems and fine roots).

Plant growth (net primary production) is determined by temperature, light availability, nutrient availability and moisture conditions (Sect. S1). In the model, there are temperature thresholds for plant growth thus excluding growth during the winter season. Graminoids and dwarf shrubs compete for the incoming light based on their leaf area. It is assumed that graminoids and dwarf shrubs are equally tall. The moisture content in the upper 10 cm of the soil can strongly reduce PFT growth as both graminoids and dwarf shrubs have an optimum growth only in part of the range of possible soil moisture conditions. Dwarf shrubs prefer drier conditions, and cannot grow if the soil is completely water-saturated. The graminoids in the model do not grow well under dry conditions, but can grow on water-saturated soils.

Mosses acquire nitrogen by nitrogen fixation from the atmosphere and can absorb available nitrogen from the upper centimetre of the soil profile. Vascular plant nitrogen uptake is determined by the fine root length of both graminoids and dwarf shrubs present in each layer and the amount of nutrients available. At the start of the growing season, when the air temperature is above the threshold for growth but the soil is still mostly frozen, the plants can use nitrogen from an internal storage, which is filled by reallocated nitrogen from senescing leaves and roots. Dying plant material enters the soil organic carbon and nitrogen litter pools. Soil organic carbon is lost by microbial decomposition, whereas the mineralised nitrogen from soil organic nitrogen becomes available for plant uptake. The rate of decomposition and nitrogen mineralisation depends on soil temperature. Part of the pool of available nitrogen can be lost by denitrification under high soil moisture conditions (Sect. S1).

A simple hydrological module is included in NUCOM-tundra, which simulates the volumetric water content of the organic and mineral soil layers (Sect. S1). Water from snowmelt, rainfall and inflow from a neighbouring vegetation type (Fig. 2) fills up the pore space in the soil layers. Evapotranspiration, surface runoff, and lateral drainage out of the moss and organic layer lower the water content. The lateral drainage includes transport of dissolved nitrogen. The hydrological processes follow a seasonal pattern. A snow layer accumulates during the winter season, and snowmelt occurs with positive air temperatures at the start of the growing season. During this period, the shallow active layer becomes water-saturated and the excess of water runs off over the soil surface. During the growing season, evapotranspiration generally exceeds precipitation, resulting in gradual drying of the soil.

2.2 Parameter values and model input

Parameter values for plant properties such as root characteristics, mortality, reallocation and decomposition have been derived from literature or have been calibrated using field data collected at the Chokurdakh Scientific Tundra Station, located 70°49′ N, 147°29′ E; altitude 10 m (Sect. S2). The Chokurdakh Scientific Tundra Station, also known as Kytalyk field station, is located in the lowlands of the Indigirka River, north-eastern Siberia, which is in the continuous permafrost zone and the Low Arctic climate zone. The vegetation is classified as tussock-sedge, dwarf-shrub moss tundra (vegetation type G4 on the Circumpolar Arctic Vegetation Map; Walker et al., 2005). The parameter values are provided in Appendix A.

NUCOM-tundra requires daily temperature and precipitation data as input for the model simulations. Weather data from Chokurdakh weather station (WMO station 21946, located 70°62′ N, 147°88′ E; altitude 44 m) for the years 1954 to 1994 obtained through the KNMI climate explorer tool (Klein Tank et al., 2002, http://climexp.knmi.nl) were input to the model. Initial values of the model simulations are provided in Sect. S3. The biomass start values were based on field measurements at the Chokurdakh Scientific Tundra Station.

2.3 Vegetation types

We defined five initial vegetation types representing a gradient from relatively dry to wet sites for the climate change simulations in NUCOM-tundra. These initial vegetation types represent five landscape positions, ranging from relatively well-drained shrub patches to waterlogged graminoid-dominated wetland (Fig. 2). The first vegetation type represents dry shrub-dominated vegetation. Vegetation types 2, 3 and 4 represent moist mixed vegetation from

relatively dry to wet sites. Vegetation type 5 represents a wet graminoid-dominated vegetation downslope which receives water from the neighbouring cell. In vegetation type 1, only outflow of both surface water and water in the organic layer occur, whereas moist sites are characterised by having both water inflow and water outflow. The water flow into a downslope landscape position is the actual water outflow from the adjacent upslope located simulation cell. This water movement over the gradient includes transport of dissolved nitrogen from the elevated shrub patch to the sedge-dominated depression.

2.4 Comparison with field data

The performance of several model parts was evaluated by comparing outputs with data from the Kytalyk field station and Chokurdakh weather station. The simulated timing of snow accumulation and snowmelt was compared with snow height data from the Chokurdakh weather station between 1944 and 2008. Time series of soil temperature at different depths and measurements of thawing depth were used to evaluate the soil temperature calculations. Furthermore, simulated PFT total biomass, biomass partitioning among leaves, woody parts, rhizomes and fine roots, and vertical root distribution were compared with field data. Field biomass collections were done for both graminoids and dwarf shrubs in graminoid-dominated, mixed and dwarf shrub-dominated vegetation sites at the tundra field site in north-eastern Siberia (Wang et al., 2016). Roots were collected over different depths, enabling the comparison of field data with simulated root distribution over depth. These field data were compared with simulations that were run with climate input from the Chokurdakh weather station. A detailed description of these comparisons of simulated and field data is provided in Sect. S4.

2.5 Climate scenario simulations

For all vegetation types, a period of 40 years was simulated to initialise the model using precipitation and temperature data from the Chokurdakh weather station from 1 August 1954 to 31 July 1994 as input. This period excludes the most pronounced warming that took place over the last few decades. Annual precipitation was, however, variable with both increasing and declining trends in the 40-year time period (Sect. S2). After the initialisation phase, 16 different climate change scenarios were run for all five vegetation types for the period 1 August 1994–31 July 2074. Inspired by the RCP emission scenarios over the 21st century, we combined four temperature increases with four precipitation increases to simulate climatic changes over this 80-year period. The combinations include temperature increases of 0, 2.5, 5 or 8 °C and precipitation changes of 0, 15, 30 or 45 % increase over 100 years. In the Arctic region, increases of 2.5 °C and 15 % precipitation are expected under emission scenario

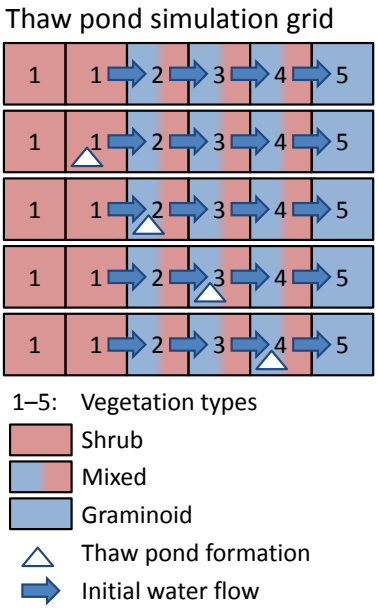

Figure 3. Simulation grid used to simulate thaw pond initiation in the vegetation types 1–4. Water flows at the start of the simulation are as indicated in the diagram. After the local permafrost collapse, the water flow from the cell with the thaw pond formation to the following downslope cell is stopped (see Fig. 8 for the consequences).

RCP2.6 and increases of 8 °C and 45 % precipitation are expected over the 21st century under emission scenario RCP8.5 (IPCC, 2014). A scenario with 5 °C increase and 30 % precipitation increase is regarded here as an "Intermediate" scenario.

The weather data series over the period 1 August 1954–31 July 1994 from the Chokurdakh weather station was used twice to create a baseline ("No change") for the climate scenario simulations between 1994 and 2074. For all climate change scenarios, temperature and precipitation were gradually increased over this 80-year simulation period. For precipitation, only the intensity of rainfall was increased and not the number of days at which rainfall occurred.

To evaluate the effects of climate change on the vegetation composition, we compared the biomass of moss, graminoids and dwarf shrubs on 31 July, averaged over the last 10 years of the simulation (corresponding with 2065–2074). Furthermore, several factors that influenced plant growth and competition were evaluated using the simulations for moist mixed vegetation sites (vegetation type 3) in which all three PFTs co-occur. The following factors were evaluated for the last 10 years of the simulations:

1. Growing season length is the average number of days per year at which the temperature threshold for vascular plant growth was exceeded.

2. Soil moisture is the average soil moisture content in the upper 10 cm of the soil profile during the growing season.

3. Light competition is the average percentage of light intercepted by graminoids and shrubs during the growing season.

4. Moisture conditions are the percentage of time in the growing season with optimal soil moisture content for growth of graminoids and dwarf shrubs.

5. Nutrient limitation is the limitation of the growth of graminoids and dwarf shrubs due to insufficient availability of nutrients in the growing season, expressed as the percentage of potential growth realised.

2.6 Thaw pond simulations

Thaw pond initiation was simulated for dry and moist vegetation types (1–4) under three different climate change scenarios: "No change", RCP2.6 and RCP8.5. Thaw pond collapse was simulated by imposing a sudden alternation of water flows. Upon a collapse event, water inflow, including surface runoff and lateral drainage through the soil organic layer, doubled whereas water outflow stopped. To evaluate the effects of thaw pond collapse on downslope vegetation sites, simulations were performed in series that included all five vegetation types (Fig. 3). Thaw pond formation was initiated at a fixed time step halfway through the simulation (corresponding to 31 July 2034). The change in vegetation composition after collapse was evaluated by determining the abundance of graminoids (in %) in the vascular plant community biomass in the last 10 summers of the simulation (31 July in the years 2065–2074), when the vegetation is at its peak biomass.

3 Results

3.1 Comparison with field data

Simulated snow height, soil temperature, active layer thickness, total PFT biomass, biomass partitioning and vertical root distribution were compared with observations from Chokurdakh Scientific Tundra Station or weather station (detailed description in Sect. S4). Simulated timing of accumulation and melt of the snow layer between 1944 and 2008 was in agreement with observations of snow depth at the Chokurdakh weather station. Simulated shallow soil temperatures were in agreement with observations from the Kytalyk meteorological tower, but simulated deep soil temperatures were higher than observed, resulting in simulated thawing depths that were on average 14 cm higher than observed thawing depths (Fig. S4.2). This deeper active layer thickness resulted in an overestimation of graminoid biomass, as was

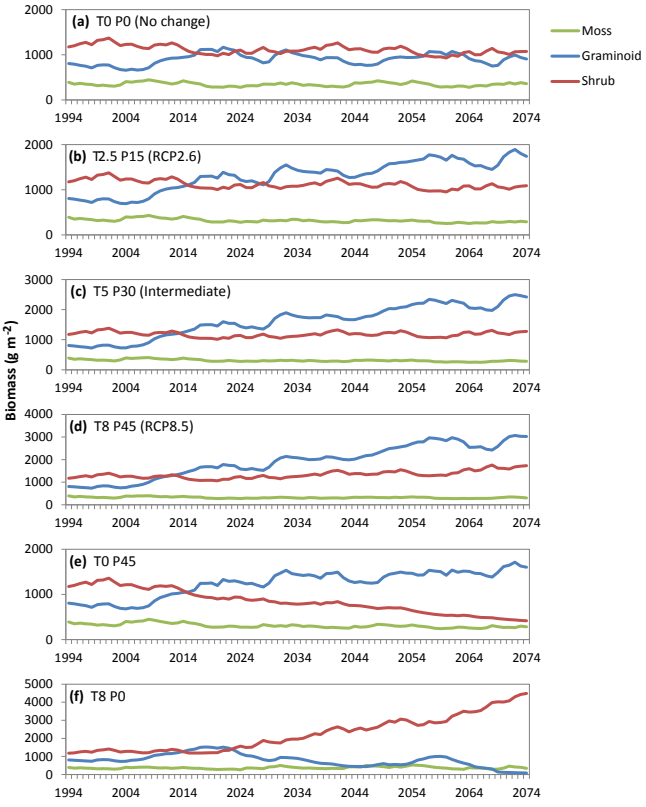

Figure 4. Simulated summer biomass of moss, graminoids and dwarf shrubs between 1994 and 2074 under different temperature (T, °C increase) and precipitation (P, % increase) change scenarios over the 21st century.

demonstrated by simulations with lowered active layer thickness (Fig. S4.3 in the Supplement). However, the patterns of changing graminoid biomass among the main climate change scenarios remained when the active layer thickness was lowered, indicating that the uncertainty about the simulated deep soil temperatures did not significantly affect the vegetation composition changes for the climate change scenario simulations.

NUCOM-tundra simulated total biomass for graminoids and dwarf shrubs within the range of biomass values obtained for shrub, mixed and graminoid vegetation types at the field site. Simulated biomass partitioning over leaves, stems and fine roots was comparable to the partitioning observed in the field with high total biomass, although the simulated biomass partitioning was rather constant and did not change with increasing total biomass, as observed in the field. Fine root vertical distribution patterns were similar between observed and simulated data as NUCOM-tundra took into account the different rooting patterns of graminoids and dwarf shrubs, and variations in active layer thickness.

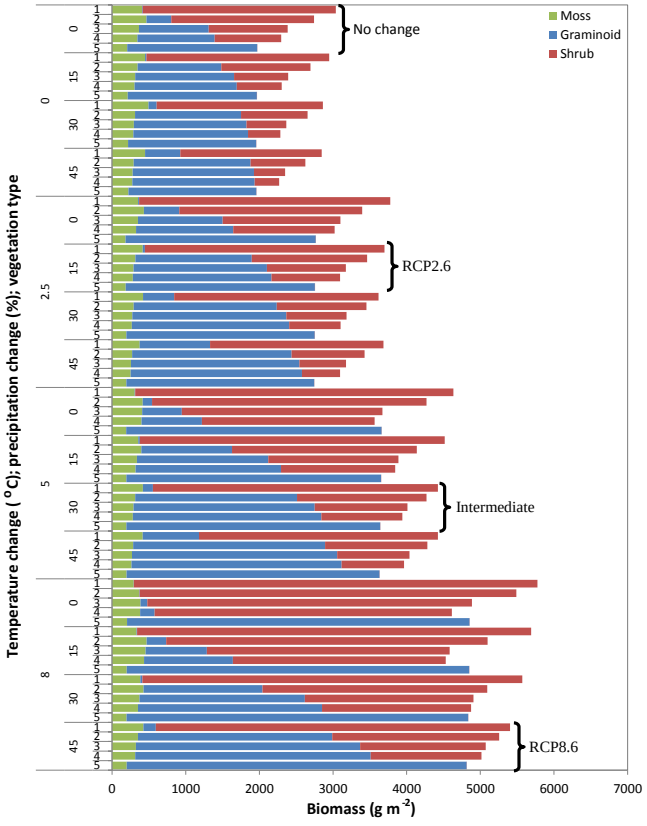

Figure 5. Simulated summer biomass of moss, graminoids and shrubs averaged over 2065–2074 for 16 climate scenario simulations in five vegetation types representing a gradient from relatively dry to wet conditions. Temperature and precipitation changes were based on 21st century RCP climate change scenarios. Biomass is total biomass (above and belowground).

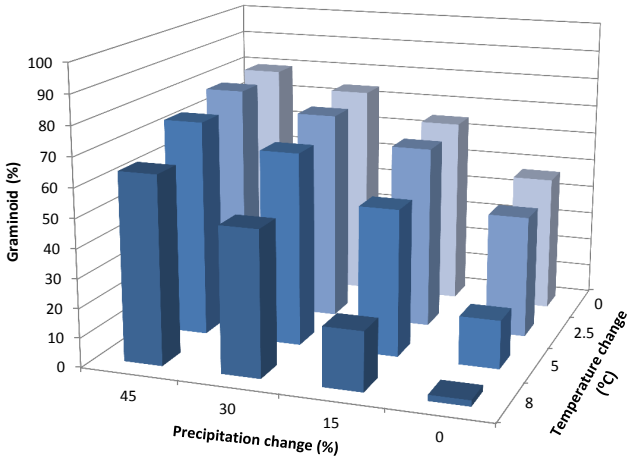

Figure 6. Percentage of graminoid biomass in the vascular plant community biomass, averaged over 2065–2074, for vegetation type 3 (initial moist mixed vegetation) for 16 temperature and precipitation scenarios in the 21st century.

3.2 Climate scenario simulations: vegetation changes

In the "No change" scenario, the total vegetation biomass was rather stable throughout the simulation in all vegetation types (Fig. 4a for vegetation type 3, data not shown for other vegetation types). Gradual biomass increases between 1994 and 2074 were simulated under the three climate change scenarios based on the RCP scenarios (Fig. 4b–d). Considering all combinations of temperature and precipitation scenarios in all vegetation types, simulated total biomass of the vegetation responded strongly to increased temperature (Fig. 5). The average total (aboveground and belowground) summer biomass between 2065 and 2074 ranged from 1970 to 3037 g m^{-2} with no temperature change, whereas total biomass ranged between 4815 and 5402 g m^{-2} with a gradual increase of 8 °C over the 21st century. In contrast, precipitation change did not affect the total vegetation biomass.

The vegetation composition in relatively well-drained sites dominated by shrub vegetation (type 1) and wet graminoid-dominated vegetation (type 5) did not change under any of the climate change scenarios (Fig. 5). In mixed vegetation (type 3), graminoids increased in abundance with the RCP2.6 scenario (2.5 °C temperature and 15 % precipitation increases over the 21st century), "Intermediate" and RCP8.5 scenario (8 °C temperature and 45 % precipitation increases over the 21st century; Figs. 4b–d, 6). In other climate change scenarios, the magnitude of both precipitation and temperature change determined changes in vegetation composition in currently mixed vegetation sites (Fig. 6). The proportion of graminoids in the vascular plant community increased in simulations with more pronounced precipitation changes and lower temperature changes (Figs. 4e, 6). In contrast, graminoids were outcompeted by shrubs by the end of simulations of initially mixed vegetation sites under a scenario with 8 °C temperature increase but no precipitation change over the 21st century (Fig. 4f).

Simulated moss biomass was in general lowest in wet graminoid-dominated vegetation sites (Fig. 5), and showed little variation among the climate scenario simulations (Figs. 4, 5).

3.3 Nutrient availability, light competition and moisture conditions

In comparison to the "No change" scenario, the growing season was on average 39 days longer in the years 2065–2074 in simulations with an 8 °C temperature increase scenario (Table 1). During the same time period, the averaged soil moisture at mixed vegetation sites was higher in simulations with more pronounced precipitation change and lower temperature changes (Table 1). Consequently, soil moisture conditions became more favourable for graminoids under these scenarios, whereas moisture conditions became more favourable for shrubs with large changes in temperature and small changes in precipitation. For the RCP2.6, "In-

Table 1. Simulated growth-limiting factors for the vascular PFTs in vegetation type 3 under different climate change scenarios. Growing season length, soil moisture, and light, moisture and nutrient conditions during the growing season were averaged for years 2064–1974.

				Graminoids			Shrubs		
T change[a] (°C)	P change[a] (%)	Growing season length[b] (days)	Soil moisture (vol. %)	Light[c] (%)	Moisture[d] (%)	Nutrients[e] (%)	Light[c] (%)	Moisture[d] (%)	Nutrients[e] (%)
0	0	101	62.1	4.9	78.0	89.3	8.6	49.5	40.2
0	15	101	63.8	7.8	82.5	87.4	4.1	42.7	41.1
0	30	101	64.9	9.3	86.1	86.3	1.7	36.0	41.3
0	45	101	65.7	10.1	87.8	85.4	0.6	32.6	41.6
2.5	0	115	58.3	5.0	66.8	87.1	14.7	63.7	37.4
2.5	15	115	61.5	9.8	73.7	84.0	7.9	49.5	39.1
2.5	30	115	62.9	11.8	77.5	82.3	4.9	45.1	40.0
2.5	45	115	64.0	13.3	81.1	81.1	2.7	39.2	40.6
5	0	128	52.8	0.6	45.7	86.9	25.8	70.7	36.1
5	15	128	58.6	7.7	67.4	83.9	15.6	61.1	36.5
5	30	128	61.3	12.6	73.4	81.1	9.3	49.1	38.1
5	45	128	62.7	14.8	75.1	79.4	6.3	44.7	39.0
8	0	140	45.6	0.0	38.9	89.1	33.7	77.5	36.5
8	15	140	53.2	1.4	47.0	86.0	28.0	69.5	35.8
8	30	140	58.3	8.7	66.5	82.8	18.9	60.7	36.0
8	45	140	60.9	13.7	72.3	80.1	12.9	49.3	37.3

[a] Temperature (T) and precipitation (P) change scenarios over the 21st century. [b] Growing season length is defined as the number of days with mean temperature above 0 °C. [c] Percentage of incoming light absorbed during the growing season. [d] Percentage of time at which soil moisture conditions were optimal for growth during the growing season (100 % = optimal soil moisture conditions during the whole growing season). [e] Percentage of realised potential growth (100 % = no nutrient limitation).

termediate" and RCP8.5 scenario, moisture conditions became slightly less favourable for graminoid growth and remained unchanged for shrub growth in comparison to the "No change" scenario.

In general, shrubs were able to intercept more light in comparison to graminoids in pronounced climate change scenarios (Table 1). Both graminoids and shrubs intercepted more light when moisture conditions became more favourable. The effect of temperature changes on light interception differed between graminoids and shrubs. Shrubs intercepted more light when temperature changes were more pronounced. Light interception in graminoids, however, decreased under scenarios with 8 °C temperature increase and less pronounced precipitation increase over the 21st century. Nutrients limited shrub growth under all climate scenarios (Table 1). For both graminoids and shrubs, nutrients became less limiting under less suitable growth conditions.

3.4 Thaw pond simulations

All thermokarst events (initiated in 2034) led to the complete domination of graminoids over shrubs within 15 years after initiation of thaw pond development (Figs. 7, 8). The vegetation composition on collapsed sites became similar to the composition on wet graminoid-dominated sites (vegetation type 5). After abrupt permafrost thaw, bryophytes took advantage of the decreased vascular plant leaf area, but stabilised later at a biomass that was equal to the moss biomass in non-collapsed, wet graminoid-dominated vegetation sites (Fig. 8). When a collapse occurred in vegetation type 1, 2 or 3, the collapse enhanced shrub expansion in the next grid cell. The thermokarst pond acted as a water sink due to which water flows into the next grid cell were halted. Consequently, the grid cell adjacent to the thermokarst pond became drier which favoured shrub growth (Fig. 7). Similar patterns for the thaw pond simulations were observed for "No change", RCP2.6 and RCP8.5 climate scenarios.

4 Discussion

The effects of climate change on tundra vegetation are complex since temperature and precipitation drive changes in hydrology, active layer depths, nutrient availability and growing season length, which interact with each other (Serreze et al., 2000; Hinzman et al., 2005). NUCOM-tundra has been developed to explore future changes in the Arctic tundra vegetation composition in response to climate scenarios, thereby taking changes in soil moisture, thawing depth and nutrient availability into account.

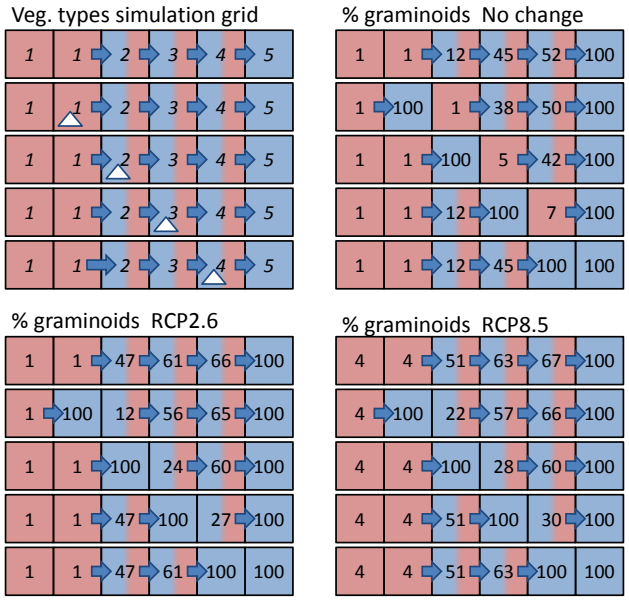

Figure 7. Results of thaw pond simulations: simulation settings (top left panel) in which vegetation types (numbers), initial water flows (arrows) and permafrost collapse sites are indicated. The other grids show the percentage of graminoids in total vascular plant biomass during the summers of 2065–2074 and the altered water flows for "No change", RCP2.6 and RCP8.5 climate scenarios. Red cells: shrub-dominated, blue cells: graminoid-dominated, both blue and red cells: mixed vegetation.

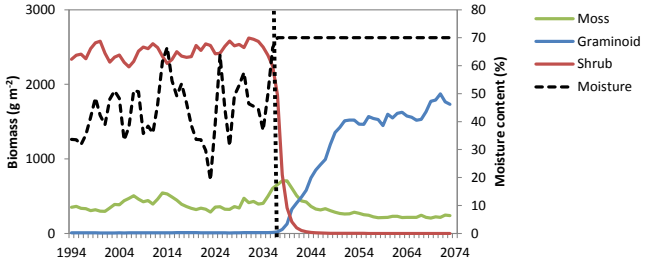

Figure 8. Biomass of moss, graminoids and shrubs and organic layer moisture content during the thaw pond formation simulation in an initially dry shrub-dominated vegetation type (1) under the "No change" scenario. The dotted line indicates the moment of ice wedge collapse.

4.1 Effects of increases in temperature and precipitation

Our climate scenario simulations suggest a significant increase in biomass with continuing climate change, and especially, increased graminoid abundance under scenarios with different magnitudes of climate change. For modest and strong emission scenarios ("Intermediate" and RCP8.5), both shrub and graminoid biomass increased. These simulations are in line with biomass increases in both shrubs and graminoids that have been observed during the past decades in Arctic tundra landscapes as a response to temperature increase (Dormann and Woodin, 2002; Walker et al., 2006; Hudson and Henry, 2009). Shrub expansion has been observed in many places in the Arctic (Sturm et al., 2001; Tape et al., 2006; Myers-Smith et al., 2011), but is not explicitly simulated by NUCOM-tundra for the RCP-based climate change scenarios which combine temperature and precipitation increases.

As nutrient availability limits plant growth in tundra landscapes (Shaver et al., 2001), a positive effect of warming on nutrient availability is a likely explanation for biomass increase observed in tundra vegetation (Hudson and Henry, 2009). Climate warming might influence nutrient availability positively by lengthening of the growing season, active layer deepening and increased microbial activity. In our simulations, nutrients were especially limiting for the shrubs, likely due to their shallow rooting systems. Compared to shrubs, graminoids root relatively deeply (Wang et al., 2016). As a consequence, active layer deepening is expected to favour, especially, graminoids. It is, however, unclear how plant root morphology responds to climate warming. An experimental warming study in dry tundra demonstrated that plants do not necessarily root deeper in response to warmer temperatures, but instead may concentrate their main root biomass in the organic layer where most nutrient mineralisation takes place (Björk et al., 2007). Nevertheless, it is likely that growing season lengthening and increased microbial mineralisation of soil organic matter improve growing conditions for both shrubs and graminoids, as also graminoids have been shown to respond strongly upon fertilisation (e.g. Jonasson, 1992).

Strikingly, the climate simulations in this study show that shifts in vegetation composition are not only dependent on temperature change, but are strongly affected by precipitation changes as well. Simulated soil moisture contents decreased with higher temperature and lower precipitation scenarios. Evapotranspiration is an important hydrological process determining soil moisture during the growing season. Throughout the growing season, the top soil layer dries out as evapotranspiration exceeds precipitation during this period, which is in agreement with observations at our study site (Sect. S2). Higher summer temperatures increase potential evapotranspiration, and thus lead to drier soils, if precipitation remains unchanged. Consequently, the area of relatively dry sites characterised by dense dwarf shrub vegetation might increase. A similar imbalance of temperature and precipitation change between 1950 and 2002 has been proposed by Riordan et al. (2006) as one of the possible causes for drying of thermokarst ponds in Alaska. A second mechanism for tundra drying with higher temperatures is increased water drainage enabled by gradual deepening of the active layer or permafrost degradation. The latter mechanism is especially important in the discontinuous permafrost zone, where climate change may cause loss of permafrost at thermokarst sites and subsequently lead to increased drainage to adjacent areas (Yoshikawa and Hinzman, 2003).

Whereas NUCOM-tundra predicts that graminoids especially benefit under the main climate change scenarios, other Arctic vegetation models mainly simulate shrub expansion (e.g. Epstein et al., 2000; Euskirchen et al., 2009; Yu et al., 2011). As moisture conditions did not differ much between the combined climate change scenarios (Table 1), the relatively large increase in graminoids in those scenarios is likely enabled by active layer deepening. Nutrients that become available in deeper soil layers are easily accessible by graminoids which are able to root throughout the whole active layer, whereas shrubs rely on the nutrient availability in the top soil layers as their root system is confined to that region. It is important to note that NUCOM-tundra currently uses a simple soil temperature soil module which calculates soil temperature based on air temperature (Sect. S1.3.4). Especially for deeper soil layers, this module lacks accuracy in precisely predicting changes in active layer thickness for different temperature change scenarios, which results in uncertainty in both the depth of the active layer and the amount of nutrients that becomes available. These processes influence graminoid growth more than shrub growth. Coupling NUCOM-tundra to an advanced soil temperature model is needed to simulate the physical soil processes more accurately.

Previously, the effectiveness of shrubs in dealing with increased nutrient levels has been proposed as an explanation for observed shrub expansion in the Arctic (Shaver et al., 2001; Tape et al., 2006). *Betula nana* responds to higher nutrient availability by increasing its biomass, which is mainly due to increased secondary stem growth (Shaver et al., 2001). However, *Betula nana* is also known to respond to increased temperatures and fertilisation by growing taller and by producing more shoots and tillers, thereby increasing its ability to compete for light with other species (Chapin and Shaver, 1996; Hobbie et al., 1999; Bret-Harte et al., 2001; Shaver et al., 2001). In NUCOM-tundra, competition for light or nutrients is determined by a combination of several plant traits (parameters values). For light competition, leaf area and light extinction are important, which are influenced by parameters such as specific leaf area, biomass allocation to leaves, leaf mortality and light extinction coefficient. Similarly, nutrient competition is influenced by parameters such as specific root length, root distribution and nutrient requirements. Although tiller production is not explicitly included in NUCOM-tundra, shrubs had an advantage in the competition for light as they have a higher specific leaf area and higher light extinction coefficient than the graminoids. Yet, this advantage for shrubs was, in the combined climate change scenarios, overruled by the advantageous ability of graminoids to root deep into the mineral soil layers. Based on our observations at our study site in the north-eastern Siberian tundra and at Toolik Lake moist tussock tundra, we assumed the (dwarf) shrubs and graminoids to be equally tall in the model. With warming-induced increases in aboveground biomass for both graminoids and shrubs, the competition for light becomes more important. In parts of the tundra area, shrubs, including *Betula nana*, can grow taller than graminoids. For a wider application of the vegetation model, i.e. to include transitions to tall shrub vegetation, a variable plant height up to a maximum would be required.

Overall, our results from the climate change scenarios mainly highlight the importance of changes in annual precipitation, as they have a large influence on the water table and thus on the tundra vegetation composition. Precipitation, especially in summer, compensates for evapotranspiration water losses, thereby having a direct positive influence on soil moisture and water table position. Climate models predict considerable precipitation increases for the Arctic region (IPCC, 2014) as the retreat of sea ice in the Arctic Ocean results in strongly increased evaporation and precipitation (Bintanja and Selten 2014). In agreement with these predictions, significant increases in precipitation over the last few decades have been demonstrated for several Arctic weather stations (Hinzman et al., 2005; Urban et al., 2014). Changes in precipitation are, however, less consistent in comparison to climate warming (Urban et al., 2014). In Chokurdakh, the location used for the model simulations, precipitation has not increased along with temperature change between 1981 and 2010 (temperature $+0.0565\,^{\circ}\mathrm{C\,yr^{-1}}$; precipitation $-1.127\,\mathrm{mm\,yr^{-1}}$; http://climexp.knmi.nl/atlas; Li et al., 2016). Continuation of the climate trends observed in Chokurdakh between 1981 and 2010 would lead to a scenario that most resembles a temperature increase of 5 °C and no precipitation change by the end of this century. This scenario would imply that currently mixed vegetation will shift towards shrub-dominated vegetation in the near future due to tundra drying.

4.2 Thaw pond formation

Formation and expansion of shrub vegetation might be set back by the degradation and collapse of ice wedges in the permafrost. Even in dry vegetation type simulations, the initiation of thermokarst led, as a result of water accumulation in thaw ponds, to complete replacement of shrubs by graminoids. The simple thaw pond module in NUCOM-tundra simulated a peak of moss biomass shortly after ground collapse and before significant colonisation of graminoids. After the collapse, the shrubs were dying because of the water-saturated soil, while the graminoids had not yet colonised the new thaw pond, and the mosses took advantage of the increased light availability. At the Siberian field site we also observe that mosses mostly drown and the first colonisers of thaw ponds are mostly graminoids, for example *Eriophorum angustifolium* (Jorgenson et al., 2006), although mosses can also be the first colonisers. NUCOM-tundra does not (yet) take surface water depth into account for the calculation of plant and bryophyte growth, due to which drowning of mosses could not be simulated. The model is also not able to simulate further vegetation

succession in thaw ponds. Most likely, after graminoid and moss establishment, an organic layer starts to accumulate, shrubs recolonise the collapsed sites, after which permafrost aggradation can take place. Water runoff out of collapsed sites is expected to increase when the organic layer accumulates, probably aided by newly developing ice structures which lift the surface.

Simulated thermokarst events favoured shrub growth in adjacent grid cells due to increased drainage. Although graminoids become dominant in thaw ponds, ice wedge collapses may provide opportunities for shrub growth on the pond margins due to small-scale changes in water flows. Such a mechanism was observed in Alaska, where shrubs became dominant around thermokarst spots as a result of increased drainage from shrub-dominated patches to the new ponds (Osterkamp et al., 2009). These results further reveal that tundra drying is an important mechanism for shrub expansion in the Arctic. Thermokarst ponds, however, may also act as a heat source and thereby stimulate further permafrost collapse (Li et al., 2014). Overall, permafrost degradation should be recognised as an important, potentially graminoid stimulating factor when studying climate change in Arctic landscapes (Jorgenson et al., 2006). Rapid expansion of shrubs might be partly compensated by the formation of graminoid-dominated thaw ponds, particularly in poorly drained lowland tundra.

The inclusion of thaw pond formation is a new but not yet fully developed element of NUCOM-tundra. There are models that simulate tundra vegetation change (ArcVeg; Epstein et al., 2000; TEM-DVM; Euskirchen et al., 2009; LPJ-Guess; Wolf et al., 2008; Zhang et al., 2013) and models that simulate thaw lake cycle dynamics (van Huissteden et al., 2011). Taking into account the formation of thaw ponds and the subsequent vegetation succession is, however, essential for a full analysis of climate change effects on the tundra ecosystem (Van Huissteden and Dolman, 2012). This model feature should, therefore, receive special attention with further model developments.

5 Data availability

Data are available upon request.

Appendix A: Parameter values in NUCOM-tundra

Table A1. Plant functional type parameter values in NUCOM-tundra.

Parameter	Description	Unit	Moss	Gram.	Shrub	Source
BD_m	bulk density moss	$g\,m^{-3}$	15 660			Heijmans et al. (2004)
maxheight	maximum height of moss layer	m	0.045			Blok et al. (2010)
minheight	minimum height of moss layer	m	0.005			
minleafarea	minimum leaf area	$m^2\,m^{-2}$		0.001	0.001	
Kext	light extinction coefficient	–		0.5	0.6	Heijmans et al. (2008) (Gram.)
SLA	specific leaf area	$m^2\,g^{-1}$		0.0060	0.0139	Shaver and Chapin (1991)
B	rooting depth coefficient	–		0.938	0.850	Murphy et al. (2009) (Gram.); van Wijk (2007) (Shrub)
SRL	specific root length	$m\,g^{-1}$		37.5	141.0	Eissenstat et al. (2000) (Gram.); Pettersson et al. (1993) (Shrub)
Gmax	maximum growth	$g\,m^{-2}\,day^{-1}$	12.0	29.0	32.5	calibrated
seedbiom	daily seed biomass input	$g\,m^{-2}\,day^{-1}$	0.000033	0.000033	0.000033	
w_{min}	minimum volumetric soil water content for growth	%	20	20	0	
w_{low}	lowest volumetric soil water content for optimal growth	%	40	40	10	
w_{high}	highest volumetric soil water content for optimal growth	%	70	70	65	
w_{max}	maximum volumetric soil water content for growth	%	70	70	70	
T_{min}	minimum air T for growth	°C	0	1	1	
T_{low}	lowest air T for optimal growth	°C	3	4	4	
N_{min}	minimum N concentration for growth	$g\,N\,g^{-1}$	0.0102	0.0122	0.0172	Hobbie (1996)
N_{max}	maximum N concentration for N uptake	$g\,N\,g^{-1}$	0.0184	0.0352	0.0278	Hobbie (1996)
Kallor	allocation of growth to fine roots	–		0.30	0.33	calibrated (Gram.); Shaver and Chapin (1991) (Shrub)
Kallos	allocation growth towards stems	–		0.24	0.14	calibrated (Gram.); Shaver and Chapin (1991) (Shrub)
Kallol	allocation growth towards leaves	–		0.46	0.53	calibrated (Gram.); Shaver and Chapin (1991) (Shrub)
Krear	reallocation of N in roots to storage	–		0.30	0.10	Heijmans et al. (2008)
Kreas	reallocation of N in stems to storage	–		0	0	Heijmans et al. (2008)
Kreal	reallocation of N in leaf to storage	–		0.34	0.25	Chapin et al. (1975) (Graminoid)
$mort_{moss}$	mortality moss	day^{-1}	0.000914			Chapin et al. (1996)
$mort_r$	mortality root	day^{-1}		0.000825	0.001015	calibrated
$mort_s$	mortality stems	day^{-1}		0.000232	0.000067	calibrated
$mort_l$	mortality leaf	day^{-1}		0.007315	0.010790	calibrated
$maxmort_s$	maximum mortality stems	day^{-1}		0.002500	0.002500	
kdec_m	decomposition moss litter	day^{-1}	0.001560			Lang et al. (2009)
kdec_r	decomposition root litter	day^{-1}		0.001691	0.000946	Heal and French (1974)
kdec_s	decomposition stems litter	day^{-1}		0.000758	0.001256	Heal and French (1974)
kdec_l	decomposition leaf litter	day^{-1}		0.001564	0.002167	Hobbie and Gough (2004)

Table A2. Parameter values related to the soil profile, microbial processes and hydrology in NUCOM-tundra.

Parameter	Description	Unit	Value	Source
maxlayer	number of mineral layers	–	10	
layerdepth	thickness of mineral layer	m	0.10	
BD_{org}	organic matter density	$g\,m^{-3}$	150 000	Marion and Miller (1982)
Nfixation_m	nitrogen fixation rate (by moss)	$g\,N\,day^{-1}$	0.00025	
Ndeposition	nitrogen deposition rate	$g\,N\,day^{-1}$	0.00027	
NCcrit	critical N : C ratio for mineralisation	$g\,N\,g\,C^{-1}$	0.008	
e^{asseff}	microbial assimilation efficiency	–	0.2	Heijmans et al. (2008)
α	optimal denitrification rate	day^{-1}	0.1	Heinen (2006)
S_{tres}	minimum fraction of water-filled pores for denitrification		0.9	
S_{max}	fraction of water-filled pores for maximum denitrification		1	
Q_{10}	denitrification increase factor with 10 °C increase		2	Heinen (2006)
T_{ref}	reference temperature(for denitrification)	°C	20	Heinen (2006)
DDF	degree day factor for snowmelt	$mm\,°C^{-1}\,day^{-1}$	5.3	Lundberg and Beringer (2005)
$FieldCap_{org}$	volumetric water content at field capacity in organic layer	$mm\,mm^{-1}$	0.36	Zotarelli et al. (2010)
$MaxCap_{org}$	maximum volumetric water content in organic layer (saturation)	$mm\,mm^{-1}$	0.70	
$FieldCap_{min}$	volumetric water content at field capacity in mineral layer	$mm\,mm^{-1}$	0.42	Saxton and Rawls (2006)
$MaxCap_{min}$	maximum volumetric water content in mineral layer (saturation)	$mm\,mm^{-1}$	0.50	Saxton and Rawls (2006)
runoffr	surface water runoff	day^{-1}	0.10	
interflowr	lateral drainage of water through organic layer	day^{-1}	0.01	
evaporation	fraction evaporation of total evapotranspiration	–	0.5	
evapodepth	soil depth over which evaporation occurs	cm	10	
wheight	height of the upper soil layer for moisture calculation	cm	10	
leachr	fixed nitrogen leach rate to deeper soil layer	day^{-1}	0.00163	
$leachr_{max}$	maximum nitrogen leach rate	day^{-1}	0.00747	

The Supplement related to this article is available online at doi:10.5194/bg-13-6229-2016-supplement.

Acknowledgements. We acknowledge financial support from the Netherlands Organisation for Scientific Research (NWO–ALW, VIDI grant 864.09.014) and thank P. Wang and L. Belelli Marchesini for providing dwarf shrub and graminoid vegetation biomass data, and latent heat flux (evapotranspiration) and soil temperature profile data for the Chokurdakh Scientific Tundra Station in north-eastern Siberia. We thank J. L. van de Poel, N. D. Nobel and E. S. Bargeman for their contributions to the initial development of NUCOM-tundra. Furthermore, we thank two anonymous referees for their helpful comments and suggestions.

Edited by: A. Rammig
Reviewed by: two anonymous referees

References

Anisimov, O. A. and Nelson, F. E.: Permafrost zonationa and climate change in the northern hemisphere: results from transient general circulation models, Climatic Change, 35, 241–258, 1997.

Berendse, F.: Litter decomposition – a neglected component of plant fitness, J. Ecol., 82, 187–190, 1994a.

Berendse, F.: Competition between plant populations at low and high nutrient supplies, Oikos, 71, 253–260, 1994b.

Bintanja, R. and Selten, F. M.: Future increases in Arctic precipitation linked to local evaporation and sea-ice retreat, Nature, 509, 479–482, 2014.

Björk, R. G., Majdi, H., Klemedtsson, L., Lewis-Jonsson, L., and Molau, U.: Long-term warming effects on root morphology, root mass distribution, and microbial activity in two dry tundra plant communities in northern Sweden, New Phytol., 176, 862–873, 2007.

Blok, D., Heijmans, M. M. P. D., Schaepman-Strub, G., Kononov, A. V., Maximov, T. C., and Berendse, F.: Shrub expansion may reduce summer permafrost thaw in Siberian tundra, Glob. Change Biol., 16, 1296–1305, 2010.

Bonfils, C. J. W., Phillips, T. J., Lawrence, D. M., Cameron-Smith, P., Riley, W. J., and Subin, Z. M.: On the influence of shrub height and expansion on northern high latitude climate, Environ. Res. Lett., 7, 015503, doi:10.1088/1748-9326/7/1/015503, 2012.

Bret-Harte, M. S., Shaver, G. R., Zoerner, J. P., Johnstone, J. F., Wagner, J. L., Chavez, A. S., Gunkelman IV, R. F., Lippert, S. C., and Laundre, J. A.: Developmental plasticity allows *Betula nana* to dominate tundra subjected to an altered environment, Ecology, 82, 18–32, 2001.

Chapin, F. S., Van Cleve, K., and Tieszen, L. L.: Seasonal nutrient dynamics of tundra vegetation at Barrow, Alaska, Arct. Alp. Res., 7, 209–226, 1975.

Chapin, F. S. and Shaver, G. R.: Physiological and growth responses of arctic plants to a field experiment simulating climatic change, Ecology, 77, 822–840, 1996.

Chapin, F. S., Bret-Harte, M. S., Hobbie, S. E., and Zhong, H.: Plant functional types as predictors of transient responses of arctic vegetation to global change, J. Veg. Sci., 7, 347–358, 1996.

Chapin, F. S., Sturm, M., Serreze, M. C., McFadden, J. P., Key, J. R., Lloyd, A. H., McGuire, A. D., Rupp, T. S., Lynch, A. H., Schimel, J. P., Beringer, J., Chapman, W. L., Epstein, H. E., Euskirchen, E. S., , L. D., Jia, G., Ping, C.-L., Tape, K. D., Thompson, C. D. C., Walker, D. A., and Welker, J. M.: Role of land-surface changes in Arctic summer warming, Science, 310, 657–660, 2005.

Christensen, T. R., Johansson, T., Åkerman, H. J., Mastepanov, M., Malmer, N., Friborg, T., Crill, P., and Svensson, B. H.: Thawing sub-arctic permafrost: Effects on vegetation and methane emissions, Geophys. Res. Lett., 31, L04501, doi:10.1029/2003GL018680, 2004.

Dormann, C. F. and Woodin, S. J.: Climate change in the Arctic: using plant functional types in a meta-analysis of field experiments, Funct. Ecol., 16, 4–17, 2002.

Dutta, K., Schuur, E. A. G., Neff, J. C., and Zimov, S. A.: Potential carbon release from permafrost soils of Northeastern Siberia, Glob. Change Biol., 12, 2336–2351, 2006.

Eissenstat, D. M., Wells, C. E., Yanai, R. D., and Whitbeck, J. L.: Research view: Building roots in a changing environment: Implications for root longevity, New Phytol., 147, 33–42, 2000.

Elmendorf, S. C., Henry, G. H., Hollister, R. D., Björk, R. G., Boulanger-Lapointe, N., Cooper, E. J., Cornelissen, J. H. C., Day, T. A., Dorrepaal, E., Elumeeva, T. G., Gill, M., Gould, W. A., Harte, J., Hik, D. S., Hofgaard, A., Johnson, D. R., Johnstone, J. F., Jónsdóttir, I. S., Jorgenson, J. C., Klanderud, K., Klein, J. A., Koh, S., Kudo, G., Lara, M., Lévesque, E., Magnússon, B., May, J. L., Mercado-Díaz, J. A., Michelsen, A., Molau, U., Myers-Smith, I. H., Oberbauer, S. F., Onipchenko, V. G., Rixen, C., Schmidt, N. M., Shaver, G. R., Spasojevic, M. J., Þórhallsdóttir, Þ. E., Tolvanen, A., Troxler, T., Tweedie, C. E., Villareal, S., Wahren, C., Walker, X., Webber, P. J., Welker, J. M., and Wipf, S.: Plot-scale evidence of tundra vegetation change and links to recent summer warming, Nature Climate Change, 2, 453–457, 2012

Epstein, H. E., Walker, M. D., Chapin, F. S., and Starfield, A. M.: A transient, nutrient-based model of arctic plant community response to climatic warming, Ecol. Appl., 10, 824–841, 2000.

Euskirchen, E. S., McGuire, A. D., Chapin, F. S., Yi, S., and Thompson, C. C.: Changes in vegetation in northern Alaska under scenarios of climate change, 2003–2100: implications for climate feedbacks, Ecol. Appl., 19, 1022–1043, 2009.

Hallinger, M., Manthey, M., and Wilmking, M.: Establishing a missing link: warm summers and winter snow cover promote shrub expansion into alpine tundra in Scandinavia, New Phytol., 186, 890–899, 2010.

Heal, O. W. and French, D. D.: Decomposition of organic matter in tundra. Soil organisms and decomposition in tundra, Tundra Biome Steering Committee, Stockholm, 279–309, 1974.

Heijmans, M. M. P. D., Arp, W. J., and Chapin, F. S.: Carbon dioxide and water vapour exchange from understory species in boreal forest, Agr. Forest Meteorol., 123, 135–147, 2004.

Heijmans, M. M. P. D., Mauquoy, D., van Geel, B., and Berendse, F.: Long-term effects of climate change on vegetation and carbon dynamics in peat bogs, J. Veg. Sci., 19, 307–320, 2008.

Heijmans, M. M. P. D., van der Knaap, Y. A., Holmgren, M., and Limpens, J.: Persistent versus transient tree encroachment of temperate peat bogs: effects of climate warming and drought events, Glob. Change Biol., 19, 2240–2250, 2013.

Heinen, M.: Simplified denitrification models: overview and properties, Geoderma, 133, 444–463, 2006.

Hinzman, L. D., Bettez, N. D., Bolton, W. R., Chapin, F. S., Dyurgerov, M. B., Fastie, C. L., Griffith, B., Hollister, R. D., Hope, A., Huntington, H. P., Jensen, A. M., Jia, G. J., Jorgenson, T., Kane, D. L., Klein, D. R., Kofinas, G., Lynch, A. H., Lloyd, A. H., McGuire, A. D., Nelson, F. E., Nolan, M., Oechel, W. C., Osterkamp, T. E., Racine, C. H., Romanovsky, V. E., Stone, R. S., Stow, D. A., Sturm, M., Tweedie, C. E., Vourlitis, G. L., Walker, M. D., Walker, D. A., Webber, P. J., Welker, J. M., Winker, K. S., and Yoshikawa, K.: Evidence and implications of recent climate change in northern Alaska and other Arctic regions, Climatic Change, 72, 251–298, 2005.

Hobbie, S. E.: Temperature and plant species control over litter decomposition in Alaskan tundra, Ecol. Monogr., 66, 503–522, 1996.

Hobbie, S. E., Shevtsova, A., and Chapin, F. S.: Plant responses to species removal and experimental warming in Alaskan tussock tundra, Oikos, 84, 417–434, 1999.

Hobbie, S. E. and Gough, L.: Litter decomposition in moist acidic and non-acidic tundra with different glacial histories, Oecologia, 140, 113–124, 2004.

Hudson, J. M. and Henry, G. H. R.: Increased plant biomass in a High Arctic heath community from 1981 to 2008, Ecology, 90, 2657–2663, 2009.

IPCC: Climate Change 2014: Synthesis Report, Contribution of Working Groups I, II and III to the Fifth Assessment Report of the Intergovernmental Panel on Climate Change, edited by: Core Writing Team, Pachauri, R. K., and Meyer, L. A., IPCC, Geneva, Switzerland, 151 pp., 2014.

Iversen, C. M., Sloan, V. L., Sullivan, P. F., Euskirchen, E. S., McGuire, A. D., Norby, R. J., Walker, A. P., Warren, J. M., and Wullschleger, S. D.: The unseen iceberg: plant roots in arctic tundra, New Phytol., 205, 34–58, 2015.

Johannessen, O. M., Bengtsson, L., Miles, M. W., Kuzmina, S. I., Semenov, V. A., Alekseev, G. V., Nagurnyi, A. P., Zakharov, V. F., Bobylev, L. P., Pettersson, L. H., Hasselmann, K., and Cattle, H. P.: Arctic climate change: Observed and modelled temperature and sea-ice variability, Tellus A, 56, 328–341, 2004.

Jonasson, S.: Plant responses to fertilization and species removal in tundra related to community structure and clonality, Oikos, 63, 420–429, 1992.

Jorgenson, M. T., Racine, C. H., Walters, J. C., and Osterkamp, T. E.: Permafrost degradation and ecological changes associated with a warming climate in central Alaska, Climatic Change, 48, 551–579, 2001.

Jorgenson, M. T., Shur, Y. L., and Pullman, E. R.: Abrupt increase in permafrost degradation in Arctic Alaska, Geophys. Res. Lett., 33, L02503, doi:10.1029/2005GL024960, 2006.

Klein Tank, A. M. G., Wijngaard, J. B., Können, G. P., Böhm, R., Demarée, G., Gocheva, A., Mileta, M., Pashiardis, S., Hejkrlik, L., Kern-Hansen, C., Heino, R., Bessemoulin, P., Müller- Westermeier, G., Tzanakou, M., Szalai, S., Pálsdóttir, T., Fitzgerald, D., Rubin, S., Capaldo, M., Maugeri, M., Leitass, A., Bukantis, A., Aberfeld, R., Van Engelen, A. F. V., Forland, E., Mietus, M., Coelho, F., Mares, C., Razuvaev, V., Nieplova, E., Cegnar, T., Antonio López, J., Dahlström, B., Moberg, A., Kirchhofer, W., Ceylan, A., Pachaliuk, O., Alexander, L. V., and Petrovic, P.: Daily dataset of 20th-century surface air temperature and precipitation series for the European Climate Assessment, Int. J. Climatol., 22, 1441–1453, 2002.

Lang, S. I., Cornelissen, J. H., Klahn, T., Van Logtestijn, R. S., Broekman, R., Schweikert, W., and Aerts, R.: An experimental comparison of chemical traits and litter decomposition rates in a diverse range of subarctic bryophyte, lichen and vascular plant species, J. Ecol., 97, 886–900, 2009.

Lawrence, D. M. and Slater, A. G.: A projection of severe near-surface permafrost degradation during the 21st century, Geophys. Res. Lett., 32, L24401, doi:10.1029/2005GL025080, 2005.

Li, S., Zhan, H., Lai, Y., Sun, Z., and Pei, W.: The coupled moisture-heat process of permafrost around a thermokarst pond in Qinghai-Tibet Plateau under global warming, J. Geophys. Res.-Earth, 119, 836–853, 2014.

Li, B., Heijmans, M. M. P. D., Berendse, F., Blok, D., Maximov, T. C., and Sass-Klaassen, U.: The role of summer precipitation and summer temperature in establishment and growth of dwarf shrub *Betula nana* in northeast Siberian tundra, Polar Biol., 39, 1245–1255, doi:10.1007/s00300-015-1847-0, 2016.

Lundberg, A. and Beringer, J.: Albedo and snowmelt rates across a tundra-to-forest transition, in: Proceedings of the 15 northern research basins international symposium and workshop, Department of Water Resources Engineering, Lund University, 1–10, 2005.

MacDougall, A. H., Avis, C. A., and Weaver, A. J.: Significant contribution to climate warming from the permafrost carbon feedback, Nat. Geosci., 5, 719–721, 2012.

Marion, G. M. and Miller, P. C.: Nitrogen mineralization in a tussock tundra soil, Arct. Alp. Res., 287–293, 1982.

McGuire, A. D., Anderson, L. G., Christensen, T. R., Dallimore, S., Guo, L., Hayes, D. J., Heimann, M., Lorenson, T. D., Macdonald, R. W., and Roulet, N.: Sensitivity of the carbon cycle in the Arctic to climate change, Ecol. Monogr., 79, 523–555, 2009.

Murphy, M. T., McKinley, A., and Moore, T. R.: Variations in above-and below-ground vascular plant biomass and water table on a temperate ombrotrophic peatland, Botany, 87, 845–853, 2009.

Myers-Smith, I. H., Forbes, B. C., Wilmking, M., Hallinger, M., Lantz, T., Blok, D., Tape, K. D., Macias-Fauria, M., Sass-Klaassen, U., Lévesque, E., Boudreau, S., Ropars, P., Hermanutz, L., Trant, A., Collier, L. S., Weijers, S., Rozema, J., Rayback, S. A., Schmidt, N. M., Schaepman-Strub, G., Wipf, S., Rixen, C., Ménard, C. B., Venn, S., Goetz, S., Andreu-Hayles, L., Elmendorf, S., Ravolainen, V., Welker, J., Grogan, P., Epstein, H. E., and Hik, D. S.: Shrub expansion in tundra ecosystems: dynamics, impacts and research priorities, Environ. Res. Lett., 6, 045509, doi:10.1088/1748-9326/6/4/045509, 2011.

Myers-Smith, I. H., Elmendorf, S. C., Beck, P. S. A., Wilmking, M., Hallinger, M., Blok, D., Tape, K. D., Rayback, S. A., Macias-Fauria, M., Forbes, B. C., Speed, J. D. M., Boulanger-Lapointe, N., Rixen, C., Levesque, E., Schmidt, N. M., Baittinger, C., Trant, A. J., Hermanutz, L., Collier, L. S., Dawes, M. A., Lantz, T. C., Weijers, S., Jorgensen, R. H., Buchwal, A., Buras, A., Naito, A. T., Ravolainen, V., Schaepman-Strub, G., Wheeler, J. A., Wipf, S., Guay, K. C., Hik, D. S., and Vellend, M.: Climate sensitivity of shrub growth across the tundra biome, Nature Climate Change, 5, 887–891, 2015.

Nadelhoffer, K., Shaver, G., Fry, B., Giblin, A., Johnson, L., and McKane, R.: ^{15}N natural abundances and N use by tundra plants, Oecologia, 107, 386–394, 1996.

Nauta, A. L., Heijmans, M. M. P. D., Blok, D., Limpens, J., Elberling, B., Gallagher, A., Li, B., Petrov, R. E., Maximov, T. C., van Huissteden, J., and Berendse, F.: Permafrost collapse after shrub removal shifts tundra ecosystem to a methane source, Nature Climate Change, 5, 67–70, 2015.

Osterkamp, T. E., Jorgenson, M. T., Schuur, E. A. G., Shur, Y. L., Kanevskiy, M. Z., Vogel, J. G., and Tumskoy, V. E.: Physical and ecological changes associated with warming permafrost and thermokarst in interior Alaska, Permafrost Periglacial Process, 20, 235–256, 2009.

Pearson, R. G., Phillips, S. J., Loranty, M. M., Beck, P. S., Damoulas, T., Knight, S. J., and Goetz, S. J.: Shifts in Arctic vegetation and associated feedbacks under climate change, Nature Climate Change, 3, 673–677, 2013.

Pettersson, R., McDonald, A. J. S., and Stadenberg, I.: Response of small birch plants (*Betula pendula* Roth.) to elevated CO_2 and nitrogen supply, Plant Cell Environ., 16, 1115–1121, 1993.

Riordan, B., Verbyla, D., and McGuire, A. D.: Shrinking ponds in subarctic Alaska based on 1950–2002 remotely sensed images, J. Geophys.-Res.Biogeo., 111, G04002, doi:10.1029/2005JG000150, 2006.

Saxton, K. E. and Rawls, W. J.: Soil water characteristic estimates by texture and organic matter for hydrologic solutions, Soil Sci. Soc. Am. J., 70, 1569–1578, 2006.

Schuur, E., Bockheim, J., Canadell, J., Euskirchen, E., Field, C., Goryachkin, S., Hagemann, S., Kuhry, P., Lafleur, P., and Lee, H.: Vulnerability of permafrost carbon to climate change: Implications for the global carbon cycle, BioScience, 58, 701–714, 2008.

Schuur, E. A. G., McGuire, A. D., Schädel, C., Grosse, G., Harden, J. W., Hayes, D. J., Hugelius, G., Koven, C. D., Kuhry, P., Lawrence, D. M., Natali, S. M., Olefeldt, D., Romanovsky, V. E., Schaefer, K., Turetsky, M. R., Treat, C. C., and Vonk, J. E.: Climate change and the permafrost carbon feedback, Nature, 520, 171–179, 2015.

Serreze, M. C., Walsh, J. E., Chapin, F. S., Osterkamp, T., Dyurgerov, M., Romanovsky, V., Oechel, W. C., Morison, J., Zhang, T., and Barry, R. G.: Observational evidence of recent change in the northern high-latitude environment, Climatic Change, 46, 159–207, 2000.

Shaver, G. R. and Chapin, F. S.: Production: biomass relationships and element cycling in contrasting arctic vegetation types, Ecol. Monogr., 61, 1–31, 1991.

Shaver, G. R. and Cutler, J. C.: The vertical distribution of live vascular phytomass in cottongrass tussock tundra, Arct. Alp. Res., 11, 335–342, 1979.

Shaver, G. R., Bret-Harte, M. S., Jones, M. H., Johnstone, J., Gough, L., Laundre, J., and Chapin, F. S.: Species composition interacts with fertilizer to control long-term change in tundra productivity, Ecology, 82, 3163–3181, 2001.

Sturm, M., Racine, C., and Tape, K.: Climate change: increasing shrub abundance in the Arctic, Nature, 411, 546–547, 2001.

Tape, K. E. N., Sturm, M., and Racine, C.: The evidence for shrub expansion in northern Alaska and the Pan-Arctic, Glob. Change Biol., 12, 686–702, 2006.

Tarnocai, C., Canadell, J. G., Schuur, E. A. G., Kuhry, P., Mazhitova, G., and Zimov, S.: Soil organic carbon pools in the northern circumpolar permafrost region, Global Biogeochem. Cy., 23, GB2023, doi:10.1029/2008GB003327, 2009.

Turetsky, M. R., Wieder, R. K., and Vitt, D. H.: Boreal peatland C fluxes under varying permafrost regimes, Soil Biol. Biochem., 34, 907–912, 2002.

Urban, M., Forkel, M., Eberle, J., Hüttich, C., Schmullius, C., and Herold, M.: Pan-arctic climate and land cover trends derived from multi-variate and multi-scale analyses (1981–2012), Remote Sens., 6, 2296–2316, 2014.

van Huissteden, J., Berrittella, C., Parmentier, F. J. W., Mi, Y., Maximov, T. C., and Dolman, A. J.: Methane emissions from permafrost thaw lakes limited by lake drainage, Nature Climate Change, 1, 119–123, 2011.

van Huissteden, J. and Dolman, A. J.: Soil carbon in the Arctic and the permafrost carbon feedback, Current Opinion in Environmental Sustainability, 4, 545–551, 2012.

van Oene, H., Berendse, F., and de Kovel, C. G.: Model analysis of the effects of historic CO_2 levels and nitrogen inputs on vegetation succession, Ecol. Appl., 9, 920–935, 1999.

van Wijk, M. T.: Predicting ecosystem functioning from plant traits: results from a multi-scale ecophysiological modeling approach, Ecol. Modell., 203, 453–463, 2007.

Vavrus, S. J., Holland, M. M., Jahn, A., Bailey, D. A., and Blazey, B. A.: Twenty-first-century Arctic climate change in CCSM4, J. Climate, 25, 2696–2710, 2012.

Walker, D. A., Raynolds, M. K., Daniels, F. J. A., Einarsson, E., Elvebakk, A., Gould, W. A., Katenin, A. E., Kholod, S. S., Markon, C. J., Melnikov, E. S., Moskalenko, N. G., Talbot, S. S., and Yurtsev, B. A.: The circumpolar Arctic vegetation map, J. Veg. Sci., 16, 267–282, 2005.

Walker, M. D., Wahren, C. H., Hollister, R. D., Henry, G. H. R., Ahlquist, L. E., Alatalo, J. M., Bret-Harte, M. S., Calef, M. P., Callaghan, T. V., Carroll, A. B., Epstein, H. E., Jonsdottir, I. S., Klein, J. A., Magnusson, B., Molau, U., Oberbauer, S. F., Rewa, S. P., Robinson, C. H., Shaver, G. R., Suding, K. N., Thompson, C. C., Tolvanen, A., Totland, O., Turner, P. L., Tweedie, C. E., Webber, P. J., and Wookey, P. A.: Plant community responses to experimental warming across the tundra biome, P. Natl. Acad. Sci. USA, 103, 1342–1346, 2006.

Walter, K. M., Zimov, S. A., Chanton, J. P., Verbyla, D., and Chapin, F. S.: Methane bubbling from Siberian thaw lakes as a positive feedback to climate warming, Nature, 443, 71–75, 2006.

Wang, P., Mommer, L., van Ruijven, J., Berendse, F., Maximov, T. C., and Heijmans, M. M. P. D.: Seasonal changes and vertical distribution of root standing biomass of graminoids and shrubs at a Siberian tundra site, Plant Soil, 407, 55–65, doi:10.1007/s11104-016-2858-5, 2016.

Wolf, A., Callaghan, T. V., and Larson, K.: Future changes in vegetation and ecosystem function of the Barents Region, Climatic Change, 87, 51–73, 2008.

Yoshikawa, K., and Hinzman, L. D.: Shrinking thermokarst ponds and groundwater dynamics in discontinuous permafrost near Council, Alaska, Permafrost Periglacial Processes, 14, 151–160, 2003.

Yu, Q., Epstein, H. E., Walker, D. A., Frost, G. V., and Forbes, B. C.: Modeling dynamics of tundra plant communities on the Yamal Peninsula, Russia, in response to climate change and graz-

ing pressure, Environ. Res. Lett., 6, 045505, doi:10.1088/1748-9326/6/4/045505, 2011.

Zhang, T., Frauenfeld, O. W., Serreze, M. C., Etringer, A., Oelke, C., McCreight, J., Barry, R. G., Gilichinsky, D., Yang, D. Q., Ye, H. C., Ling, F., and Chudinova, S.: Spatial and temporal variability in active layer thickness over the Russian Arctic drainage basin, J. Geophys. Res.-Atmos., 110, D16101, doi:10.1029/2004JD005642, 2005.

Zhang, W., Miller, P. A., Smith, B., Wania, R., Koenigk, T., and Döscher, R.: Tundra shrubification and tree-line advance amplify arctic climate warming: results from an individual-based dynamic vegetation model, Environ. Res. Lett., 8, 034023, doi:10.1088/1748-9326/8/3/034023, 2013.

Zimov, S. A., Davydov, S. P., Zimova, G. M., Davydova, A. I., Schuur, E. A. G., Dutta, K., and Chapin, F. S.: Permafrost carbon: Stock and decomposability of a globally significant carbon pool, Geophys. Res. Lett., 33, L20502, doi:10.1029/2006GL027484, 2006a.

Zimov, S. A., Schuur, E. A., and Chapin, F. S.: Permafrost and the global carbon budget, Science, 312, 1612–1613, 2006b.

Zotarelli, L., Dukes, M. D., and Morgan, K. T.: Interpretation of soil moisture content to determine soil field capacity and avoid over-irrigating sandy soils using soil moisture sensors, University of Florida Cooperation Extension Services, AE460, 2010.

NUCOMBog: A R package to run the NUCOM-Bog model and process its outputs

J.W.M. Pullens*[1,2], M. Bagnara[3], and F. Hartig[3,4]

[1]Department of Sustainable Agro-ecosystems and Bioresources, Research and Innovation Centre, Fondazione Edmund Mach (FEM), Via E. Mach 1, 38010 San Michele all'Adige, Italy

[2]Hydromet, Department of Civil and Environmental Engineering and Environmental Research Institute, University College Cork, Cork, Ireland

[3]Department of Biometry and Environmental System Analysis, University of Freiburg, Freiburg, Germany

[4]Theoretical Ecology, Faculty of Biology and Pre-Clinical Medicine, University of Regensburg, Universitätsstraße 3, 93053 Regensburg, Germany

1 Abstract

The model NUCOM-Bog (NUtrient cycling and COMpetition) describes the vegetation, carbon, nitrogen and water dynamics of peatland ecosystems (Heijmans et al., 2008). This model is derived from earlier NUCOM models (Berendse, 1988; Van Oene et al., 1999). The NUCOMBog package links the model, which is written in Delphi, to the R infrastructure. It runs on a monthly time step and the competition is based on light and nitrogen. For more details about NUCOM-Bog, see Heijmans et al. (2008). The executable of the model is available on request at the corresponding author and available on `https://github.com/jeroenpullens/NUCOMBog`.

*corresponding author, jeroenpullens@gmail.com, executable of the model is available on request at corresponding author

2 The NUCOMBog R package

The NUCOMBog R package provides several functions to setup and run the model.

setupNUCOM

In order to run the model a setup structure needs to be made. In this way the model knows the working directory, the climatic, environmental data, the initial biomass values, the start year and the end year. The model starts in January of the start year and ends in December of the end year. In the setup also the output is specified, see section: getData. For both the single core run and the multi-core run the same setup function can be used. This can be done by setting the parameter "parallel" to TRUE or FALSE, the default value is FALSE. "Separate" can only be use in parallel, it can be used to run the model with a list of parameters where all parameters are run individually, in contrast to a complete parameter list. Parameters for which no value has been given these parameters are set to the original value, see runNUCOM.

In some runs a spin-up period is used. During this spin-up the model can reach a stable equilibrium, this can be useful when the initial biomass values are not completely known. Since the data from not spin-up is not always needed for analysis, these values can be neglected by R. In the setup function the parameter "Startval" is implemented for that reason. The "Startval" has to be the row number of the output, i.e. if the model was run from 1970-2005 and only the data from January 2000 onward is needed. The start value has to be set to (2000-1970)*12 = 360. This "Startvalue" will be used in the getData function.

getData

The getData function retrieves the monthly data from the model run. The data of monthly output file is loaded into the global environment. The output that can be retrieved is Net Primary Production ("NPP"), Heterotrophic respiration ("hetero_resp"), Net Ecosystem Exchange ("NEE") and water table depth ("WTD"). The "Startvalue" can also be set, the "Startval" has to be the row number of the output, i.e. if the model was run from 1970-2005 and only the data from January 2000 onward is needed. The start value has to be set to (2000-1970)*12 = 360.

runNUCOM

When the setupNUCOM function has run, the setup is used to run the model. The presented function here only runs on a single core, for the multi-core run, see runparallelNUCOM. To run NUCOMBog we need the setup as previously described and potentially the parameter values. The parameter values need to be in a data frame format with two columns. The column names have to be "names" and "values", both without capital letter. When no parameters or few parameters are given to the model, the model uses the values provided by Heijmans et al. (2008) for the parameters which are not provided. The names are the same as in the paper, but to identify to which PFT the variable corresponds, the first four letters are used, so eric, gram, humm, lawn and holl. For example the maximum potential growth rate of the graminoids is gram_maxgr. The shrubs are defined ericaceous, e.g. the maximum potential growth rate is eric_maxgr.

During the run the parameter file is created in the input folder. In the output folder the monthly and yearly output files are created. Example input files and the folder structure are integrated in the R package and can be copied to a user specified folder, see section: copytestdata.

runparallelNUCOM

This function is used to run the model over multiple cores, this is particularly useful when multiple parameter sets need to be run. This function makes use of the snowfall (Knaus, 2013) package. To run the model in parallel, the type of cluster is needed, by default this is set to "SOCK". The model has not been tested on other cluster types so far. In the runparallelNUCOM function also the amount of cores, that are available for the computation, are needed. By default it is set to "1".

During the parallel run of the model for each provided parameter set a new folder is created in which the files with the climatic, environmental and initial data and the executable is copied. This has the advantage that the parameter files and the output files are in one folder, so no specific tracking in the cluster is needed.

The created folders are also very small (smaller than 2 MB) and therefore disk space issues are most likely not occurring.

copytestdata

The R package also includes some test data, this data has to be copied to a user defined folder. With the use of the function copytestdata the user can copy the data and test the model.

3 Data

The model needs three types of input data, all which need to be in the input folder as a ".txt" file. An example of the structure of the folder and the data of the example can are integrated in the R package and can be copied, see section copytestdata. The data used in this publication are from Heijmans et al. (2008). The three inputs are:

Initial values The model needs to be initialized with biomass values, preferable from field measurements. In the model the biomass of the vascular plants is separated in "organs" (leaf, shoot, root), while the biomass of the mosses is only the mass of the "shoot". The biomass needs to be separated into grams of carbon and grams of nitrogen per plant organ. Also the carbon and nitrogen of each specific plant organ stored/sequestrated in the acrotelm and catotelm is needed. As well as an initial water table depth and average water table depth.

Environmental data The environmental data should contain the yearly atmospheric CO_2 concentration in ppm and nitrogen deposition (both wet and dry) in kg N per hectare.

Climatic data The climatic data should contain monthly temperature, precipitation, and potential evapotranspiration. NUCOM-Bog was designed to run with the calculated Penman potential evapotranspiration (Penman, 1946).

4 Example Lille Vildmose, Denmark

In this section we will present an example of NUCOMBog. For this run the data from the Lille Vildmose, Denmark as presented in Heijmans et al. (2008) is used.

```
test_setup_singlecore <- setupNUCOM(mainDir = "/home/jeroen/MEE_model/",
    climate = "ClimLVMhis.txt", environment = "EnvLVMhis.txt",
    inival = "inivalLVMhis.txt", start = 1766, end = 1999, type = c("NEE",
        "WTD", "NPP", "hetero_resp"), parallel = F)
output <- runNUCOM(setup = test_setup_singlecore, parameters = NULL)
```

What we can see here is that the model has been run without any given parameters and therefore the integrated values from Heijmans et al. (2008) are used. The model was run from January 1766

till December 1999. The net primary production, net ecosystem exchange and water table depth are plotted from 1960 till 1999 (Figure 1).

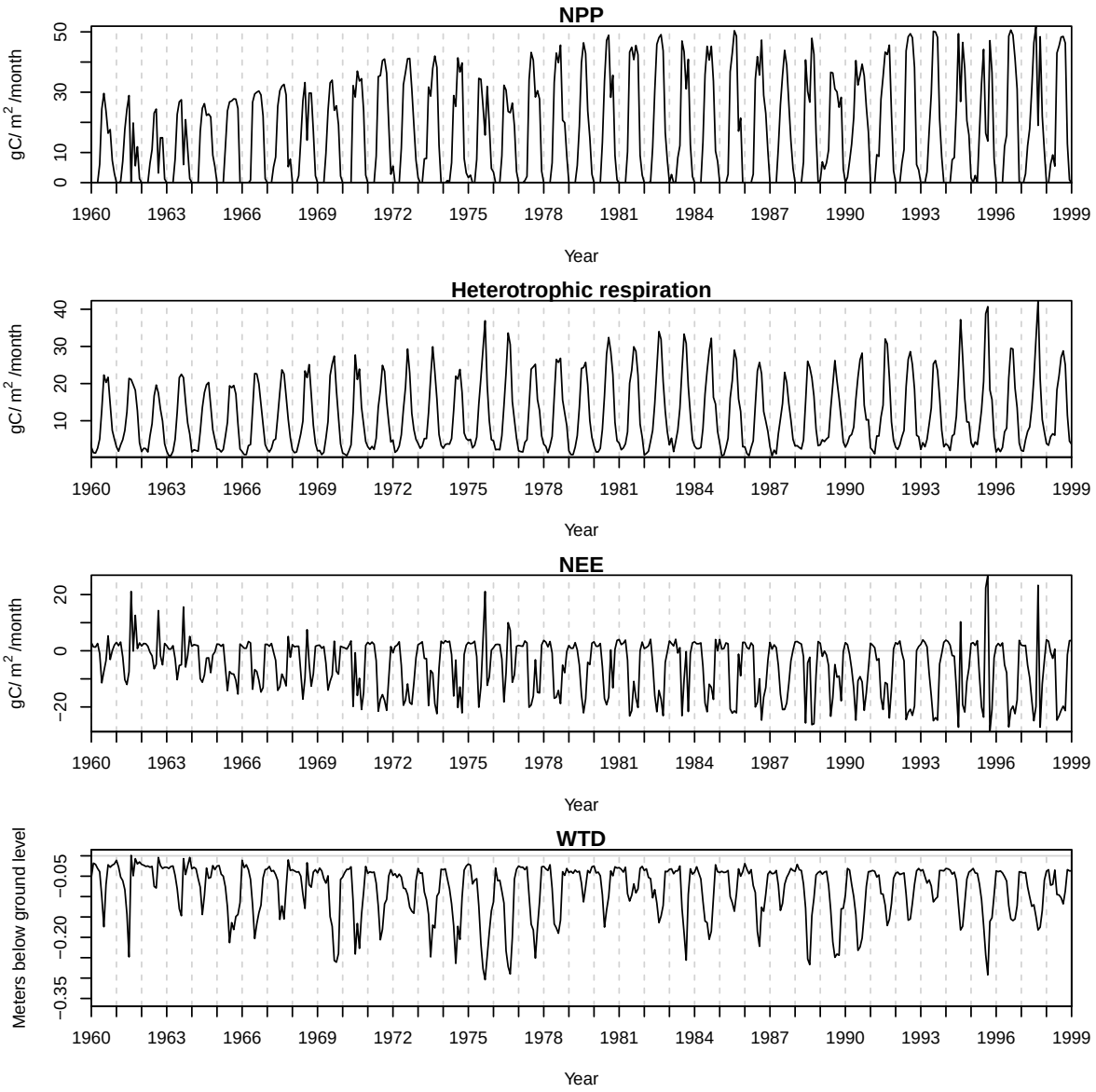

Figure 1: Simulated monthly NPP, NEE, heterotrophic respiration and WTD from 1960 till 1999.

The seasonal dynamics can be seen in the plot of the NPP, NEE and heterotrophic respiration, in which the greatest uptake takes place during the summer months. During some of the summer months the NEE 'peaks' close to zero or even above zero, these episodes match with a drop in water table depth. This could indicate that the plants were water stressed. During the winters the NEE is bigger than 0 gC m^2 $month^1$, indicating a loss of carbon, through heterotrophic respiration.

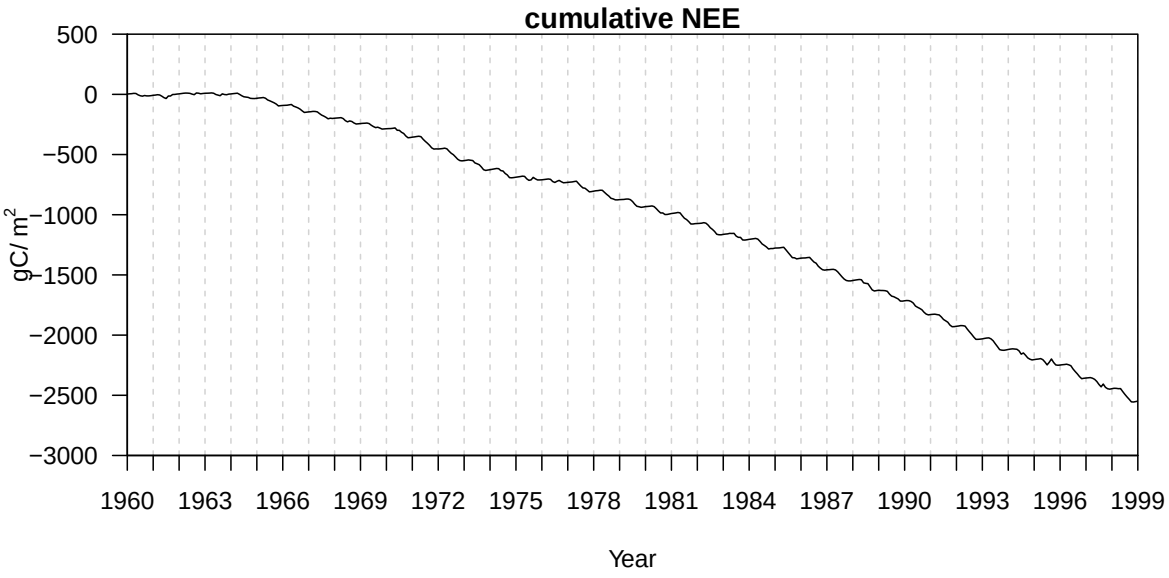

Figure 2: Cumulative monthly net ecosystem exchange from 1980 until 1999.

When we plot the cumulative modeled NEE, we see that the modeled Lil Vildmose site is acting as a carbon sink, i.e. sequestering carbon, see Figure 2 .

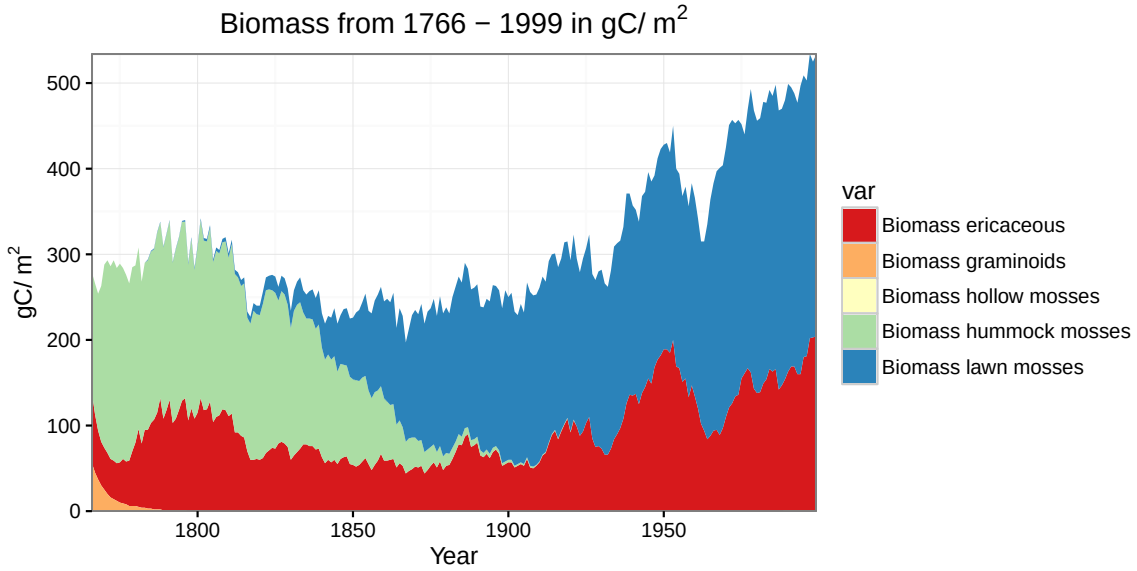

Figure 3: Biomass composition of the five different PFTs from 1766 till 1999.

Figure 3 indicates that the initial biomass of the graminoids was set too high. The plants die within 40 years and never return. At this location there is no hollow moss present and the initial values were therefore set to 0 gC m^2. The last 100 years the vegetation composition is stabilizing, only ericaceous

shrub species and lawn mosses are present. Both PFTs are increasing their biomass over time, due to CO_2 fertilization and an increase in temperature.

5 Acknowledgements

The authors would like to thank Ramiro Silveyra Gonzalez for his help with the development for this package. The authors would also like to thank Monique Heijmans for providing the NUCOM-Bog model. This work was supported by a STSM grant to JWMP from COST Action FP1304 (Profound) `http://cost-profound.eu/site/`.

References

Berendse, F. (1988). *Een simulatiemodel als hulpmiddel bij het beheer van vochtige heidevelden*. CABO, Wageningen, NL (In Dutch), Wageningen.

Heijmans, M. M. P. D., Mauquoy, D., Van Geel, B., and Berendse, F. (2008). Long-term effects of climate change on vegetation and carbon dynamics in peat bogs. *Journal of Vegetation Science*, 19(March):307–320.

Knaus, J. (2013). snowfall: Easier cluster computing (based on snow).. R package version 1.84-6.

Penman, H. L. (1946). Natural evaporation from open water, bare soil and grass. 193(1032):120–145.

Van Oene, H., Berendse, F., and de Kovel, C. (1999). Model analyses of the effects of the historic CO2 levels and nitrogen inputs on vegetation succession. *Ecological applications*, 9(3):920–935.